THE UNIVERSITY OF QUEENSLAND

AUSTRALIA

Characterisation of the α_{1B}-Adrenoceptor by Modeling, Dynamics and Virtual Screening

Kapil Jain

B.Pharm, M.S.(Pharm.)

A Thesis submitted for the degree of Master of Philosophy at

The University of Queensland in 2018

Institute for Molecular Bioscience

Abstract

G protein-coupled receptors (GPCRs) are the largest druggable class of proteins yet relatively little is known about the mechanism by which agonist binding induces the conformational changes necessary for G protein activation and intracellular signaling. Recently, the Kobilka group has shown that agonists, neutral antagonists and inverse agonists stabilise distinct extracellular surface (ECS) conformations of the β_2-adrenergic receptor (AR) opening up new possibilities for allosteric drug targeting at GPCRs. The goal of this project is to extend these studies to define how the ECS conformation of the α_{1B}-AR changes during agonist binding and develop an understanding of ligand entry and exit mechanisms that may help in the design of specific ligands with higher selectivity, efficacy and longer duration of action.

Two parallel approaches were initiated to identify likely functional residues. The role of residues lining the primary binding site were predicted by online web server (Q-Site Finder) while secondary binding sites residues were predicted from molecular dynamics (MD) simulations. Predicted functionally significant residues were mutated and their function was established using FLIPR, radioligand and saturation binding assays. Despite the α_{1B}-AR being pursued as a drug target for over last few decades, few specific agonists and antagonists are known to date. In an attempt to address this gap, we pursued ligand-based approach to find potential new leads. The outcomes of this research will help to understand the GPCR activation process. This research may open the door to the rational development of new modulators that can recognise the ECS of GPCRs in distinct conformational states.

Chapter 1 provides an overview of the GPCR including the structure, function, pharmacology and regulation of Class A GPCRs with special reference to the α_1-AR. The present work is an effort to address the issues pertaining to the activation of the α_1-AR and how the binding of the known ligands affect the ECS of the receptor and stabilise specific conformations. The ligand-based *In Silico* drug discovery approach is implemented to address rational development of leads which could be subtype specific. The use of computational tools has been shown to study the receptor for drug discovery and development.

Chapter2 describes research to characterise the egress pathway of norepinephrine (NE), the endogenous α_1-AR agonist. Using a homology model of the α_{1B}-AR built from turkey-β_1-AR as template, we performed molecular docking of NE at the orthosteric binding site. Validation of the docking model was performed using mutants generated from site directed mutagenesis and

testing those using radiolabelled, functional and binding studies to gain insights into the role played by the residues lining the egress pathway. Residues Trp121, Cys195, Tyr203 and Ser207 were identified to be particularly involved and effect the simulations at two distinct positions which may probably regulate the access and egress of NE to- and from- the orthosteric binding site to the ECS. This study revealed that the negatively charged residues lining the extracellular loop 2 (ECL2) may also provide an allosteric site for the positively charged ligands by retaining them for some time and stabilising the ECS as inferred from our MD studies.

Chapter 3 describes research to understand the activation process of the apo and NE-bound α_{1B}-AR using accelerated molecular dynamics (aMD). The receptors in both states were energy minimised, equilibrated and subjected to classical MD for a specific time frame. Residues known from the experimental studies to be involved in receptor activation were mutated individually along with additional double mutants to further characterise their role in activation process. This study identified single (W184A) and double mutant (Y223F-Y348F) in both the apo and NE-bound α_{1B}-AR that preferentially moved the receptor towards the active state.

Chapter 4 describes virtual screening (VS) for novel modulators of the α_1-AR. Using Rapid Overlay of Chemical Structures (ROCS), 17.9 million drug-like compounds were screened from the ZINC database. The initial results identified 80 "hits" which were confirmed by flexible docking to likely bind either at orthosteric or adjacent allosteric sites along the ligand binding/unbinding pathway. To validate the potential of this set of ligands to target the α_1-AR, 12 hits were selected for pharmacological evaluation across the three α_1-AR subtypes. The results of our initial characterisation revealed that several ligands that docked in the orthosteric site of the α_{1B}-AR activated all the three α_1-AR subtypes confirming the potential of this approach to identify new α_1-AR modulators.

Chapter 5 provides an overall conclusions drawn from the above work done and future prospects. In summary, this study has revealed the critical involvement of residues in TM3, TM5, TM7, ECL1 and ECL2. This study identified two distinct positions; auxiliary site 1 and auxiliary site 2 which could act as allosteric sites and might be subtype specific. aMD led to identification of single (W184A) and double mutant (Y223F-Y348F) that were close to receptor activation while VS identified leads which activated all the three α_1-AR subtypes confirming the potential of this approach to identify new α_1-AR modulators.

Declaration by the author

This thesis is composed of my original work, and contains no material previously published or written by another person except where due reference has been made in the text. I have clearly stated the contribution by others to jointly-authored works that I have included in my thesis.

I have clearly stated the contribution of others to my thesis as a whole, including statistical assistance, survey design, data analysis, significant technical procedures, professional editorial advice, financial support and any other original research work used or reported in my thesis. The content of my thesis is the result of work I have carried out since the commencement of my higher degree by research candidature and does not include a substantial part of work that has been submitted to qualify for the award of any other degree or diploma in any university or other tertiary institution. I have clearly stated which parts of my thesis, if any, have been submitted to qualify for another award.

I acknowledge that an electronic copy of my thesis must be lodged with the University Library and, subject to the policy and procedures of The University of Queensland, the thesis be made available for research and study in accordance with the Copyright Act 1968 unless a period of embargo has been approved by the Dean of the Graduate School.

I acknowledge that copyright of all material contained in my thesis resides with the copyright holder(s) of that material. Where appropriate I have obtained copyright permission from the copyright holder to reproduce material in this thesis and have sought permission from co-authors for any jointly authored works included in the thesis.

Publications included in this thesis

No publications included.

Other publications during candidature

No manuscripts submitted for publication.

Other publications during candidature

Peer-reviewed article

1. Brust, Andreas; Croker, Daniel; Colless, Barbara; Ragnarsson, Lotten; Andersson, Asa; Jain, Kapil; Caraballo, Sonia; Castro, Joel; Brierley, Stuart; Alewood, Paul; Lewis, Richard: **Conopeptide-derived κ-opioid agonists (conorphins): potent, selective and metabolic stable dynorphinA mimetics with anti-nociceptive properties**. *Journal of medicinal chemistry* 2016, **59**(6):2381-2395.

Conference abstract

1. Jain K, Ragnarsson L, Lewis RJ (2014) "Identification of functionally active residues in α_{1B}-AR by computational approaches" at 10th International Conference on Chemical structures-German Conference on Chemoinformatics-2014, The Netherlands.

Contributions by others to the thesis

Invaluable input in establishing research projects, designing experiments and interpreting results, proof reading the thesis has been given by my advisory team Professor Richard Lewis, Dr Lotten Ragnarsson and Asa Andersson.

Dr. Lotten Ragnarsson and Asa Andersson assisted me with molecular biology experiments like cell culture, FLIPR assay, radioligand binding assay and saturation binding assay along with data analysis and plotting graphs for Chapter 2 and Chapter 4. Initial molecular dynamics set up was carried out with the help of Dr. Grischa Meyer.

Results in chapter 2 and chapter 3 include data from published mutants. I acknowledge the support and co-operation provided to cross-validate the results from steered and accelerated molecular dynamics with the experimental results from Dr. Lotten Ragnarsson work.

Statement of parts of the thesis submitted to qualify for the award of another degree

No works submitted towards another degree have been included in this thesis.

Research Involving Human or Animal Subjects

No animal or human participants were involved in this research.

Acknowledgements

I would like to acknowledge my supervisor **Prof. Richard Lewis** for guiding and giving me the opportunity to complete my PhD in this field of research that I am passionate about. Richard's suggestions in presentations, designing experiments, interpreting data and writing the thesis and manuscripts were invaluable; and I could not ask for a friendlier environment to do my PhD. Thanks Richard for expert and friendly advice and for being always there when I needed you!

I would like to express my deepest appreciation to **Dr. Lotten Ragnarsson** for teaching in the lab, presentations and writing. Lotten has had an essential role in my PhD, helping me to coordinate projects, priorities and timelines. Dr. Lotten's expertise in molecular biology and training were essential in learning lab techniques used for the second and fourth result chapter of this thesis. I could not ask for a better teacher. Most importantly, I thank Lotten for encouraging, supporting and guiding during the years of my PhD. Thanks Lotten, we made it and it has been a great journey!

Very special thanks go also to **Asa Anderson** for patiently teaching the molecular biology techniques, binding assays, plotting graphs. Thanks Thea for patiently helping with administrative work. I would like to thank IT team especially Chris Hunt and Yves St-Onge for helping me with IT and software work throughout my PhD. Furthermore I would also like to acknowledge with much appreciation the crucial role of **Dr. Amanda Carozzi**, who gave great support and went much further beyond her work duties to make sure PhD students are successful.

Thanks to Prof. Mike Water, Prof. Wally Thomas and Prof. David Fairlie for participating in my PhD milestones committee and for giving inestimable suggestions for my candidature.

I would like to acknowledge the financial support from The University of Queensland providing a UQI scholarship. I would also like to acknowledge The Institute for Molecular Biosciences for a travel grant which allowed me to attend an international conference in The Netherlands; and my supervisor Richard Lewis for providing financial support to complete my PhD projects and to attend conferences.

Last but not least, many thanks go to the most important people in my life: my family and friends. I thank my family for supporting my decision to come to Australia to pursue my dream PhD. Thanks to everyone for making this journey smoother and for your company, support, love, dedication and caring.

Financial support

I acknowledge receiving UQI Fees and UQI Living scholarship during my candidature to complete MPhil.

Keywords

GPCR, alpha-1 (α_1) Adrenergic Receptor, Homology Modeling, Molecular Docking, Virtual Screening, Molecular Dynamics, FLIPR Assays, Radioligand Binding Assays, Saturation Binding Assays.

Australian and New Zealand Standard Research Classifications (ANZSRC)

ANZSRC code: 030404, Cheminformatics and Quantitative Structure-Activity Relationships, 50%

ANZSRC code: 060112, Structural Biology (incl. Macromolecular Modelling), 30%

ANZSRC code: 111599, Pharmacology and Pharmaceutical Sciences, 20%

Fields of Research (FoR) Classification

FoR code: 0304, Medicinal and Bimolecular Chemistry, 50%

FoR code: 0601, Biochemistry and Cell Biology, 30%

FoR code: 1115, Pharmacology and Pharmaceutical Sciences, 20%

Table of Contents

List of Figures

List of Table

List of Abbreviations

°C	Degree celsius
3D	Three-dimensional
α_1-AR	Alpha-1 adrenergic receptor
β-AR	Beta adrenergic receptor
δ-OR	δ-opioid receptors
aMD	Accelerated molecular dynamics
AA	Amino acid
ABF	Adaptive biasing force simulation
AR	Adrenergic receptors
B	Boundary condition
BLAST	Basic local alignment search tool
BRh	Bovine rhodopsin
BSA	Bovine serum albumin
cpm	Counts per minute
cAMP	cyclic adenylyl monocyclase
cMD	Classical molecular dynamics
Ca^{2+}	Calcium ion
Cl^-	Chloride ion
$CaCl_2$	Calcium chloride
CO_2	Carbon dioxide
Da	Daltons
DAG	Diacyl glycerol
DMEM	Dulbecco's modified eagle medium
DMSO	Dimethyl sulfoxide
EC_{50}	Half-maximal excitatory concentration
ECS	Extracellular surface
EDTA	Ethylenediaminetetraacetic acid
FBS	Foetal bovine serum
FDA	Food and drug administration

FLIPR	Fluorometric imaging plate reader
FRET	Fluorescence resonance energy transfer
GA	Genetic algorithm
GDP	Guanosine diphosphate
GIRK	G protein-coupled inwardly rectifying potassium
GOLD	Genetic optimisation for ligand docking
GPCRs	G protein-coupled receptors
GTP	Guanosine triphosphate
HBA	Hydrogen bond acceptor
HTS	High throughput screening
HVS	Hierarchical virtual screening
HY	Hydrophobic feature
IC	Initial condition
IC_{50}	Half-maximal inhibitory concentration
IFP	Interaction fingerprint
IFS	Interaction fingerprint-based similarity
IP_3	Inositol triphosphate
Iso	Isoprenaline
K	Kelvin
K_d	Dissociation constant
K_i	Inhibitory constant
KCl	Potassium chloride
N	Number of particles
Na^+	Sodium ion
pIC_{50}	Positive half-maximal inhibitory concentration
PAM	Positive allosteric modulator
PCR	Polymerase chain reaction
PEI	Polyethyleneimine
PI	Positive ionisable
PKC	Protein kinase C
PLC-β	Phospholipase C-β

PLS-DA	Partial least square-discriminant analysis
PMF	Potential of mean force
POPC	1-palmitoyl-2-oleoyl-sn-glycerol-3-phosphatidylcholine
PSS	Physiological salt solution
PVS	Parallel virtual screening
RAMD	Random accelerated molecular dynamics
RMSD	Root mean square deviation
ROCS	Rapid overlay of chemical structures
S1P1	Sphingosine-1-phosphate receptor 1
SAR	Structure activity relationship
SBDD	Structure based drug design
SEM	Standard error of the mean
SMD	Steered molecular dynamics
TM	Transmembrane
VS	Virtual screening
WT	Wildtype

List of Amino Acid Abbreviations

Ala	A	Alanine
Arg	R	Arginine
Asn	N	Asparagine
Asp	D	Aspartic Acid
Cys	C	Cysteine
Glu	E	Glutamic Acid
Gln	Q	Glutamine
Gly	G	Glycine
His	H	Histidine
Ile	I	Isoleucine
Leu	L	Leucine
Lys	K	Lysine
Met	M	Methionine
Phe	F	Phenylalanine
Pro	P	Proline
Ser	S	Serine
Thr	T	Threonine
Trp	W	Tryptophan
Tyr	Y	Tyrosine
Val	V	Valine

Chapter 1

Chapter 1: Introduction

1.1 GPCRs: An Overview

GPCRs are seven transmembrane (7TM) proteins or heptahelical protein structures [1] which comprise of the largest receptor class in the human genome [2]. GPCRs are ubiquitous throughout the plant and animal kingdom [3]. They are the largest and most diverse group of membrane receptors [4, 5]. GPCRs are present in the genomes of bacteria, yeast, plants, nematodes and other invertebrate groups highlighting their early evolutionary origin [6]. Genome sequence analysis led to the identification of >800 different human genes coding for the GPCR classes [7]. GPCRs are involved in numerous diseases and account for approximately 25–50% of all modern medicinal drugs [8]. However, these drugs target only ~30 members of the GPCR class mainly biogenic amine receptors [9]. So, there is an enormous potential to exploit the remaining family members including >100 orphan receptors [10] for which no ligands/modulators exists.

GPCRs are widely distributed in different tissues and organs and thereby play a key role in diverse physiological processes such as neurotransmission, secretion, cellular metabolism and cellular differentiation [11]. GPCR members share the general mechanism of signal transduction by G proteins, β arrestins and other downstream effectors [12]. They respond to a wide variety of stimuli ranging from extracellular signals such as light and odorants to intracellular signals such as neurotransmitters, biogenic amines, lipids, proteins, ions, chemokine's, amino acids, hormones, nucleotides and many other sensory molecules and transduce binding events into intracellular reactions [13].

Crystallisation of GPCRs has been a challenge for decades thereby hampering molecular interpretation of biophysical and biochemical findings and rational drug discovery applications. The first membrane protein crystal structure was solved in 1985 by X-ray crystallography [14]. Since then more than 300 membrane protein structures have been solved along with bovine rhodopsin in 2000 [15]. The first high resolution crystal structure of the human β_2-AR with a diffusible ligand [16] came out after 7 years of extensive and rigorous research and technology development (**Table 1-1**) followed by other class A GPCR crystal structures; β_1-AR [16], adenosine A2A-R [17], chemokine CXCR4 [18], dopamine D3 [19] and histamine H_1 [20] receptors. These structures represent diversity at various level of homology among the highly conserved 7TM helices in the GPCR classes.

GPCRs comprise of 7TM helices connected by three intracellular (ICL) and three extracellular loops (ECL) [21] (**Figure 1-1)**. Parts of the ECLs along with the N terminus are responsible for ligand binding. The length of the N terminus ranges from a short structure to large globular domain in rhodopsin like structures and other GPCR classes. The ICLs along with the C terminus interacts with downstream effectors G proteins in signaling [22]. The 7TMs are considered as the most highly conserved component among the GPCR classes. These TMs harbours important signature motifs characteristic of the GPCR classes including the D[E]RY motif in TM3, WxP motif in TM6 and NPxxY motif in TM7 [23]. These motifs contribute to GPCR internalisation and signal transduction.

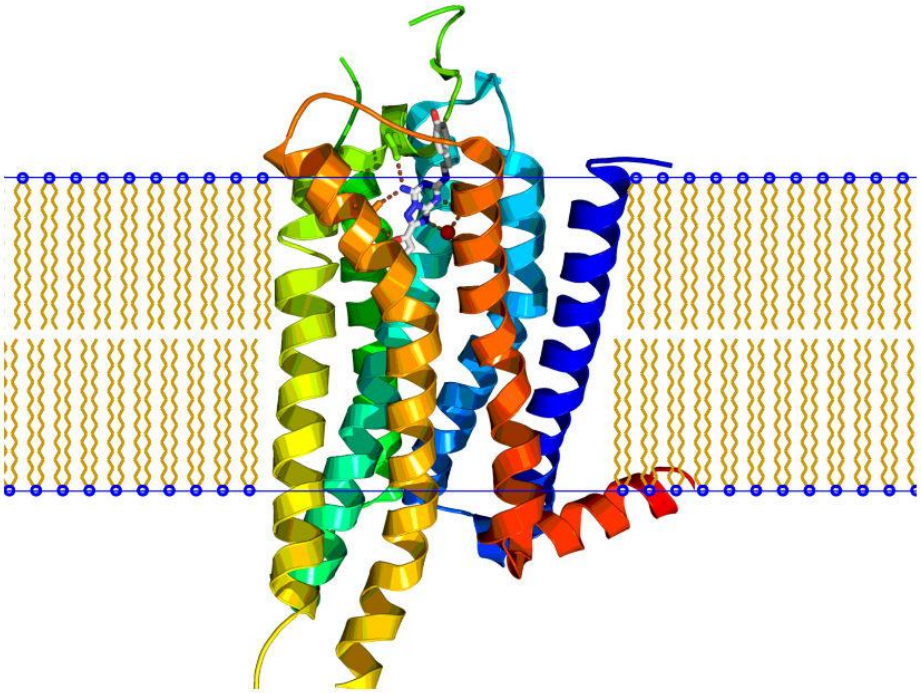

Figure 1-1: Model showing the 7TM topology of α_{1B}-AR embedded in membrane lipids.

1.2 Classification of GPCRs

GPCRs are often classified into different groups, subgroups and sub-subgroups based on the ligands they bind (**Table 1-1**) [24]. Although many classification approaches have been proposed, the GPCRs are classified mainly into six main classes (A, B, C, D, E and F) [25, 26] with limited sequence homology between the classes. All GPCRs classified into distinct classes share highly conserved 7TM domains with their structures containing four essential elements; three ECLs, three ICLs, and an N and C terminus [2].

The six classes could easily be distinguished on the basis of length and residues in the N terminus [27, 28]. The glycoprotein receptors of class A have N termini as long as some class B and the bitter taste receptors of family F have N termini similar size to many class A receptors but the smooth receptors of family F has a longer N terminus. The biggest is class A which accounts and codes for ~85% of the genes. Over half of class A GPCR genes are predicted to encode olfactory receptors while the remaining receptors are activated by known endogenous compounds or are classified as orphan receptors [10]. Phylogenetically, Class A is sub-divided into four main groups and 13 subgroups. The receptor of interest of this project α_{1B}-AR belongs to class A GPCR. Class B receptors (Secretin receptor family) encoded by 15 genes in humans bind large peptides such as secretin, parathyroid hormone, glucagon, calcitonin, vasoactive intestinal peptide, growth hormone releasing hormone and pituitary adenylyl cyclase activating protein[29].

The Class C (Glutamate receptor) members have ligand recognition domain in the long N terminus and has structural similarity with the bacterial amino acid binding proteins such as leucine/isoleucine/valine binding protein (LIVBP). Glutamate binds by venus fly trap mechanism in a cavity formed by two lobes on the amino terminal domain containing the ligand binding site. The adhesion GPCRs contain high percentage of Ser and Thr residues in the N terminus which can function as O- and N- glycosylation sites [30]. Class D (Fungal mating pheromone receptors) members comprise of pheromone receptors which are used by organisms for chemical communication [31]. Class E, the cAMP receptors forms part of the chemotactic signaling system of slime moulds [32]. Class F, the frizzled receptor has approximately 200 amino acids in the N terminus with conserved cysteine and the receptor control functions like cell fate, proliferation and polarity (**Figure 1-2**). **Table 1-1** summarises GPCRs classification.

Table 1-1: Classification of GPCR.

Category	Receptor Type
Class A (or 1)	Rhodopsin like
Class B (or 2)	Secretin receptor family
Class C (or 3)	Metabotropic glutamate/Pheromone
Class D (or 4)	Fungal mating pheromone receptors
Class E (or 5)	Cyclic AMP receptors
Class F (or 6)	Frizzled/smoothened

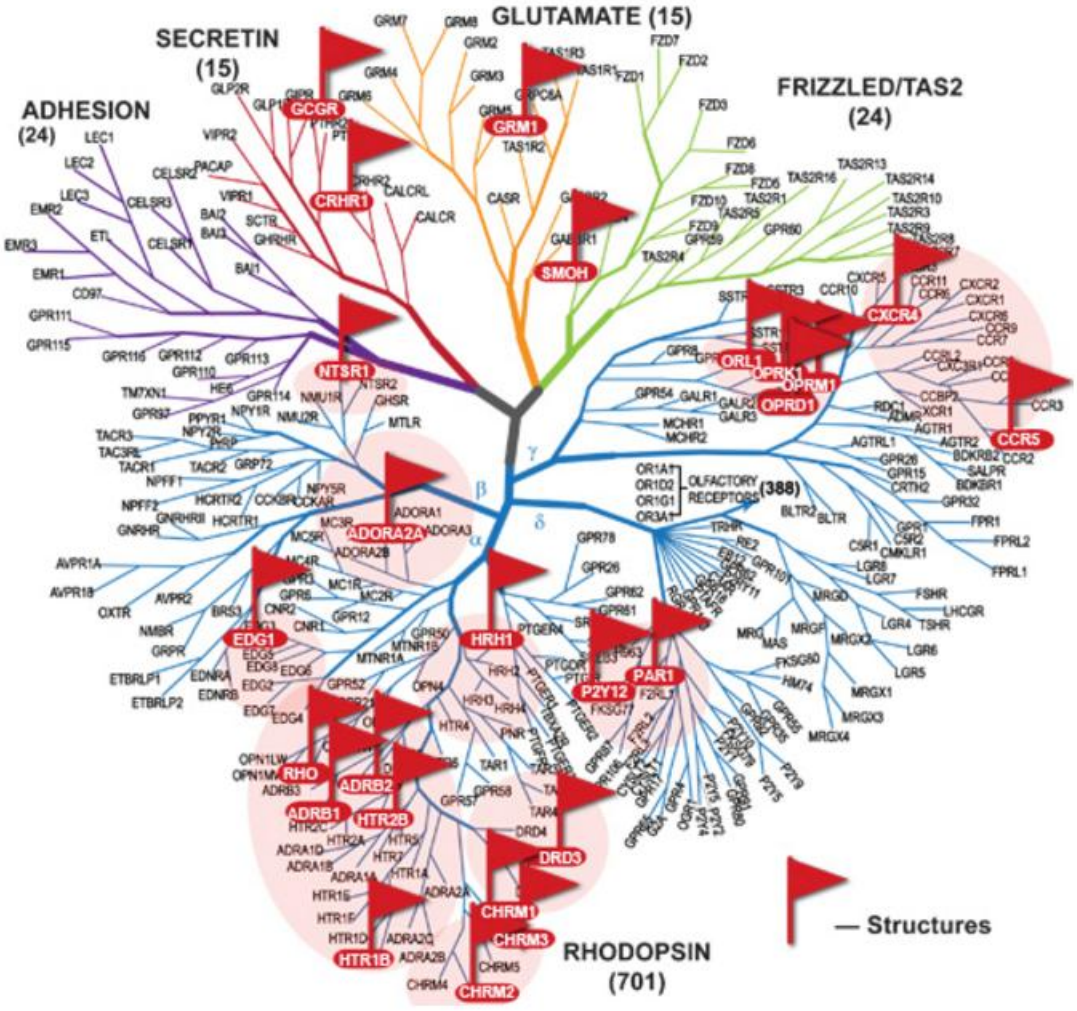

Figure 1-2: GPCR network (Image Courtesy: GPCR network; http://gpcr.usc.edu.).

The bioinformatics methodology has classified GPCRs thereby providing functional information for new GPCRs in the whole 'GPCR proteome' which is important for the development of novel drugs. Generally, the GPCR function is predicted on the basis of the hierarchical classification of the GPCR proteome but with the development of the state of art computational tools like alignment-free methods, statistical model methods and machine learning methods, GPCRs functions can be predicted irrespective of the classical hierarchical classification [33]. In hierarchical classification, the first stage is based on the discrimination of GPCRs from the non-GPCRs followed by classification of the segregated GPCRs into class, subclass, sub-subclass, groups, and subgroups. They are further classified based on protein-protein interaction type: binding G protein type, oligomerised partner type etc.

1.3 Mechanism of GPCR Activation

GPCRs are activated by a variety of signals in the form of external ligands and other signal mediators which leads to conformational changes and activation of G proteins and thereby transduce signals to downstream effectors [34-38]. Though major information about mechanism of action was based on rhodopsin structures [39, 40], recent crystal structures of ARs have provided new insights on GPCR activation mechanism. The receptor exists in an equilibration between inactive and active conformations [41].

The G protein is bound to the receptor in its inactive conformation [42, 43]. Once the ligand binds the receptor, conformational changes (bis-histidine metal ion-binding sites are generated between the cytoplasmic extensions of TM3 and TM6 in rhodopsin [44]; disruption of an ionic interaction between the highly conserved D(E)RY sequence at the cytoplasmic end of TM3 and an acidic residue at the cytoplasmic end of TM6 is observed upon activation in both rhodopsin and the β_2-AR [45]) take place within the receptor which in turn activates the associated G protein [34, 46] (**Figure 1-3**). The receptor can now either activate another G protein or switch back to its inactive state.

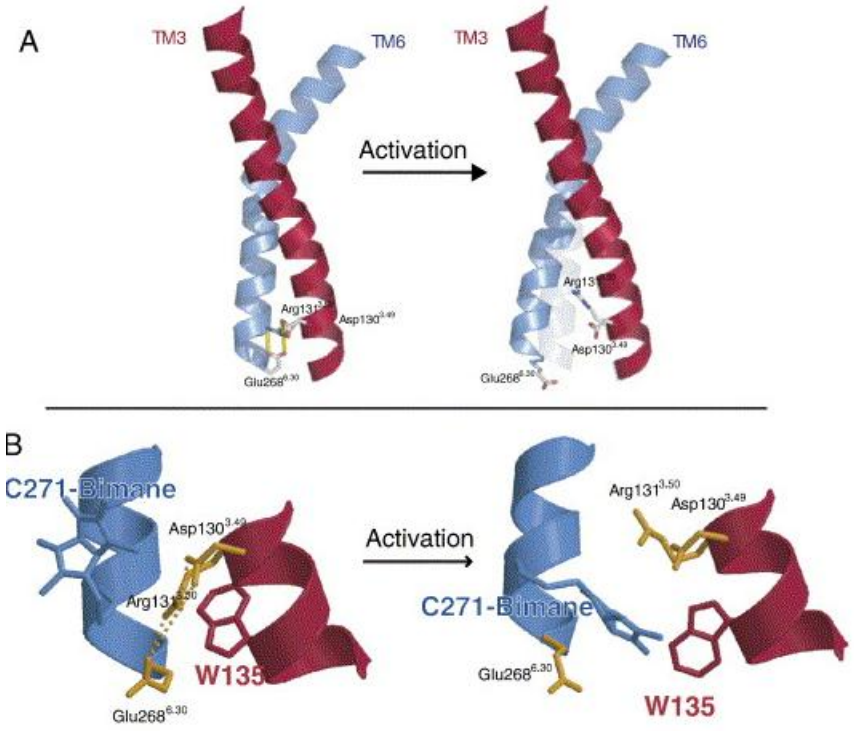

Figure 1-3: (A) Model of TM3 (red) and TM6 (blue) from the β_2-AR depicting the amino acids that comprise the ionic lock at the cytoplasmic end of these TM segments. (B) Close up view of the ionic lock and the modifications made to monitor conformational changes in this region [47] (Image courtesy: Kobilka, B. K. et al., *Biochimica et Biophysica Acta (BBA)-Biomembranes*; 2007;1768;794-807).

G proteins are heterotrimeric proteins consisting of three subunits G_α, G_β and G_γ [48]. In the inactive state receptor, the G protein is irreversibly bound to Guanosine diphosphate (GDP). Upon receptor activation, the G protein exchanges one molecule of GDP for Guanosine triphosphate (GTP) on the heterotrimeric α-subunit and then dissociates from the receptor protein as a G_α monomer and $G_{\beta\gamma}$ dimer which are now free to modulate the activity of other intracellular proteins. The GTP bound Gα subunit has the capability of slow hydrolysis of GTP to GDP which eventually regenerates the GDP bound G_α thus allowing re-association with the $G_{\beta\gamma}$ dimer to form the stable inactive G protein [49, 50] (**Figure 1-4**).

G protein signaling generates secondary messengers like cyclic adenylyl monocyclase (cAMP), calcium ions (Ca^{2+}), Inositol triphosphate/Diacyl glycerol (IP_3/DAG) which triggers further downstream processes. The phosphorylation of activated GPCRs by GPCR kinases leads to binding of activated GPCRs with high affinity to multifunctional scaffold proteins β-arrestins

[51, 52]. β-arrestins desensitise G protein signaling by preventing coupling of activated receptors with further G proteins and promote GPCR internalisation by nucleating the machinery required for clathrin-mediated endocytosis [53]. β-arrestins are also independent signal transducers, influencing signaling events such as the activation of mitogen-activated protein kinases that regulate the cytoskeleton, protein synthesis, cell migration and apoptosis, independent of G proteins [54].

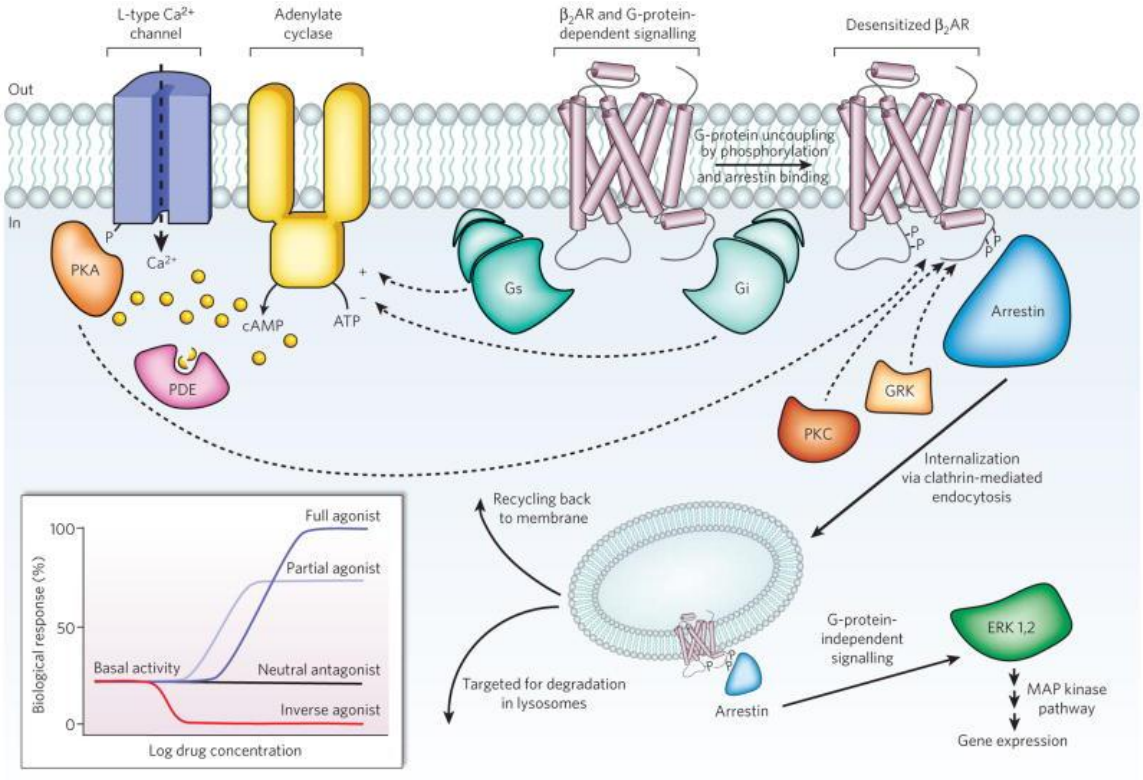

Figure 1-4: Signal transduction in GPCRs [55] (Image courtesy: Kobilka K.B. et al, *Nature*; 2009;459;356-363).

Further downstream signal transduction depends on the type of G protein attached and activation by the receptor [56-58]. GPCRs activate four distinct subclasses of G proteins; G_s proteins stimulate adenylyl cyclase, G_i proteins inhibit adenylyl cyclase while $G_{\beta\gamma}$ subunit of G_i G protein activate the G protein-coupled inwardly rectifying potassium (GIRK) channels, $G_{q/11}$ proteins activate phospholipase C-β (PLC-β) and $G_{12/13}$ proteins activate Rho guanine-nucleotide exchange factors. In addition, β and γ subunits form heterotrimers with α subunits [59] and mediate effector coupling in their own right providing a diverse array of signaling responses.

There are 4 subclasses of Gα-proteins ($G_{\alpha s}$, $G_{\alpha i/o}$, $G_{\alpha q/11}$ and $G_{\alpha 12/13}$) mediating three G protein dependent signaling pathways [60].The effector of the $G_{\alpha s}$ and $G_{\alpha i/o}$ pathways is adenylate cyclase [61] which catalyses the conversion of cytosolic adenosine triphosphate to cAMP [61]. The effector of the $G_{\alpha q/11}$ pathway is PLC-β which catalyses the cleavage of phosphatidylinositol 4,5-biphosphate into secondary messengers IP_3/DAG [62]. IP_3 elicits Ca^{2+} release from the endoplasmic reticulum while DAG diffuses along the plasma membrane and activates a Ser/Thr kinase; protein kinase C (PKC). The downstream effector of the $G_{\alpha 12/13}$-mediated signaling is the monomeric GTPaseRhoA which regulates intracellular processes such as formation of actin stress fibers, gene transcription and cell growth [63].

1.3.1 The Two-State Model of Receptor Activation vs. Multi-State Models of Receptor Activation

Ternary complex model also known as the two-state model is the most widely used model to understand the mechanism of receptor activation [64]. This model is based on the principle that in the absence of agonists, receptors can spontaneously adopt an active conformation and couple to the G protein [65]. This model classifies the receptor into two states as active and inactive states with a sufficiently low energy barrier which leads to easy transformation of low fraction of receptors to pass from inactive to active state. This model has been superseded by theories which explain the incompetency of the two-state model to understand the complex mechanism of GPCR activation.

This two-state model is replaced by multi-state model which explains and provides support and evidence of existence of multiple conformational states [66]. In the multistate model, the receptor is proposed to alternate spontaneously between multiple active and inactive conformations [67]. The observation that different constitutively active mutants of the α_{1B}-AR are differentially phosphorylated and internalised, although they convey a similar agonist-independent activity to the receptor supports the multi-state model [68, 69]. Fluorescence spectroscopy analysis of the purified β_2-AR indicated that most ligands promote alterations in receptor structure consistent with the existence of multiple ligand-specific conformational states [70].

1.3.2 Implications from Biophysical Studies on Receptor Activation Models

The biophysical analyses of rhodopsin and β_2-AR structures have provided novel insights into the critical conformational changes accompanying receptor activation. Rhodopsin covalently bounds an inverse agonist; *cis*-retinal and upon absorption of a photon isomerises to an agonist; *trans*-retinal within the binding pocket [71]. The efficient activation of rhodopsin by *trans*-retinal requires that *cis*-retinal is pre-bound and that *cis*-retinal can be rapidly converted to *trans*-retinal by photoisomerisation.

In contrast to the rapid activation and slow inactivation kinetics observed for rhodopsin, spectroscopic analyses of the purified β_2-AR labelled with a conformationally sensitive fluorophore revealed slow agonist-induced conformational changes ($t_{1/2}$ ~2–3 min) which is significantly slower than the predicted association rate of the agonist [72]. Biophysical studies has provided direct structural analyses of conformational change in the receptor molecule as an important first step toward a more profound understanding of GPCR function at a molecular level [38].

1.4 GPCR Oligomers

GPCRs are known to exist as dimers (or oligomers) and these dimers can play essential role in activation process for the glutamate family of GPCRs where ligand induced changes in the dimer interface of the amino terminal ligand binding domain has been demonstrated by crystallography [73]. The heterodimerisation between receptor subtypes suggested a potential level of receptor complexity that could account for unexpected pharmacological diversities. There are distinctive dimerisation interfaces or domains both within the TM helices [74] and also at the extracellular N terminus [75] or the intracellular C terminus [76] depending on the GPCR. The GPCRs are stabilised as dimers/oligomers via non-covalent interactions. Two modes of interaction have been described (**Figure 1-5**) A) Contact dimerisation in which the relevant helix (helices) from one monomer contact(s) partner(s) in the other monomer stabilising the dimer pair; and B) Domain swapping in which several helices from each receptor are "swapped" in the dimer such that the functional monomer within the dimer contains helices contributed by both receptors [77]. As GPCRs are major pharmacological targets, the existence of dimers could have important implications for the development and screening of new drugs [78].

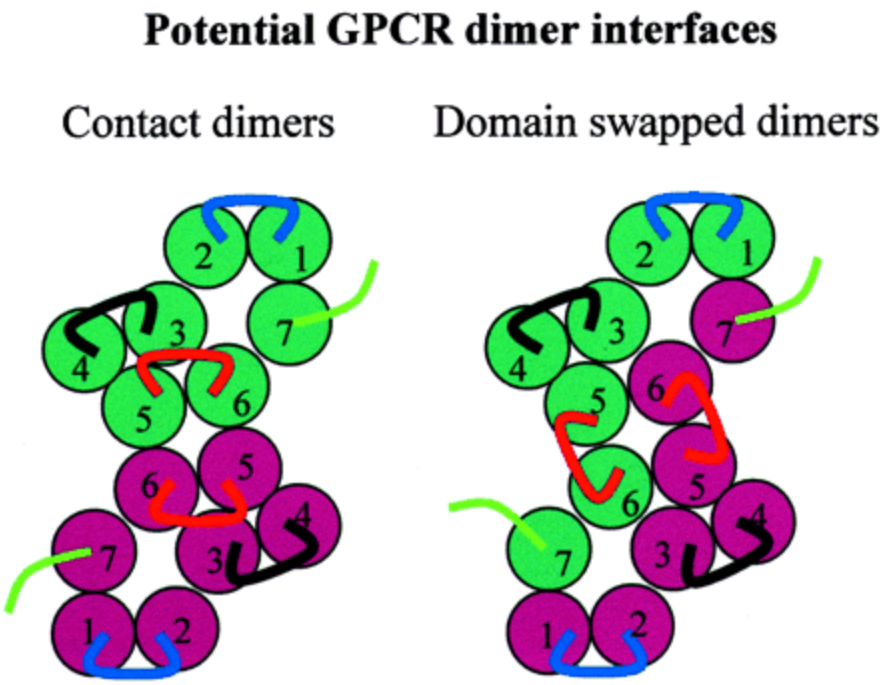

Figure 1-5: Potential GPCR dimer interfaces [77] (Image courtesy: GE Breitwieser et al., *Circulation Res.*; 2004;94;17-27).

1.5 GPCRs as Drug Targets

The GPCRs comprises of over 800 7TM receptors for hormones, neurotransmitters, chemokines and ions in both central and peripheral nervous system. Not surprisingly, GPCRs are important targets for therapeutics [79] especially class A GPCRs. They are universally considered to be challenging drug targets primarily due to lack of stability of the 7TM receptor structure and the lack of information on how small molecules bind to and impact function of the receptor. Although drugs in the clinic currently target only about 10% of the known GPCRs, these drugs represent about 45% of current pharmaceuticals available [80-82]. Researchers have been immensely presented with the discovery of novel drugs by elucidation of X-ray structures of different class A, class B, class C and frizzled GPCR structures in the recent years thereby giving the opportunity to use these structures for drug design purposes. Most especially, the very recent structures of non-class A GPCRs may serve as invaluable templates for ligand design for very difficult target classes [83]. Structure based drug design (SBDD) for GPCRs is currently limited to virtual screening (VS) or to modeling a ligand of interest into a public domain X-ray structure of a GPCR (or homology model) [84].

GPCRs regulate wide variety of human physiological processes including growth, metabolism and homeostasis. GPCRs serve as drug targets for the treatment of a multitude of conditions that includes hypertension, pain, ulcers, allergies, alcoholism, obesity, glaucoma, psychotic disorders and HIV. The routinely used drugs targeting GPCRs includes angiotensin receptor blockers (ARBs) for hypertension, bronchodilators for asthma, antihistamines for allergy and H2 blockers for acid reflux. Several worlds' top 10 best-selling drugs including Advair Diskus (fluticasone propionate and salmeterol) and Abilify (aripiprazole) target GPCR. **Table 1-2** and **Table 1-3** list the commonly used drugs that targets GPCRs and top selling drugs that targets GPCRs.

Table 1-2: Commonly used drugs targeting GPCRs.

GPCR Class	Drug(s)	Indication
Adrenoreceptor		
Alpha-1	alfuzosin, terazosin	Benign prostate hyperplasia, high blood pressure
Alpha-2	clonidine, bisoprolol, betaxolol	High blood pressure
Beta-1	metoprolol, atenolol	High blood pressure
Beta-2	albuterol, nadolol, penbutolol	Asthma
Acetylcholine Receptor		
M1, M2, M3, M4 and M5	tolterodine	Overactive bladder
M1, M2, M3, M4 and M5	atropine	Poisoning
M1	scopolamine	Motion sickness; diarrhea
Calcitonin	calcimar	Osteoporosis
Dopamine		
D2	metoclopramide	Heartburn
D2	haloperidol, olanzapine	Schizophrenia
D2	ropinirole, pramipexole	Parkinson's disease; Restless legs syndrome
Histamine		
H1	loratadine, cetirizine	Allergies
H1	demenhydrinate	Motion sickness
H2	cimetidine, ranitidine	Ulcers/heartburn
5-HT (serotonin)		
5-HT1B	trazodone	Anxiety; depression
5-HT1D	sumatriptan	Migraine headaches
GLP-1	exenatide	Type-2 diabetes

Opioid		
Mu	fentanyl, codein, meperidine	Pain
Mu/kappa	oxycodone	Pain
CysLT1	montelukast	Asthma
Prostaglandin E2 receptors	misoprostol	Gastric ulcers

Table 1-3: Top selling drugs that target GPCRs.

Trade name	**Generic name**	**Indication**
Plavix	clopidogrel	anti-clotting
Abilify	aripiprazole	schizophrenia, bipolar disorders, depression
Seroquel	Quetiapine	bipolar disorders, neuro-degenerative disorders
Singulair	Montelukast	asthma
Zyprexa	olanzapine	schizophrenia
Diovan	valsartan	blood pressure

1.6 GPCRs: Discovery and Structures

To understand the structure-function relationship of GPCRs regulating signal transduction and their prevalence as therapeutic targets, detailed atomic structures of GPCRs has been sought for long [85]. The structural determination of bovine rhodopsin in 2000 [15] was a remarkable advancement in drug discovery which paved the way for understanding the molecular mechanism of closely related GPCRs by homology modeling [86]. The second breakthrough appeared in 2007 with crystallisation of the first human β_2-AR [87] followed by structure elucidation of other class A members over the subsequent years.

The crystal structures of rhodopsin, β_2-AR share same overall design with a core structure composed of seven α-helical TM segments. The ligand binding cavity is formed by sidechains of amino acids from TM2-TM7. The ECL2 in β_2-AR is a β-hairpin shaped structure and forms a lid over the binding cavity. The disulphide bridge between ECL2 and TM3 is highly conserved among all class A GPCRs from rhodopsin to β-AR to A2A-R [88, 89]. In β-AR, ECL2 is partly folded as α-helix and is further stabilised by additional disulphide bond found only in β_1- and β_2-ARs [90]. A conserved aspartic acid residue in TM3 acts as an anchoring point for the positively charged amine group of the agonists in all the ARs.

The crystal structures are known to exist in active or inactive states. The active state is defined as the state in which agonists stabilise the active receptor conformation which leads to G protein activation. The inactive state is defined as the state where inverse agonists and antagonists favors an inactive receptor state that reduces G protein signaling [91]. Mostly, the crystal structures elucidated so far have mostly captured the inactive states with few active state structures crystallised with nanobodies and G protein fusions by X-ray crystallography [92] and NMR spectroscopy [93]. This advancement in visualisation of GPCRs and their signaling complexes is the result of the technological advances in methodological development such as protein engineering, new detergents, lipid cubic phasebased crystallisation and microfocus synchrotron beamlines [94].

GPCRs can thus be viewed as molecular engines that oscillate between the inactive and active states of which the inactive state being the most stable and the most highly represented. Agonist binding stabilises conformational states that bind and activate G proteins and other signaling molecules such as arrestins. The availability of multistate structural data facilitates the application of computational approaches to approximate active state binding pockets from

inactive state crystal structures enabling structure based docking studies to identify new agonists. The crystallisation of the active state of the β_2-AR was a remarkable milestone in understanding the activation mechanism and different conformational states of the receptor.

G proteins comprising of 4 subclasses of Gα-proteins ($G_{\alpha s}$, $G_{\alpha i/o}$, $G_{\alpha q/11}$ and $G_{\alpha 12/13}$), relay signals from GPCRs to a wide array of downstream effectors [95]. Gs has a higher affinity for GTP than GDP and the β_2-AR has an approximately 100-fold higher affinity for agonists in this agonist-β_2AR-Gs ternary complex [96]. Laurila et al., has shown that some specific antagonists like ARC239, chlorpromazine, prazosin, spiperone, spiroxatrine bind to the human α_{2A}-AR with 10- to 100-fold lower affinity than to the α_{2B}- and α_{2C}-ARs [97]. This study showed that the TM1 has indirect conformational effects related to the charge distribution or overall shape of the binding pocket. Also, TM1 does not participate in specific side-chain interactions with amino acids within the binding pocket of the receptor or with ligands bound therein.

The active state of GPCR is thus defined as a conformation that couples to and stabilises nucleotide-free G protein. This ternary crystal structure was solved by molecular replacement technique using Phaser [98]. The process of molecular replacement was carried out in the following order; the β and γ subunits from a G_i heterotrimer (PDB: 1GP2) [99], the G_s alpha RAS like domain (PDB: 1AZT) [100], the active-state β_2-AR (PDB: 3P0G), a β_2-AR binding nanobody (PDB: 3P0G) [101], T4 lysozyme (PDB: 2RH1) [102] and the $G_{s\alpha}$ helical domain (PDB: 1AZT). This milestone achieved followed the direct visualisation of a GPCR-β-arrestin complex (PDB: 4JQI, 5DGY) by electron microscopy [103, 104].

The rate of discovery of new GPCR crystal structures has accelerated in the recent years and has shed light on the differences in ligand binding patterns within class A GPCR [105-107]. Homology modeling is an automated comparative modeling of the three-dimensional (3D) protein structures from the experimentally determined structures of related family members as templates [108]. The possibility of building accurate class B and class C GPCR structures based on class A GPCR structures by homology modeling is ruled out due to structural differences. However, recent approaches in crystallisation techniques has ledto the elucidation of new class B and class C GPCR structures for drug discovery and rational drug design [109]. These structures provided unparalleled insights into the structural and functional diversity along with the class A GPCR structures like the molecular changes that the receptor undergo during activation, molecular signatures of the GPCR fold etc. **Table 1-4** lists the crystal structures resolved.

Table 1-4: Example of GPCR crystallised structures.

Protein Name	Ligand	PDB	Resolution (Å)	Year
Adenosine A2A receptor	CGS21680	4UG2	2.60	2015
	Ergotamine	4IB4	2.70	2013
	ZM241385	3EML	2.60	2008
	UK-432097	3QAK	2.71	2011
	ZM241385	4EIY	1.80	2012
Beta-1 Adrenergic receptor	Cyanopindolol	2VT4	2.70	2008
	Cyanopindolol	4BVN	2.10	2014
Beta-2 Adrenergic receptor	Carazolol	2RH1	2.40	2007
	Timolol	3D4S	2.80	2008
	Alprenolol	3NYA	3.16	2010
	ICI 118,551	3NY8	2.84	2010
	Compound 1	3NY9	2.84	2010
	Nanobody	3P0G	3.50	2011
CCR1 chemokine receptor		2LNL	NMR	2012
CCR5 chemokine receptor	vMIP-II	4RWS	3.10	2015
	CVX15	3OE0	2.90	2010
	IT1t	3ODU	2.50	2010
	IT1t (I222)	3OE6	3.20	2010
	IT1t (P1)	3OE8	3.10	2010
	IT1t (P1)	3OE9	3.10	2010
CCR5 Chemokine Receptor		4MBS	2.71	2013
D3 Dopamine receptor	Eticlopride	3PBL	2.89	2010
Bovine rhodopsin	Retinal	1U19	2.20	2004
Opioid receptor	Naltrindole	4N6H	1.80	2013
	peptide	4RWA	3.28	2015
Glucagon receptor (GLR)		4L6R	3.30	2013
Histamine receptor H1	Doxepin	3RZE	3.10	2011
Kappa opioid receptor		4RWA	3.28	2015

	JDTic	4DJH	2.90	2012
M2 Muscarinic receptor		3UON	3.00	2012
	Iperoxo	4MQS	3.50	2013
	Iperoxo and LY2119620	4MQT	3.70	2013
M3 Muscarinic receptor		4DAJ	3.40	2012
	Tiotropium	4U15	2.80	2014
Neurotensin receptor		4GRV	2.80	2012
	Lysozyme	4BWB	3.57	2014
Nociceptin opioid receptor (ORL-1)	Compound-24	4EA3	3.01	2012
Protease-activated receptor 1 (PAR1)		3VW7	2.20	2012
P2Y purinoceptor 12	AZD1283	4NTJ	2.62	2014
Sphingosine 1-phosphate receptor 1	ML056	3V2W	3.35	2012
		3V2Y	2.80	2012
5-hydroxytryptamine receptor 1B	dihydroergotamine	4IAQ	2.80	2013
	ergotamine	4IAR	2.70	2013
Smoothened Receptor	LY2940680	4N4W	2.80	2014
	Cyclopamine	4O9R	3.20	2014
Class B GPCR		4K5Y	2.98	2013
		4L6R	3.30	2016
Class C G protein-coupled metabotropic glutamate receptor		4OR2	2.80	2014
		4OO9	2.60	2014
Free fatty acid receptor 1 (FFAR1)	TAK-875	4PHU	2.33	2014
Sphingosine 1-phosphate receptor		3V2W	3.35	2012
		3V2Y	2.80	2012

1.7 GPCRs Modulators

Endogenous ligands bind to the orthosteric binding site in GPCRs which initiates the signaling process. However drugs targeting the orthosteric sites have limitations of selectivity, clinical efficacy and undesirable effects on receptor regulation [110, 111]. Allosteric modulators that bind at sites other than the orthosteric site provide opportunities to target topographically distinct sites present on many GPCRs [112, 113]. Targeting these sites with synthetic small molecules is now an emerging approach to develop receptor subtype selective leads as new therapeutics [113-115].

Such allosteric modulators have the potential to exhibit improved physicochemical profiles, selectivity, specificity, efficacy and safety (improved pharmacological profile). Studies on GPCR activation have shown existence of multiple active states which can be stabilised by different ligands targeting both orthosteric and allosteric sites at once [116-118]. Recent studies have demonstrated that linking orthosteric and allosteric ligands can yield bitopic ligands with improved subtype selectivity and affinity [117, 118].

Identification, development and discovery of these allosteric and bitopic ligands that can stabilise distinct conformational states may help us to better understand the role of distinct conformations in signaling and generating structure-function relationships [119]. To reduce the false-positive rates; state of the art computational techniques are useful in discovery of these new class of modulators [120]. Both allosteric and bitopic ligands possess advantages over orthosteric ligands, so their discovery is a new and novel approach in drug design.

1.8 Adrenergic Receptors

ARs belongs to class A GPCRs which respond to catecholamines, particularly NE and epinephrine (E) [121, 122]. They function primarily by increasing or decreasing the intracellular production of secondary messengers such as cAMP and/or IP_3/DAG [61]. Sometimes, the activated G protein itself operates on K^+ (potassium) or Ca^{2+} channels or increases prostaglandin production [123].

ARs have been classified into two types α and β-ARs on the basis of two distinct rank orders of potencies of adrenergic agonists [124] (**Table 1-5**). α and β-ARs share a high degree of amino acid identity between each other especially within the TMs forming the ligand binding pocket (68−77% identity for α_1-AR, 79−82% for α_2-AR and 63−73% for β-AR) [125].

Table 1-5: Classification of adrenergic receptors [126].

Parameters	**α**	**β**
Rank order of potency of Agonists	E ≥ NE > Isoprenaline (Iso)	Iso > E > NE
Antagonist	Phenoxybenzamine	Propranolol
Effector pathway	IP_3/DAG↑, cAMP↓, K^+ channel ↑	cAMP↑.Ca^{2+} channel ↑

1.8.1 α Adrenergic Receptors

The α-ARs upon activation triggers a complex range of autonomic responses [126]. Theyare subdivided into α_1 and α_2 subtypes based on the pharmacological action rather than anatomical location (**Table 1-6**). Molecular cloning has further identified three subtypes of α_1 receptors (α_{1A}, α_{1B} and α_{1D}) [127-129] and α_2 receptors (α_{2A}, α_{2B} and α_{2C}) [130, 131]. The evolutionary distance between the α_{1A}-AR and α_{1B}-AR is relatively nearer and their sequence similarity is relatively higher within the three α_1-AR subtypes compared to the evolutionary distance with the α_2-AR subtypes. α_{2A}-AR and α_{2C}-AR shows high sequence similarity within the α_2-AR subtypes [132].

Table 1-6: α-AR localisation, function, ligands and effector pathway influenced [133, 134].

Parameters	**α_1**	**α_2**
Location	Postjunctional on effector organs	Mostly prejunctional on nerve endings and postjunctional on blood vessels
Functions	Gland-secretion, Gut-contraction, Liver-glycogenolysis, Heart-arrhythmia	Transmitter release inhibition, Vasoconstriction, ↓ Central sympathetic flow, ↓ Insulin release
Selective agonist	Phenylephrine, Methoxamine	Clonidine
Selective Antagonist	Prazosin	Yohimbine
Effector pathway	IP_3/DAG ↑, Ca^{2+} ↑, Phospholipase A_2 ↑-PG release	cAMP ↓, K^+ channel ↑, IP_3/DAG ↑ Ca^{2+} channel ↑ or ↓,

1.8.1.1 α_1 Adrenergic Receptors

The α_1-ARs are activated by E released from the adrenal medulla and NE released from sympathetic nerve endings. They associate with the Gq heterotrimeric G proteins and triggers downstream signaling processes by increasing IP_3 production [135]. The subtypes mediate many effects of the sympathetic nervous system including different and sometimes opposing physiological effects for eg., the α_{1A}-AR promotes automaticity and arrhythmias during myocardial ischemia whereas the α_{1B}-AR activates Na^+/K^+ pump leading to cell hyperpolarisation thus decreasing the propensity for abnormal heart rhythms [135, 136].

There are many drugs available in the market which exerts their effects through α_1-ARs but they are not subtype specific and selective. Non-selective α_1-AR agonists and antagonists have been used for a long time for the treatment of various diseases like controlling the cardiovascular, respiratory and neuronal functions, digestion, pupil dilation and contraction, energetic metabolism and endocrinal functions. The lack of information about the structure of the receptors has limited the development of subtype-selective compounds and this in turn has hindered our

understanding of the roles of each subtype (α_{1A}, α_{1B} and α_{1D}) in physiology and disease [137]. The subtype differences observed because of sequence differences in the subtypes are mainly due to non-conserved residues in the TM spanning domain. However, there are only few subtype-selective drugs available that can differentiate between the subtypes with ≥100 fold affinity [138-140].

Because α_1-AR crystal structure has not been defined experimentally, protein structure prediction using different methods like *de novo* or *ab initio* modeling [141] and comparative modeling (such as threading and homology modeling) can be used to overcome these limitations [142, 143]. To design selective drugs, an understanding of subtype differences in the ligand binding pockets and an insight into the architecture of α_1-ARs would be invaluable. Therefore, molecular modeling studies may provide some insights into the structural requirements of receptor binding which may be of great value to discover new and more selective compounds.

The homology models of the α-ARs [144] and ligand docking has been described by many research groups using low resolution cryo-electron microscope [145] and X-ray structure [146] of bacteriorhodopsin as templates [147]. Since bacteriorhodpsin is not a GPCR, significantly improved bovine rhodopsin (BRh) based homology models were developed [15]. A combination of molecular modeling methods and experimental data has provided useful insights into the process of ligand binding and the superiority of BRh based model to study human ARs [148, 149].However, BRh shares only ~22% sequence identity with α_1-ARs [150] which pose limitations but since the overall structure is conserved (7TMs), it is still useful and sufficient to generate predictive models.

In 2007, the first human GPCR crystal structure of β_2-AR [102] was resolved by Brian Kobilka's group. Hence, it is advisable to use β_2-AR for homology model building of α_1-AR due to the close evolutionary relationship between the two receptors and the higher resolution crystal structure as β_2-AR shares a total degree of sequence identity (~35% with α_1-AR and ~40% in the TM helical regions) which are more acceptable values for developing homology models.

Although the α_1-AR orthosteric binding pocket residuehave been defined mostly experimentally [138, 151, 152], key interactions between the receptor and ligand are expected to be similar to those of the β-ARs as both receptors are activated by the catecholamines, NE and E. Studies on the α_1-AR have shown key points of interaction to occur between Asp125 in the TM3 with that of the protonated amine of the agonists, and between two serine residues Ser207 and Ser208 in

TM5 which form hydrogen-bonds with the meta- and parahydroxyl groups of the catechol ring moiety of ligands [138]. These critical binding contacts with the natural ligands are conserved within and between the α- and β-AR subtypes [153].

Putative agonist and antagonist binding sites have been proposed based on the mutagenesis studies for β_2-AR which commensurates with the agonist and antagonist bound active and inactive states [154, 155]. Experimental analysis found that Asp125, Asn344 and Ser207 play an important role in both agonist and antagonist binding. However, Ser208, Ser211 and Asn279 are involved in agonist binding in α_{1B}-AR [137]. The ligand binding residues proposed for α_1-AR are almost similar to β_2-AR (**Figure 1-6**) [156] due to the higher identity between residues in the TM region (**Figure 1-7**).

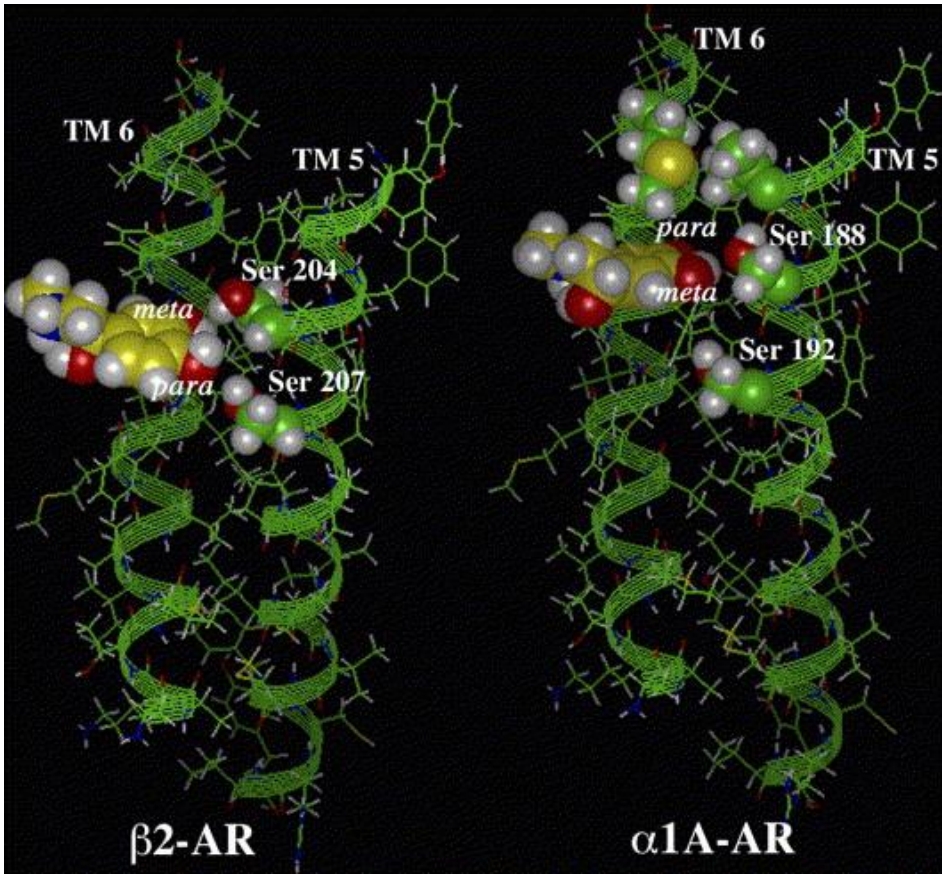

Figure 1-6: Serine–hydroxyl interactions between the β_2- and α_{1A}-AR [152] (Image Courtesy: Perez, D. M et al., *J. Biochem. Phamacol.*; 2007;73:1051-1062).

Mutagenesis studies on α- and β-ARs have shown that the protonated amine of catecholamines forms an electrostatic interaction with an aspartic acid residue on TM3 (Asp106) [157]. The catechol ring forms aromatic/hydrophobic interactions with phenylalanine residues in TM4 (Phe163) and TM5 (Phe187) while the catechol hydroxyl groups form hydrogen bonds with serine residues in TM5 (Ser188 with meta-hydroxyl and Ser192 with para-hydroxyl) [158].

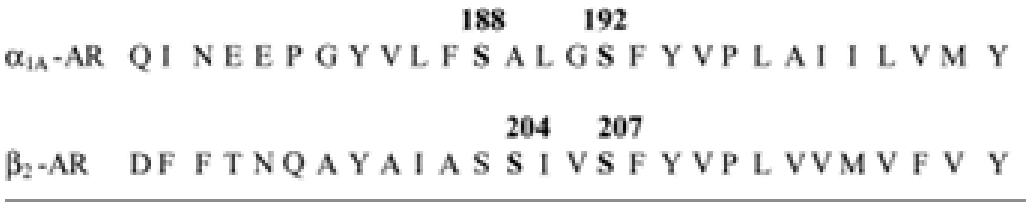

Figure 1-7: Sequence alignment between the α_{1A}-AR and the β_2-AR for the TM5 serine residues involved in hydrogen bonding with the catechol hydroxyls [152] (Image Courtesy: Perez, D. M. et al., *J. Biochem. Phamacol.*; 2007;73:1051-1062).

In contrast, extracellular site residues show higher diversity which might be helpful in ligand selectivity for GPCRs (**Figure 1-8**).

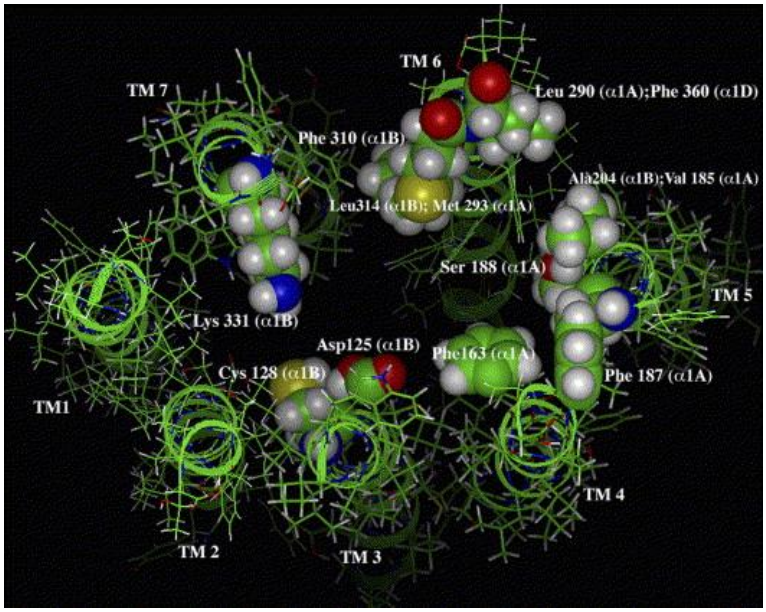

Figure 1-8: Residues involved in agonist binding in the α_1-ARs. The view is looking down upon the extracellular face of the binding pocket[152](Image Courtesy: Perez, D. M. et al., *J. Biochem. Phamacol.*; 2007;73:1051-1062).

Binding of agonist and antagonist to the receptor leads to receptor activation and inactivation in a multi-step process at the molecular level. The inactive state of rhodopsin like GPCRs is stabilised by salt bridge formation between TM3 and TM6 at the cytoplasmic end also known as "ionic lock" ($Arg^{3.50}$-$Glu^{6.30}$) (**Figure 1-9**) [123, 159]. Activation of rhodopsin like GPCRs suggests rotation of TM3 and TM6 helices. Furthermore, activation of ARs by agonist implicate rotamer toggle of various hydrophobic amino acids surrounding $Pro^{6.50}$ also known as the "rotamer toggle switch" [160].

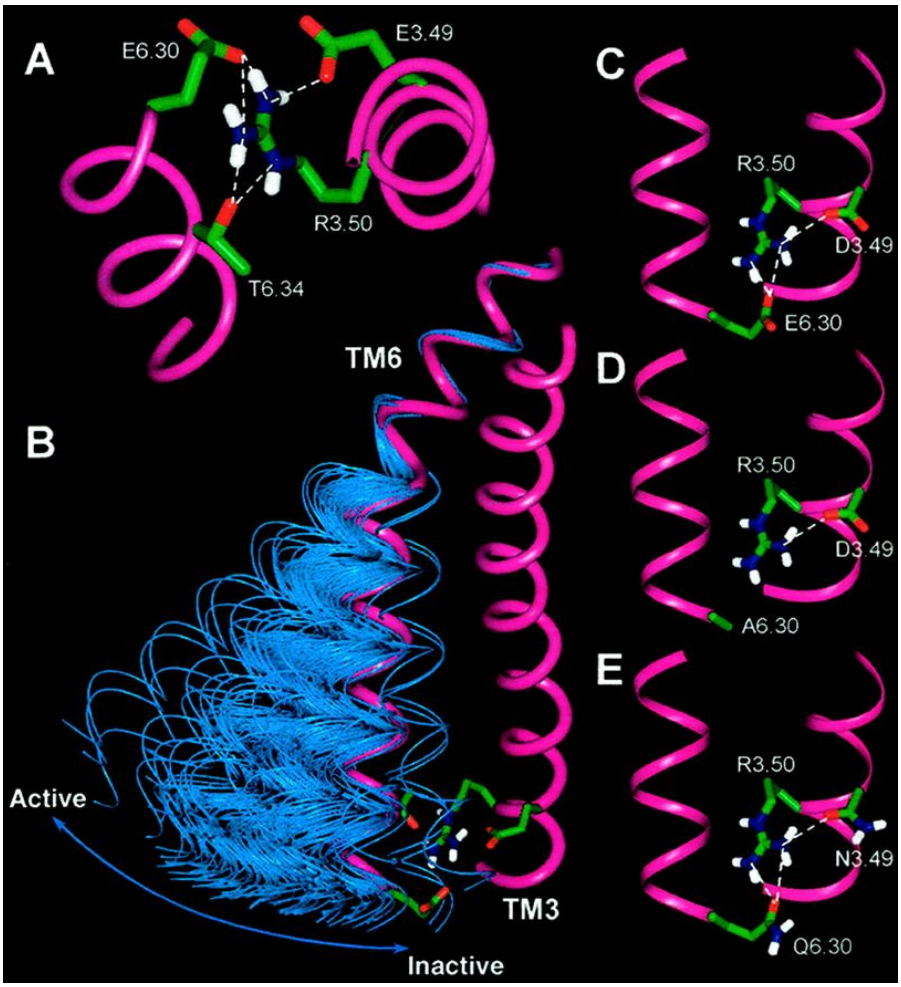

Figure 1-9: Molecular 3D representations of the interaction of TM3 and TM6 at their cytoplasmic ends and the effects of 6.30 mutations [44] (Image Courtesy: Juan A. Ballesteros et al., *J. Biol. Chem*.; 2001;276:29171-29177).

Activation/inactivation mechanism is further influenced by the change in interaction pattern between the E(D)RY and NPxxY motifs respectively. Scheer *et al.*, suggested that the $Arg^{3.50}$ is constrained in a polar pocket formed by residues in TMs 1, 2, and 7 in the inactive state based on α_{1B}-ARsimulations [66]. Arginine shifts out of the polar pocket upon protonation of the adjacent $Asp^{3.49}$ leading to long range conformational changes. The conserved aspartic acid in TM2 ($Asp^{2.50}$, Asp79 in β_2-AR) was predicted to be the ionic counterpart of the arginine in the inactive state. Ballesteros *et al.*, proposed that the ionic counterpart of $Arg^{3.50}$ in the inactive state could be the adjacent $Asp^{3.49}$ and that in the active state $Asp^{3.49}$ is protonated and $Arg^{3.50}$ interacts instead with $Asp^{2.50}$ [161]. In the inactive state, $Arg^{3.50}$ not only interacts with $Asp^{3.49}$ but also with $Glu^{6.30}$ and this ionic interaction between the cytoplasmic ends of TM6 and TM3 is an ionic lock that maintains the receptor in the inactive state.

The binding mode of antagonists to α_1-AR is affected by mutations at Asn106. Two conserved phenylalanine residues on TM7; Phe308 and Phe312 are known to form π–π stacking interactions with almost all α_{1A}-AR antagonists [162]. Three set of consecutive residues on ECL 2; Gln177, Ile178 and Asn179 forms interaction with selective α_{1A}-AR antagonists (WB-4101 and phentolamine) [137].

1.8.2 β-Adrenergic Receptors

In contrast to α-ARs, β-ARs respond to circulating catecholamines that regulate heart functions [163]. Congestive heart failure is the condition associated with up- and down- regulation of the β-ARs by change in expression and functions [164]. Three β-AR subtypes (β_1, β_2 and β_3) have been classified pharmacologically at the molecular level. β_1- and β_2-AR share 54% homology, while β_3-AR shares 51% and 46% identity with β_1- and β_2-AR [165].

β-ARs activate the G_s protein which in turn activates adenylyl cyclase thereby increasing the concentration of intracellular cAMP which activates protein kinase A and phosphorylates cellular proteins [35, 166]. β-ARs are involved in many patho-physiological conditions like increased chronotropy and ionotropy in heart, increased renin secretion (β_1); Bronchodialation, uterine relaxation, hyperglycaemia and lipolysis in liver and vasoconstriction (β_2); and lipolysis and regulation of bodyweight (β_3) [167].

1.9 Adrenergic Modulators Classification

Broadly, adrenergic modulators can be classified into two groups (adrenergic agonists and adrenergic antagonists) based on their mode of action, pharmacological activity, selectivity for specific subtypes, chemically and level of therapeutic response.

1.9.1 Adrenergic Agonists

Adrenergic modulators are classified as agonists due to their ability of binding and activating the receptor that leads to downstream signaling process. These act on both α- and β-ARs [168] and their subtypes [3, 13, 166]. Adrenergic agonists are broadly classified based on their pharmacological activity and their ability to bind with the receptor as:

a) Direct acting- on each adrenoceptor and its subtypes;
b) Mixed acting- on both the adrenoceptor like ephedrine (α_1, α_2, β_1, β_2 and releasing agents) and
c) Indirect acting- by releasing agents such as amphetamine, tyramine; uptake inhibitors like cocaine; MOA inhibitors like selegiline [169] and COMT inhibitors like entacapone [170].

Direct acting could be selective; acting specifically on particular subtype and non-selective; acting on either subtypes [171].

Compounds which show selectivity for the α_{1A}-AR subtype include 5-methyl-urapidil, niguldipine, oxymetazoline, A-61603, SNAP5089, KMD-3213 and RS17053. Compounds selective for the α_{1B}-AR subtype include espisperone, respisperone, risperidone and the compound AH11110A. α_{1D}-AR subtype specific ligands include compounds BMY7378 and SKF105854. The following table provides few examples of adrenergic agonists (**Table 1-7)**:

Table 1-7: Examples of Adrenergic agonists.

Selective Agonists		**Non-Selective Agonists**	
α_1	Phenylephrine	α_1, α_2	Oxymetazoline
α_2	Clonidine	β_1, β_2	Isoproterenol
β_1	Dobutamine	$\alpha_1, \alpha_2, \beta_1, \beta_2$	Epinephrine
β_2	Terbutaline	$\alpha_1, \alpha_2, \beta_1$	Norepinephrine
β_3	BRL 37344, CGP 12177		

1.9.2 Adrenergic Antagonists

These modulators antagonise the receptor action of adrenaline and related drugs by blocking the receptor [172]. Adrenergic antagonists are competitive against either α- or β-ARs or both α- and β-ARs. Adrenergic antagonists are therefore classified as α adrenergic blocking drugs and β adrenergic blocking drugs.

1.9.2.1 α Adrenergic Blocking Drugs

α Adrenergic blocking drugs are chemically classified into two types as

a) Non-equilibrium (B-haloalkylamines: Phenoxybenzamine) or
b) Equilibrium type.

Equilibrium is further subdivided into three subtypes based on their subtype specificity and chemically as follows [173-175] (**Table 1-8**):

Table 1-8: Table listing α adrenergic blocking drugs.

α_1 Selective		Prazosin, Terazosin, Doxazosin, Tamsulosin
α_2 Selective		Yohimbine
Nonselective	Ergot Alkaloids	Ergotamine, Ergotoxine
	Hydrogenated Ergot Alkaloids	Dihydroergotamine, Dihydroergotoxine
	Imidazolines	Phentolamine
		Chlorpromazine

1.9.2.2 β Adrenergic Blocking Drugs

β adrenergic blocking drugs are classified as cardioselective (β_1) such as metoprolol, atenolol, acebutolol, bisoprolol and nonselective (β_1 and β_2) drugs. Nonselective β_1 and β_2 is further subdivided into three categories based on their intrinsic sympathomimetic activities and additional α blocking activity (**Table 1-9**) [176].

Table 1-9: Table listing β adrenergic blocking drugs.

With Intrinsic Sympathomimetic Activity	Propranolol, Sotalol, TImolol
Without Intrinsic Sympathomimetic Activity	Pindolol
Additional α Blocking Activity	Labetalol, Carvedilol

1.9.3 Therapeutic Classification of Adrenergic Drugs

Adrenergic drugs are also classified therapeutically [172] into various classes as summarised in **Table 1-10**:

Table 1-10: Table classifying adrenergic drugs based on their therapeutic action.

Pressure Agents	NE, Ephedrine, Dopamine, Phenylephrine, Methoxamine
Cardiac Stimulants	E, Dobutamine, Isoprenaline
Bronchodilators	Isoprenaline, Salbutamol, Salmeterol, Formoterol
Nasal Decongestants	Phenylephrine, Xylometazoline, Oxymetazoline, Naphazoline
CNS Stimulants	Amphetamine, Methamphetamine, Dezamphetamine
Anorectics	Fenfluramine, Sebutramine, Dexfluramine
Uterine relaxant and Vasodilators	Ritodrine, Isoxsuprine, Salbutamol, Terbutaline

1.10 α_1-AR in Health and Disease

α_1-ARs belongs to well-studied family of class A GPCRs that mediate smooth and cardiac muscle contraction and thus play important physiological roles in vasculature, prostate, heart, gut and gall bladder [177-180]. The α_1-AR expression is tissue specific with α_{1A}-AR mostly found in liver, heart and cerebral cortex; α_{1B}-AR mostly in liver, heart and cerebral cortex and α_{1D}-AR mostly in bladder along with prostate and blood vessels. α_1-ARs are also present in the brain and spinal cord [181] and are upregulated in nociceptors following chronic constriction of the sciatic nerve in rats [182]. Blood vessels are important targets for α_1-AR drugs. Given this broad distribution it is not surprising that α_1-AR antagonists are important for the treatment of hypertension and benign prostatic hyperplasia while α_1-AR agonists have potential in a range of other α_1-AR-related diseases including heart failure [183].

1.11 Homology Modeling of Membrane Proteins

The biochemical function of a protein at the molecular level can be inferred from its 3D structure [85]. However, the number of experimentally determined crystal structures is much less than the number of available GPCR protein sequences [184]. As of February 2018, the number of crystal structures deposited in the protein data bank [185] are 137,692, which is relatively very small when compared with more than 6 million sequences held in the uniprot knowledge database [186]. Homology modeling or comparative protein structure modeling is a tool to build the 3D structure of a protein from its amino acid sequence based on sequence similarity and alignment with a protein (template) whose crystal structure is known and deciphered [187].

De novo or *ab initio* methods have also been developed to determine 3D structures for a protein where a suitable template is not available or because of very low sequence identity between the template and target structure [86]. Although *de novo* or *ab initio* methods can be used without the need of a homologous template structure, it falls short in terms of accuracy when compared to comparative structures [184]. Therefore, homology modeling is the method of choice to build reliable 3D *in silico* models of a protein in all cases where template structures are known [188]. Homology models have many applications in VS, docking, designing site-directed mutagenesis experiments or in rationalising the effects of sequence variations [189].

Homology modeling generally consists of four steps.

1) Template identification for modeling the protein of interest.

2) Mapping corresponding residues of the target with the template by sequence alignment and sometimes manually.

3) 3D model generation and

4) Evaluation of quality of generated models [141, 190].

The smaller the root mean square deviation between template and target structure is, the better and more accurate is the model. Therefore, structures with greater than 50% sequence identity are considered reasonable while the structures with less than 30% sequence identity (twilight zone) are unreliable as the relationship between sequence and structure similarity gets increasingly dispersed [150].

The accuracy of the protein structure model is a crucial step in the whole process which depends on the evolutionary distance between the target and template structures [191]. Scoring functions such as statistical potential of mean force have been developed to estimate the overall accuracy

[192]. The stereo-chemical plausibility of the generated models can be assessed using the tools such as PROCHECK and WHATCHECK [193]. One way to improve accuracy is to subject the built homology models to MD simulations thereby improving their RMSD to the experimental structure [194].

This technique also comes with certain limitations as of availability of homologous templates [195] i.e., only regions of the protein corresponding to an identified template can be modeled accurately. Modeling oligomeric proteins or structural changes caused by insertion, deletion, mutation and fusion proteins cannot be modeled accurately by comparative modeling. There are many programs and online web servers available for homology modeling. SWISS-MODEL has been the first automated modeling server publicly available [188]. In the meantime, similar services have been developed by other groups, e.g., ModPipe, ESyPred3D, 3D-JIGSAW or M4T [196]. Programs such as Homology and WHAT-IF can be run locally on a computer. Commercial packages like Schrodinger and Discovery Studio also provide a range of modules like PRIME for effective homology modeling [197].

Homology models have demonstrated that their accuracy in building and predicting the 3D structures of proteins from their amino acid sequences is comparable to the structures obtained through X-ray crystallography [198]. Initially, GPCR models were based on the bacteriorhodopsin template [39]. Later on, crystal structure of BRh was used as a template for the homology modeling with the availability of experimental information and thus all efforts were based on this structure [15, 199]. Homology modeling with BRh had a limitation of availability of high resolution GPCR structures and showed a lower sequence identity of 21% and lower TM identity of 26% compared to α_1-ARs. Thereafter, homology modeling to derive structural models of class A GPCR was carried out based on the crystal structure of the human β_2-AR with high resolution and showed a sequence identity of 29 −31% and TM identity of 37 − 43% compared to α_1-ARs [200].

Jayaraman et al., performed homology modeling and docking studies of human α_2-AR subtypes based on crystal structure of human dopamine D3 receptor as it showed highest TM identity in comparison to available crystal structures [201]. These models were in accordance with the experimental findings and suggested role of important residues in binding and showed correct orientation of the conserved residues involved in binding.

In another study by Pedretti et al., homology model of α_{1A}-AR was constructed followed by molecular docking of endogenous agonist NE and antagonist WB-4101. The homology model was constructed by using rhodopsin structure (PDB: 1F88) as template. The results were in concordance with the mutagenesis data thereby confirming the approach used and identified key binding residues interacting with agonist and antagonist [202] (**Figure 1-10; Figure 1-11**).

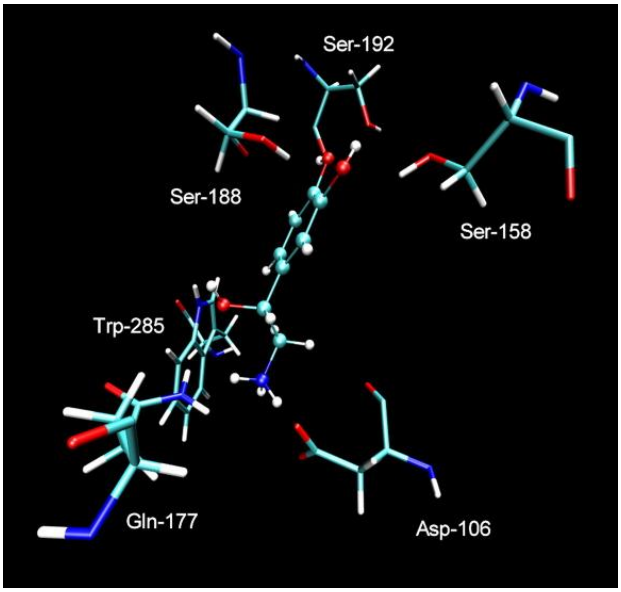

Figure 1-10: Main interactions in α_{1a}-AR–NE complex [202]. (Image Courtesy: Pedretti et al., *Biochem. Biophys. Res. Comm.*; 2004;319:493-500).

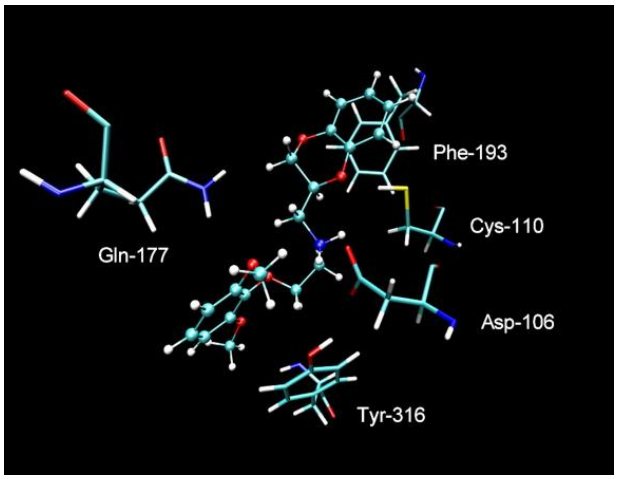

Figure 1-11: Main interactions in α_{1A}-AR–WB-4101 complex [202]. (Image Courtesy: Pedretti et al., *Biochem. Biophys. Res. Comm.*; 2004;319:493-500).

Halip LO et al, demonstrated key interactions between ligands and α_2-ARs and compared the predicted results with the experimental results by homology modeling and docking. The 3D homology model of three α_2-AR subtypes were constructed using X-ray structure of the β_2-AR (PDB: 2RH1) as template [142]. Although the squid rhodopsin has the highest sequence similarity with α_2-ARs, the β_2-AR structure (PDB code: 2RH1) was chosen as structural template because it belongs to class A GPCR and binds a biogenic amine like α_2-ARs. The study analysed the similarities and differences between the ECLs and binding sites of three α_2-AR subtypes. The results from this study could be used for VS of chemical databases to identify α_2-AR subtype specific ligands.

Lupei Du and Minyong Li modeled the interactions between α_1-ARs and their antagonists by use of ligand-based (pharmacophore identification and QSAR modeling) and structure-based (comparative modeling and molecular docking) approaches. These computational approaches helped to understand the structural basis of antagonist binding and the molecular basis of receptor activation [203].

1.12 Molecular Dynamics of Membrane Proteins

The structural determination of the high-resolution membrane proteins comparable to globular and soluble proteins lags with the realisation that the dynamics of these systems require large conformational sampling space over long time-scale [204]. Computational tools in particular MD have become indispensable and as an alternate source to improve our current mechanistic knowledge of membrane protein structure and dynamics [205].This limits our understanding of the physiological functions and the structure-function relationship of the GPCRs [206].

MD simulation is a technique which generates the atomic trajectories for a system of number of particles (N) for a specific interatomic potential with a certain initial condition (IC) and boundary condition (BC) [207]. It is a computer simulation of physical movements of atoms and molecules wherein they are allowed to interact for a given period of time which gives a view of motion of the atoms [208] (**Figure 1-12)**. The macroscopic properties of a system are explored through microscopic simulations such as calculating changes in the binding free energy of a drug candidate or to examine the energetics and mechanisms of conformational change. The connection between microscopic simulations and macroscopic properties is made via statistical mechanics [209].

MD simulations provide the means to solve the equation of motion of the particles and evaluate these mathematical formulas. These are being increasingly partnered with wet lab experiments because simulations can track system behavior across a vast spatiotemporal domain length that can be scaled up to thousands of Angstroms with atomic precision and timescales scaled to milliseconds [210].

The classical MD simulation method is based on Newton's second law or the equation of motion,

F=m*a, where

F is the force exerted on the particle,

m is its mass and

a is its acceleration [211].

From knowledge of the force on each atom, the acceleration of each atom can be determined in the system. Integration of the equations of motion then yields a trajectory which describes the positions, velocities and accelerations of the particles as they vary with time. From this trajectory, the average values of properties are determined. The method is deterministic; once the

positions and velocities of each atom are known, the state of the system can be predicted at any time in the future or the past.

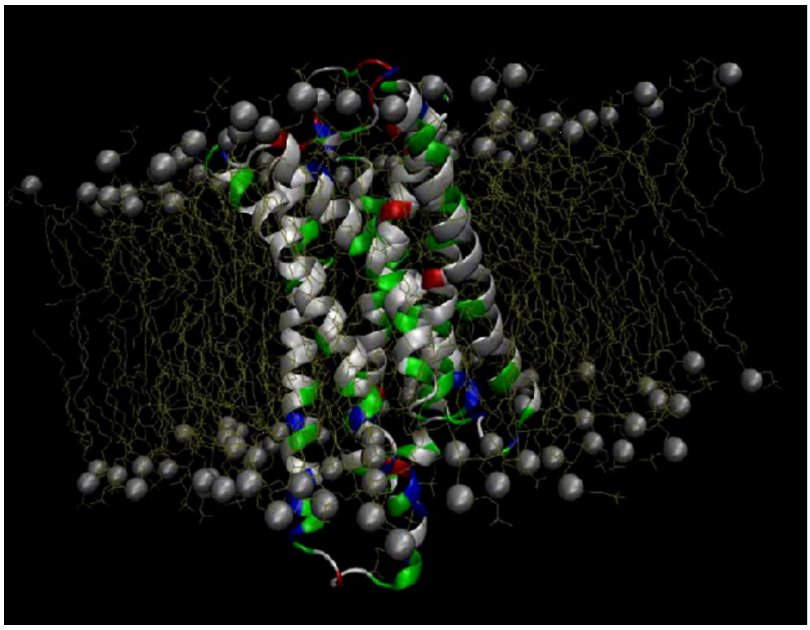

Figure 1-12: A typical classical MD simulation system with protein embedded in lipid bilayers.

The biological systems studied using all-atom MD simulations can be very large comprising millions of atoms. MD simulations can be used for studying membrane proteins which present particular challenges for experimental methods like X-ray crystallography and NMR spectroscopy for receptor crystallization [210]. MD simulations have provided detailed information on the fluctuations and conformational changes of proteins and nucleic acids. These methods are now routinely used to investigate the structure, dynamics and thermodynamics of biological molecules and their complexes. They are also used in the determination of structures from X-ray crystallography and NMR experiments. The limitation of MD simulations is that it is time consuming and computationally expensive [212].

Many studies on membrane proteins, ion channels and transporters have appeared in the literature emphasising the role of MD simulations in activation and inactivation mechanism, flow of ions and other transporters through ion channels, egress route of agonist and antagonists from the binding cavity [213-215]. MD simulations have been successfully applied to study the GPCR functioning and activation mechanism [205, 216]. GPCRs bind with an array of ligands which promotes the receptor to active and inactive states. The binding of ligands to GPCRs is of crucial

importance in understanding the drug-binding pathways through MD simulations for rational drug design that identifies the important residues lining the pathway which could then be used for SBDD. Previous studies on the activation mechanism of β_1- and β_2-AR [217, 218], the process of ligand binding to the Src protein kinase [219], accelerated dynamics on M2 and M3 muscarinic receptors for enhanced sampling of the active states [220, 221] have shed light on the structure-function relationship thereby increasing our understanding of the rational drug design process [222]. The application of MD simulations to GPCRs is illustrated below in following examples.

Tikhonova IG. et al., demonstrated the role of biased agonists in the β_2-AR bound to the β-arrestin and the empty receptor to further characterise the receptor conformational changes caused by biased agonists with aMD simulations aMD [223]. aMD simulations captured the known microscopic characteristics of the inactive states such as the ionic lock and water clusters. Simulations with the G protein biased agonist salbutamol involved perturbations of the network of interactions within the NPxxY motif.

Sahane G. et al., provided molecular insights into the dynamics of pharmacogenetically important N terminal variants of the human β_2-AR. The N terminal region of the arginine variant showed greater dynamics compared to the Gly variant which lead to differential placement. Further, the position and dynamics of the N terminal region affects the ligand binding site accessibility. This study revealed the key differences between the variants providing a molecular framework towards understanding the variable drug response in asthma patients [224].

Nygaard R. et al., have shown evidence for conformational states which are not observed in crystal structures as well as substantial conformational heterogeneity in agonist- and inverse-agonist-bound preparations by NMR spectroscopy [41]. This study revealed that an agonist alone does not stabilise a fully active conformation suggesting that the conformational link between the agonist binding pocket and the G protein coupling surface is not rigid.

Chan H. C. S. et al, investigated the impact of ligands on β_2-AR through a total of 12*100ns MD simulations. This study generated the molecular fingerprints that exemplified propensities of protein-ligand interactions [225]. Further the ligands exhibited a distinct mode of interaction with TM5 and TM6 thereby altering the shape and eventually the state of the receptor. This study provided insightful prospectives into GPCR targeted structure based drug discoveries.

Deupi et al., has shown the use of steered molecular dynamics (SMD) simulation to describe in atomic detail the unbinding process of two inverse agonists which have been co-crystallised with β_1- and β_2-AR subtypes along four different channels [226]. These compounds access the orthosteric binding site of β-ARs from the extracellular water environment. This study also identified the presence of secondary binding sites located in the ECL2 and ECL3 and TM7 where ligands are transiently retained by electrostatic and van der Waals interactions.

Ab Initio modeling and MD Simulation was employed by De Benedetti. PG. et al., to build an activation model of the α_{1B}-AR [227]. A combined approach of MD simulation and mutagenesis was used to determine the structural and dynamic features characterising the inactive and active states of α_{1B}-AR.

Results from microsecond MD simulations and community network analysis of the β_2-AR-G_s complex with $G_{\alpha s}$ in the open and closed conformations revealed strong allosteric communication between the β_2-AR and $G_{\beta\gamma}$ mediated by $G_{\alpha s}$ in a study by Xianqiang S. et al [228]. Further the complex is stabilised differently in the open and closed conformations.

Spijker P. et al., predicted the 3D structure of the human β_2-AR and the binding site of several agonists and antagonists bound to β_2-AR [229]. The apo-β_2-AR shows less dynamic flexibility whereas the antagonist bound β_2-AR structure is quite rigid in the MD simulations. This MD validation for the structure predictions of GPCRs in explicit lipid and water environment suggested that these methods can be trusted for studying the activation mechanism and the design of subtype specific agonists and antagonists. This study identified that antagonist-protein simulations differ substantially from the dynamics of the apo-protein and of the agonist-β_2-AR systems.

1.13 Virtual Screening of Membrane Proteins

Drug discovery is a process of identification of initial hits that are optimised to improve the potency, selectivity, metabolic stability and oral bioavailability that led to potential leads as agonists, antagonists and inverse agonists [230]. This process of identification of initial hits in the drug discovery pipeline can be categorised into two main types; HTS and VS. HTS has a very low hit rate of 0.1% against one or few therapeutic targets [231] whereas VS has emerged as an important tool over HTS in terms of cost incurred in discovering new molecules which can therefore be implemented as the starting point in drug discovery campaigns. HTS is technology-driven and hampered by phenomena like limited solubility or aggregation while VS is knowledge-driven with a loophole to discriminate true hits from non-binders and this critically relies on the capacity of extracting knowledge from existing data [231].

The number of putative compounds with a molecular weight <500Da is estimated to be around 10^{200} of which approximately 10^{60} are assumed to be drug-like compounds [232]. A complete sampling of such a large chemical space is impossible. Therefore, it is assumed that molecules with similar structures and properties exhibit similar biological activity and that molecules being located closely together in chemical space tend to be functionally related. For screening such a large chemical space, techniques encompassing data mining, machine learning or physics-based methods are used for VS.

The process of VS can be classified into two types;

a) Classical VS in which one or more chemical database is screened for hits against a few specific targets. This screening is focused on specific regions of the chemical space encompassing a chemical moiety to be necessary for hits to form interactions with the amino acids in the proteins;

b) Inverse virtual screening is a process in which a large protein library is screened against one or few small molecules. This practice of inverse VS is uncommon (**Figure 1-13**).

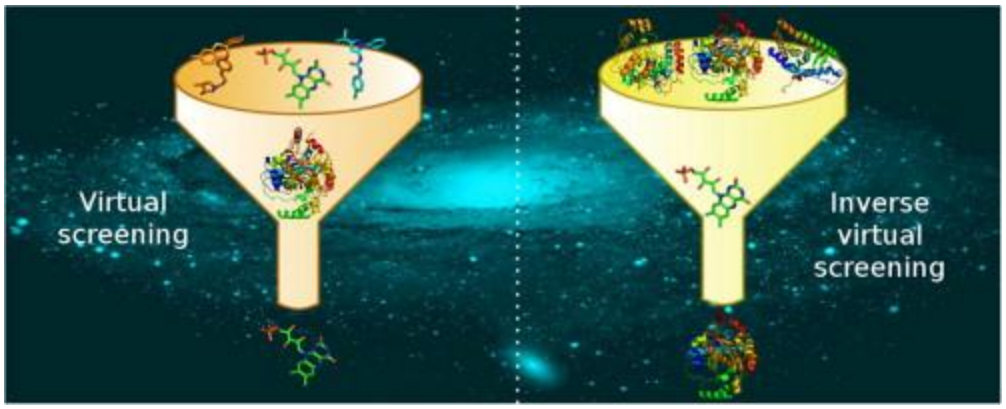

Figure 1-13: Classical and inverse VS flow [231] (Image Courtesy: Scapozza L. et al., *Methods*; 2015;71;44-57).

Ligand and structure-based VS approaches were developed to help identify small molecule ligands for proteins of interest (**Figure 1-14**). Structure-based VS utilise the structural information of the protein as target and include methods like molecular docking [233], structure based pharmacophores [234] and *de novo* design [235]. Ligand-based VS use the chemical structure of known bioactive molecules to identify new active molecules against a particular target [236]. These approaches are often combined in either hierarchical or parallel manner to take advantage of the strength and avoid the limitations associated with individual methods (**Figure 1-15)**.

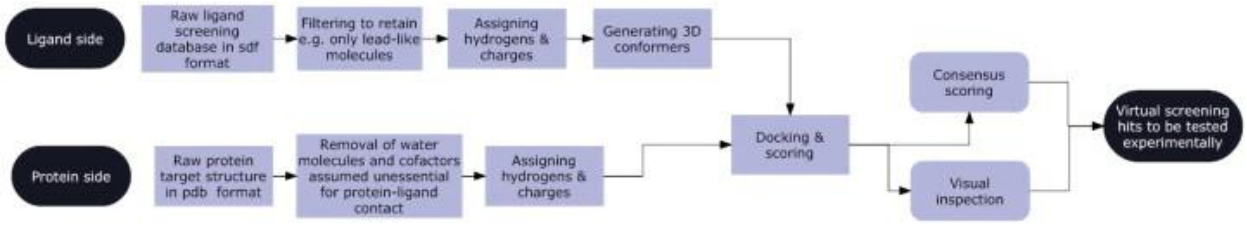

Figure 1-14: Flow-chart of a target-based virtual screening procedure and analysis [231] (Image Courtesy: ScapozzaL. et al., *Methods*; 2015;71;44-57).

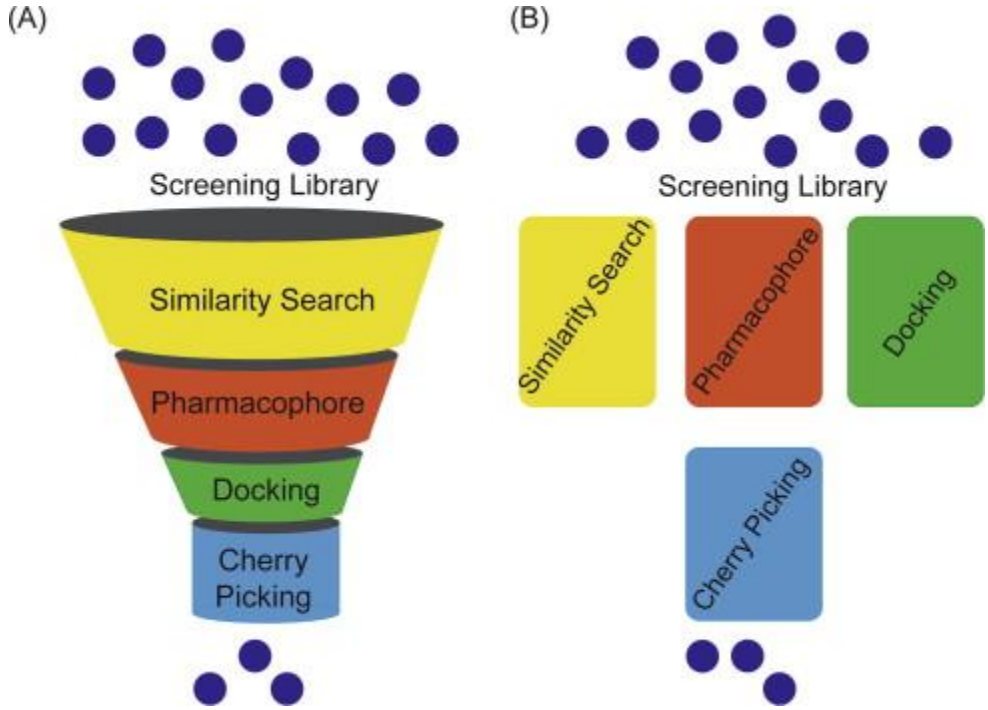

Figure 1-15: Integration of ligand and structure-based approaches. (A) Hierarchical virtual screening, (B) Parallel virtual screening (PVS) [230] (Image Courtesy: Kumar A. et al., *Methods*; 2015;71;26-37).

In hierarchical VS, several filters using ligand and structure-based approaches are sequentially applied to reduce a large screening library to a number small enough for experimental testing. Some of the VS studies are discussed to demonstrate the successful application of VS in small molecule drug discovery.

Chris de Graaf and Didier Rognan used selective structure-based VS to retrieve full and partial agonists of the β_2-AR. In this study, the X-ray structure of the ground state receptor could not distinguish true ligands with different functional effects thereby modifying this structure to reflect early conformational events in receptor activation that led to a receptor model which was able to selectively retrieve full and partial agonists by structure-based VS [237].

Chris de Graaf et al., described a VS method that combines energy based docking scoring function with a molecular interaction fingerprint (IFP) to identify new ligands based on GPCR crystal structures. This approach resulted in the experimental validation of 53% of the β_2-AR and 73% of the histamine receptor hits with up to nanomolar affinities and potencies [238]. Costanzi S. et al., evaluated the applicability of ligand-based and structure-based models to quantitative affinity predictions and VS for ligands of the β_2-AR [239].

Saxena A.K. described the hierarchical VS (HVS) study consisting of pharmacophore modeling, docking and VS to identify novel high affinity and selective β_3-AR agonists [240]. The focused virtual library was generated using the structure-based insights gained from the earlier reported comprehensive study focusing on the structural basis of β-AR subtype selectivity of representative agonists and antagonists. This study led to the identification of potential virtual leads as novel highaffinity and selective β_3-AR agonists.

1.14 Project Overview

GPCRs are the largest class of proteins. Despite the recent progress in evolution of large number of crystal structures relatively little is understood about the structure-function relationships and the correlation of conformational changes required for G protein activation and intracellular signaling. GPCR structure-function studies have mainly focused on the conserved 7TM residues with the role of residues lining the ECS being poorly defined despite their potential to allosterically modulate the GPCR signaling.

Kobilka group revealed the synergy between the stabilisation of the distinct ECS conformations and orthosteric binding site of the β_2-AR with the agonists, neutral antagonists and inverse agonists opening up new possibilities for allosteric drug targeting at β_2-AR [241]. Comparison of the orthosteric binding sites of the β_1- AR and β_2-AR revealed that 15 of 16 (94%) residues are identical [87, 242]. In contrast 22 of 39 residues (56%) differ in ECL2 and ECL3 although their backbone structure domain is similar (**Figure 1-16**). This difference in residues at the ECS could provide allosteric drug targeting sites specific to the β_1- and β_2-AR.

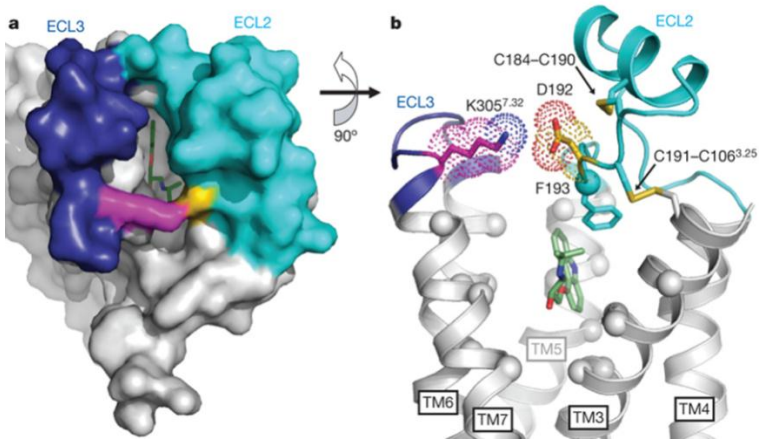

Figure 1-16: A) The ECS of β_2-AR showing ECL2, ECL3 and inverse agonist carazolol (green); B) Intramolecular and ligand binding interactions [243] (Image courtesy: Bokoch M. P. et al., *Nature;* 2010;463;108-112).

Phe193 in ECL2 forms a favorable edge-to-face interaction with the tricyclic aromatic ring of carazolol in the β_2-AR crystal structure attributed to conformational change by inverse agonist carazolol. MD simulations has shown that the Phe193 adopts the *trans* conformation pointing towards TM5 in the presence of carazolol but it has increased mobility and is able to assume multiple conformations in the alprenolol-bound state.

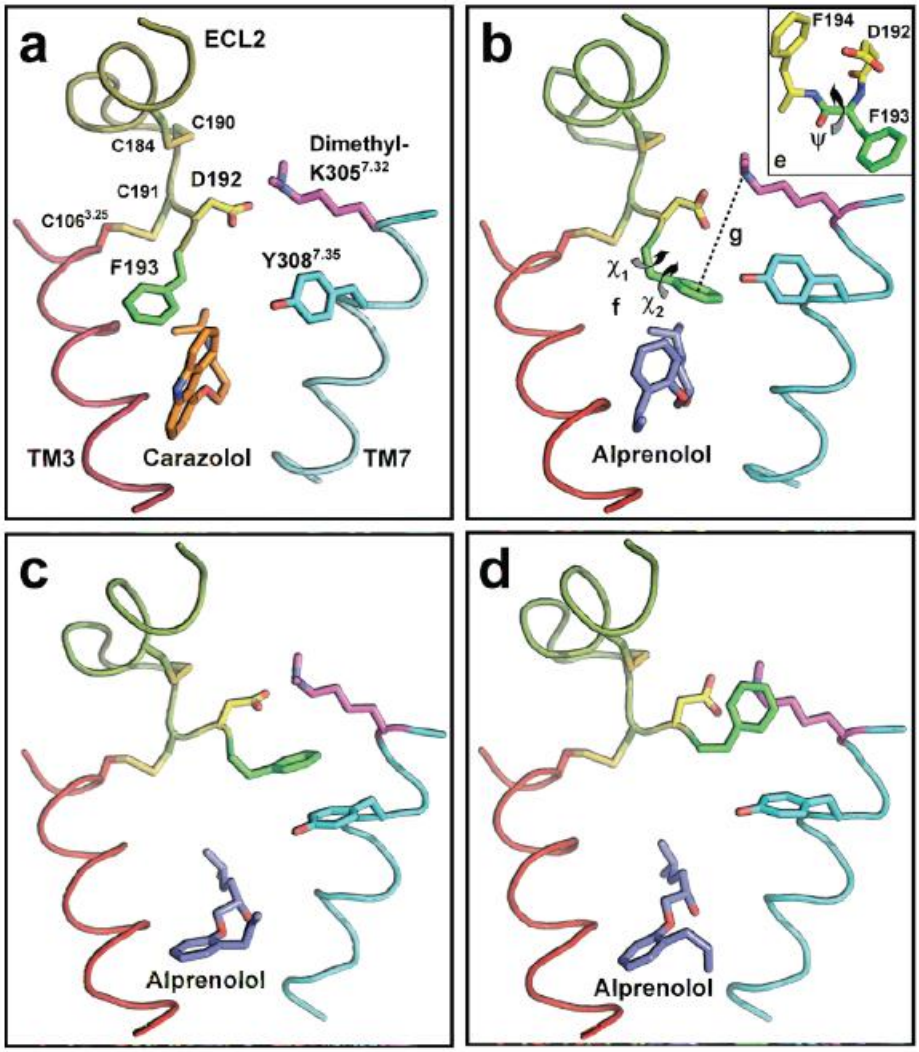

Figure 1-17: MD simulations of inverse agonist (carazolol) and neutral antagonist (alprenolol) in complex with the β_2-AR [243] (Image courtesy: Bokoch M. P. et al., *Nature*; 2010;463;108-112).

However, the agonists induced conformations differ from those that are induced by inverse agonists in that the Lys305–Asp192 salt bridge is weakened in the β_2-AR active state. Further, the extracellular end of TM6 and TM7 moves upon activation. The TM6 motion necessitates a lateral displacement of TM7 that reorients the Lys305 salt bridge in agreement with NMR spectroscopy (**Figure 1-18**). This study provided direct evidence for the three distinct conformations of the β_2-AR ECS; a) one for an unliganded receptor or a neutral antagonist; b) one for an inverse agonist and c) one for an agonist.

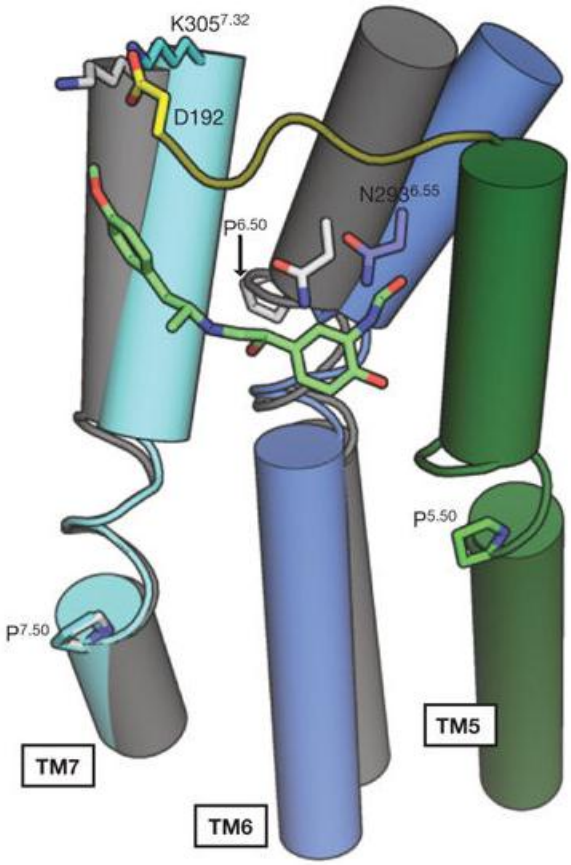

Figure 1-18: Model of β_2-AR activation by formoterol [243] (Image courtesy: Bokoch M. P. et al., *Nature*; 2010;463;108-112).

Ragnarsson L. et al., established the specific ECS molecular interactions between the refined NMR structure of ρ-TIA (a conopeptide from the piscivorous *Conus Tulipa*) and homology model of the α_{1B}-AR derived from the turkey β_1-AR [243, 244]. Fourteen residues were identified on the ECS of the α_{1B}-AR that influenced ρ-TIA binding. ρ-TIA binding was dominated by a salt bridge and cation-π interaction between Arg4-ρ-TIA and Asp327 and Phe330 respectively and a T-stacking-π interaction between Trp3-ρ-TIA and Phe330. Water-bridging hydrogen bonds between Asn2-ρ-TIA and Val197, Trp3-ρ-TIA and Ser318, and the positively charged N terminus and Glu186, were also identified (**Figure 1-19**). These interactions revealed that peptide binding to the ECS on TM6 and TM7 at the base of ECL3 are sufficient to allosterically inhibit agonist signaling at GPCR.

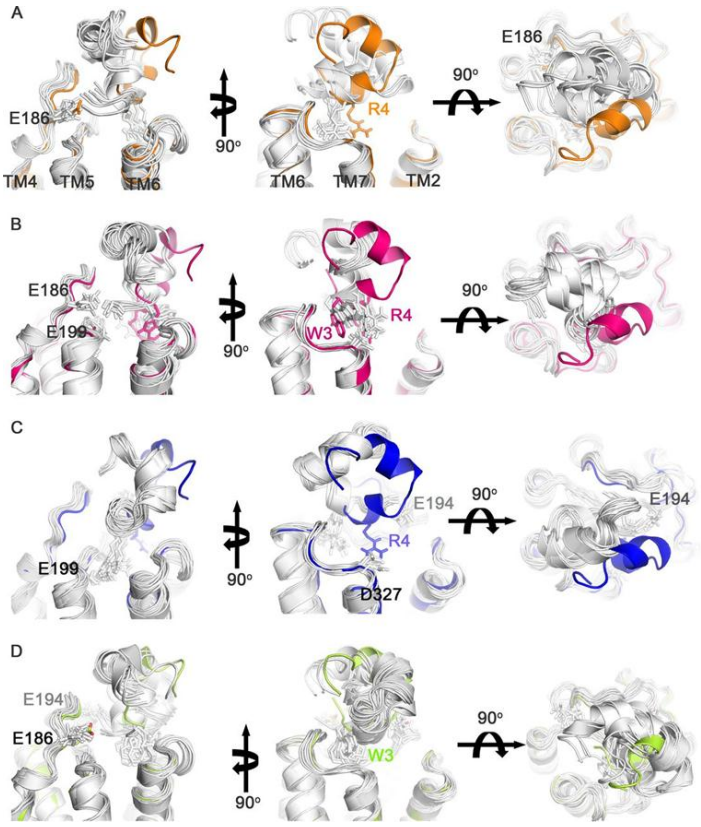

Figure 1-19: Docking of ρ-TIA analogs and ρ-TIA to the α_{1B}-AR and mutants [244] (Image courtesy: Ragnarsson. L. et al., *J. Biol. Chem.*; 2013;288:1814-1827).

In another study Ragnarsson L. et al., systematically mutated all ECS residues of the α_{1B}-AR to alanine (**Figure 1-20**). This study provided contribution of residues in ECL1 and ECL2 affecting NE potency and/or affinity at the α_{1B}-AR to function [140]. Half (24 of 48) of the ECS mutations significantly decreased NE potency in an inositol 1-phosphate assay. Most of the mutations reduced NE affinity (17) determined from [^{3}H] prazosin displacement studies whereas four mutations at the entrance to the NE binding pocket enhanced NE affinity.

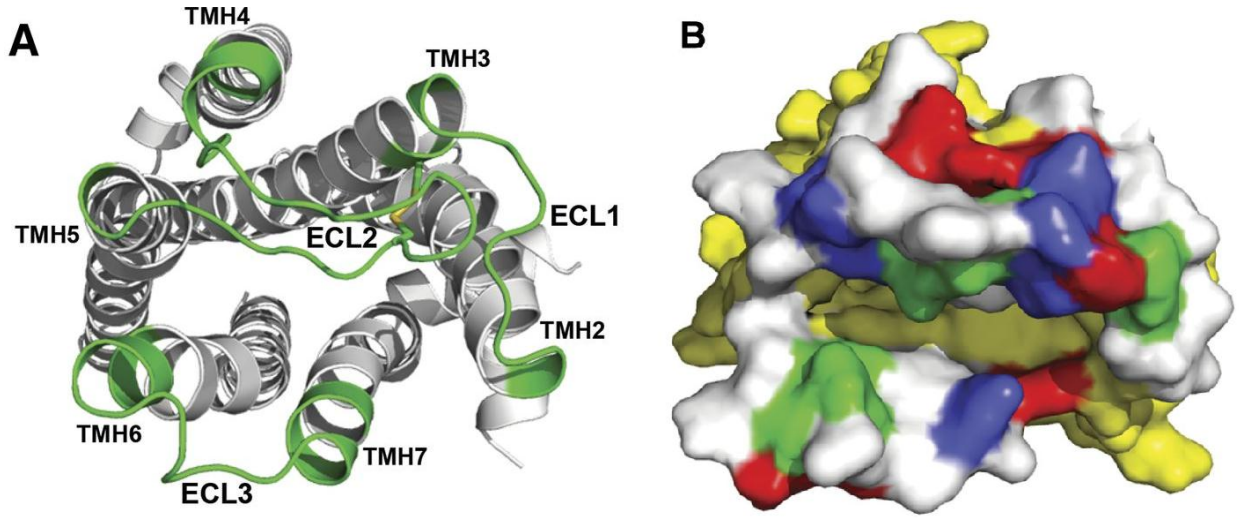

Figure 1-20: Structure and ECS of α_{1B}-AR. (A) Top view of α_{1B}-AR showing the backbone for mutated ECS in green, with the disulfide bond between ECL2 and TM3 in yellow. The cleft between ECL2 and TM6 and TM7, where agonists access the orthosteric binding site, is further illustrated in B. (B) Top view of α_{1B}-AR in the same orientation as (A), with the surface of ECS residues colored by type, with nonpolar side chains in white, polar side chains in green, positively charged side chains in red, and negatively charged side chains in blue. Non-ECS residues are shown in yellow [140] (Image courtesy: Ragnarsson L. et al., *J. Biol. Chem*.; 2015;878:121-129).

This study found that most of the residues lining ECL1 and ECL2 contributed significantly to α_{1B}-AR affinity and/or efficacy. The ECS residues either lined the entrance to the NE binding pocket or they lay outside the entrance which might modulate NE function at allosteric sites. In contrast to the majority of ECL1 and ECL2 mutations affecting α_{1B}-AR function, only L323A in ECL3 decreased NE affinity whereas the K324A and P326A mutants associated with TM7 significantly reduced NE potency.

The role of ECL3 in receptor activation is in agreement with results from a study on the adenosine A_1 receptor [245]. Residues lining the upper lip of the entrance to the NE binding pocket reduced NE affinity whereas mutant residues lining the lower lip mostly enhanced NE affinity. These residues directly influence the NE binding kinetics as these residues are present at the entrance to the NE binding pocket. This study provided insights into potency of NE that can be attributed to effects on NE affinity. This is due to the residues lining the NE entrance pocket present around ECL1 and ECL2 or from effects on signaling efficacy that arise mostly through buried or structurally significant residue.

The goal of this project is to extend these studies to define how the ECS conformation of the α_{1B}-AR changes during agonist activation. An understanding of ligand entry and exit mechanisms may help in receptor subtype selectivity of ligand binding and design of specific drugs with higher efficacy and longer duration of action. Two parallel approaches were initiated to define the role of residues lining the primary and secondary binding sites. Residues predicted from binding site server lining the orthosteric site were mutated experimentally for their role in signaling while the role of residues at secondary site were predicted from MD simulations.

Moreover, only a few specific agonists and antagonists are known till date for the above receptor. Therefore, a ligand basedor structure based approach will help in finding possible new leads. The outcomes of this research will help to understand the GPCR activation process. This research is expected to open the door to the rational development of new modulators that can recognise the ECS of GPCRs in distinct conformational states.

Here, we built the homology model of the α_{1B}-AR and carried out MD simulations with docked agonist (NE) to understand the activation process. Moreover, we were also interested in studying the putative ligand binding residues in the active site and the importance of the ECS in agonist binding. Previous studies on the β_2-AR have shown that the orthosteric binding site is accessed by the ligand through an opening on the ECS [246, 247]. Conversely, in opsin structures the same binding site is accessed through TM helices [248]. The ECL2 in opsin forms a β hairpin structure thus folding into the TM core and covering the ligand binding pocket. While in the β_2-AR structure, the same loop forms a two and a half turn short α helix slightly displaced away from the orthosteric binding site thereby providing a pathway and entrance to the binding pocket [249].

The crystal structure provides only a static view of the ligand-receptor bound state [41] but lacks the dynamics and information about the access and exit of ligands from the receptor during its activation and inactivation process [156]. In addition, there is a high sequence similarity among the three α_1 subtypes [250]; therefore a subtle difference in residues lining the orthosteric binding pocket may influence the access and exit routes and thereby play a vital role in the receptor subtype selectivity of ligand binding. Our MD results are in consonance with the known information regarding the activation and inactivation processes of the GPCR.

Further, we investigated the process of receptor activation by aMD simulations on the apo and NE-bound form of the built homology model. Similar to the approach, the residues known from

the experimental studies to be involved in receptor activation were mutated individually along with some double mutants to further characterise their role. Surprisingly, we found few single and double mutants which are of pivotal importance in activation process. At last, we decided to perform VS of the known modulator (NE) for α_1-AR to come out with new leads which could be subtype specific. This process led to identification of new leads which activated all the three α_1-AR subtypes confirming the approach of this process to identify new α_1-AR modulators.

1.15 Aim and Objectives

The aim of this project is to study the changes in ECS conformation of the α_{1B}-AR upon agonist binding and understand the activation process computationally and to use this information to rationally identify new modulators.

The specific outcomes to be achieved include:

1. To develop a new molecular model that describes the conformational changes during agonist activation of α_1-AR (Chapter 2).
2. To characterise the egress pathway of NE from the orthosteric binding site to identify additional contributions to NE affinity (Chapter 2).
3. To determine the effects of selected ECS residues on agonist binding and NE signaling (Chapter 2, 3).
4. To understand the activation process of the α_{1B}-AR in both apo and NE- bound form (Chapter 3).
5. Use these models to help identify new modulators acting at ECS conformations of the α_1-AR (Chapter 4).

1.16 References

1. Barton N, Blaney F, Garland S, Tehan B, Wall I: **Seven transmembrane G protein-coupled receptors: Insights for drug design from structure and modeling**. *Compmedchem II* 2007, **4**:669-701.
2. Fredriksson R, Lagerström MC, Lundin L-G, Schiöth HB: **The G protein-coupled receptors in the human genome form five main families. Phylogenetic analysis, paralogon groups and fingerprints**. *Molecular pharmacology* 2003, **63**(6):1256-1272.
3. Tuteja N: **Signaling through G protein-coupled receptors**. *Plant signaling & behavior* 2009, **4**(10):942-947.
4. Horn F, Bettler E, Oliveira L, Campagne F, Cohen FE, Vriend G: **GPCRDB information system for G protein-coupled receptors**. *Nucleic acids research* 2003, **31**(1):294-297.
5. Foord SM, Bonner TI, Neubig RR, Rosser EM, Pin JP, Davenport AP, Spedding M, Harmar AJ: **International Union of Pharmacology. XLVI. G protein-coupled receptor list**. *Pharmacological reviews* 2005, **57**(2):279-288.
6. Kroeze WK, Sheffler DJ, Roth BL: **G protein-coupled receptors at a glance**. *Journal of cell science* 2003, **116**(24):4867-4869.
7. **Fredricksson R,** Schiöth H**B:The repertoire of G protein-coupled receptors in fully sequenced genomes. *Molecular Pharmacology*2005, 67(5):1414-1425.**
8. Overington JP, Al-Lazikani B, Hopkins AL: **How many drug targets are there?** *Nature reviews drug discovery* 2006, **5**(12):993-996.
9. **Tyndall JD, Sandilva R: GPCR agonists and antagonists in the clinic. *Medicinal chemistry* 2005, 1(4):405-421.**
10. Civelli O: **GPCR deorphanisations: The novel, the known and the unexpected transmitters**. *Trends in pharmacological sciences* 2005, **26**(1):15-19.
11. Lappano R, Maggiolini M: **G protein-coupled receptors: Novel targets for drug discovery in cancer**. *Nature reviews drug discovery* 2011, **10**(1):47-60.
12. Whalen EJ, Rajagopal S, Lefkowitz RJ: **Therapeutic potential of β-arrestin and G protein-biased agonists**. *Trends in molecular medicine* 2011, **17**(3):126-139.
13. Neve K: **Functional selectivity of G protein-coupled receptor ligands: New opportunities for drug discovery**.*Chemmedchem* 2010, **5**(2):303-304.

14. Deisenhofer J, Epp O, Miki K, Huber R, Michel H: **X-ray structure analysis of a membrane protein complex. Electron density map at 3Å resolution and a model of the chromophores of the photosynthetic reaction center from rhodopseudomonas viridis**. *Journal of molecular biology* 1984, **180**(2):385-398.
15. Palczewski K, Kumasaka T, Hori T, Behnke CA, Motoshima H, Fox BA, Le Trong I, Teller DC, Okada T, Stenkamp RE: **Crystal structure of rhodopsin: A G protein-coupled receptor**. *Science* 2000, **289**(5480):739-745.
16. Warne T, Serrano-Vega MJ, Baker JG, Moukhametzianov R, Edwards PC, Henderson R, Leslie AG, Tate CG, Schertler GF: **Structure of a β_1-adrenergic G protein-coupled receptor**. *Nature* 2008, **454**(7203):486-491.
17. Jaakola VP, Griffith MT, Hanson MA, Cherezov V, Chien EYT, Lane JR, IJzerman AP, Stevens RC: **The 2.6 angstrom crystal structure of a human A2A adenosine receptor bound to an antagonist**. *Science* 2008, **322**(5905):1211-1217.
18. Wu B, Chien EYT, Mol CD, Fenalti G, Liu W, Katritch V, Abagyan R, Brooun A, Wells P, Bi FC: **Structures of the CXCR4 chemokine GPCR with small-molecule and cyclic peptide antagonists**. *Science* 2010, **330**(6007):1066-1071.
19. Chien EYT, Liu W, Zhao Q, Katritch V, Won Han G, Hanson MA, Shi L, Newman AH, Javitch JA, Cherezov V: **Structure of the human dopamine D3 receptor in complex with a D2/D3 selective antagonist**. *Science* 2010, **330**(6007):1091-1095.
20. Shimamura T, Shiroishi M, Weyand S, Tsujimoto H, Winter G, Katritch V, Abagyan R, Cherezov V, Liu W, Han GW: **Structure of the human histamine H1 receptor complex with doxepin**. *Nature* 2011, **475**(7354):65-70.
21. Deupi X: **Quantification of structural distortions in the transmembrane helices of GPCRs**. *Methods in molecular biology* 2012,**914**: 219-235.
22. Tobin AB, Butcher AJ, Kong KC: **Location, location, location… site-specific GPCR phosphorylation offers a mechanism for cell-type-specific signalling**. *Trends in pharmacological sciences* 2008, **29**(8):413-420.
23. Nygaard R, Frimurer TM, Holst B, Rosenkilde MM, Schwartz TW: **Ligand binding and micro-switches in 7TM receptor structures**. *Trends in pharmacological sciences* 2009, **30**(5):249-259.

24. Schiöth HB, Fredriksson R: **The GRAFS classification system of G protein-coupled receptors in comparative perspective**. *General and comparative endocrinology* 2005, **142**(1):94-101.

25. Davies MN, Secker A, Freitas AA, Mendao M, Timmis J, Flower DR: **On the hierarchical classification of G protein-coupled receptors**. *Bioinformatics* 2007, **23**(23):3113-3118.

26. Kolakowski Jr LF: **GCRDB: A G protein-coupled receptor database**. *Receptors & channels* 1993, **2**(1):1-7.

27. Wallin E, von Heijne G: **Properties of N terminal tails in G protein-coupled receptors: A statistical study**. *Protein engineering, design and selection* 1995, **8**(7):693-698.

28. Martin B, de Maturana RL, Brenneman R, Walent T, Mattson MP, Maudsley S: **Class II G protein-coupled receptors and their ligands in neuronal function and protection**. *Neuromolecular medicine*2005, **7**(1-2):3-36.

29. Cardoso JC, Pinto VC, Vieira FA, Clark MS, Power DM: **Evolution of secretin family GPCR members in the metazoa**. *BMC evolutionary biology* 2006, **6**(1):108-124.

30. Fredriksson R, Lagerström MC, Höglund PJ, Schiöth HB: **Novel human G protein-coupled receptors with long N-terminals containing GPS domains and Ser/Thr-rich regions**. *FEBS letters* 2002, **531**(3):407-414.

31. Nakagawa T, Sakurai T, Nishioka T, Touhara K: **Insect sex-pheromone signals mediated by specific combinations of olfactory receptors**. *Science* 2005, **307**(5715):1638-1642.

32. Prabhu Y, Eichinger L: **The Dictyostelium repertoire of seven transmembrane domain receptors**. *European journal of cell biology* 2006, **85**(9):937-946.

33. Suwa M: **Bioinformatics tools for predicting GPCR gene functions**. *Advances in experimental medicine and biology* 2014, **796**:205-224.

34. Deupi X, Li X-D, Schertler GF: **Ligands stabilize specific GPCR conformations: But how?** *Structure* 2012, **20**(8):1289-1290.

35. Dror RO, Pan AC, Arlow DH, Borhani DW, Maragakis P, Shan Y, Xu H, Shaw DE: **Pathway and mechanism of drug binding to G protein-coupled receptors**. *Proceedings of the national academy of sciences* 2011, **108**(32):13118-13123.

36. Sorkin A, von Zastrow M: **Signal transduction and endocytosis: Close encounters of many kinds**. *Nature reviews molecular cell biology* 2002, **3**(8):600-614.

37. Gether U, Kobilka BK: **G protein-coupled receptors II. Mechanism of agonist activation**. *Journal of biological chemistry* 1998, **273**(29):17979-17982.

38. Gether U: **Uncovering molecular mechanisms involved in activation of G protein-coupled receptors**. *Endocrine reviews* 2000, **21**(1):90-113.

39. Schertler GF, Villa C, Henderson R: **Projection structure of rhodopsin**. *Nature* 1993, **362**(6422):770-772.

40. Okada T, Ernst OP, Palczewski K, Hofmann KP: **Activation of rhodopsin: New insights from structural and biochemical studies**. *Trends in biochemical sciences* 2001, **26**(5):318-324.

41. Nygaard R, Zou Y, Dror RO, Mildorf TJ, Arlow DH, Manglik A, Pan AC, Liu CW, Fung JJ, Bokoch MP: **The dynamic process of β_2-adrenergic receptor activation**. *Cell* 2013, **152**(3):532-542.

42. Fanelli F, De Benedetti PG: **Inactive and active states and supramolecular organization of GPCRs: Insights from computational modeling**. *Journal of computer-aided molecular design* 2006, **20**(7-8):449-461.

43. Samama P, Bond RA, Rockman HA, Milano CA, Lefkowitz RJ: **Ligand-induced overexpression of a constitutively active β_2-adrenergic receptor: Pharmacological creation of a phenotype in transgenic mice**. *Proceedings of the national academy of sciences* 1997, **94**(1):137-141.

44. Ballesteros JA, Jensen AD, Liapakis G, Rasmussen SG, Shi L, Gether U, Javitch JA: **Activation of the β_2-adrenergic receptor involves disruption of an ionic lock between the cytoplasmic ends of transmembrane segments 3 and 6**. *Journal of biological chemistry* 2001, **276**(31):29171-29177.

45. Farrens DL, Altenbach C, Yang K, Hubbell WL, Khorana HG: **Requirement of rigid-body motion of transmembrane helices for light activation of rhodopsin**. *Science* 1996, **274**(5288):768-770.

46. Oldham WM, Hamm HE: **Heterotrimeric G protein activation by G protein-coupled receptors**. *Nature reviews molecular cell biology* 2008, **9**(1):60-71.

47. Kobilka BK: **G protein-coupled receptor structure and activation**. *Biochimica et biophysica acta (BBA)-Biomembranes* 2007, **1768**(4):794-807.

48. Lambright DG, Sondek J, Bohm A, Skiba NP, Hamm HE, Sigler PB: **The 2.0 Å crystal structure of a heterotrimeric G protein**. 1996,**379**;311-319.

49. Goetz A, Lanig H, Gmeiner P, Clark T: **Molecular dynamics simulations of the effect of the G protein and diffusible ligands on the β_2-adrenergic receptor**. *Journal of molecular biology* 2011, **414**(4):611-623.

50. Natochin M, Gasimov KG, Artemyev NO: **Inhibition of GDP/GTP exchange on Gα subunits by proteins containing G protein regulatory motifs**. *Biochemistry* 2001, **40**(17):5322-5328.

51. Kang DS, Tian X, Benovic JL: **Role of β-arrestins and arrestin domain-containing proteins in G protein-coupled receptor trafficking**. *Current opinion in cell biology* 2014, **27**:63-71.

52. Tian X, Kang DS, Benovic JL: **β-arrestins and G protein-coupled receptor trafficking**. *Methods in enzymology* 2013, **521**:91-108.

53. Goodman Jr OB, Krupnick JG, Santini F, Gurevich VV, Penn RB, Gagnon AW, Keen JH, Benovic JL: **β-arrestin acts as a clathrin adaptor in endocytosis of the β_2-adrenergic receptor**. *Nature* 1996, **383**(6599):447-449.

54. Shukla AK, Xiao K, Lefkowitz RJ: **Emerging paradigms of β-arrestin-dependent seven transmembrane receptor signaling**. *Trends in biochemical sciences* 2011, **36**(9):457-469.

55. Rosenbaum DM, Rasmussen SG, Kobilka BK: **The structure and function of G protein-coupled receptors**. *Nature* 2009, **459**(7245):356-363.

56. Pawson T, Scott JD: **Signaling through scaffold, anchoring and adaptor proteins**. *Science* 1997, **278**(5346):2075-2080.

57. Janetopoulos C, Jin T, Devreotes P: **Receptor-mediated activation of heterotrimeric G proteins in living cells**. *Science* 2001, **291**(5512):2408-2411.

58. Kristiansen K: **Molecular mechanisms of ligand binding, signaling and regulation within the superfamily of G protein-coupled receptors: Molecular modeling and mutagenesis approaches to receptor structure and function**. *Pharmacology & therapeutics* 2004, **103**(1):21-80.

59. Pierce KL, Premont RT, Lefkowitz RJ: **Seven-transmembrane receptors**. *Nature review molecular cell biology* 2002, **3**(9):639-650.

60. Strathmann MP, Simon MI: **G alpha 12 and G alpha 13 subunits define a fourth class of G protein alpha subunits**. *Proceedings of the national academy of sciences* 1991, **88**(13):5582-5586.

61. May DC, Ross EM, Gilman AG, Smigel MD: **Reconstitution of catecholamine-stimulated adenylate cyclase activity using three purified proteins**. *Journal of biological chemistry* 1985, **260**(29):15829-15833.

62. Camps M, Carozzi A, Schnabel P, Scheer A, Parker PJ, Gierschik P: **Isozyme-selective stimulation of phospholipase C-β_2 by G protein $\beta\gamma$-subunits**. *Nature* 1992, **360**(6405):684-686.

63. Suzuki N, Hajicek N, Kozasa T: **Regulation and physiological functions of G12/13-mediated signaling pathways**. *Neurosignals* 2009, **17**(1):55-70.

64. Leff P: **The two-state model of receptor activation**. *Trends in pharmacological sciences* 1995, **16**(3):89-97.

65. Samama P, Cotecchia S, Costa T, Lefkowitz R: **A mutation-induced activated state of the β_2-adrenergic receptor. Extending the ternary complex model**. *Journal of biological chemistry* 1993, **268**(7):4625-4636.

66. Scheer A, Fanelli F, Costa T, De Benedetti P, Cotecchia S: **Constitutively active mutants of the α_{1B}-adrenergic receptor: Role of highly conserved polar amino acids in receptor activation**. *The EMBO journal* 1996, **15**(14):3566-3578.

67. Schwartz TW, Gether U, Schambye HT, Hjorth SA: **Molecular mechanism of action of non-peptide ligands for peptide receptors**. *Current pharmaceutical design* 1995, **1**:325-342.

68. Cotecchia S: **The α_1-adrenergic receptors: Diversity of signaling networks and regulation**. *Journal of receptors and signal transduction* 2010, **30**(6):410-419.

69. Doze VA, Handel EM, Jensen KA, Darsie B, Luger EJ, Haselton JR, Talbot JN, Rorabaugh BR: **α_{1A}-and α_{1B}-adrenergic receptors differentially modulate antidepressant-like behavior in the mouse**. *Brain research* 2009, **1285**:148-157.

70. Gether U, Lowe J, Schwartz T: **Tachykinin non-peptide antagonists: Binding domain and molecular mode of action**. *Biochemical society transactions* 1995, **23**(1):96-102.

71. Sakmar TP: **Rhodopsin: A prototypical G protein-coupled receptor**. *Progress in nucleic acid research and molecular biology* 1997, **59**:1-34.

72. Gether U, Seifert R, Ballesteros JA, Sanders-Bush E, Weinstein H, Kobilka BK: **Structural instability of a constitutively active G protein-coupled receptor agonist-independent activation due to conformational flexibility**. *Journal of biological chemistry* 1997, **272**(5):2587-2590.

73. Kunishima N, Shimada Y, Tsuji Y, Sato T: **Structural basis of glutamate recognition by a dimeric metabotropic glutamate receptor**. *Nature* 2000, **407**(6807):971-977.

74. Overton MC, Blumer KJ: **The extracellular N-terminal domain and transmembrane domains 1 and 2 mediate oligomerization of a yeast G protein-coupled receptor**. *Journal of biological chemistry* 2002, **277**(44):41463-41472.

75. Ray K, Hauschild BC, Steinbach PJ, Goldsmith PK, Hauache O, Spiegel AM: **Identification of the cysteine residues in the amino-terminal extracellular domain of the human Ca^{2+} receptor critical for dimerization implications for function of monomeric Ca^{2+} receptor**. *Journal of biological chemistry* 1999, **274**(39):27642-27650.

76. Calver AR, Robbins MJ, Cosio C, Rice SQ, Babbs AJ, Hirst WD, Boyfield I, Wood MD, Russell RB, Price GW: **The C-terminal domains of the GABA-B receptor subunits mediate intracellular trafficking but are not required for receptor signaling**. *Journal of neuroscience* 2001, **21**(4):1203-1210.

77. Breitwieser GE: **G protein–coupled receptor oligomerisation**. *Circulation research* 2004, **94**(1):17-27.

78. Bouvier M: **Oligomerisation of G protein-coupled transmitter receptors**. *Nature reviews neuroscience* 2001, **2**(4):274-286.

79. Jacoby E, Bouhelal R, Gerspacher M, Seuwen K: **The 7 TM G protein-coupled receptor target family**. *Chemmedchem* 2006, **1**(8):760-782.

80. Drews J: **Drug discovery: A historical perspective**. *Science* 2000, **287**(5460):1960-1964.

81. Wise A, Gearing K, Rees S: **Target validation of G protein-coupled receptors**. *Drug discovery today* 2002, **7**(4):235-246.

82. Alexander SH, Attwood MM, Mathias RA, Schioth HB, Gloriam DE: **Trends in GPCR drug discovery: New agents, targets and indications** *Nature reviews drug discovery* 2017, **16**:829-842.

83. Tautermann CS: **GPCR structures in drug design, emerging opportunities with new structures**. *Bioorganic & medicinal chemistry letters* 2014, **24**(17):4073-4079.

84. Shoichet BK, Kobilka BK: **Structure-based drug screening for G protein-coupled receptors**. *Trends in pharmacological sciences* 2012, **33**(5):268-272.

85. Topiol S, Sabio M: **X-ray structure breakthroughs in the GPCR transmembrane region**. *Biochemical pharmacology* 2009, **78**(1):11-20.

86. Al-Lazikani B, Jung J, Xiang Z, Honig B: **Protein structure prediction**. *Current opinion in chemical biology* 2001, **5**(1):51-56.

87. Rasmussen SG, Choi H-J, Rosenbaum DM, Kobilka TS, Thian FS, Edwards PC, Burghammer M, Ratnala VR, Sanishvili R, Fischetti RF: **Crystal structure of the human β_2 adrenergic G protein-coupled receptor**. *Nature* 2007, **450**(7168):383-387.

88. Wheatley M, Wootten D, Conner MT, Simms J, Kendrick R, Logan R, Poyner DR, Barwell J: **Lifting the lid on GPCRs: The role of extracellular loops**. *British journal of pharmacology* 2012, **165**(6):1688-1703.

89. Cherezov V, Rosenbaum DM, Hanson MA, Rasmussen SG, Thian FS, Kobilka TS, Choi H-J, Kuhn P, Weis WI, Kobilka BK: **High-resolution crystal structure of an engineered human β_2-adrenergic G protein–coupled receptor**. *Science* 2007, **318**(5854):1258-1265.

90. Forfar R, Lu Z-L: **Role of the transmembrane domain 4/extracellular loop 2 junction of the human gonadotropin-releasing hormone receptor in ligand binding and receptor conformational selection**. *Journal of biological chemistry* 2011, **286**(40):34617-34626.

91. Azzi M, Charest PG, Angers S, Rousseau G, Kohout T, Bouvier M, Piñeyro G: **β-arrestin-mediated activation of MAPK by inverse agonists reveals distinct active conformations for G protein-coupled receptors**. *Proceedings of the national academy of sciences* 2003, **100**(20):11406-11411.

92. Wacker D, Fenalti G, Brown MA, Katritch V, Abagyan R, Cherezov V, Stevens RC: **Conserved binding mode of human β_2-adrenergic receptor inverse agonists and**

antagonist revealed by X-ray crystallography. *Journal of the american chemical society* 2010, **132**(33):11443-11445.

93. Gautier A, Mott HR, Bostock MJ, Kirkpatrick JP, Nietlispach D: **Structure determination of the seven-helix transmembrane receptor sensory rhodopsin II by solution NMR spectroscopy**. *Nature structural & molecular biology* 2010, **17**(6):768-774.

94. Ghosh E, Kumari P, Jaiman D, Shukla AK: **Methodological advances: The unsung heroes of the GPCR structural revolution**. *Nature reviews molecular cell biology* 2015, **16**(2):69-81.

95. Neer EJ, Clapham DE: **Roles of G protein subunits in transmembrane signaling**. *Nature* 1988, **333**(6169):129-134.

96. Rasmussen SG, DeVree BT, Zou Y, Kruse AC, Chung KY, Kobilka TS, Thian FS, Chae PS, Pardon E, Calinski D: **Crystal structure of the β_2-adrenergic receptor-Gs protein complex**. *Nature* 2011, **477**(7366):549-555.

97. Laurila J, Wissel G, Xhaard H, Ruuskanen J, Johnson M, Scheinin M: **Involvement of the first transmembrane segment of human α_2-adrenoceptors in the subtype-selective binding of chlorpromazine, spiperone and spiroxatrine**. *British journal of pharmacology* 2011, **164**(5):1558-1572.

98. McCoy AJ: **Solving structures of protein complexes by molecular replacement with Phaser**. *Acta crystallographica section D, biological crystallography* 2007, **63**(1):32-41.

99. Wall MA, Coleman DE, Lee E, Iñiguez-Lluhi JA, Posner BA, Gilman AG, Sprang SR: **The structure of the G protein heterotrimer $G_i\alpha_1\beta_1\gamma_2$**. *Cell* 1995, **83**(6):1047-1058.

100. Sunahara RK, Tesmer JJ, Gilman AG, Sprang SR: **Crystal structure of the adenylyl cyclase activator $G_{s\alpha}$**. *Science* 1997, **278**(5345):1943-1947.

101. Rasmussen SG, Choi H-J, Fung JJ, Pardon E, Casarosa P, Chae PS, DeVree BT, Rosenbaum DM, Thian FS, Kobilka TS: **Structure of a nanobody-stabilised active state of the β_2-adrenoceptor**. *Nature* 2011, **469**(7329):175-180.

102. Cherezov V, Rosenbaum DM, Hanson MA, Rasmussen SG, Thian FS, Kobilka TS, Choi H-J, Kuhn P, Weis WI, Kobilka BK: **High-resolution crystal structure of an engineered human β_2-adrenergic G protein–coupled receptor**. *Science* 2007, **318**(5854):1258-1265.

103. Shukla AK, Manglik A, Kruse AC, Xiao K, Reis RI, Tseng W-C, Staus DP, Hilger D, Uysal S, Huang L-Y: **Structure of active β-arrestin-1 bound to a G protein-coupled receptor phosphopeptide**. *Nature* 2013, **497**(7447):137-141.

104. Zhou X: **X-ray laser diffraction for structure determination of the rhodopsin-arrestin complex**. *Scientific data* 2016,**3**:160021-160034.

105. Douglas S, Wesley K, Bryan R: **G protein-coupled receptors at a glance**. *Journal of cell science* 2003, **116**:4867-4869.

106. Granier S, Kobilka B: **A new era of GPCR structural and chemical biology**. *Nature chemical biology* 2012, **8**(8):670-673.

107. Lebon G, Warne T, Tate CG: **Agonist-bound structures of G protein-coupled receptors**. *Current opinion in structural biology* 2012, **22**(4):482-490.

108. Bordoli L, Kiefer F, Arnold K, Benkert P, Battey J, Schwede T: **Protein structure homology modeling using SWISS-MODEL workspace**. *Nature protocols* 2009, **4**(1):1-13.

109. Klabunde T, Hessler G: **Drug design strategies for targeting G-protein-coupled receptors**. *Chembiochem* 2002, **3**(10):928-944.

110. Smith NJ, Bennett KA, Milligan G: **When simple agonism is not enough: Emerging modalities of GPCR ligands**. *Molecular and cellular endocrinology* 2011, **331**(2):241-247.

111. Violin JD, Crombie AL, Soergel DG, Lark MW: **Biased ligands at G protein-coupled receptors: Promise and progress**. *Trends in pharmacological sciences* 2014, **35**(7):308-316.

112. Lu S, Huang W, Zhang J: **Recent computational advances in the identification of allosteric sites in proteins**. *Drug discovery today* 2014, **19**(10):1595-1600.

113. Liu W, Chun E, Thompson AA, Chubukov P, Xu F, Katritch V, Han GW, Roth CB, Heitman LH, IJzerman AP: **Structural basis for allosteric regulation of GPCRs by sodium ions**. *Science* 2012, **337**(6091):232-236.

114. Milligan G, Smith NJ: **Allosteric modulation of heterodimeric G protein-coupled receptors**. *Trends in pharmacological sciences* 2007, **28**(12):615-620.

115. Wu B, Chien EY, Mol CD, Fenalti G, Liu W, Katritch V, Abagyan R, Brooun A, Wells P, Bi FC: **Structures of the CXCR4 chemokine GPCR with small-molecule and cyclic peptide antagonists**. *Science* 2010, **330**(6007):1066-1071.

116. Keov P, Sexton PM, Christopoulos A: **Allosteric modulation of G protein-coupled receptors: A pharmacological perspective**. *Neuropharmacology* 2011, **60**(1):24-35.

117. Valant C, Sexton PM, Christopoulos A: **Orthosteric/allosteric bitopic ligands**. *Molecular interventions* 2009, **9**(3):125-135.

118. Lane JR, Sexton PM, Christopoulos A: **Bridging the gap: Bitopic ligands of G protein-coupled receptors**. *Trends in pharmacological sciences* 2013, **34**(1):59-66.

119. Feng Z, Hu G, Ma S, Xie X-Q: **Computational advances for the development of allosteric modulators and bitopic ligands in G protein-coupled receptors**. *The AAPS journal* 2015, **17**(5):1080-1095.

120. Lane JR, Chubukov P, Liu W, Canals M, Cherezov V, Abagyan R, Stevens RC, Katritch V: **Structure-based ligand discovery targeting orthosteric and allosteric pockets of dopamine receptors**. *Molecular pharmacology* 2013, **84**(6):794-807.

121. Zhao MM, Hwa J, Perez DM: **Identification of critical extracellular loop residues involved in α_1-adrenergic receptor subtype-selective antagonist binding**. *Molecular pharmacology* 1996, **50**(5):1118-1126.

122. Weiner N: **Norepinephrine, epinephrine and the sympathomimetic amines**. *Goodman and Gilman's the pharmacological basis of therapeutics 7th ed newyork: MacMillan publishing company* 1985:145-180.

123. Rosenbaum DM, Rasmussen SG, Kobilka BK: **The structure and function of G protein-coupled receptors**. *Nature* 2009, **459**(7245):356-363.

124. Foord SM, Bonner TI, Neubig RR, Rosser EM, Pin J-P, Davenport AP, Spedding M, Harmar AJ: **International union of pharmacology. XLVI. G protein-coupled receptor list**. *Pharmacological reviews* 2005, **57**(2):279-288.

125. Berthelsen S, Pettinger WA: **A functional basis for classification of α-adrenergic receptors**. *Life sciences* 1977, **21**(5):595-606.

126. Furchgott RF: **The classification of adrenoceptors (adrenergic receptors). An evaluation from the standpoint of receptor theory**. *Catecholamines* 1972, **33**:283-335.

127. Cotecchia S, Schwinn DA, Randall RR, Lefkowitz RJ, Caron MG, Kobilka BK: **Molecular cloning and expression of the cDNA for the hamster α_1-adrenergic receptor**. *Proceedings of the national academy of sciences* 1988, **85**(19):7159-7163.

128. Schwinn DA, Lomasney JW, Lorenz W, Szklut PJ, Fremeau RT, Yang-Feng TL, Caron MG, Lefkowitz RJ, Cotecchia S: **Molecular cloning and expression of the cDNA for a novel α_1-adrenergic receptor subtype**. *Journal of biological chemistry* 1990, **265**(14):8183-8189.

129. Lomasney JW, Cotecchia S, Lorenz W, Leung WY, Schwinn DA, Yang-Feng TL, Brownstein M, Lefkowitz RJ, Caron MG: **Molecular cloning and expression of the cDNA for the α_{1A}-adrenergic receptor. The gene for which is located on human chromosome 5**. *Journal of biological chemistry* 1991, **266**(10):6365-6369.

130. Simonneaux V, Ebadi M, Bylund D: **Identification and characterisation of α_{2D}-adrenergic receptors in bovine pineal gland**. *Molecular pharmacology* 1991, **40**(2):235-241.

131. Kobilka B, Matsui H, Kobilka T, Yang-Feng T, Francke U, Caron M, Lefkowitz R, Regan J: **Cloning, sequencing and expression of the gene coding for the human platelet α_2-adrenergic receptor**. *Science* 1987, **238**(4827):650-656.

132. Yu H, Xu Y, Xiao Y, Li X: **The research on the relationship between adrenergic receptor subtypes**. *Third international conference on natural computation* 2007, 233-238.

133. Young WS, Kuhar MJ: **Noradrenergic α_1 and α_2 receptors: Light microscopic autoradiographic localization**. *Proceedings of the national academy of sciences* 1980, **77**(3):1696-1700.

134. Bylund D: **Subtypes of α_1-and α_2-adrenergic receptors**. *The FASEB journal* 1992, **6**(3):832-839.

135. Dorn GW, Brown JH: **Gq signaling in cardiac adaptation and maladaptation**. *Trends in cardiovascular medicine* 1999, **9**(1):26-34.

136. Molkentin JD, Dorn II GW: **Cytoplasmic signaling pathways that regulate cardiac hypertrophy**. *Annual review of physiology* 2001, **63**(1):391-426.

137. Zhao M-M, Hwa J, Perez DM: **Identification of critical extracellular loop residues involved in α_1-adrenergic receptor subtype-selective antagonist binding**. *Molecular pharmacology* 1996, **50**(5):1118-1126.

138. Hwa J, Graham RM, Perez DM: **Identification of critical determinants of α_1-adrenergic receptor subtype selective agonist binding**. *Journal of biological chemistry* 1995, **270**(39):23189-23195.

139. Waugh DJ, Gaivin RJ, Zuscik MJ, Gonzalez-Cabrera P, Ross SA, Yun J, Perez DM: **Phe-308 and Phe-312 in transmembrane domain 7 are major sites of α_1-adrenergic receptor antagonist binding imidazoline agonists bind like antagonists**. *Journal of biological chemistry* 2001, **276**(27):25366-25371.

140. Ragnarsson L, Andersson Å, Thomas WG, Lewis RJ: **Extracellular surface residues of the α_{1B}-adrenoceptor critical for G protein–coupled receptor function**. *Molecular pharmacology* 2015, **87**(1):121-129.

141. Mobarec JC, Sanchez R, Filizola M: **Modern homology modeling of G protein coupled receptors: Which structural template to use?** *Journal of medicinal chemistry* 2009, **52**(16):5207-5216.

142. Ostopovici-Halip L, Curpăn R, Mracec M, Bologa CG: **Structural determinants of the α_2-adrenoceptor subtype selectivity**. *Journal of molecular graphics and modeling* 2011, **29**(8):1030-1038.

143. Evers A, Klabunde T: **Structure-based drug discovery using GPCR homology modeling: Successful virtual screening for antagonists of the α_{1A}-adrenergic receptor**. *Journal of medicinal chemistry* 2005, **48**(4):1088-1097.

144. Carrieri A, Fano A: **The *in silico* insights of α-adrenergic receptors over the last decade: Methodological approaches and structural features of the 3D models**. *Current topics in medicinal chemistry* 2007, **7**(2):195-205.

145. Ruprecht JJ, Mielke T, Vogel R, Villa C, Schertler GF: **Electron crystallography reveals the structure of metarhodopsin I**. *The EMBO journal* 2004, **23**(18):3609-3620.

146. Okada T, Palczewski K: **Crystal structure of rhodopsin: Implications for vision and beyond**. *Current opinion in structural biology* 2001, **11**(4):420-426.

147. Archer E, Maigret B, Escrieut C, Pradayrol L, Fourmy D: **Rhodopsin crystal: New template yielding realistic models of G protein-coupled receptors?** *Trends in pharmacological sciences* 2003, **24**(1):36-40.

148. Teller DC, Okada T, Behnke CA, Palczewski K, Stenkamp RE: **Advances in determination of a high-resolution three-dimensional structure of rhodopsin, a model of G protein-coupled receptors (GPCRs)**. *Biochemistry* 2001, **40**(26):7761-7772.

149. Lavoie H, Gallant J, Grandbois M, Blaudez D, Desbat B, Boucher F, Salesse C: **The behavior of membrane proteins in monolayers at the gas–water interface: comparison between photosystem II, rhodopsin and bacteriorhodopsin**. *Materials science and engineering: C* 1999, **10**(1):147-154.

150. Rost B: **Twilight zone of protein sequence alignments**. *Protein engineering* 1999, **12**(2):85-94.

151. Piascik MT, Perez DM: **α_1-adrenergic receptors: New insights and directions**. *Journal of pharmacology and experimental therapeutics* 2001, **298**(2):403-410.

152. Perez DM: **Structure–function of α_1-adrenergic receptors**. *Biochemical pharmacology* 2007, **73**(8):1051-1062.

153. Audet M, Bouvier M: **Insights into signaling from the β_2-adrenergic receptor structure**. *Nature chemical biology* 2008, **4**(7):397-403.

154. Cavasotto CN, Phatak SS: **Homology modeling in drug discovery: Current trends and applications**. *Drug discovery today* 2009, **14**(13):676-683.

155. Costanzi S: **On the applicability of GPCR homology models to computer-aided drug discovery: A comparison between *in silico* and crystal structures of the β_2-adrenergic receptor**. *Journal of medicinal chemistry* 2008, **51**(10):2907-2914.

156. Wang T, Duan Y: **Ligand entry and exit pathways in the β_2-adrenergic receptor**. *Journal of molecular biology* 2009, **392**(4):1102-1115.

157. Porter JE, Hwa J, Perez DM: **Activation of the α_{1B}-adrenergic receptor is initiated by disruption of an interhelical salt bridge constraint**. *Journal of biological chemistry* 1996, **271**(45):28318-28323.

158. Hwa J, Perez D: **The unique nature of the serine residues involved in α_1-adrenergic receptor binding and activation**. *Journal of biolgical chemistry*1996, **271**:6322-6327.

159. Ballesteros J, Weinstein H: **Integrated methods for modeling G protein-coupled receptors**. *Methods neuroscience*1995, **25**:366-428.

160. Shi L, Liapakis G, Xu R, Guarnieri F, Ballesteros JA, Javitch JA: **β_2-adrenergic receptor activation modulation of the proline kink in transmembrane 6 by a rotamer toggle switch**. *Journal of biological chemistry* 2002, **277**(43):40989-40996.

161. Ballesteros J, Kitanovic S, Guarnieri F, Davies P, Fromme BJ, Konvicka K, Chi L, Millar RP, Davidson JS, Weinstein H: **Functional microdomains in G protein-coupled receptors the conserved arginine-cage motif in the gonadotropin-releasing hormone receptor**. *Journal of biological chemistry* 1998, **273**(17):10445-10453.

162. Waugh DJ, Gaivin RJ, Zuscik MJ, Gonzalez-Cabrera P, Ross SA, Yun J, Perez DM: **Phe308 and Phe312 in TM VII are a major site of α_1-adrenergic receptor antagonist binding: Imidazoline agonists bind like antagonists**. *Journal of biological chemistry* 2001.**276**:25366-25371.

163. Wallukat G: **The β-adrenergic receptors**. *Herz* 2002, **27**(7):683-690.

164. Post SR, Hammond HK, Insel PA: **β-adrenergic receptors and receptor signaling in heart failure**. *Annual review of pharmacology and toxicology* 1999, **39**(1):343-360.

165. Skeberdis VA: **Structure and function of β_3-adrenergic receptors**. *Medicina (kaunas, lithuania)* 2003, **40**(5):407-413.

166. Johnson M: **Molecular mechanisms of β_2-adrenergic receptor function, response and regulation**. *Journal of allergy and clinical immunology* 2006, **117**(1):18-24.

167. Wachter SB, Gilbert EM: **β-adrenergic receptors from their discovery and characterisation through their manipulation to beneficial clinical application**. *Cardiology* 2012, **122**(2):104-112.

168. Furchgott RF: **The pharmacological differentiation of adrenergic receptors**. *Annals of the newyork academy of sciences* 1967, **139**(3):553-570.

169. Schubert B, VanDongen AM, Kirsch GE, Brown AM: **β-adrenergic inhibition of cardiac sodium channels by dual G protein pathways**. *Science* 1989, **245**(4917):516-519.

170. Jordan J, Lipp A, Tank J, Schröder C, Stoffels M, Franke G, Diedrich A, Arnold G, Goldstein DS, Sharma AM: **Catechol-o-methyltransferase and blood pressure in humans**. *Circulation* 2002, **106**(4):460-465.

171. Weiland GA, Minneman KP, Molinoff PB: **Fundamental difference between the molecular interactions of agonists and antagonists with the β-adrenergic receptor**. *Nature* 1979, **281**(5727):114-117.

172. Westfall TC, Westfall DP: **Adrenergic agonists and antagonists**. *Goodman and Gilman's the pharmacological basis of therapeutics, 11th ed edited by Brunton LL, Lazo JS, Parker KL newyork, McGraw-Hill* 2006:237-315.

173. Kobinger W: **Central α-adrenergic systems as targets for hypotensive drugs**. *Reviews of physiology, biochemistry and pharmacology* 1978, **81**:39-100.

174. Foye WO, Lemke TL, Williams DA: **Foye's principles of medicinal chemistry**: Lippincott Williams & Wilkins; 2008.

175. Tripathi K: **Essentials of medical pharmacology**: JP Medical Ltd; 2013.

176. Mehvar R, Brocks DR: **Stereospecific pharmacokinetics and pharmacodynamics of beta-adrenergic blockers in humans**. *Journal of pharmacy & pharmaceutical sciences* 2001,**4**(2):185-200.

177. Andersson KE, Gratzke C: **Pharmacology of α_1-adrenoceptor antagonists in the lower urinary tract and central nervous system**. *Nature clinical practice urology* 2007, **4**(7):368-378.

178. Finch AM, Graham RM: **The $\alpha_{(1D)}$-adrenergic receptor: Cinderella or ugly stepsister**. *Molecular pharmacology*2006, **69**(1):1-4.

179. Graham RM, Perez DM, Hwa J, Piascik MT: **α_1-adrenergic receptor subtypes. Molecular structure, function and signaling**. *Circulation research* 1996, **78**(5):737-749.

180. Woodcock EA, Du XJ, Reichelt ME, Graham RM: **Cardiac α_1-adrenergic drive in pathological remodelling**. *Cardiovascular research* 2008, **77**(3):452-462.

181. Michelotti GA, Price DT, Schwinn DA: **α_1-adrenergic receptor regulation: Basic science and clinical implications**. *Pharmacology & therapeutics* 2000, **88**(3):281-309.

182. Drummond ES, Dawson LF, Finch PM, Bennett GJ, Drummond PD: **Increased expression of cutaneous α_1-adrenoceptors after chronic constriction injury in rats**. *The journal of pain* 2014, **15**(2):188-196.

183. O'Connell TD, Jensen BC, Baker AJ, Simpson PC: **Cardiac α_1-adrenergic receptors: Novel aspects of expression, signaling mechanisms, physiologic function, and clinical importance**. *Pharmacological reviews* 2014, **66**(1):308-333.

184. Marks DS, Colwell LJ, Sheridan R, Hopf TA, Pagnani A, Zecchina R, Sander C: **Protein 3D structure computed from evolutionary sequence variation**. *PloS one* 2011, **6**(12):e28766.

185. Berman HM, Westbrook J, Feng Z, Gilliland G, Bhat T, Weissig H, Shindyalov IN, Bourne PE: **The protein data bank**. *Nucleic acids research* 2000, **28**(1):235-242.

186. Dutta S, Burkhardt K, Young J, Swaminathan GJ, Matsuura T, Henrick K, Nakamura H, Berman HM: **Data deposition and annotation at the worldwide protein data bank**. *Molecular biotechnology* 2009, **42**(1):1-13.

187. Eswar N, Webb B, Madhusudhan MS., Marti-Renom Marc A, John B, Pieper U, Karchin R, Shen MY, Sali A: **Comparative protein structure modeling**. *Current protocols in bioinformatics* 2006, 1-47.

188. Bordoli L, Kiefer F, Arnold K, Benkert P, Battey J, Schwede T: **Protein structure homology modeling using SWISS-MODEL workspace**. *Nature protocols* 2008, **4**(1):1-13.

189. Bissantz C, Bernard P, Hibert M, Rognan D: **Protein-based virtual screening of chemical databases II. Are homology models of G-protein coupled receptors suitable targets?** *Proteins: Structure, function, and bioinformatics* 2003, **50**(1):5-25.

190. Kihara D, Chen H, Yang YD: **Quality assessment of protein structure models**. *Current protein and peptide science 2009*, **10**(3): 216-228.

191. Eswar N, Webb B, Madhusudhan MS., Marti-Renom Marc A, Pieper U, Shen MY, Sali A: **Comparative protein structure modeling**. *Current protocols in protein scence* 2007.

192. Gertz EM: **BLAST scoring parameters**. *Manuscript* 2005.

193. Wallner B, Elofsson A: **Quality assessment of protein models**. *Prediction of protein structures, functions and interactions* 2008:143-157.

194. Anishkin A, Milac AL, Guy HR: **Symmetry-restrained molecular dynamics simulations improve homology models of potassium channels**. *Proteins: Structure, function and bioinformatics* 2010, **78**(4):932-949.

195. Kundrotas PJ, Vakser IA: **Accuracy of protein-protein binding sites in high-throughput template-based modeling**. *PLoS computational biology* 2010, **6**(4):e1000727.

196. Jose Freitas da Silveira N, Eduardo BC, Andrade AH, Filgueira de Azevedo JW: **Molecular modeling databases: A new way in the search of protein targets for drug development**. *Current bioinformatics* 2007, **2**(1):1-10.

197. Liao C, Sitzmann M, Pugliese A, Nicklaus MC: **Software and resources for computational medicinal chemistry**. *Future medicinal chemistry* 2011, **3**(8):1057-1085.

198. Worth CL, Kreuchwig A, Kleinau G, Krause G: **GPCR-SSFE: A comprehensive database of G protein-coupled receptor template predictions and homology models**. *BMC bioinformatics* 2011, **12**(1):185-195.

199. Okada T, Sugihara M, Bondar A-N, Elstner M, Entel P, Buss V: **The retinal conformation and its environment in rhodopsin in light of a new 2.2Å crystal structure**. *Journal of molecular biology* 2004, **342**(2):571-583.

200. Ostopovici-Halip L, Borota A, Gruia A, Mracec M, Rad-Curpan R, Mracec M: **3D Homology model of the α_{2B}-adrenergic receptor subtype**. *Revue roumaine de chimie* 2010, **55**(5):343-348.

201. Jayaraman A, Jamil K, Kakarala K: **Homology modelling and docking studies of human α_2-adrenergic receptor subtypes**. *Journal of computer science systems biology* 2013, **6(3)**:136-149.

202. Pedretti A, Silva ME, Villa L, Vistoli G: **Binding site analysis of full-length α_{1A} adrenergic receptor using homology modeling and molecular docking**. *Biochemical and biophysical research communications* 2004, **319**(2):493-500.

203. Du L, Li M: **Modeling the interactions between α_1-adrenergic receptors and their antagonists**. *Current computer-aided drug design* 2010, **6**(3):165-178.

204. Bruno A, Costantino G: **Molecular dynamics simulations of G protein-coupled receptors**. *Molecular informatics* 2012, **31**(3-4):222-230.

205. Grossfield A: **Recent progress in the study of G protein-coupled receptors with molecular dynamics computer simulations**. *Biochimica et biophysica acta (BBA)-biomembranes* 2011, **1808**(7):1868-1878.

206. Johnston JM, Filizola M: **Showcasing modern molecular dynamics simulations of membrane proteins through G protein-coupled receptors**. *Current opinion in structural biology* 2011, **21**(4):552-558.

207. Li J: **Basic molecular dynamics**. *Handbook of Materials Modeling*. Springer; 2005: 565-588.

208. Rapaport DC: **The art of molecular dynamics simulation**: Cambridge university press; 2004.

209. Ghirardi GC, Rimini A, Weber T: **Unified dynamics for microscopic and macroscopic systems**. *Physical review. D, particles and fields* 1986, **34**(2):470-491.

210. Borhani DW, Shaw DE: **The future of molecular dynamics simulations in drug discovery**. *Journal of computer-aided molecular design* 2012, **26**(1):15-26.

211. Van Gunsteren WF, Berendsen HJC: **Computer simulation of molecular dynamics: Methodology, applications and perspectives in chemistry**. *Angewandte chemie international edition in english* 2003, **29**(9):992-1023.

212. Van der Kamp MW, Shaw KE, Woods CJ, Mulholland AJ: **Biomolecular simulation and modelling: Status, progress and prospects**. *Journal of the royal society interface* 2008, **5**(Suppl 3):173-190.

213. Lindahl E, Sansom MS: **Membrane proteins: Molecular dynamics simulations**. *Current opinion in structural biology* 2008, **18**(4):425-431.

214. Khalili-Araghi F, Gumbart J, Wen P-C, Sotomayor M, Tajkhorshid E, Schulten K: **Molecular dynamics simulations of membrane channels and transporters**. *Current opinion in structural biology* 2009, **19**(2):128-137.

215. Arinaminpathy Y, Khurana E, Engelman DM, Gerstein MB: **Computational analysis of membrane proteins: The largest class of drug targets**. *Drug discovery today* 2009, **14**(23):1130-1135.

216. Chipot C: **Milestones in the activation of a G protein-coupled receptor. Insights from molecular-dynamics simulations into the human cholecystokinin receptor-1**. *Journal of chemical theory and computation* 2008, **4**(12):2150-2159.

217. Dror RO, Arlow DH, Maragakis P, Mildorf TJ, Pan AC, Xu H, Borhani DW, Shaw DE: **Activation mechanism of the β_2-adrenergic receptor**. *Proceedings of the national academy of sciences* 2011, **108**(46):18684-18689.

218. Soriano-Ursúa MA, Trujillo-Ferrara JG, Correa-Basurto J, Vilar S: **Recent structural advances of β_1 and β_2 adrenoceptors yield keys for ligand recognition and drug design**. *Journal of medicinal chemistry* 2013, **56**(21):8207-8223.

219. Shan Y, Kim ET, Eastwood MP, Dror RO, Seeliger MA, Shaw DE: **How does a drug molecule find its target binding site?** *Journal of the american chemical society* 2011, **133**(24):9181-9183.

220. Dror RO, Green HF, Valant C, Borhani DW, Valcourt JR, Pan AC, Arlow DH, Canals M, Lane JR, Rahmani R: **Structural basis for modulation of a G protein-coupled receptor by allosteric drugs**. *Nature* 2013, **503**(7475):295-299.

221. Kruse AC, Hu J, Pan AC, Arlow DH, Rosenbaum DM, Rosemond E, Green HF, Liu T, Chae PS, Dror RO: **Structure and dynamics of the M3 muscarinic acetylcholine receptor**. *Nature* 2012, **482**(7386):552-556.

222. Kappel K, Miao Y, McCammon JA: **Accelerated molecular dynamics simulations of ligand binding to a muscarinic G protein-coupled receptor**. *Quarterly reviews of biophysics* 2015, **48**(4):479-487.

223. Tikhonova IG, Selvam B, Ivetac A, Wereszczynski J, McCammon JA: **Simulations of biased agonists in the β_2-adrenergic receptor with accelerated molecular dynamics**. *Biochemistry* 2013, **52**(33):5593-5603.

224. Shahane G, Parsania C, Sengupta D, Joshi M: **Molecular insights into the dynamics of pharmacogenetically important N terminal variants of the human β_2-adrenergic receptor**. *PLoS computational biology* 2014, **10**(12):e1004006.

225. Chan HS, Filipek S, Yuan S: **The principles of ligand specificity on β_2-adrenergic receptor**. *Scientific reports* 2016, **6:**34736-34747.

226. González A, Perez-Acle T, Pardo L, Deupi X: **Molecular basis of ligand dissociation in β-adrenergic receptors**. *PLoS one* 2011, **6**(9):e23815.

227. Fanelli F, Menziani C, Scheer A, Cotecchia S, De Benedetti PG: ***Ab initio* modeling and molecular dynamics simulation of the α_{1B}-adrenergic receptor activation**. *Methods* 1998, **14**(3):302-317.

228. Sun X, Ågren H, Tu Y: **Microsecond molecular dynamics simulations provide insight into the allosteric mechanism of the G_s protein uncoupling from the β_2-adrenergic receptor**. *The journal of physical chemistry B* 2014, **118**(51):14737-14744.

229. Spijker P, Vaidehi N, Freddolino PL, Hilbers PA, Goddard WA: **Dynamic behavior of fully solvated β_2-adrenergic receptor embedded in the membrane with bound agonist or antagonist**. *Proceedings of the national academy of sciences* 2006, **103**(13):4882-4887.

230. Kumar A, Zhang KY: **Hierarchical virtual screening approaches in small molecule drug discovery**. *Methods* 2015, **71**:26-37.

231. Westermaier Y, Barril X, Scapozza L: **Virtual screening: An *in silico* tool for interlacing the chemical universe with the proteome**. *Methods* 2015, **71**:44-57.

232. Jacob L, Hoffmann B, Stoven V, Vert J-P: **Virtual screening of GPCRs: An *in silico* chemogenomics approach**. *BMC bioinformatics* 2008, **9**(1):363-379.

233. Yuriev E, Ramsland PA: **Latest developments in molecular docking: 2010–2011 in review**. *Journal of molecular recognition* 2013, **26**(5):215-239.

234. Pirhadi S, Shiri F, Ghasemi JB: **Methods and applications of structure based pharmacophores in drug discovery**. *Current topics in medicinal chemistry* 2013, **13**(9):1036-1047.

235. Kutchukian PS, Shakhnovich EI: ***De novo* design: Balancing novelty and confined chemical space**. *Expert opinion on drug discovery* 2010, **5**(8):789-812.

236. Stahura FL, Bajorath J: **New methodologies for ligand-based virtual screening**. *Current pharmaceutical design* 2005, **11**(9):1189-1202.

237. De Graaf C, Rognan D: **Selective structure-based virtual screening for full and partial agonists of the β_2-adrenergic receptor**. *Journal of medicinal chemistry* 2008, **51**(16):4978-4985.

238. Kooistra AJ, Vischer HF, McNaught-Flores D, Leurs R, De Esch IJ, De Graaf C: **Function-specific virtual screening for GPCR ligands using a combined scoring method**. *Scientific reports* 2016, **6**:1-21.

239. Vilar S, Karpiak J, Costanzi S: **Ligand and structure-based models for the prediction of ligand-receptor affinities and virtual screenings: Development and application to the β_2-adrenergic receptor**. *Journal of computational chemistry* 2010, **31**(4):707-720.

240. Saxena AK, Roy KK: **Hierarchical virtual screening: Identification of potential high-affinity and selective β_3-adrenergic receptor agonists**. *SAR and QSAR in environmental research* 2012, **23**(5-6):389-407.

241. Bokoch MP, Zou Y, Rasmussen SGF, Liu CW, Nygaard R, Rosenbaum DM, Fung JJ, Choi HJ, Thian FS, Kobilka TS: **Ligand-specific regulation of the extracellular surface of a G protein-coupled receptor**. *Nature* 2010, **463**(7277):108-112.

242. Warne T, Serrano-Vega MJ, Baker JG, Moukhametzianov R, Edwards PC, Henderson R, Leslie AG, Tate CG, Schertler GF: **Structure of a β_1-adrenergic G protein-coupled receptor**. *Nature* 2008, **454**(7203):486-491.

243. Bokoch MP, Zou Y, Rasmussen SG, Liu CW, Nygaard R, Rosenbaum DM, Fung JJ, Choi H-J, Thian FS, Kobilka TS: **Ligand-specific regulation of the extracellular surface of a G protein-coupled receptor**. *Nature* 2010, **463**(7277):108-112.

244. Ragnarsson L, Wang C-IA, Andersson Å, Fajarningsih D, Monks T, Brust A, Rosengren KJ, Lewis RJ: **Conopeptide ρ-TIA defines a new allosteric site on the extracellular surface of the α_{1B}-adrenoceptor**. *Journal of biological chemistry* 2013, **288**(3):1814-1827.

245. Peeters M, Wisse L, Dinaj A, Vroling B, Vriend G, Ijzerman A: **The role of the second and third extracellular loops of the adenosine A1 receptor in activation and allosteric modulation**. *Biochemical pharmacology* 2012, **84**(1):76-87.

246. Isin B, Estiu G, Wiest O, Oltvai ZN: **Identifying ligand binding conformations of the β_2-adrenergic receptor by using its agonists as computational probes**. *PLoS One* 2012, **7**(12):e50186.

247. Plazinska A, Plazinski W, Jozwiak K: **Agonist binding by the β_2-adrenergic receptor: An effect of receptor conformation on ligand association–dissociation characteristics**. *European biophysics journal* 2015, **44**(3):149-163.

248. Scheerer P, Park JH, Hildebrand PW, Kim YJ, Krauß N, Choe H-W, Hofmann KP, Ernst OP: **Crystal structure of opsin in its G protein-interacting conformation**. *Nature* 2008, **455**(7212):497-502.

249. González A, Perez-Acle T, Pardo L, Deupi X: **Molecular basis of ligand dissociation in β-adrenergic receptors**. *PLoS one* 2011, **6**(9):e23815.

250. Balogh B, Szilágyi A, Gyires K, Bylund DB, Mátyus P: **Molecular modelling of subtypes (α_{2A}, α_{2B} and α_{2C}) of α_2-adrenoceptors: A comparative study**. *Neurochemistry international* 2009, **55**(6):355-361.

Chapter 2

Chapter 2: Role of the Extracellular Surface as a Secondary Site for Agonist Interactions at the α_{1B} Adrenoceptor: A Molecular Dynamics Study

2.1 Introduction

GPCRs are the largest class of proteins [1]. α_1-ARs are members of the class A GPCRs that are activated by the catecholamines E and NE released from the adrenal medulla and sympathetic nerve endings respectively [2]. α_1-ARs are present post-junctionally on effector organs and contribute to glycogenolysis in the liver, arrhythmias in the heart, secretion from glands and contraction of the gut [3]. Three α_1-ARs (α_{1A}, α_{1B} and α_{1D}) have been pharmacologically characterized [4, 5] but their roles are still not fully understood due to the lack of structure-function relationship of selective agonists and antagonists that can distinguish between each of the subtypes [6-8].

The mechanism by which agonist binding induces the conformational changes in α_1-ARs necessary for G protein activation and intracellular signaling are inferred from the recent work of the Kobilka laboratory which has shown that agonists, neutral antagonists and inverse agonists stabilise distinct ECS conformations of the β_2-AR [9, 10]. Kobilka demonstrated the role of ligand-specific conformational changes around the ECS of the β_2-AR by NMR spectroscopy. A more detailed understanding of the contributions played by ECS residues in agonist activation is expected to identify new possibilities for allosteric drug targeting at GPCRs [11, 12] (**Figure 2-1**).

The crystallised 7TM structures harbors conserved structural motifs common to all class A GPCRs members; D(E)RY on TM3, CWxP(Y/F/L) on TM6 and NPxxY on TM7 [13]. The Arg residue in D(E)RY motif forms a cytoplasmic salt bridge (ionic lock) with Glu on TM6 (Arg135-Glu247, PDB ID 1F88) in the inactive class A GPCRs [14]. This ionic lock contributes to an energy barrier limiting transitions from the inactive to active-state rhodopsin [15]. The Tyr in the NPxxY motif form a structurally important hydrogen bond with the Asn on TM2 (Y306-N73 in PDB ID 1F88) specific to rhodopsin [16].

The extracellular disulphide bond between TM3 and ECL2 is important for ligand binding and activation in many GPCRs including rhodopsin [17], CXCR4 [18], β_2-AR [19], muscarinic receptors [20], gonadotropin releasing hormone receptor [21] and thyrotropin releasing hormone receptor [22]. This disulphide bond constrains ECL2 close to TM3 to form part of the entrance cavity for ligand binding in non-rhodopsin class A crystal structures.

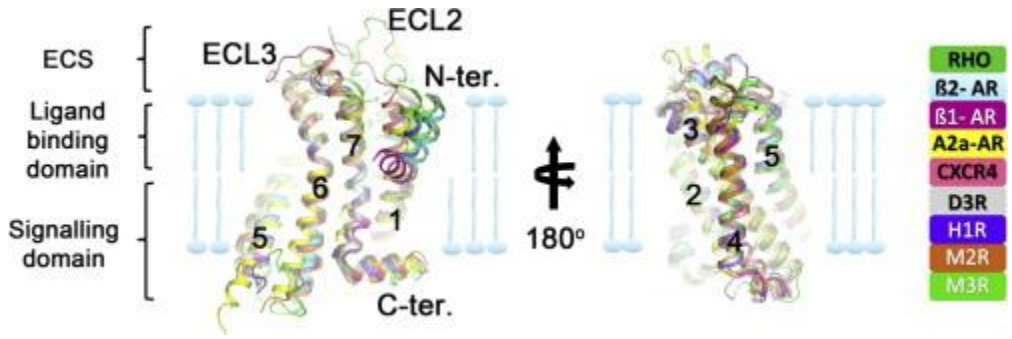

Figure 2-1: Comparison of the overall architecture of GPCR crystal structures between subfamilies [23] (Image courtesy: Lewis R. J. et al., *Biochem. Pharmacol.*; 2013;85;153-162).

The orthosteric binding sites are positioned deep (rhodopsin) or shallow (CXCR4) into the 7TM structures (**Figure 2-2**). A common feature of the orthosteric binding sites in all determined crystal structures of class A GPCR is their high rigidity as evidenced by their relatively low crystallographic B-factors (higher crystallographic resolution tends to correlate with lower B-factor) and the negatively charged surface present in all other class A GPCRs except the positively charged H_1R [24]. These features contribute to the challenge of designing selective orthosteric drugs that target only specific GPCR subtypes. Superimposition of the orthosteric binding sites reveals extensive structural and sequence overlap of class A GPCRs.

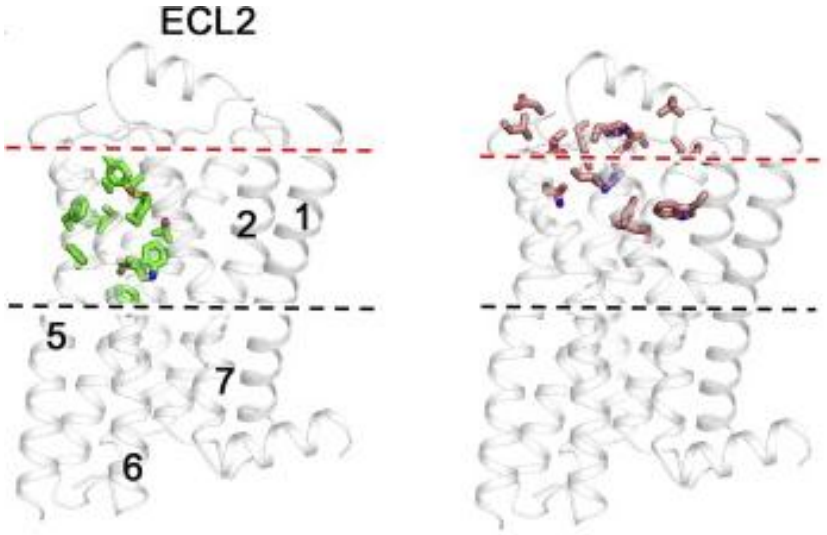

Figure 2-2: Location of the orthosteric binding site in rhodopsin (flanked by residues in green) and CXCR4 (residues flanked in brown) [23] (Image courtesy: Lewis R. J. et al., *Biochem. Pharmacol.*; 2013;85;153-162).

Figure 2-3 reveals a high degree of structural conservation despite the low overall protein sequence identity of nine class A GPCRs across four different subclasses in complex with a wide

variety of orthosteric ligands. For clarity, only the extracellular regions of TM6, TM7 and ECL3 are shown in the left panel and all ECLs are removed in the rotated view. This information can be used to shed light on possibilities to develop subtype selective allosteric modulators that act at less conserved structural motifs.

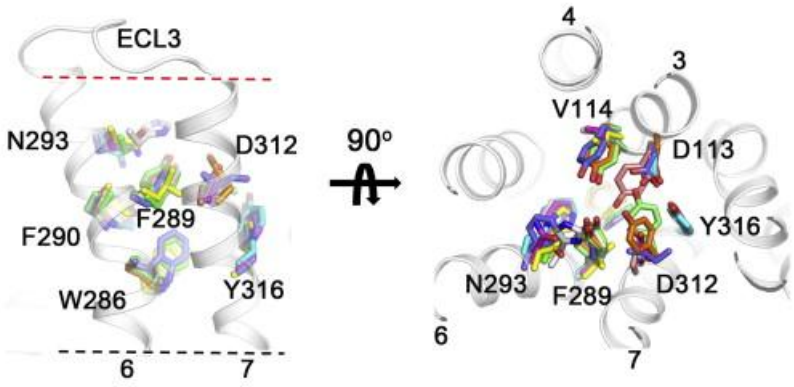

Figure 2-3: Residues lining the ECL and orthosteric site of class A GPCR members superimposed on the backbone of β_2-AR [23] (Image courtesy: Lewis R. J. et al., *Biochem. Pharmacol.;* 2013;85;153-162).

The route ligands follow to enter the orthosteric binding site is of crucial importance to understand the importance of ECS residues in receptor activation [9, 10, 25]. Studies on β-ARs have revealed that specific residues in the ECS were important to ligand entry and exit [25]. These results were supported by random accelerated MD (RAMD) studies [26] that suggest the ligands access the primary binding site via the ECS in contrast to TM helices as observed in rhodopsin [13, 14, 27] where ECL2 covers the entrance to the binding pocket [10]. Thus, it is plausible to suggest an importance of the ECS as a secondary site for ligand binding. Though recent progress in crystal structure evolution has provided an atomistic view of the ligand-receptor interactions, insights into the detailed receptor-ligand interactions are still not known. The detailed process by which the ligand dissociates from its receptor and the pattern it follows during dissociation remains hidden.

Deupi et al., demonstrated in atomic detail the molecular basis of ligand binding/unbinding events by SMD simulation; the unbinding process of two inverse agonists (cyanopindolol and carazolol) which were co-crystallised with β_1-AR and β_2-ARs subtypes. This study revealed that these compounds are likely to access the orthosteric binding site of β-ARs along four different channels (C1, C2, C3 and C4, **Figure 2-4c**) from the extracellular water environment there by

suggesting the presence of secondary binding sites located in the ECL2, ECL3 and TM7 where ligands are transiently retained by electrostatic and van der Waals interactions (**Figure 2-4**).

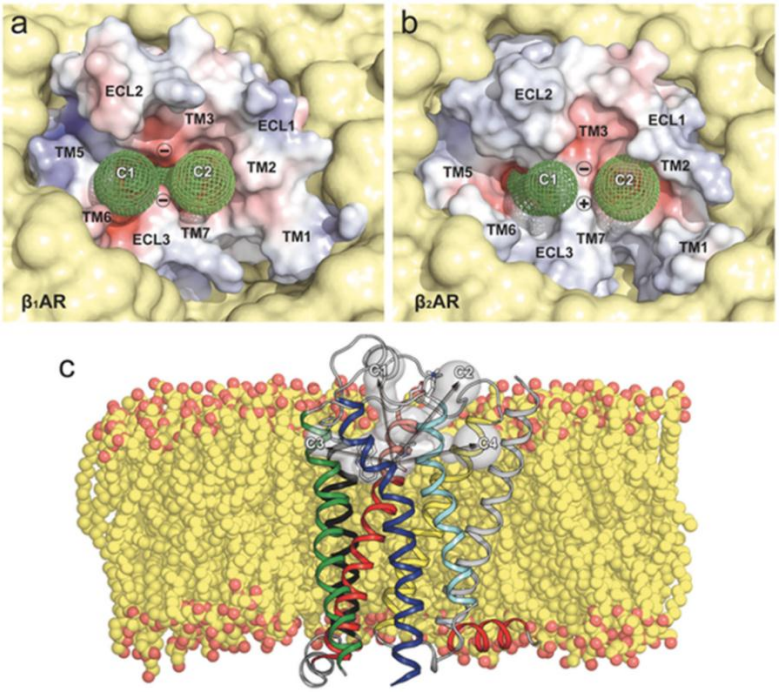

Figure 2-4: Extracellular molecular surfaces of the a) β_1-AR,b) and β_2-AR and c) embedded in a lipid bilayer[28] (Image courtesy: Deupi X. et al., *PloS one*; 2011;6;e23815).

Charged residues in ECL2 (Asp217 and Asp356 in β_1-AR) and ECL3 (Asp192 and Lys305 in β_2-AR) separate the C1 and C2 channel from each other.This study identified that in the process of ligand entry Phe218 in β_1-AR and Phe193 in β_2-AR serve as a floodgate by removing the water solvent shell around the compounds during binding.

Guo D .et al., investigated the molecular basis of ligand dissociation process (antagonist ZM241385) in the A2A-R [29]. This study identified the characteristic mutant receptors that alter the ligand dissociation rate while only marginally influencing its binding affinity demonstrating that even receptor features with little contribution to affinity might prove critical to the dissociation process. Further, the antagonist ZM241385 follows a multistep dissociation pathway there by consecutively interacting with distinct receptor regions, a mechanism that may also be common to many other GPCRs (**Figure 2-5**).

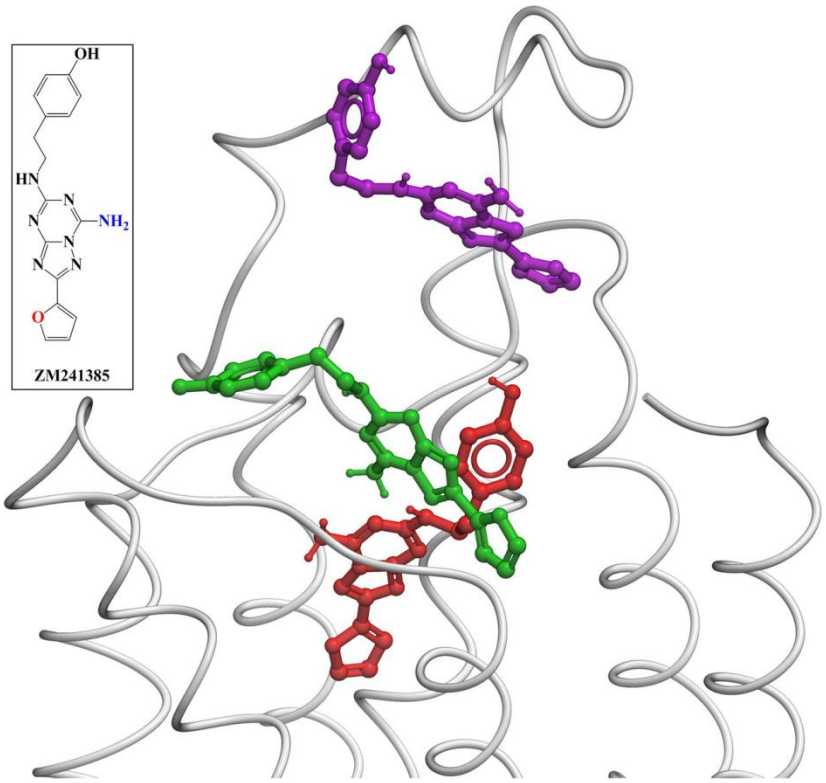

Figure 2-5: MD simulation of ZM241385 passes through multiple distinct consecutive steps represented by three superimposed snapshots: red (initial pose, 0ns), green (28ns), and magenta (32ns) [29] (Image courtesy: Guo D. et al,, *Mol. Pharmacol.*; 2016;89;485-491).

In this study antagonist ZM241385 follows a multistep dissociation pathway from the A2A-R first breaking the hydrogen bond network formed by the triad of Glu169 in ECL2, Thr256 in TM6 and His264 in TM7 and transiently contacting the hydrophobic pocket above Tyr271 in TM7 consisting of Ile66 and Ser67 in TM2 and Leu267 in TM7 before moving further away from the binding pocket into the extracellular domain and bulk solvent (**Figure 2-6**).

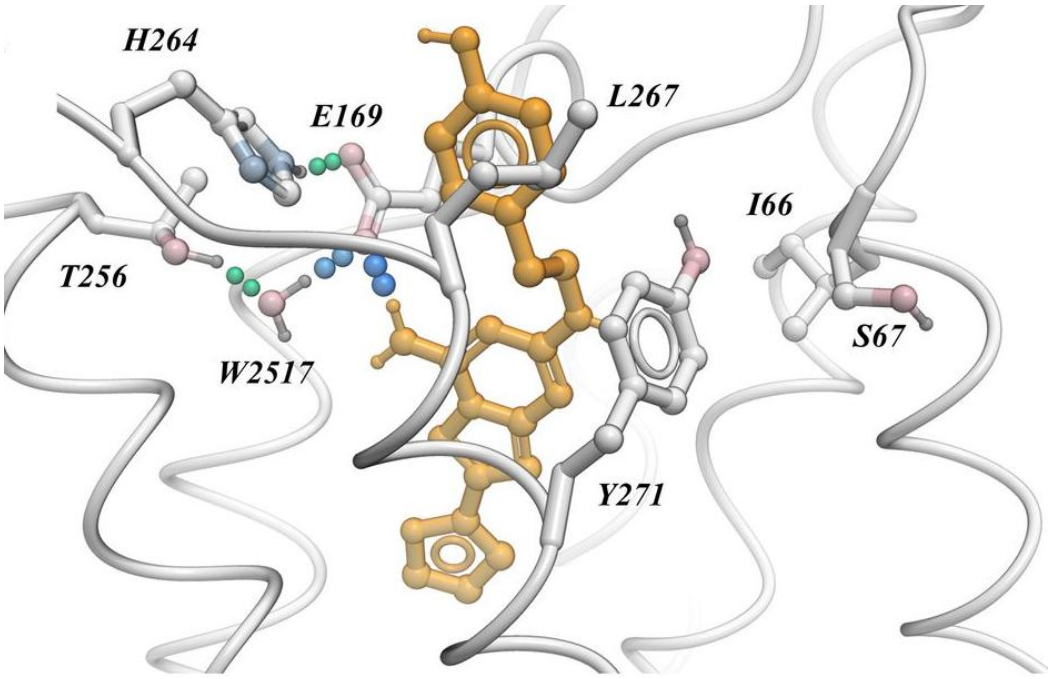

Figure 2-6: Amino acid residues in A2A-R interacting with ZM241385 during its dissociation process [29] (Image courtesy: Guo D. et al., Mol. *Pharmacol.*; 2016;89;485-491).

Craik D. J. et al., delineated the unbinding pathway of α-conotoxin ImI from the α_7 nicotinic acetylcholine receptor [30]. This study identified three exit routes using RAMD simulations. Of the three exit routes that involved smallest perturbation in conformation had three subpathways which were studied by SMD simulation. The two subpathways correlated well experimentally indicating that these two subpathways are sampled more frequently.

In the present study, we used a turkey β_1-AR (PDB ID: 2YCW) [31, 32] derived homology model of hamster α_{1B}-AR and SMD to find the egress pathway of NE from the orthosteric binding site of the α_{1B}-AR (**Figure 2-7**). This study led to the identification of residues on the ECS of α_{1B}-AR and two potential secondary sites; first at the entrance of the orthosteric binding site around TM5 and ECL2 and second around ECL1 which might be subtype specific.

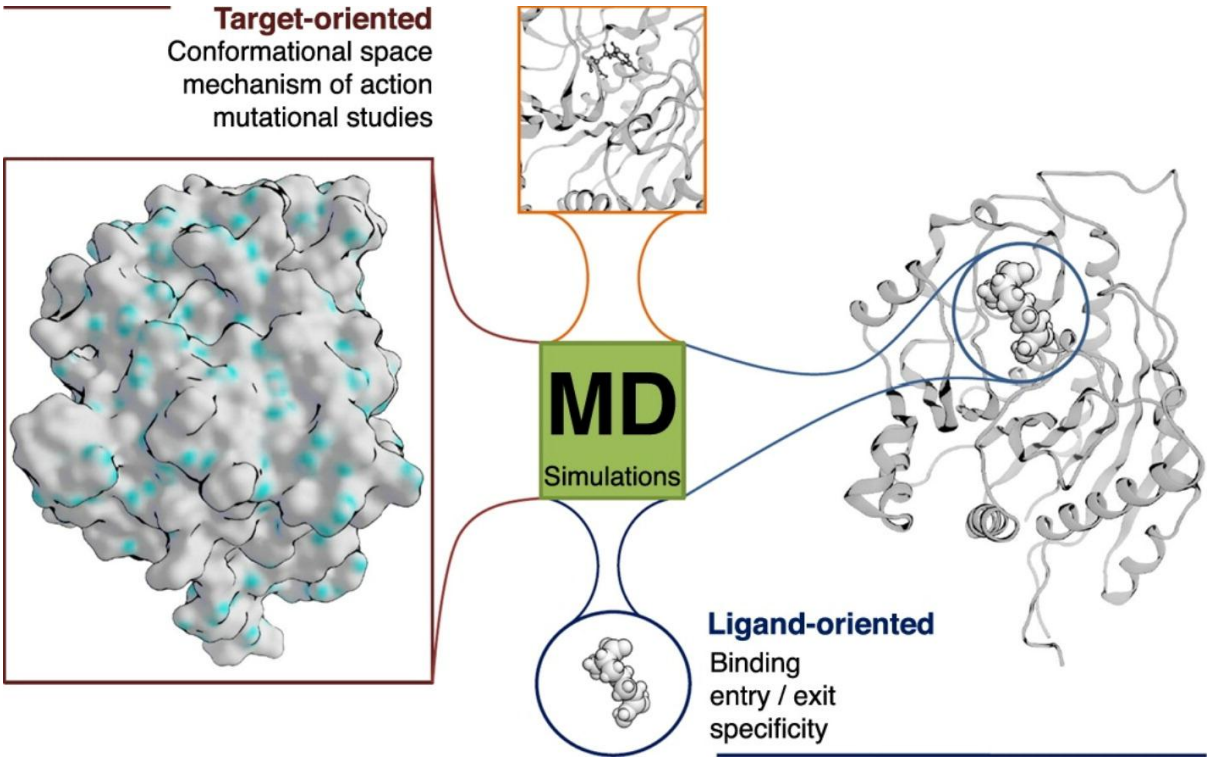

Figure 2-7: Role of MD in delineation of binding/unbinding pathway [33] (Image courtesy: Mortier J. et al., *Drug Discov. Today;* 2015;20;686-702).

The residues identified during egress were subsequently mutated and the resulting mutant receptors were then subjected to experimental determination of the ligand's affinity. An analysis of these results suggests that aromatic residues may play a key role in stabilising specific ECS conformations of the receptor with potential to differentially interact with NE. This multi-step process of ligand dissociation from the receptor could be speculated to be common to other members of the class A GPCR.

2.2 Material and Methods

2.2.1 Homology Modeling

The hamster α_{1B}-AR sequence retrieved from SwissProtKB/TrEMBL database [34, 35] (primary accession number: P18841) was subjected to a NCBI BLASTp [36] search against Protein Data Bank (PDB) (**Figure 2-8**). The crystal structure of the turkey β_1-AR at 3.0Å resolution (PDB ID: 2YCW) was selected as template for homology modeling of the hamster α_{1B}-AR due to its high (31.4%) sequence identity using the program MODELLER 9.10 [37]. Secondary structure prediction of the TM helices as well as the ICLs and ECLs prediction was performed with the PSIPRED server (http://bioinf.cs.ucl.ac.uk/psipred/psiform.html).

MODELLER (ver.9.10) used for homology modeling of hamster α_{1B}-AR is a computer program that models 3D structures of proteins and their assemblies by satisfaction of spatial restrains. Ten crude models were generated initiallyby the automated class in MODELLER and the model with the lowest DOPE score and molpdf score was selected for further ligand modeling. PROCHECK programme was used to validate the stereochemistry using Ramachandran plot.

The loops in the initial crude homology model showed steric clashes as observed from the ERRAT plot were subjected for loop modeling by Modeller Loop class and validated by ERRAT plot. This gives the measure of the structural error at each amino acid residues in the 3D structure model which should be below 95% cut-off value. Some of the amino acid residues of hamster α_{1B}-AR that formed secondary structure had an error value more than 95% cut-off value. 10 models generated from loop modeling were validated by PROCHECK and ERRAT plot. Binding site for NE docking in the resulting model was predicted by Q-SiteFinder [38]. Energy minimisation was performed on the crude models and default settings were used in Modeller for model building.

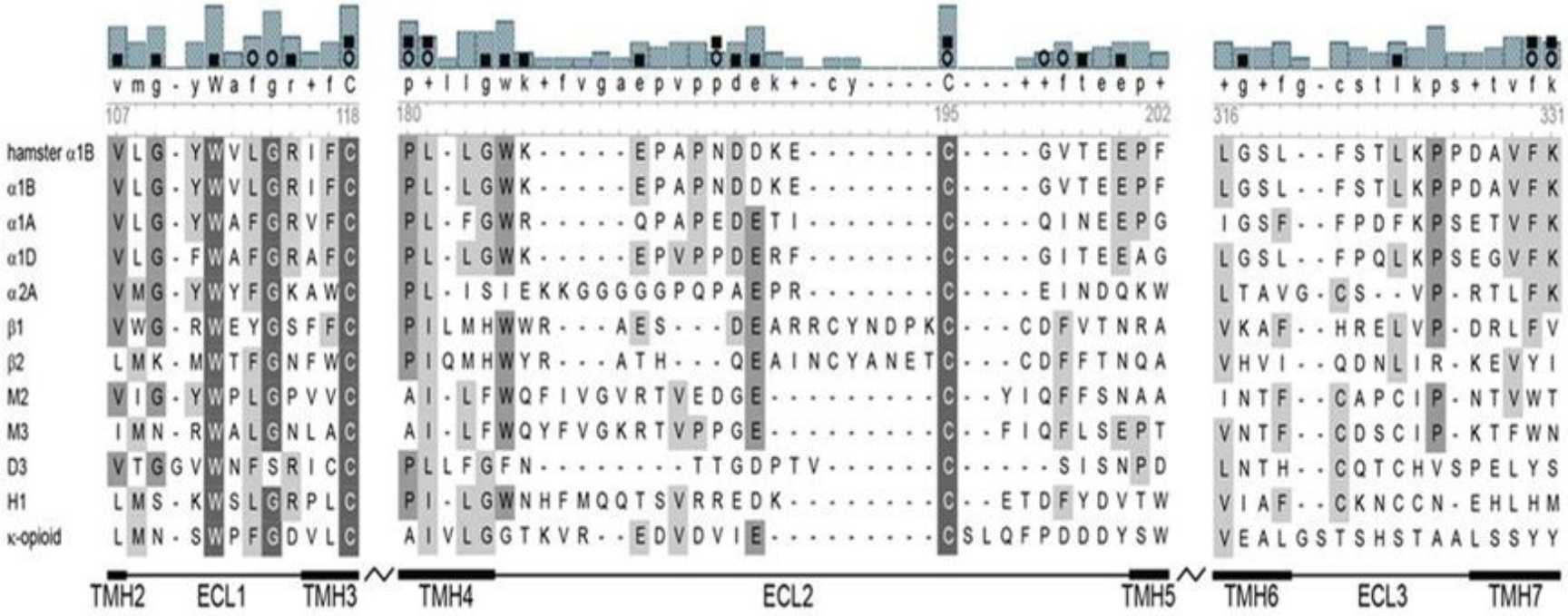

Figure 2-8: Comparison of hamster α_{1B}-AR sequences with α-ARs, β-ARs, muscarinic, dopamine, histamine and opioid receptors obtained from UniProt [39] (Image courtesy: Ragnarsson L. et al., *J. Biol. Chem*.; 2013;288;1814-1827).

2.2.2 Molecular Docking

Molecular docking is a computationally intensive structure-based VS technique which generates and scores putative protein-ligand complexes according to their calculated binding affinities. It has been successfully used for identifying active compounds by filtering out those that do not fit into the binding sites. In the absence of the structural information of the target, a homology model can be constructed and used for molecular docking analysis.

In the present study, molecular docking was performed with the developed homology model of hamster α_{1B}-AR using Genetic Optimisation for Ligand Docking (GOLD) program. For the purpose of docking, homology model structure of hamster α_{1B}-AR was prepared with the structure preparation tool available in AutoDock and GOLD. Hydrogen atoms were added and Gasteiger-Hückel charges were appropriately assigned.

Docking of NE to the orthosteric binding site of hamster α_{1B}-AR was performed with AutoDock [40] and GOLD [41]. In AutoDock, the grid maps were prepared using the AutoGrid utility with 54*52*48 points which is sufficiently large to accommodate all active site residues and grid spacing was set to 0.375Å. Docking parameters were kept as per following; number of individuals in the population was set to 150, maximum number of energy evaluations was set to 2500000, maximum number of generations was set to 2700 and number of genetic algorithm (GA) runs was set to 20. A docking pose of NE which showed the lowest binding energy was selected for MD simulation studies.

In GOLD two scoring functions; Gold Score fitness function and Chem Score fitness function was used to estimate the efficiency of docking. For each of the five independent GA runs, a maximum number of 100000 GA operations were performed on a set of five groups with a population size of 100 individuals. Operator weights for crossover, mutation, and migration were set to 95, 95 and 10 respectively. Default cut off values of 2.5Å and 4.0Å was employed for hydrogen bonds and van der Waals distance. GA docking was terminated when the top three solutions had an RMSD within 1.5Å. The best ranked solutions were always among the first 10 GA runs and the conformations of NE based on the best fitness score were further analysed.

2.2.3 Molecular Dynamics Simulations

All MD trajectories were calculated using NAMD2.9 [42, 43]. The protein was internally hydrated using SOLVATE program [44]. To imitate the membrane environment, the modeled hamster α_{1B}-AR was inserted into the phospholipid bilayer generated from membrane builder module of VMD 1.9 [45]. The membrane consisted of 184 molecules of 1-palmitoyl-2-oleoyl-sn-glycerol-3-phosphatidylcholine (POPC) and was equilibrated for 0.5ns. The system was neutralised by adding chloride ions and additional sodium and chloride ions were added to a final concentration of 0.15mol/L.

The parameters for NE were partly obtained from the work published on β_2-AR by Spijker. et al., [46] and remaining were derived from parameters already present in the CHARMM force field [47] for similar chemical groups. Temperature control was maintained at 310K with Langevin dynamics and a damping constant of $5ps^{-1}$; applied to non-hydrogen atoms. Periodic boundary conditions were used with the Nosé-Hoover Langevin piston method [48] (piston period 200fs, decay rate 50fs) to maintain a constant pressure of 1.013Bar.

The Particle-mesh Ewald algorithm [49] was used to account for long-range electrostatic effects (grid resolution <1Å). The van der Waals interactions were determined using a Leonard–Jones function. The cut off radius for including atoms in the nearest-neighbor list was set to 13.5Å. 1-2 and 1-3 interactions were excluded while 1-4 interactions were scaled by multiplication with a predefined factor. All other non-bonded interactions were calculated using a switching function to smooth the interactions to zero between 10 and 12Å. The integration time steps were 2, 1, and 2fs for bonded, nonbonded and long-range electrostatic interactions respectively. The lengths of all chemical bonds were constrained by the SHAKE algorithm [50] involving hydrogen atoms at their equilibrium values while the SETTLE algorithm [51] was used to set the water geometry restrained rigid. The system was first minimised for lipids and water (1ns) while keeping the protein and ligand fixed followed by an all-atom conjugate gradient minimisation of the entire system during which protein was relaxed and allowed to move freely. After this the system was equilibrated for 10ns at 310K and constant pressure.

2.2.3.1 Steered Molecular Dynamics Simulations

The process of NE dissociation from the orthosteric binding site of the hamster α_{1B}-AR was studied by SMD [52] implemented in NAMD2.9. Simulations were carried out using NPT ensemble with a constant number of molecules, temperature and pressure with periodic boundary conditions after equilibrating the system for 10ns to ensure system is thermodynamically stable. The initial structures for the simulations were the snapshots that were taken randomly from the equilibration states during conventional MD. The direction of the applied forces was defined with respect to the centre of mass of the NE (catechol moiety). SMD simulations were performed at constant velocity of 10Å/ns and the spring constant was set to 250pN/Å. The exponent for harmonic constraints applied to the Cα atoms of helix was set to a value of 2. The process was repeated 5 times for 5ns until the NE was displaced towards ECS. The potential of mean force (PMF) was calculated according to Jarzynski's equation [53].

2.2.4 Site-Directed Mutagenesis

The site directed mutagenesis reactions were carried out using the QuikChange^{TM} Mutagenesis kit (Stratagene Cloning Systems, La Jolla, CA, USA) following the manufacturer's instructions with the hamster α_{1B}-AR vector (a kind gift from Prof. Bob Graham, Victor Chang Cardiac Research Institute, Sydney, Australia) as template to produce mutant cDNAs. Sense and antisense oligonucleotide primers (Sigma Aldrich, Sydney, Australia) were designed to produce the following mutations in the α_{1B}-AR; C129A, F117A, A204G, A204T, S208A, F212A and Y338A. TOP-10 *E.coli* cells (invitrogen) were transformed with wildtype (WT) and mutant cDNA and plated onto LB plates containing ampicillin and incubated at 37ºC for 16-20 hrs. Plasmid preparation was performed using a Miniprep and High Speed Maxi kit (Invitrogen). Purified cDNA was used to confirm all mutations by sequencing at the Australian genome Research Facility.

2.2.5 Transient Expression of α_{1B}-AR and Membrane Preparation

COS-1 cells (ATCC, Manassas, VA) were cultured in Dulbecco's modified Eagle's medium (DMEM) supplemented with 5% fetal bovine serum (FBS) in a humidified incubator at 37ºC and 5% CO_2. Cells were transiently transfected with purified plasmid DNA encoding WT or mutant hamster α_{1B}-AR using FuGENE HD (Roche) (6µg DNA/25cm^2, 36µg DNA/145 cm^2) following the manufacturer's protocol. Cell membranes were prepared 48h post transfection

wherein cells were harvested and homogenised by Polytron homogeniser in HEM buffer (20mM HEPES, 1.5mM EGTA, 12.5mM MgCl2, pH 7.4) mixed with complete protease inhibitor. The homogenate was centrifuged at 2000rpm for 10 min (RCF/G-Force, 45) and resulting supernatant was centrifuged at 14000rpm for 30 mins (RCF/G-Force, 6586) at 4°C. The pellet was re-suspended in HEM buffer with 10% v/v glycerol stored at -80°C. BCA protein assay kit was used to determine the protein concentration following manufacturer's protocol.

2.2.6 FLIPR Assay Measuring Intracellular Ca^{2+} Responses

On the day of the assay cells were loaded with the Calcium 4 No-wash dye (Molecular Devices) by diluting the lyophilised dye in physiological salt solution and incubated for 30 min at 37°C in a 5% humidified CO_2 incubator. Intracellular Ca^{2+} responses were measured in response to increasing concentrations of agonist (NE) (10pM–100µM), in a Fluorometric Imaging Plate Reader (FLIPR) (Molecular Devices, Sunnyvale, CA) using a cooled CCD camera with excitation at 470–495nM and emission at 515–575nM. Camera gain and intensity were adjusted for each plate to yield a minimum of 1000 arbitrary fluorescence units (AFU) baseline fluorescence. Prior to addition of NE, 10 baseline fluorescence readings were taken followed by fluorescent readings every second for 300s. Concentration-response curves were established by plotting DeltaF/F_0 values where F_0 is the base-line level of fluorescence and Delta F is the change in fluorescence from the baseline level against agonist concentration using Prism (GraphPad Software).

2.2.7 Radioligand Binding Assay

The affinity of the NE at the α_{1B}-AR mutants was determined using the radiolabeled α_1-AR antagonist [^{3}H] prazosin (0.5nm). Reactions were carried out in a round bottom 96 well plate with radioligand, membranes from α_{1B}-AR-transfected COS-1 cells (5µg of protein) and increasing concentration of NE (10pM - 10µM) in HEM buffer. Saturation binding assays were also performed to determine the Kd value for prazosin at each of the mutant. The assays were performed in triplicates in a total reaction volume of 150µl. The membranes were incubated for 60 mins at room temperature followed by harvesting onto Whatman GF/B filter mats pretreated with 0.6% polyethyleneimine using a TomTec harvester. Beta plate scintillant was then applied and the filter bound radioactivity was then measured using WallacMicroBeta.

2.2.8 Statistics and Data Analysis

Sigmoidal curves for the calculation of EC_{50} were fitted to individual data points by nonlinear regression using the software package Prism (GraphPad Software, San Diego, CA).The NE signaling efficiency was calculated as the NE pEC_{50} value minus the NEK_i value with additional adjustment for the significantly reduced expression levels (observed only for the C118A mutant). B_{max}values were determined from two 12-point saturation binding experiments with 95% confidence intervals overlapping WT values were considered not significantly different fromWT, otherwise these experiments were performed in triplicate.

2.3 Results and Discussion

2.3.1 Homology Modeling

A 3D structure of the hamster α_{1B}-AR was built by homology modeling [37]. Hits retrieved from the BLASTp [36] search were compared for %identity and %similarity. Turkey-β_1-AR (PDB ID: 2YCW) [31, 54] was selected as template for model building (31.4% identity and 47.9% similarity). The residues comprising the TM regions of GPCRs were found to be relatively conserved upon sequence alignment between the hamster α_{1B}-AR and turkey β_1-AR (**Figure 2-9**).

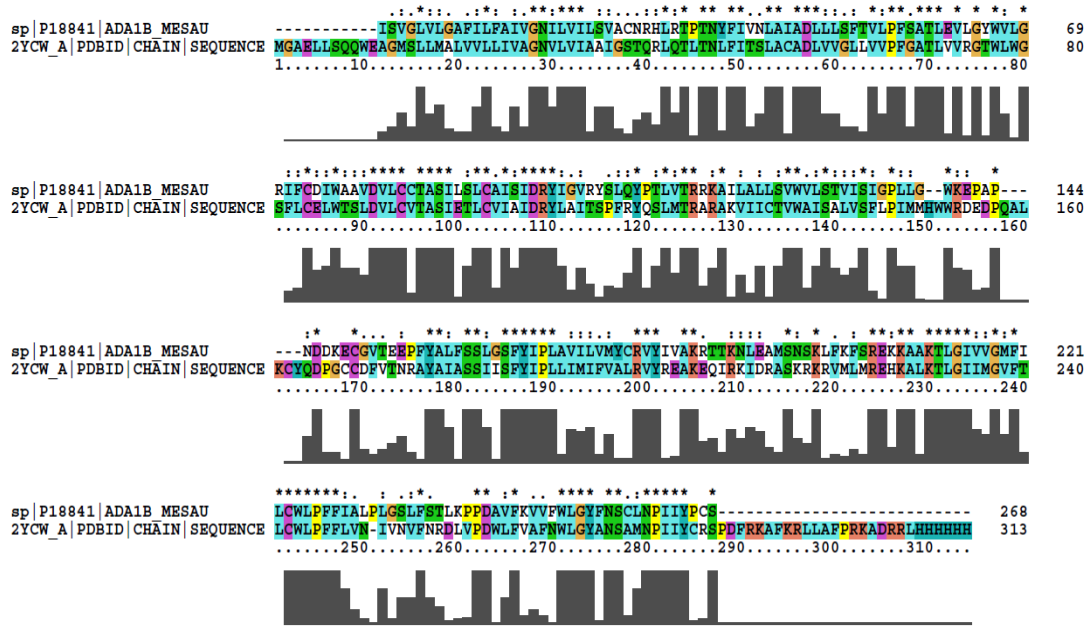

Figure 2-9: Sequence alignment between hamster α_{1B}-AR and turkey β_1-AR (grey bars showing the % identity between the residues in α_{1B}-AR and turkey β_1-AR; * represent the similar residues).

The structural superposition of the Cα atoms of the hamster α_{1B}-AR with that of the turkey β_1-AR for 268 Cα atom pairs resulted in a root mean square deviation (RMSD) of 0.22Å (**Figure 2-10**).

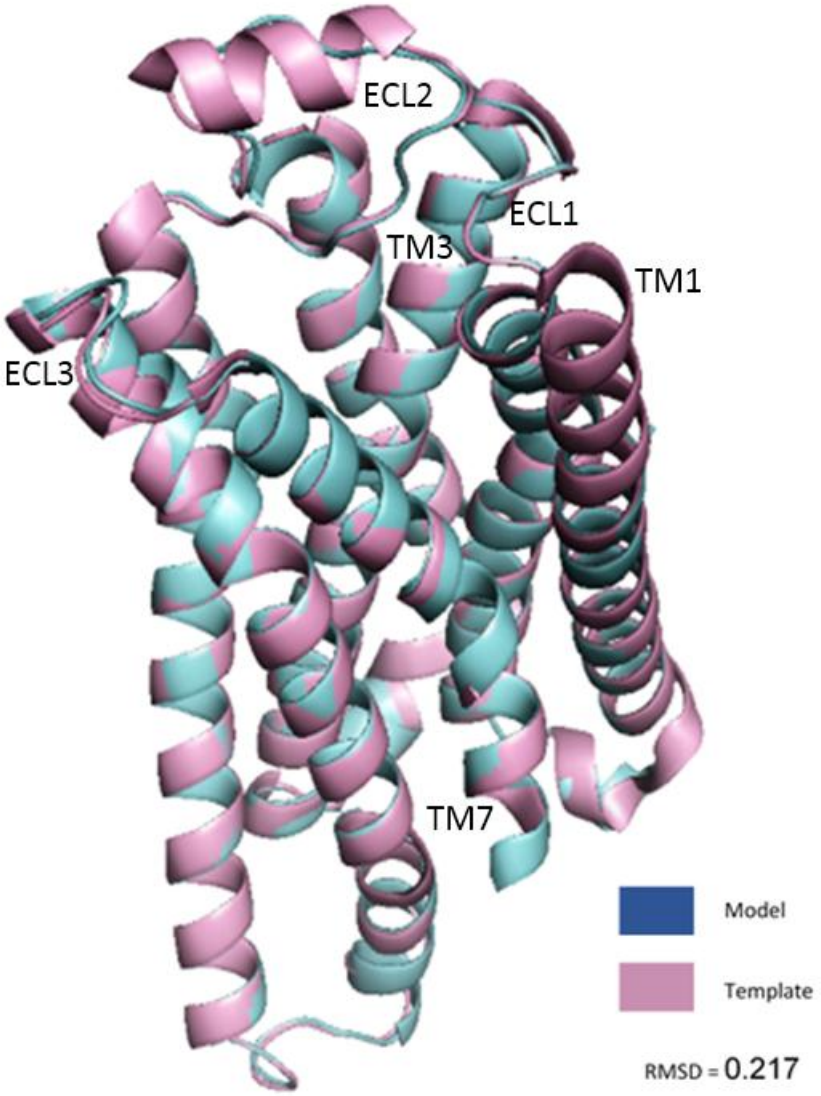

Figure 2-10: Superimposition of Cα backbone of hamster α_{1B}-AR (cyan) with the X-ray crystal structure of turkey-β_1-AR (PDB ID: 2YCW) (magenta) and RMSD calculated.

The homology model of hamster α_{1B}-AR showed an ERRAT quality factor of 85.38%. Ramachandran plot (93.7%, 6.3%, 0.0%, and 0.0%) indicated that 100.0% of the residues in the α_{1B}-AR model are either in the most favored or in the additionally allowed regions with no residues in generously allowed or disallowed regions (**Figure 2-11**) [55].

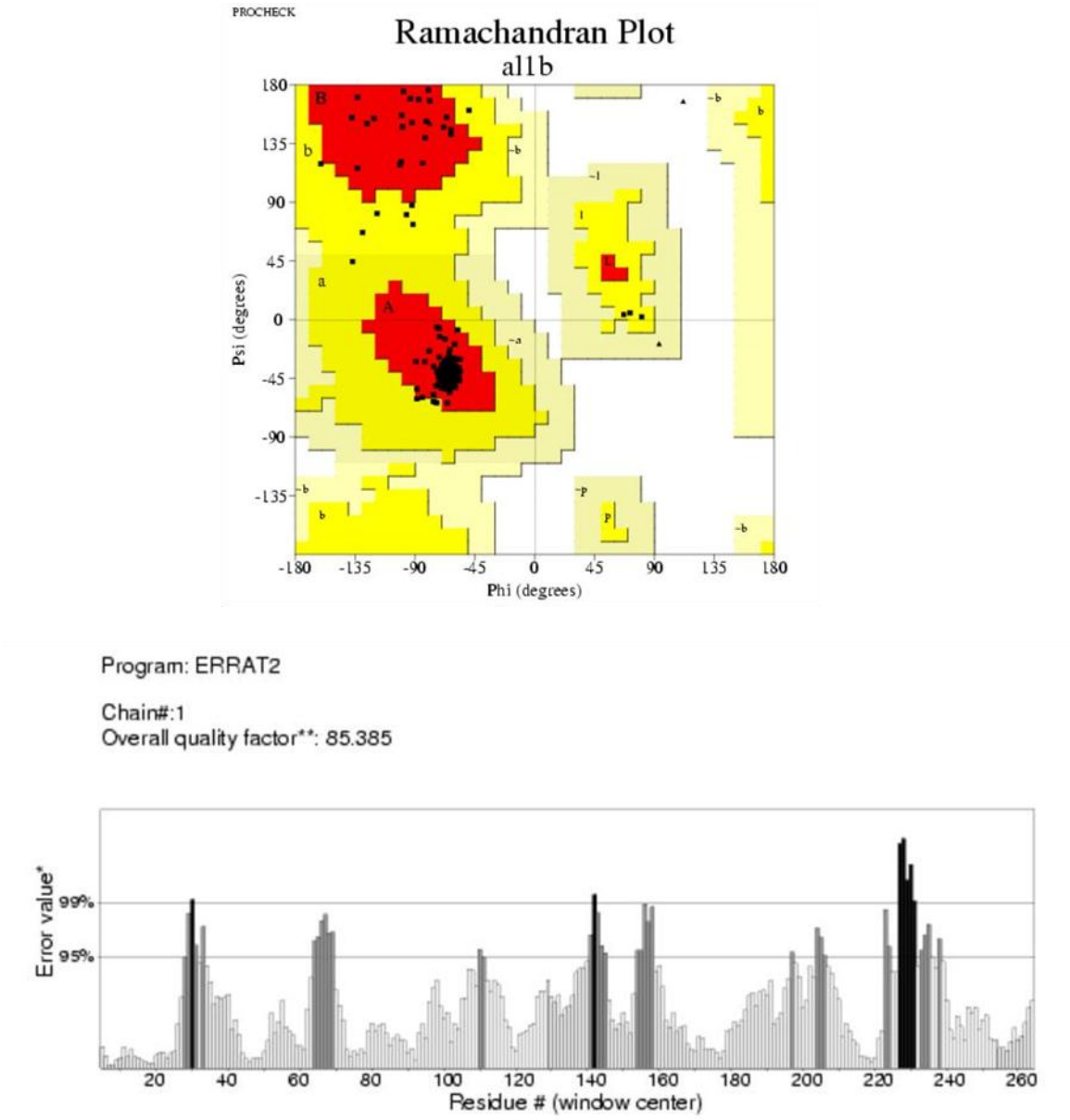

Figure 2-11: Ramachandran plot showing the percentage of residues in the favored and allowed region while Errat plot displays the steric clashes with an overall quality factor of 85.38.

2.3.2 Molecular Docking

Binding site for NE docking in the hamster α_{1B}-AR model as predicted by Q-SiteFinder is shown in **Figure 2-12**. Binding site analysis of the modeled hamster α_{1B}-AR identified similarity in residues lining the orthosteric binding pocket with that of the turkey β_1-AR (Asp125, Val122, Tyr207, Ser211, Ser215, Trp303, Phe306 and Phe307). Therefore, we proceeded with the modeled structure for docking studies of NE in the orthosteric binding site by AutoDock and GOLD software. Docking was evaluated based on two criteria;

(i) Binding pose and

(ii) Scoring function.

Binding pose was evaluated based on consistency with experimentally determined NE interactions while the scoring function considered the lowest energy value for AutoDock and highest GOLD Score function for GOLD as parameters of docking efficiency.

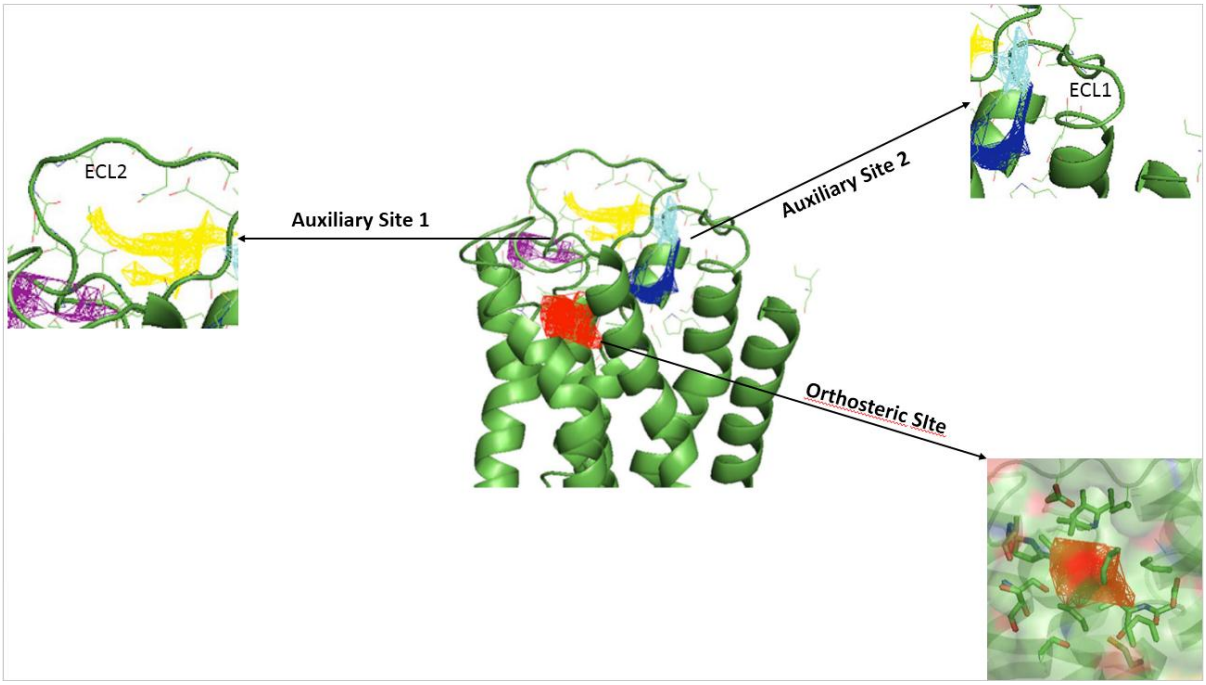

Figure 2-12: Binding site prediction in the hamster α_{1B}-AR model by Q-SiteFinder. One orthosteric site (red) and two auxiliary sites were predicted in ECL1 (Cyan) and ECL2 (Yellow).

Molecular docking of NE revealed formation of strong hydrogen bond interactions with Asp125, Glu199 and Ser207 of the α_{1B}-AR with both AutoDock and GOLD (**Figure 2-13**) which is consistent with interactions observed for ligand binding in orthosteric sites of related GPCR co-crystal structures including cyanapindolol bound turkey-β_1-AR [33] and carazolol bound β_2-AR [14] (RMSD 0.245 and 0.119) suggesting correct docking of NE in the binding cavity. Additionally, NE was seen to form a strong hydrogen bond with Val197 in ECL2 and

weak hydrogen bonds with residues Glu186, Leu314, Ser315, Leu333 and Pro335 in some of the binding poses as observed with AutoDock. Water mediated hydrogen bond between the N terminal positive charge of ρ-TIA and Glu-186, Asn-2-ρ-TIA and the backbone Val-197, was observed in a study by Ragnarsson et al. However, hydrogen bond formation between Asn-2-ρ-TIA and the backbone of Val-197 was not validated via mutational approaches [39].

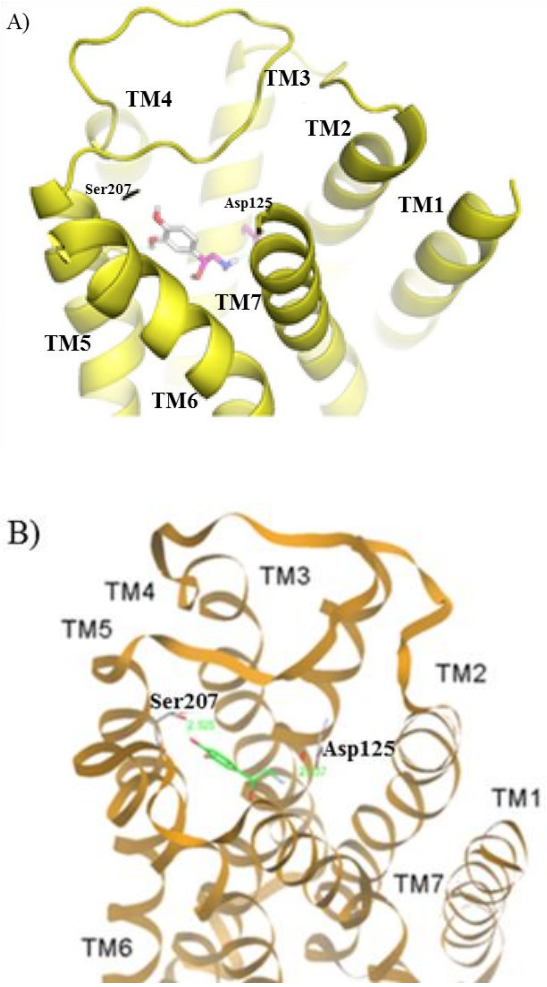

Figure 2-13: Docked pose of NE into hamster α_{1B}-AR obtained from A) AutoDock (Ligand: Silver color) and B) GOLD (Ligand: Green color) (Side view).

NE also formed hydrogen bonds with the backbone of the Cys129 in TM3, Ala204 in TM5 and other short-range contacts like van der Waals and hydrophobic interactions with Trp184, Tyr203, Trp307 and Phe311 in some of the docking poses as observed with GOLD. The best pose has a docking score of 38.40 (DOPE and molpdf score). In the docking poses evaluated, NE consistently docked in tilted position (% occurrence ±5%) with the catechol moiety forming hydrogen bonds with residues in TM5 and terminal amine side chain forming hydrogen bond with TM3.

2.3.3 Molecular Dynamics

2.3.3.1 Stability of Trajectories

The trajectory for the whole system was analysed for total energy, potential energy, temperature and pressure (**Figure 2-14**).

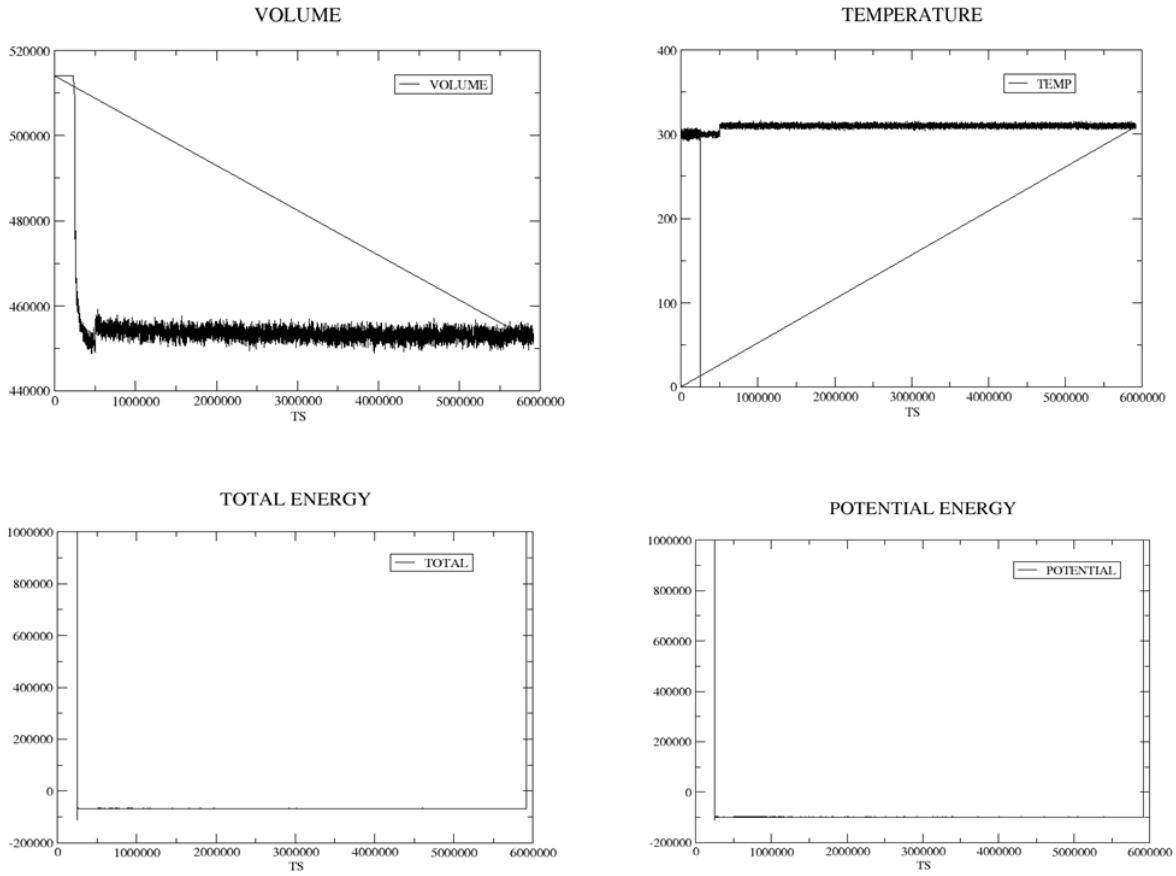

Figure 2-14: The equilibrated system of NE with hamster α_{1B}-AR obtained after 10ns showing constant level of Volume, Temperature, Total Energy and Potential Energy.

The **Figure 2-14** shows the curve for total energy with respect to number of frames for all the structures during a 10ns equilibration run which includes equilibration with protein constrained and relaxed. The system is stabilised at an average total energy of -98,000Kcal/mol at 310K and 1.013bar. The RMSD stability for the whole system and three ECLs was also analysed to study the effective conformational sampling. The RMSD plot shows that the whole system is stable at an average value of 2.7Å after approximately 6ns while the three ECLs have relatively higher average RMSD of 25Å, 30Å and 40Å for ECL1, ECL2 and ECL3 probably because the loops are exposed to the solvent at extracellular side.

2.3.4 Route Preference for NE Dissociation

A docking pose of NE which showed the highest Gold Score fitness function and lowest binding energy was selected for MD simulations studies. Initially the receptor was embedded in a lipid bilayer and equilibrated for 10ns. After equilibration, forces were applied on the centre of mass of the catechol group of NE. Before performing the actual simulation, the direction of the pulling vector was determined based on position and orientation of the ligand in the binding site.

The most preferable route was found to be in +z direction (**Figure 2-15**) towards the ECS (**Figure 2-16**) and not from the TM helices as observed in rhodopsin. The process of ligand dissociation from the orthosteric binding site to ECS also suggests the probable entry route for NE. The ligand is found to be retained in the receptor along with extracellular solvent to a distance of ~15Å from the orthosteric binding site.

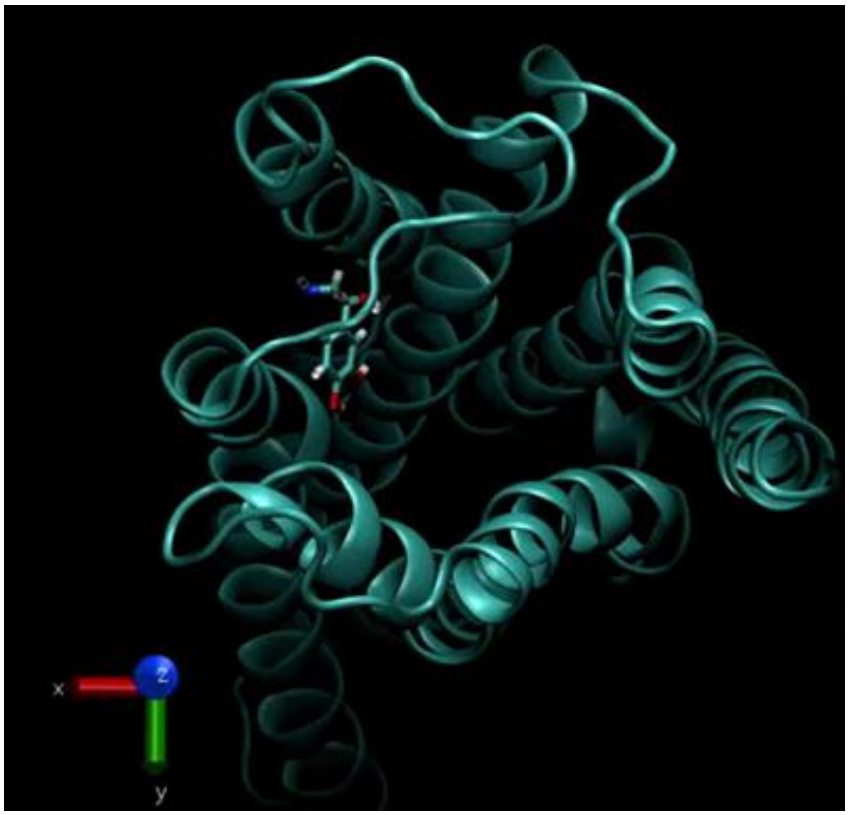

Figure 2-15: The dissociation process of NE from the orthosteric site in +z direction as observed by visual molecular dynamics pluggin (VMD).

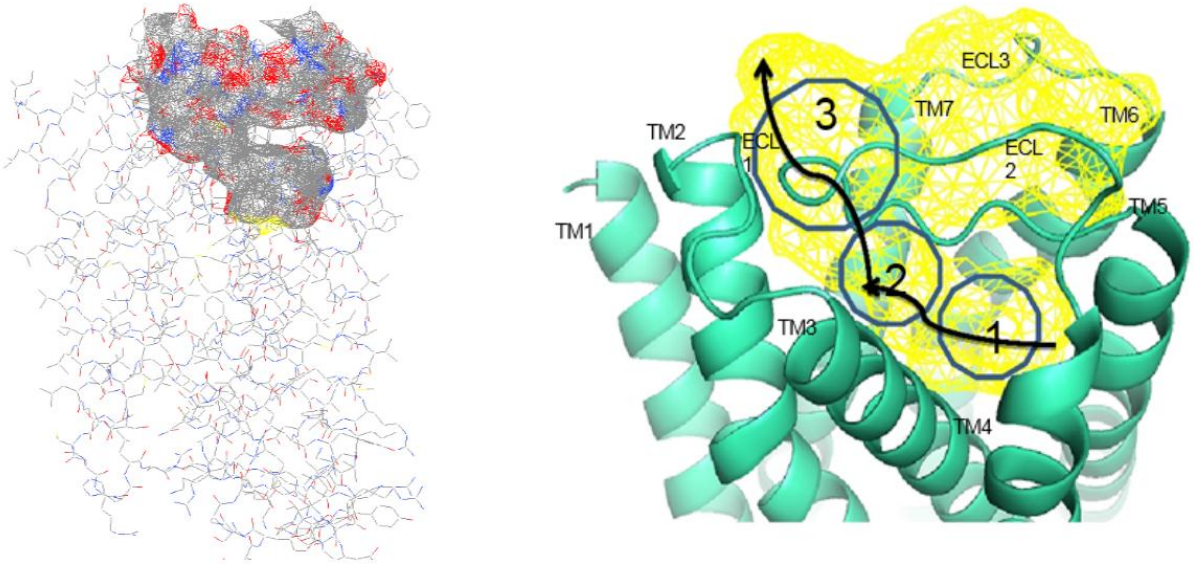

Figure 2-16: The binding cavity and the NE egress pathway. A) Position 1 represents the orthosteric binding site; B) Position 2 (ECL2) represents the auxiliary site 1 and c) Position 3 (ECL1) represent the auxiliary site 2.

2.3.5 Force Profile of NE during Dissociation

The force profile of NE pulling experiments is shown in **Figure 2-17.** The initial force required to pull NE from the orthosteric binding site averages to ~600pN which is considered to be an average value in ligand diffusion SMD experiments showing that initially large amount of force is required to break the strong hydrogen bonds between the NE and Asp125 in TM3 and Ser207 in TM5. Position 1 represents the orthosteric binding site while position 2 represent the auxiliary site 1 (at ECL2) and position 3 represent the auxiliary site 2 (at ECL1). An overlap between the orthosteric binding site and auxiliary site 1 (at ECL2) is also observed along the egress pathway where NE interacts with Tyr203, Ser207 and Ser208 residues in TM5.

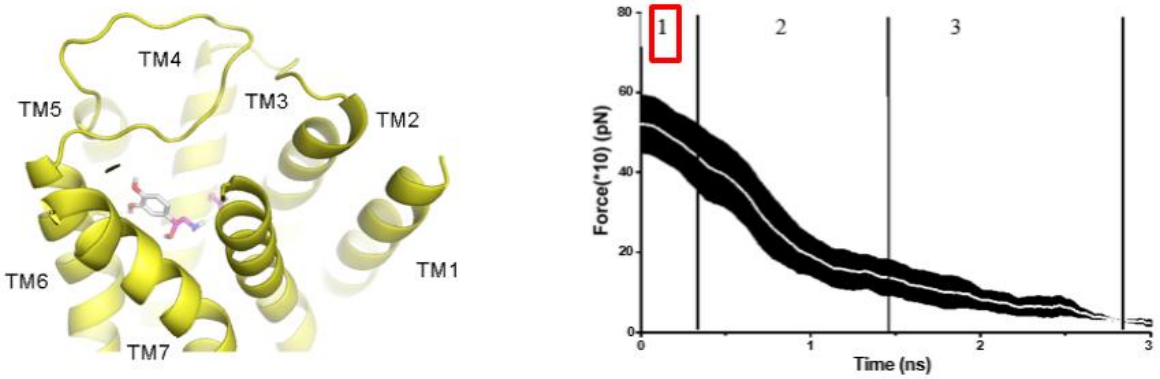

Figure 2-17: Force (averaged) vs Time. Plot showing the force profile of NE SMD simulation run at different time intervals along with three characteristic positions 1, 2 and 3. Highlighted position 1 in red color corresponds to orthosteric site similar to NE docking pose.

The positive slope found in the potential of mean force (PMF) profile (**Figure 2-17**) and an increased force required to pull NE characterises secondary retention sites of NE while exiting from the orthosteric site. The positively charged NE is attracted by the negatively charged residues lining the ECS which may account for ligand binding affinity at these sites.

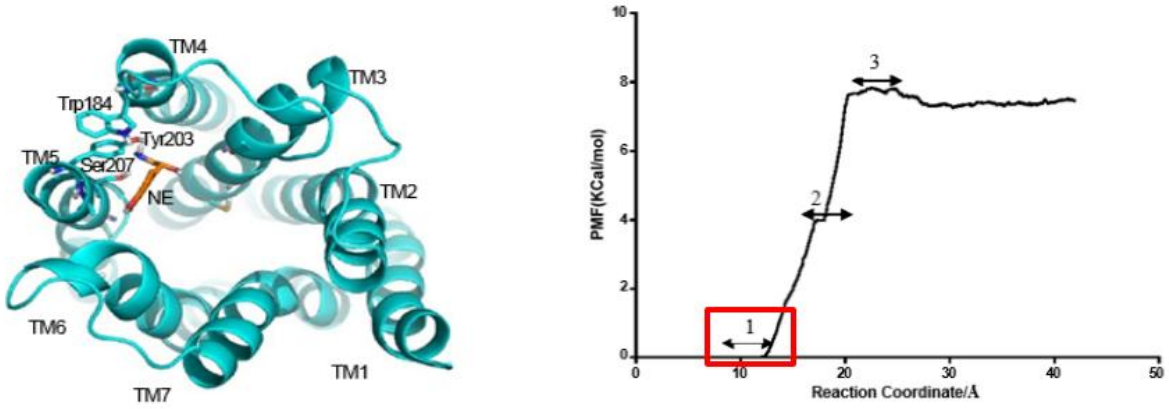

Figure 2-18: PMF plot obtained from adaptive biasing force (ABF) simulation of NE during egress pathway. Highlighted position 1 in red color corresponds to orthosteric site similar to NE docking pose and an overlap site between the orthosteric and auxiliary site 1 (ECL2).

As shown in **Figure 2-17**, NE encounters the biggest energy barrier at the beginning of the simulations wherein the force required to move NE from the cavity averages to 500–600pN during the first 0.4ns and thereafter force decreases gradually as NE move towards ECS. At this position, NE completely dissociates from the orthosteric binding site and is shown to be interacting with the residues Tyr203, Ser207 and Ser208 in TM5.

Our results infer a characteristic pi-pi interaction between side chain of Trp184 in ECL2 and Tyr203 in TM5 (**Figure 2-19**) while hydroxyl group of Tyr203 forms a weak hydrogen bond with amine side chain of NE. At this point, catechol ring of NE flips its position by approximately 180º while still maintaining weak interactions with Tyr203. As the ligand is displaced further, a strong interaction with Glu194 and Val197 in the ECL2 and a salt bridge between the tertiary amine side chain of the NE and Ser207 in TM5 deters further exit of NE. Trp121 in TM3 is at ~3Å to NE and forms intermolecular hydrogen bonds with Val98 in TM2 and stabilises the protein. At this point, NE is stabilised at the interface of ECL1 and ECL2 by Cys195 in ECL2 and Gly109 in ECL1 along with a weak salt bridge formed between the amine side chain and Glu194 in ECL2 which retains NE at this auxiliary site.

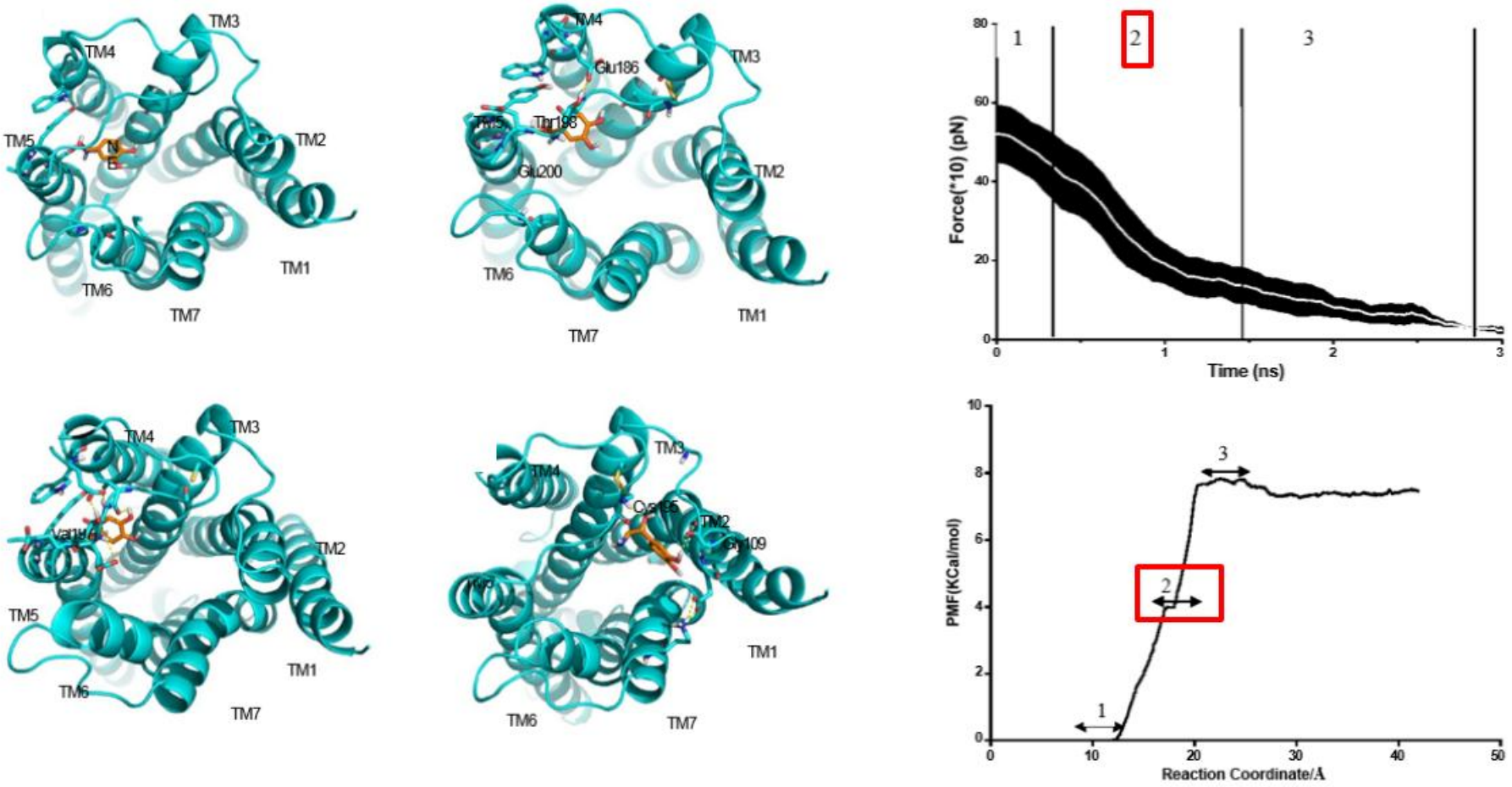

Figure 2-19: Egress route of NE along the position 2 (auxiliary site 1; ECL2 (highlighted in red color)) interacting with residues Cys195, Val197, Thr198, Glu199 and Glu200 along with its respective position as represented in Force averaged vs time and PMF plot.

A characteristic weak pi-pi interaction is observed along the egress pathway between catechol moiety of NE and phenyl ring of Tyr110 in ECL1 which accounts for a short energy barrier and a small force required to break the subsequent interactions (**Figure 2-20**). This position is further stabilised by weak interactions between ligand and residues in ECL1, ECL2 and TM2. As the ligand moves along during simulation, the distance between ligand and ECL1 further decreases and an increment in force is required to overcome the energy barrier formed by strong hydrogen bond between Cys195 and the β-hydroxyl group of NE. Further, a salt bridge between Gly109 and a tertiary amine side chain and a T-pi interaction between catechol moiety of NE and phenyl ring of Tyr110 hinders the egress.

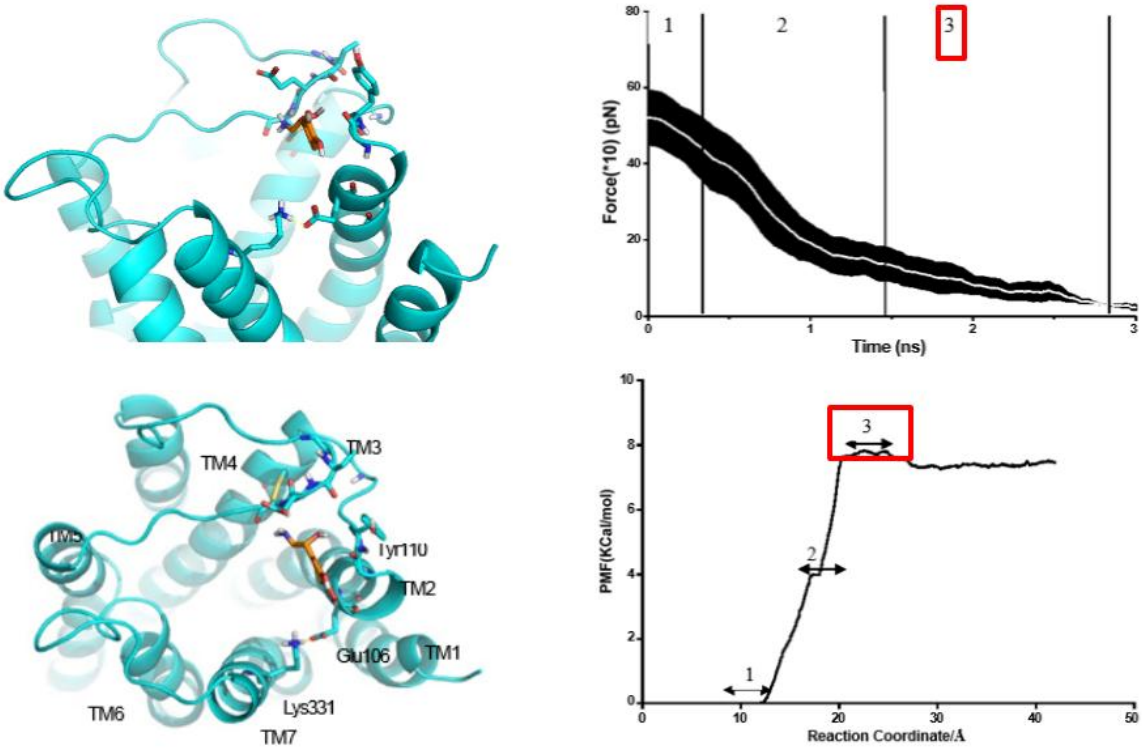

Figure 2-20: Egress route of NE along the position 3 (auxiliary site 2; ECL1 (highlighted in red color)) interacting with residues Gly109 and Tyr110 with its position in Force averaged vs time and PMF plot.

2.3.6 Characterisation of Residues Lining the ECS

From the results obtained, it can be inferred that the positively charged NE is attracted by the negatively charged residues lining the ECS which may account for ligand binding affinity at these sites. Because the ECS is flanked by negative side chains, these help in strong NE binding interactions and hence an extra force is required to break these interactions setting NE free. Thus, these sites may also act as secondary sites for NE retention during its egress from the orthosteric binding site and probably it can be inferred that same route is followed by NE whileentering into the orthosteric binding site. The various residues interacting with NE during egress are listed in **Table 2-1**.

Table 2-1: List of residues in different regions of TM and ECLs interacting with NE during egress pathway as predicted from docking and MD studies.

Residue	TMII	TMIII	TMV	TMVII	ECL1	ECL2	GOLD	AutoDock	Q-SiteFinder	Interaction SIte
Asp125		√					√	√	√	Orthosteric Site
Cys129		√							√	
Trp184						√	√		√	
Phe212			√						√	
Tyr338				√					√	
Tyr203			√				√		√	Overlap b/n orthosteric & Auxiliary site 1
Ser207			√				√	√	√	
Ser208			√						√	
Cys195						√			√	Auxiliary Site 1
Val197						√		√	√	
Thr198						√			√	
Glu199						√	√	√	√	
Glu200						√			√	
Ala204			√				√	√	√	
Gly109					√				√	Auxiliary Site 2
Tyr110					√				√	
Phe117	√								√	
Trp121		√							√	

The route preferred by NE during egress is in conjunction with the results obtained from PDBSUM for crude homology model implying that the egress pathway is same, before and after refining the model and after performing SMD simulations. The refinement of crude homology model was done for steric clashes and loop refinement after initial homology model was obtained. **Figure 2-21** shows a characteristic path taken by NE in which position 1 represents the primary site where NE originally binds in the orthosteric site. Position 2 (auxiliary site 1) represents the probable constriction site for ligand entry and exit surrounded by residues from TM4, TM5 and ECL2 while position 3 (auxiliary site 2) is located in between ECL1 and ECL2.

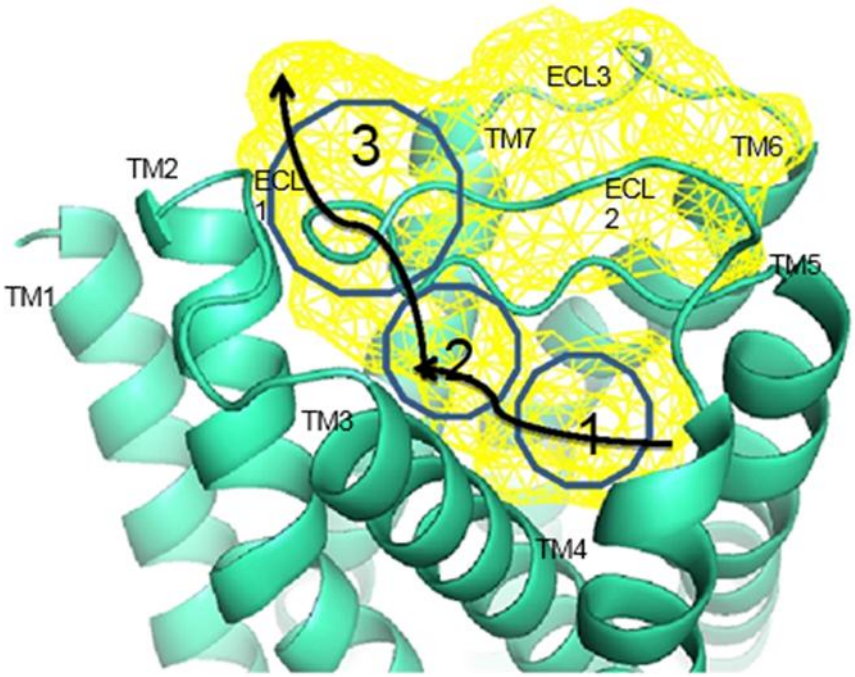

Figure 2-21: Likely egress route for NE from the orthosteric binding site to ECS highlighting position 1 as orthosteric or primary binding site; position 2 as auxiliary site 1 between TMV and ECL2 and position 3 as auxiliary site 2 at ECL1.

2.3.7 Characterisation of Egress Pathway Residue Effect on Prazosin Affinity at α_{1B}-AR

Prazosin binds in the orthosteric pocket below the ECS of the α_{1B}-AR and was used to evaluate the expression levels and structural integrity of the ECS mutants. There was no change in prazosin K_d for the mutants in the TMs adjoining ECL1, TM2, and TM3. In ECL2, no mutants significantly affected prazosin affinity. Alanine mutations in ECL3 and the ECS residues in the adjoining TM6 and TM7 had no significant effect on prazosin affinity. B_{max} values were generated for all mutants.

To determine the contribution of the residues for NE binding identified from SMD of NE from α_{1B}-AR, we mutated these residues to the alanine and glycine across the extracellular portions of associated TM helices. To further confirm the stability of the protein for any conformation changes and structural integrity, K_d value was calculated for antagonist prazosin (**Figure 2-22**) which binds in the site like NE and other agonists. COS-1 cells were used for the expression of the WT and the mutants which were tested initially for their affinity to bind with the antagonist prazosin.

As shown in **Figure 2-22**, no significant changes in the K_d value for prazosin compared to WT (Kd = 0.85 ± 0.197 (3), nM) was observed for Y110A, F117A, Y121A, C129A, W184A,C195A, V197A, T198A, E199A, E200A, Y203A, A204G, A204T, S207A, S08A and F212A. The prazosin K_d increased by 10 fold for G109A and decreased by 8 fold for Y338A. **Table 2-2** summarises the pharmacological characterisation of WT and α_{1B}-AR mutants showing Prazosin $K_{d.}$ and B_{max} determined from saturation binding assays.

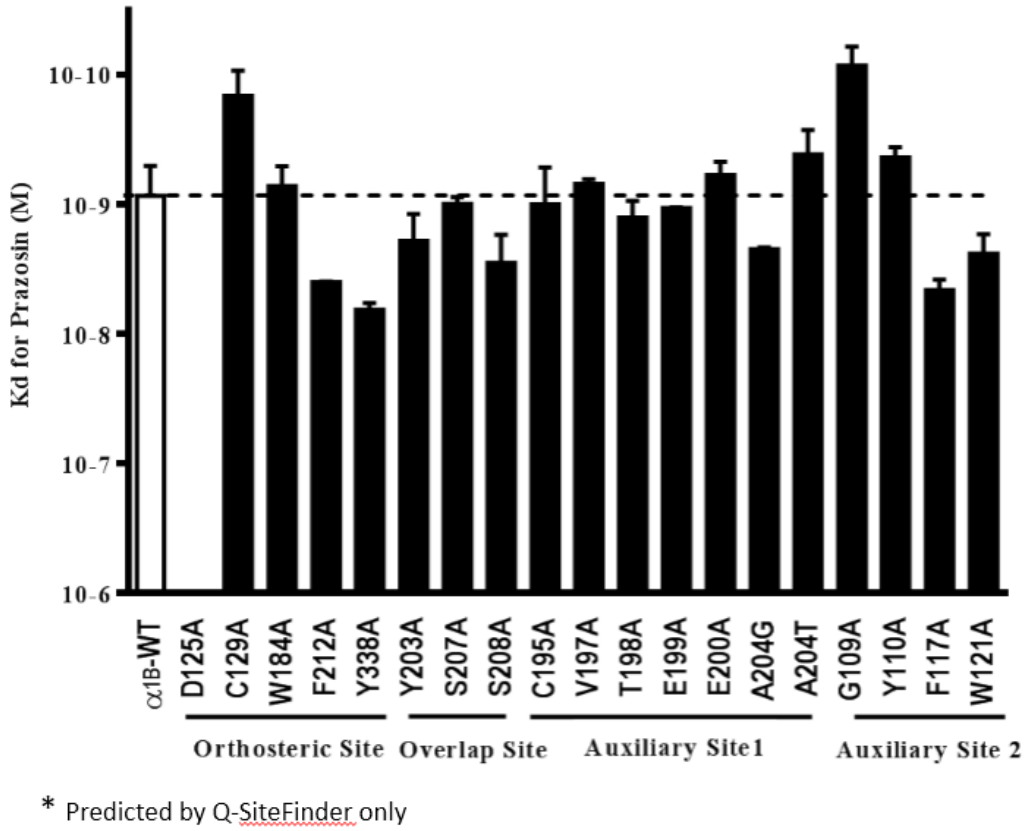

* Predicted by Q-SiteFinder only

Mutants	Prazosin Kd	Interaction Sites
D125A	-	Orthosteric Site
C129A*	X	
W184A	X	
F212A*	X	
Y338A*	8x ↓	
Y203A	X	Overlap b/n Orthosteric and Auxiliary Site 1
S207A	X	
S208A*	X	
C195A	X	Auxiliary Site 1
V197A	X	
T198A	X	
E199A	X	
E200A	X	
A204G	X	
A204T	X	
G109A	10x ↑	Auxiliary Site 2
Y110A	X	
F117A	X	
W121A	X	

Figure 2-22: Effect of α_{1B}-AR mutants on prazosin K_d. A comparison of WT and α_{1B}-AR mutants K_d for prazosin determined from saturation binding curves where nonspecific binding was determined in the presence of 10nM phentolamine. Values are means ± S.E. of 2–4 separate experiments for mutants and n=6 for WT, each performed in triplicate.

2.3.8 Characterisation of NE Efficacy

The binding site mutations predicted from egress pathway and Q-SiteFinder studies were also assessed for altered signaling using the FLIPR platform. These residues were Asp125, Trp184 at orthosteric site (Position 1), Cys195, Val197, Thr198, Glu199, Glu200 and Ala204 at auxiliary site 1 (position 2), Gly109, Tyr110, Phe117 and Trp121 at auxiliary site 2 (position 3) (**Figure 2-21**) plus Cys129, Ser208, Phe212 and Tyr338 predicted from Q-SiteFinder surrounding the orthosteric binding site. Mutation of D125A resulted in total loss of function for NE alike in a study by Hwa et al., [56], while potency decreased by 1000 folds for W121A, C195A and Y203A compared with the WT (5 ± 0.69 (7), nM) α_{1B}-AR receptor. The F212A and Y338A mutants showed a 100 fold decrease in NE potency and Y110A, C129A, W184A, T198A, E200A, A204G, A204T, S207A mutants reduced NE potency by 10 fold. In contrast, G109A, F117A, V197A, E199A and S208A mutants had no effect on signaling as shown in **Figure 2-23**. These residues line the orthosteric binding site and ECS with Gly109, Tyr110 in ECL1; Phe117, Trp121, Asp125, Cys129 in TM3; Trp184, Cys195, Val197, Thr198, Glu199, Glu200 in ECL2; Tyr203, Ala204, Ser207, Ser208, Phe212 in TM5 and Tyr338 in TM7.

Weak interactions between residues lining the ECL2 and NE present in position 2 may account for smaller change (<10 fold reduction) implying mutation of these residues does not have a major influence on NE binding and less force is required to extract the NE from the position 2. Similarly, weak pi-pi and T-pi interactions between the catechol ring of NE and phenolic ring of Tyr110 in ECL1 along with formation of a very weak hydrogen bond between Trp121 and Val98 in TM2 present around the orthosteric binding site may account for greater reduction in NE potency.

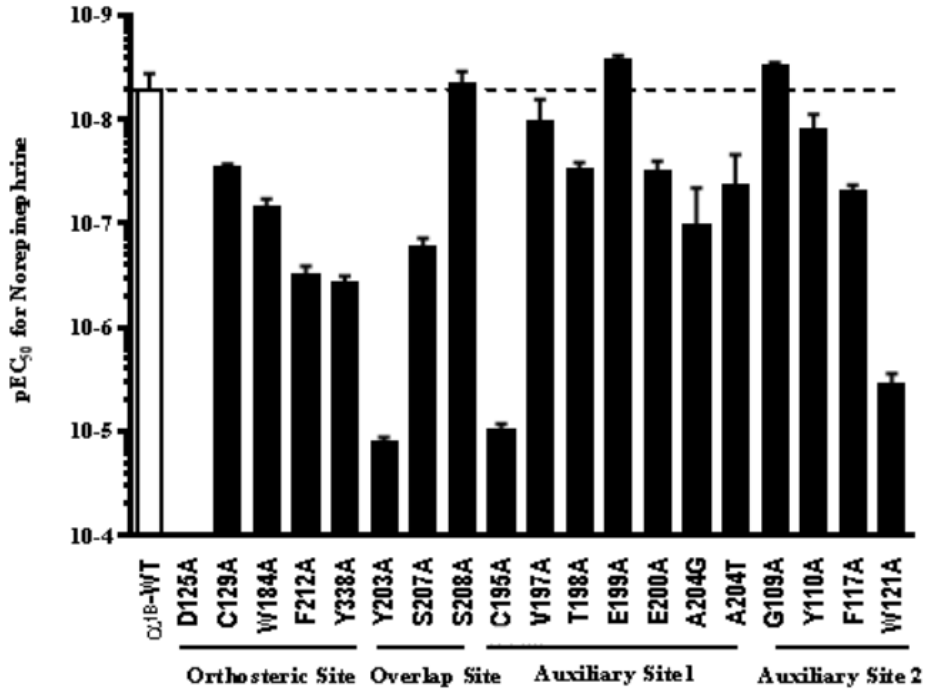

* Predicted by Q-SiteFinder only

Mutants	NE EC_{50}	Interaction Sites
D125A	-	Orthosteric Site
C129A*	10x ↓	
W184A	10x ↓	
F212A*	100x ↓	
Y338A*	100 x↓	
Y203A	1000x ↓	Overlap b/n Orthosteric and Auxiliary Site 1
S207A	50x ↓	
S208A*	X	
C195A	1000x ↓	Auxiliary Site 1
V197A	X	
T198A	10x ↓	
E199A	X	
E200A	10 x↓	
A204G	10 x↓	
A204T	10 x↓	
G109A	X	Auxiliary Site 2
Y110A	X	
F117A	10 x↓	
W121A	1000x ↓	

Figure 2-23: Bar graph showing NE potency at mutated a_{1B}-AR. Comparison of NE EC_{50} values for WT and α_{1B}-AR mutants in response to increasing concentrations of NE in transiently transfected COS-1 cells. Values are means ± S.E.M. of 7 separate experiments for WT and three to four separate experiments for each mutant (each performed in triplicate).

Previous studies on the mutation of residues in ECL1, ECL2, TM3, TM5 and TM7 have revealed their functional importance in receptor activation [7, 11, 19, 28, 39, 56]. Mutation of the D125A in TM3 conserved to class A GPCRs leads to complete loss of the activity while mutation of S207A in TM5 reduces NE affinity by 100 fold. Ser207 forms hydrogen bond with the hydroxyl group of the NE while Asp125 forms hydrogen bond with the amine group of the NE [56]. Residues conserved in the NPxxY motif of TM7 are significant for receptor activation by formation of hydrogen bond between the Tyr223 (TM5) and Tyr338 (TM7) [57]. **Table 2-2** summarises the pharmacological characterisation of WT and mutant α_{1B}-ARs showing NE EC_{50} determined measuring Ca^{2+} in response to increasing concentrations of NE in a FLIPR assay.

2.3.9 Characterisation of NE Affinity at α_{1B}-AR Mutants

To evaluate the effects of mutants on NE binding, the affinity of NE (*Ki*) was determined from the radioligand binding experiments. Similar to loss of activity for D125A in signaling assay, NE did not bind to the receptor when Asp125 was mutated to alanine. This is evident in a study by Cotechhia S [57] where mutation of Asp125 to alanine profoundly impaired the ability of the hamster α_{1B}-AR to bind antagonists. Similar results were obtained by Ragnarsson et al., [39]. In contrast to D125A, the affinity for W184A, Y203A and S207A is significantly decreased by 17-, 67- and 168 folds in position 1 of egress pathway compared to the WT (21.5 ± 0.66 (4) μm). This could be referred as an initial step in egress pathway of NE where NE initially forms strong hydrogen bond with Asp125 and Ser207 and as it moves out of the binding site, a strong pi-pi interaction between the Trp184 and Tyr203 and a hydrogen bond formation between the Tyr203 and NE leads to retention of NE at this secondary site, part of which overlaps with the primary orthosteric binding site.

The residues at auxiliary position 1 in ECL2 (Cys195, Val197, Thr198, Glu199, Glu200 and Ala204) has mixed change in NE affinity. Mutation of V197A resulted in increased affinity for NE by 2- fold whereas affinity drop observed for C195A, T198A, E200A and A204G was 160-, 11-, 5- and 18-fold respectively as shown in **Figure 2-24**. The affinity remains unaffected for E199A compared to WT. The results support the signaling data where mutation of C195A results in breaking of disulphide bond with C118 that provides stability to ECL2 and ECS. The ECL2 along with upper half of TM2, TM3, TM5 and TM7 has mixed ratio of hydrophilic and hydrophobic residues which imparts specific physio-chemical nature to the receptor.

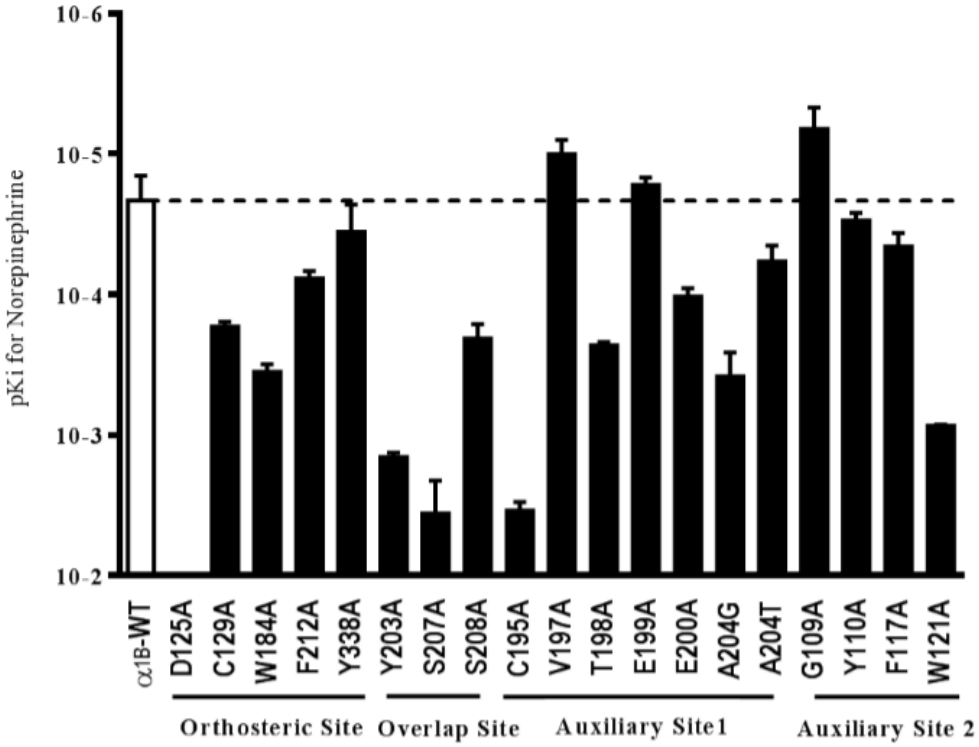

* Predicted by Q-SiteFinder only

Mutants	NE Ki	Interaction Sites
D125A	-	Orthosteric Site
C129A*	8x ↓	
W184A	17x ↓	
F212A*	4x ↓	
Y338A*	2x ↓	
Y203A	67x ↓	Overlap b/n Orthosteric and Auxiliary Site 1
S207A	168x ↓	
S208A*	10x ↓	
C195A	160x ↓	Auxiliary Site 1
V197A	2x ↑	
T198A	11x ↓	
E199A	X	
E200A	5x ↓	
A204G	18x ↓	
A204T	3x ↓	
G109A	3x ↑	Auxiliary Site 2
Y110A	X	
F117A	2x ↓	
W121A	39x ↓	

Figure 2-24: Comparison of *Ki* values for α_{1B}-AR mutants in response to increasing concentrations of NE (n=4). Comparison of NE *Ki* values for WT and a_{1B}-AR mutants. The affinity of NE at the WT receptor and α_{1B}-AR mutants was determined from displacement of the radiolabeled α_1-AR antagonist [^{3}H] prazosin (0.5nM) using membranes from α_{1B}-AR–transfected COS-1 cells (5µg protein) and increasing concentrations of NE. Values are means ± S.E.M. of 4 separate experiments for WT and two to three separate experiments for each mutant (each performed in triplicate).

In position 3 of egress route, the NE affinity for G109A is increased by 3 folds whereas affinity remains unchanged for Y110A and decreases for F117A and W121A by 2- and 39-folds respectively. Trp121 in TM3 around the orthosteric site forms intermolecular hydrogen bond with backbone of Val98 in TM2 and imparts additional stability to the binding site network residues. G109A and Y110A adjacent to each other in ECL1 do not have effect on potency but affinity increases for G109A by 3-folds. At this position, Tyr110 forms a weak T-pi stacking interaction with NE and Gly109 forms a salt bridge with amine side chain of NE during egress.

Phe117 located at tip of TM3 is in close proximity to NE egress pathway and therefore mutation of Phe117 to alanine reduces affinity. Additionally predicted residues from Q-Site finder lining the orthosteric binding site contributes differently to the binding affinity. C129A, S208A, F212A and Y338A have reduced affinity for NE by 8-, 10-, 4- and 2-folds respectively. **Table 2-2** summarises the pharmacological characterisation of WT and mutant α_{1B}-ARs showing NE *Ki* determined from radioligand binding assays.

Table 2-2: Pharmacological characterisation of WT and mutant α_{1B}-ARs showing B_{max} determined from saturation binding assays, Prazosin K_d, NE *Ki* determined from radioligand binding assays and NE EC_{50} determined measuring Ca^{2+} in response to increasing concentrations of NE in FLIPR with NE efficiency = pEC_{50} – pKi [58].

Mutants[a]	B_{max} % of WT	Prazosin K_d (nM)	NE EC_{50} (nM)	NE K_i (µM)	Efficiency (Log Scale)
α_{1B}-WT	100	0.85 ± 0.19 (3)	5 ± 0.69 (7)	21.5 ± 0.66 (4)	3.61 ± 0.33 (4)
D125A	-	-	-	-	-
W184A	77.00 ±16.00 (2)	0.72 ± 0.11 (3)	69 ± 0.82 (6)	354.8 ± 0.88 (3)	3.70 ± 0.13 (3)
Y203A	146.25 ±21.07 (4)	1.92 ± 0.39 (3)	12547 ± 0.90 (6)	1433.9 ± 0.93 (3)	2.05 ± 0.07 (3)
S207A	170.5 ±17.50 (2)	0.99 ± 0.05 (3)	169 ± 0.81 (6)	3613.2 ± 0.58 (3)	4.32 ± 0.32 (3)
C195A	38.50 ±25.50 (2)	1.00 ± 0.28 (3)	9632 ± 0.87 (6)	3440.8 ± 0.86 (3)	2.55 ± 0.11 (3)
V197A	46.00 ±27.00 (2)	0.69 ± 0.02 (3)	10 ± 0.59 (6)	10.0 ± 0.78 (3)	2.97 ± 0.33 (3)
T198A	112.75 ±2.29 (4)	1.26 ± 0.16 (3)	30 ± .0.85 (6)	229.0 ± 0.95 (3)	3.87 ± 0.09 (3)
E199A	113.00 ±58.00 (2)	1.06 ± 0.00 (3)	2 ± 0.89 (6)	16.5 ± 0.88 (3)	3.78 ± 0.10 (3)
E200A	56.00 ±18.00 (2)	0.59 ± 0.06 (3)	31 ± 0.79 (6)	103.1 ± 0.87 (3)	3.51 ± 0.16 (3)
A204G	121.63 ± 20.34 (2)	2.22 ± 0.03 (2)	105 ± 0.42 (4)	383.1 ± 0.67 (3)	3.56 ± 0.53 (3)
A204T	10.89 ± 38.25 (2)	0.41 ± 0.07 (3)	43 ± 0.49 (6)	58.0 ± 0.77 (3)	3.12 ± 0.53 (3)
G109A	49.67 ±11.85 (3)	0.08 ± 0.01 (3)	3 ± 0.93 (7)	6.6 ± 0.70 (3)	3.34 ± 0.18 (3)
Y110A	3.67 ±0.33 (3)	0.43 ± 0.03 (3)	12 ± 0.70 (3)	29.7 ± 0.88 (3)	3.37 ± 0.20 (3)
F117A	62.77 ± 31.53 (2)	4.59 ± 0.37 (2)	50 ± 0.84 (4)	45.7 ± 0.79 (3)	2.95 ± 0.16 (3)
W121A	240.00 ±15.70 (2)	2.39 ± 0.35 (3)	3530 ± 0.79 (6)	831.7 ± 0.98 (3)	2.38 ± 0.11 (3)
C129A	6.92 ± 59.59 (2)	0.14 ± 0.02 (2)	29 ± 0.91 (3)	168.9 ± 0.92 (3)	3.75 ± 0.07 (3)
S208A	172.3 ± 32.63 (2)	2.83 ± 0.61 (2)	4 ± 0.74 (3)	205.4 ± 0.78 (3)	4.65 ± 0.22 (3)
F212A	12.04 ± 66.27 (2)	3.99 ± 0.01 (2)	311 ± 0.82 (3)	76.6 ± 0.88 (3)	2.39 ± 0.13 (3)
Y338A	17.69 ± 20.29 (2)	6.54 ± 0.36 (2)	372 ± 0.85 (3)	35.8 ± 0.63 (4)	1.98 ± 0.26 (4)

[a]Values are the mean ± S.E.M., with the number (n) of separate experiments indicated for each mutant.

2.3.10 Characterisation of NE Signaling Efficiency

NE signaling efficiency for the WT and other mutants was obtained by subtracting the effect of pKi from pEC_{50} (pEC_{50} - pKi). Efficiency characterises the effectiveness of NE for receptor activation on the individual mutants (**Figure 2-25**). In position 1, Y203A showed reduced efficiency by 36-folds and S207A had an increase in efficiency by 5-folds when compared with WT (log 3.61 ± 0.33 (4)) while in position 2, C195A, V197A, T198A and A204T decreased signaling efficiency by 11-, 2-, 4- and 3-folds while rest of the mutants remained unaffected. Position 3 mutants also had effect on efficiency where F117A and W121A reduced efficiency by 5- and 17-folds respectively. Other predicted residues also affected efficiency where F212A and Y338A decreased efficiency by 17- and 43-folds and S208A increased efficiency by 11-folds. Table 2 summarises the pharmacological characteristion of WT and mutant α_{1B}-ARs showing NE efficiency = pEC50 – pKi.

We addressed the exit pathway of NE from the homology model of hamster α_{1B}-AR, the most prevalent drug target involved in many diseases. At the time we conducted our study, no crystal structure of α_{1B}-AR was available in the repository hence to study the ligand dissociation process we built the homology model of hamster α_{1B}-AR from turkey β_1-AR based on the sequence similarity. The successful implementation of the MD simulations in the biological systems has been known and cited many times in the literature.

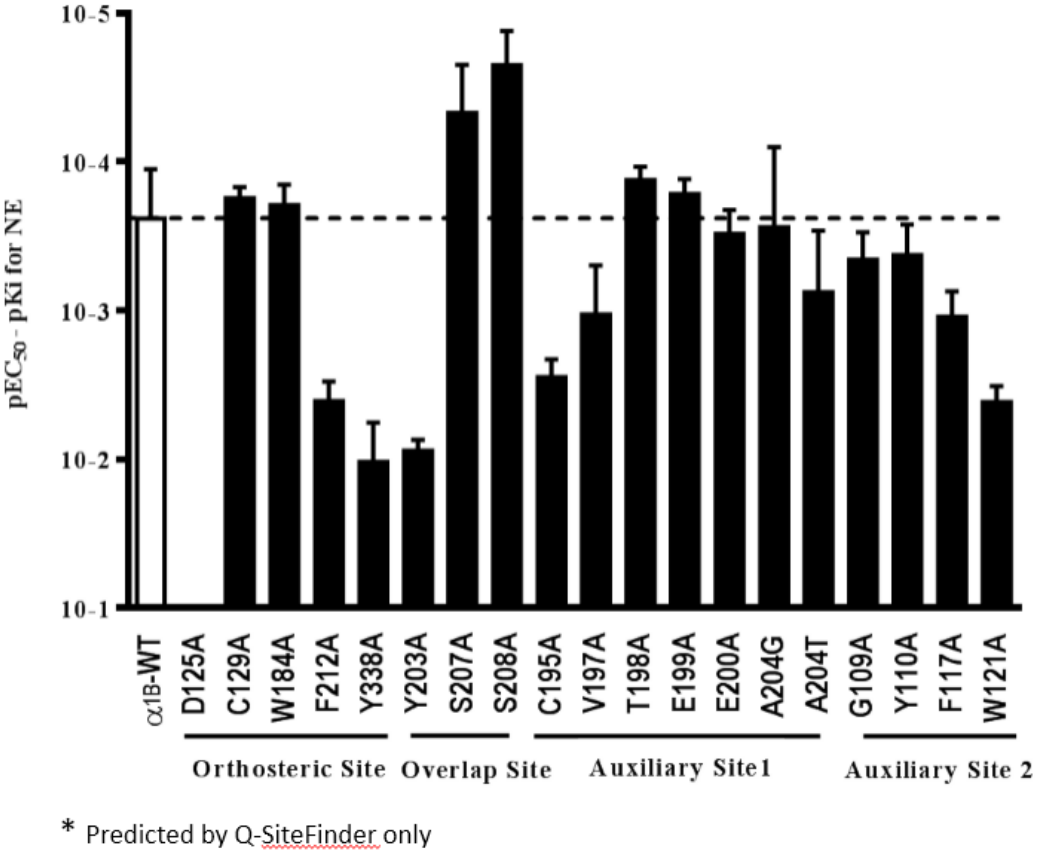

* Predicted by Q-SiteFinder only

Mutants	NE Efficacy	Interaction Sites
D125A	-	Orthosteric Site
C129A*	X	
W184A	X	
F212A*	17x ↓	
Y338A*	43x ↓	
Y203A	36x ↓	Overlap b/n Orthosteric and Auxiliary Site 1
S207A	5x ↑	
S208A*	11x↑	
C195A	11x ↓	Auxiliary Site 1
V197A	4x ↓	
T198A	2x ↑	
E199A	X	
E200A	X	
A204G	X	
A204T	3x ↓	
G109A	X	Auxiliary Site 2
Y110A	X	
F117A	5x ↓	
W121A	17x ↓	

Figure 2-25: Plot showing NE signaling efficiency for α_{1B}-AR mutants. To characterise how effectively NE activated WT and mutant receptors, NE efficacy was calculated as the NE pEC_{50} value minus the NE K_i value (pEC_{50} - pK_i) for NE at WT and α_{1B}-AR mutants. Values are means ± S.E.M. of 7 separate experiments for WT and three separate experiments for each mutant (each performed in triplicate).

MD simulations have been used to study structure-activity relationship at the atomistic level along with association and dissociation of ligand from its drug target. This study helped us to identify the residues that would have gone unnoticed in a more classical site directed mutagenesis study with a primary emphasis on loss- or gain-of-affinity mutations [39, 58]. These residues form transient interactions with NE that contribute to the energetic barriers along the dissociation pathway which may further influence the global conformation of the receptor. Interestingly, the mutants involved in the ligand dissociation process are located in two topographically different clusters at auxiliary sites 1 and 2 apart from the orthosteric binding site. Docking studies of the fenoterol derivatives with β_2-AR indicated that the ligand carazolol and BI-167107 bind to the orthosteric site and their pattern of the interaction is very similar to that of the BI-167107 molecule originally co-crystallised with β_2-AR (active conformation). The 3,5-dihydroxyphenyl group of fenoterol interacts with serines (Ser203, Ser204, Ser207) located at TM5 while the protonated amine group of the ligand is involved in formation of the ionic bridge with the carboxyl group of Asp113 (TM3) [59-61]. Carazolol closely interacts in β_2-AR with TM polar residues like Asp113 (TM3), Asn312 (TM7), Tyr316 (TM7), Ser203 (TM5) and Ser207 (TM5) similar to that observed with docking of NE in our hamster α_{1B}-AR homology model (Asp125 (TM3), Tyr203 (TM5) and Ser207 (TM5)) [25].

The crystal structure of carazolol bound β_2-AR provided static view of β_2-AR-ligand bound state but lacks information about how a ligand diffuses in and out of the receptor or any conformational changes of the receptor accompanying ligand binding and dissociation. The residues lining the orthosteric pocket are mostly conserved among the GPCRs except for residues that line the ECLs which are non-conserved and thus might be responsible for subtype selectivity. ECL2 not only plays specific role in allosterism [62], ligand recognition, ligand specificity [63] and receptor activation process [64, 65] but studies have shown that ECL2 is critical to the ligand binding kinetics due to its conformational flexibility [62, 66]. The interactions broken along the path of NE exit may create resistance for NE dissociation as well as the obstacles for NE entry. RAMD simulations have suggested that ligands access the orthosteric binding site of the β_2-AR mainly through an opening at the ECS.

Ting Wang and Yong Duan have shown that carazolol exited from the binding pocket of β_2-AR through the opening on the ECS via diverse routes; the ECS opening (pathway A i.e., the putative entrance), the cleft between TM4 and TM5 (pathway B), the cleft between TM5 and

TM6 (pathway C), the cleft between TM1 and TM2 (pathway D), the cleft between TM1 and TM7 (pathway E) and the cleft between TM6 and TM7 (pathway F) [25]. The amino acid differences at the entrance/exit, to and from the ligand-binding pocket may contribute to the receptor subtype-selectivity of ligand-binding in the β-AR subfamily.

The residues at the ECS of β_2-AR suggests the existence of an electronegative funnel that attracts positively charged ligands into the orthosteric binding site [67] similar to that observed in our hamster α_{1B}-AR model where electronegatively charged ECS attracts the positively charged NE. The initial force peaks to remove ligands from the orthosteric binding site via extracellular channels C1 or C2 in β_2-AR were on average ~600pN, like extraction of NE from the α_{1B}-AR orthosteric pocket (**Figure 2-4; 2-17**). The force required for pulling ligands from the rhodopsin is double compared to α- and β-ARs for channels other than extracellular route (via TMs 1 and 7 or TMs 5 and 6) [68].

Similar to unbinding of cyanopindolol by disruption of the initial interactions (electrostatic interaction with Asp113 (TM3) and hydrogen bonds with Ser207 (TM5) and Asn312 (TM7) and breaking of interactions with Asp125 (TM3) and Ser207 (TM5) in α_{1B}-AR homology model), the maximal force fall as the ligands displace further from the orthosteric binding site towards the exit channels [69]. The process of ligand extraction shows two retention sites at ~0.9ns and ~1.5ns in both β_1- and β_2-AR identical to the auxiliary position 1 (ECL2) and auxiliary position 2 (ECL1) as observed in our α_{1B}-AR homology model. In the final steps of the simulations, ligand drifted apart from the receptors with no further retention and the force decays to zero.

During dissociation, ligands (carazolol and cyanopindolol) are retained in the boundary with the extracellular solvent (~9–15Å from the orthosteric binding site) in both β_1-AR and β_2-AR while NE is placed at ~13Å from the centre of mass of the protein and is displaced by ~10-13Å towards the ECS during the force pulling experiment as depicted by PMF plot (**Figure 2-18**). These retention sites serve as secondary binding pockets during ligand entry and exit process in the ARs. The residues Asp192 in ECL2 and Lys305 in TM7 forms a salt bridge and separates the two subcavities in β_2-AR [70]. Similar to this, a strong salt bridge is observed in the hamster α_{1B}-AR homology model between the Glu106 in TM1 and Lys331 in TM7.

A systematic alanine scan of the ECL and TM mutants was performed to help understand the role of these residues in class A GPCR function and the contribution of these residues to NE potency, affinity and signaling efficiency. This study identified that ECS residues contributed

significantly to the α_{1B}-AR affinity and efficiency. These residues lined the entrance to the orthosteric binding site where they might affect the NE function allosterically or its access to the binding pocket. Tikhonova I. G. et al., compared the unbinding process of β_1- and β_2-selective antagonists from β_1- and β_2-AR by applying SMD simulations and have shown the potential for a kinetic basis of antagonist selectivity [70].

Clark et al., [71] and Peeters et al., [72, 73] demonstrated the role of residues in ECL1, ECL2 and ECL3 in A2A-R activation including the structurally important WxFG motif similar to WVLG motif in ECL1 of α_{1B}-AR. The adjoining ECL1 mutant Y110A reduced potency but not efficacy. ECL1 is critical to maintain the structural scaffold of class A GPCRs [74], and mutations in ECL1 affect affinity and efficacy that distorts the ECS confirmation. ECL2 is least conserved loop in sequence and structure and participates in the orthosteric binding pocket of rhodopsin [14] andbinding of dopamine to the dopamine receptor [75]. ECL2 influence the agonist versus antagonist function in human-rat $P2Y_4$ receptor [76] and point mutations in ECL2 produced constitutively active receptors [64] or inhibitory effects on signaling when ECL2 flexibility was affected [62].

11 of the 16 mutants in ECL2 of the α_{1B}-AR reduces NE potency including 9 mutants that reduce NE affinity (W184A, K185A, E186A, N190A, D191A, D192A, C195A, T198A and E200A) and four that reduce NE efficacy (N190A, C195A, G196A and V197) [58]. Hwa et al, swapped three of the residues (G196Q, V197I and T198N) in ECL2 of α_{1B}-AR to the corresponding residues in α_{1A}-AR and showed these residues influence the antagonist selectivity between the three α_1-AR subtypes [77]. In our model of hamster α_{1B}-AR, these residues are present at the auxiliary site 1 and might influence the access of NE to the orthosteric binding pocket.

ECL2 is further stabilised by intramolecular interactions in addition to being anchored to the extracellular end of TM3 via conserved cysteine bond that may promote stabilisation of the inactive state [78]. Therefore the conserved disulfide bond between the C118A and C195A mutants (TM3 and ECL2) affect the NE and agonist potency as shown by Ragnarsson et al., [39] in hamster α_{1B}-AR model and other class A GPCRs [18-22, 79-83]. The effect of these mutations can be clustered in various regions based on their affinity and signaling efficiency like at the start of ECL1, mutants tend to reduce NE affinity while mutants across ECL2 reduce efficacy. Disruption of the disulfide bond between Cys118 and Cys195 enhances the ρ-TIA affinity but has no effect on prazosin affinity and reduces NE potency [39].

In the unbound WT-α_{1B}-AR, Asp125 in TM3 forms a salt bridge with Lys331 in TM7 equivalent to what has been established for the rhodopsin receptor but not observed in our α_{1B}-AR model [56]. Mutation of Asp125 has shown specific radioligand binding as demonstrated by Perez et al., [56] on α_{1B}-AR similar to mutation in α_2-AR [84] and β_2-AR [85]. Specific radioligand binding has also been shown for similar aspartic acid counterion mutations in the serotonin receptor [86]. Substitution of a serine or asparagine for the conserved Asp113 in TM3 of the β_2-AR resulted in a reduction of affinity by 10,000-fold for selective AR agonists and antagonists [87]. A functional response in α_{1A}-ARs was observed between AR agonists and specific serine residues in TM5 [88]. The ability to constitutively activate α_{1B}-ARs by substituting many types of amino acids at multiple and diversified positions in the protein suggests the importance of maintaining the basal conformation of the WT receptor [56, 89].

The MD simulation of NE egress from the α_{1B}-AR provides support to the experimental observations and our speculation of unbinding process of the ligand which is a multi-step process. The atomic-level descriptions of the process as observed in this study will deepen our understanding of ligand-GPCR interactions and will lay the structural foundation for future rational design of drugs with optimised binding kinetics.

2.4 References

1. Katritch V, Cherezov V, Stevens RC: **Diversity and modularity of G protein-coupled receptor structures**. *Trends in pharmacological sciences* 2012, **33**(1):17-27.
2. O'Connell TD, Jensen BC, Baker AJ, Simpson PC: **Cardiac α_1-adrenergic receptors: Novel aspects of expression, signaling mechanisms, physiologic function and clinical importance**. *Pharmacological reviews* 2014, **66**(1):308-333.
3. Michelotti GA, Price DT, Schwinn DA: **α_1-adrenergic receptor regulation: Basic science and clinical implications**. *Pharmacology & therapeutics* 2000, **88**(3):281-309.
4. Graham RM, Perez DM, Hwa J, Piascik MT: **α_1-adrenergic receptor subtypes molecular structure, function and signaling**. *Circulation research* 1996, **78**(5):737-749.
5. Furchgott RF: **The pharmacological differentiation of adrenergic receptors**. *Annals of the newyork academy of sciences* 1967, **139**(3):553-570.
6. Adams HR: **Adrenergic agonists and antagonists**. *Veterinary pharmacology and therapeutics* 1995, **7**:87-113.
7. Gnus J, Czerski A, Ferenec S, Zawadzki W, Witkiewicz W, Hauzer W, Rusiecka A, Bujok J: Minneman KP: **In vitro study on the effects of some selected agonists and antagonists of α_1-adrenergic receptors on the contractility of the aneurysmally-changed aortic smooth muscle in humans.** *Journal of physiology and pharmacology* 2012, **63**(1):29-34.
8. Roehrborn CG, Schwinn DA: **α_1-adrenergic receptors and their inhibitors in lower urinary tract symptoms and benign prostatic hyperplasia**. *The journal of urology* 2004, **171**(3):1029-1035.
9. Dror RO, Pan AC, Arlow DH, Borhani DW, Maragakis P, Shan Y, Xu H, Shaw DE: **Pathway and mechanism of drug binding to G protein-coupled receptors**. *Proceedings of the national academy of sciences* 2011, **108**(32):13118-13123.
10. Bokoch MP, Zou Y, Rasmussen SG, Liu CW, Nygaard R, Rosenbaum DM, Fung JJ, Choi H-J, Thian FS, Kobilka TS: **Ligand-specific regulation of the extracellular surface of a G protein-coupled receptor**. *Nature* 2010, **463**(7277):108-112.

11. Zhao M-M, Hwa J, Perez DM: **Identification of critical extracellular loop residues involved in α_1-adrenergic receptor subtype-selective antagonist binding**. *Molecular pharmacology* 1996, **50**(5):1118-1126.
12. Lappano R, Maggiolini M: **G protein-coupled receptors: Novel targets for drug discovery in cancer**. *Nature reviews drug discovery* 2011, **10**(1):47-60.
13. Nygaard R, Frimurer TM, Holst B, Rosenkilde MM, Schwartz TW: **Ligand binding and micro-switches in 7TM receptor structures**. *Trends in pharmacological sciences* 2009, **30**(5):249-259.
14. Palczewski K, Kumasaka T, Hori T, Behnke CA, Motoshima H, Fox BA, Le Trong I, Teller DC, Okada T, Stenkamp RE: **Crystal structure of rhodopsin: A G protein-coupled receptor**. *Science* 2000, **289**(5480):739-745.
15. Schneider EH, Schnell D, Strasser A, Dove S, Seifert R: **Impact of the DRY motif and the missing "ionic lock" on constitutive activity and G protein coupling of the human histamine H4 receptor**. *Journal of pharmacology and experimental therapeutics* 2010, **333**(2):382-392.
16. Mills JS, Miettinen HM, Cummings D, Jesaitis AJ: **Characterisation of the binding site on the formyl peptide receptor using three receptor mutants and analogs of Met-Leu-Phe and Met-Met-Trp-Leu-Leu**. *Journal of biological chemistry* 2000, **275**(50):39012-39017.
17. Karnik SS, Khorana HG: **Assembly of functional rhodopsin requires a disulfide bond between cysteine residues 110 and 187**. *Journal of biological chemistry* 1990, **265**(29):17520-17524.
18. Zhou H, Tai H-H: **Expression and functional characterisation of mutant human CXCR4 in insect cells: Role of cysteinyl and negatively charged residues in ligand binding**. *Archives of biochemistry and biophysics* 2000, **373**(1):211-217.
19. Fraser C: **Site-directed mutagenesis of β-adrenergic receptors. Identification of conserved cysteine residues that independently affect ligand binding and receptor activation**. *Journal of biological chemistry* 1989, **264**(16):9266-9270.
20. Kurtenbach E, Curtis C, Pedder E, Aitken A, Harris A, Hulme E: **Muscarinic acetylcholine receptors. Peptide sequencing identifies residues involved in**

antagonist binding and disulfide bond formation. *Journal of biological chemistry* 1990, **265**(23):13702-13708.

21. Cook JV, Eidne KA: **An intramolecular disulfide bond between conserved extracellular cysteines in the gonadotropin-releasing hormone receptor is essential for binding and activation**. *Endocrinology* 1997, **138**(7):2800-2806.
22. Perlman JH, Wang W, Nussenzveig DR, Gershengorn MC: **A disulfide bond between conserved extracellular cysteines in the thyrotropin-releasing hormone receptor is critical for binding**. *Journal of biological chemistry* 1995, **270**(42):24682-24685.
23. Wang C-IA, Lewis RJ: **Emerging opportunities for allosteric modulation of G protein-coupled receptors**. *Biochemical pharmacology* 2013, **85**(2):153-162.
24. Kuhne S, Kooistra AJ, Bosma R, Bortolato A, Wijtmans M, Vischer HF, Mason JS, de Graaf C, de Esch IJ, Leurs R: **Identification of ligand binding hot spots of the histamine H1 receptor following structure-based fragment optimisation**. *Journal of medicinal chemistry* 2016, **59**(19):9047-9061.
25. Wang T, Duan Y: **Ligand entry and exit pathways in the β_2-adrenergic receptor**. *Journal of molecular biology* 2009, **392**(4):1102-1115.
26. **Johnston JM, Filizola M: Beyond standard molecular dynamics: Investigating the molecular mechanisms of G protein-coupled receptors with enhanced molecular dynamics methods. *Advances in experimental medicine and biology* 2014,796:95-125.**
27. Standfuss J, Edwards PC, D'Antona A, Fransen M, Xie G, Oprian DD, Schertler GF: **Crystal structure of constitutively active rhodopsin: How an agonist can activate its GPCR**. *Nature* 2011, **471**(7340):656-660.
28. González A, Perez-Acle T, Pardo L, Deupi X: **Molecular basis of ligand dissociation in β-adrenergic receptors**. *PLoS one* 2011, **6**(9):e23815.
29. Guo D, Pan AC, Dror RO, Mocking T, Liu R, Heitman LH, Shaw DE, IJzerman AP: **Molecular basis of ligand dissociation from the adenosine A2A receptor**. *Molecular pharmacology* 2016, **89**(5):485-491.
30. Yu R, Kaas Q, Craik DJ: **Delineation of the unbinding pathway of α-conotoxin ImI from the α7 nicotinic acetylcholine receptor**. *The journal of physical chemistry B* 2012, **116**(21):6097-6105.

31. Moukhametzianov R, Warne T, Edwards PC, Serrano-Vega MJ, Leslie AG, Tate CG, Schertler GF: **Two distinct conformations of helix 6 observed in antagonist-bound structures of a β_1-adrenergic receptor**. *Proceedings of the national academy of sciences* 2011, **108**(20):8228-8232.
32. Warne T, Serrano-Vega MJ, Baker JG, Moukhametzianov R, Edwards PC, Henderson R, Leslie AG, Tate CG, Schertler GF: **Structure of a β_1-adrenergic G protein-coupled receptor**. *Nature* 2008, **454**(7203):486-491.
33. Mortier J, Rakers C, Bermudez M, Murgueitio MS, Riniker S, Wolber G: **The impact of molecular dynamics on drug design: Applications for the characterisation of ligand–macromolecule complexes**. *Drug discovery today* 2015, **20**(6):686-702.
34. Boeckmann B, Bairoch A, Apweiler R, Blatter M-C, Estreicher A, Gasteiger E, Martin MJ, Michoud K, O'Donovan C, Phan I: **The SWISS-PROT protein knowledgebase and its supplement TrEMBL in 2003**. *Nucleic acids research* 2003, **31**(1):365-370.
35. Bairoch A, Apweiler R, Wu CH, Barker WC, Boeckmann B, Ferro S, Gasteiger E, Huang H, Lopez R, Magrane M: **The universal protein resource (UniProt)**. *Nucleic acids research* 2005, **33**(suppl 1):D154-D159.
36. Gertz EM: **BLAST scoring parameters**. *Manuscript* 2005.
37. Eswar N, Webb B, Marti-Renom MA, Madhusudhan M, Eramian D, Shen My, Pieper U, Sali A: **Comparative protein structure modeling using Modeller**. *Current protocols in bioinformatics* 2006, **5**(6): 1-47.
38. Laurie AT, Jackson RM: **Q-SiteFinder: An energy-based method for the prediction of protein–ligand binding sites**. *Bioinformatics* 2005, **21**(9):1908-1916.
39. Ragnarsson L, Wang C-IA, Andersson Å, Fajarningsih D, Monks T, Brust A, Rosengren KJ, Lewis RJ: **Conopeptide ρ-TIA defines a new allosteric site on the extracellular surface of the α_{1B}-adrenoceptor**. *Journal of biological chemistry* 2013, **288**(3):1814-1827.
40. Trott O, Olson AJ: **AutoDock Vina: Improving the speed and accuracy of docking with a new scoring function, efficient optimisation and multithreading**. *Journal of computational chemistry* 2010, **31**(2):455-461.

41. Verdonk ML, Cole JC, Hartshorn MJ, Murray CW, Taylor RD: **Improved protein–ligand docking using GOLD**. *Proteins: Structure, function and bioinformatics* 2003, **52**(4):609-623.

42. Phillips JC, Braun R, Wang W, Gumbart J, Tajkhorshid E, Villa E, Chipot C, Skeel RD, Kale L, Schulten K: **Scalable molecular dynamics with NAMD**. *Journal of computational chemistry* 2005, **26**(16):1781-1802.

43. Nelson MT, Humphrey W, Gursoy A, Dalke A, Kalé LV, Skeel RD, Schulten K: **NAMD: A parallel, object-oriented molecular dynamics program**. *International journal of high performance computing applications* 1996, **10**(4):251-268.

44. Grubmüller H: **SOLVATE v. 1.0. Theoretical Biophysics Group**. *Institute for medical optics, ludwig-maximilians university, munich* 1996.

45. Humphrey W, Dalke A, Schulten K: **VMD: Visual molecular dynamics**. *Journal of molecular graphics* 1996, **14**(1):33-38.

46. Spijker P, Vaidehi N, Freddolino PL, Hilbers PA, Goddard WA: **Dynamic behavior of fully solvated β_2-adrenergic receptor embedded in the membrane with bound agonist or antagonist**. *Proceedings of the national academy of sciences* 2006, **103**(13):4882-4887.

47. Brooks BR, Bruccoleri RE, Olafson BD, States DJ, Swaminathan S, Karplus M: **CHARMM: A program for macromolecular energy, minimisation and dynamics calculations**. *Journal of computational chemistry* 1983, **4**(2):187-217.

48. Tu K, Tobias DJ, Klein ML: **Constant pressure and temperature molecular dynamics simulation of a fully hydrated liquid crystal phase dipalmitoylphosphatidylcholine bilayer**. *Biophysical journal* 1995, **69**(6):2558-2562.

49. Darden T, York D, Pedersen L: **Particle mesh Ewald: An N· log (N) method for Ewald sums in large systems**. *The Journal of chemical physics* 1993, **98**(12):10089-10092.

50. Allen MP, Wilson MR: **Computer simulation of liquid crystals**. *Journal of computer-aided molecular design* 1989, **3**(4):335-353.

51. Miyamoto S, Kollman PA: **SETTLE: An analytical version of the SHAKE and RATTLE algorithm for rigid water models**. *Journal of computational chemistry* 1992, **13**(8):952-962.

52. Izrailev S, Stepaniants S, Isralewitz B, Kosztin D, Lu H, Molnar F, Wriggers W, Schulten K: **Steered molecular dynamics**. *Computational molecular dynamics: Challenges, methods, ideas.* 1998: 39-65.

53. Gore J, Ritort F, Bustamante C: **Bias and error in estimates of equilibrium free-energy differences from nonequilibrium measurements**. *Proceedings of the national academy of sciences* 2003, **100**(22):12564-12569.

54. Berman HM, Westbrook J, Feng Z, Gilliland G, Bhat T, Weissig H, Shindyalov IN, Bourne PE: **The protein data bank**. *Nucleic acids research* 2000, **28**(1):235-242.

55. Kihara D, Chen H, Yang YD: **Quality assessment of protein structure models**. *Current protein and peptide science 2009*. **10**(3):216-228.

56. Porter JE, Hwa J, Perez DM: **Activation of the α_{1B}-adrenergic receptor is initiated by disruption of an interhelical salt bridge constraint**. *Journal of biological chemistry* 1996, **271**(45):28318-28323.

57. Cotecchia S: **Constitutive activity and inverse agonism at the α_1 adrenoceptors**. *Biochemical pharmacology* 2007, **73**(8):1076-1083.

58. Ragnarsson L, Andersson Å, Thomas WG, Lewis RJ: **Extracellular surface residues of the α_{1B}-adrenoceptor critical for G protein–coupled receptor function**. *Molecular pharmacology* 2015, **87**(1):121-129.

59. Kolinski M, Plazinska A, Jozwiak K: **Recent progress in understanding of structure, ligand interactions and the mechanism of activation of the β_2-adrenergic receptor**. *Current medicinal chemistry* 2012, **19**(8):1155-1163.

60. Plazinska A, Kolinski M, Wainer IW, Jozwiak K: **Molecular interactions between fenoterol stereoisomers and derivatives and the β_2-adrenergic receptor binding site studied by docking and molecular dynamics simulations**. *Journal of molecular modeling* 2013, **19**(11):4919-4930.

61. Plazinska A, Plazinski W, Jozwiak K: **Fast, metadynamics-based method for prediction of the stereochemistry-dependent relative free energies of ligand–receptor interactions**. *Journal of computational chemistry* 2014, **35**(11):876-882.

62. Avlani VA, Gregory KJ, Morton CJ, Parker MW, Sexton PM, Christopoulos A: **Critical role for the second extracellular loop in the binding of both orthosteric and**

allosteric G protein-coupled receptor ligands. *Journal of biological chemistry* 2007, **282**(35):25677-25686.

63. Samson M, LaRosa G, Libert F, Paindavoine P, Detheux M, Vassart G, Parmentier M: **The second extracellular loop of CCR5 is the major determinant of ligand specificity**. *Journal of biological chemistry* 1997, **272**(40):24934-24941.
64. Klco JM, Wiegand CB, Narzinski K, Baranski TJ: **Essential role for the second extracellular loop in C5a receptor activation**. *Nature structural & molecular biology* 2005, **12**(4):320-326.
65. Scarselli M, Li B, Kim S-K, Wess J: **Multiple residues in the second extracellular loop are critical for M3 muscarinic acetylcholine receptor activation**. *Journal of biological chemistry* 2007, **282**(10):7385-7396.
66. Gkountelias K, Tselios T, Venihaki M, Deraos G, Lazaridis I, Rassouli O, Gravanis A, Liapakis G: **Alanine scanning mutagenesis of the second extracellular loop of type 1 corticotropin-releasing factor receptor revealed residues critical for peptide binding**. *Molecular pharmacology* 2009, **75**(4):793-800.
67. Cherezov V, Rosenbaum DM, Hanson MA, Rasmussen SG, Thian FS, Kobilka TS, Choi H-J, Kuhn P, Weis WI, Kobilka BK: **High-resolution crystal structure of an engineered human β_2-adrenergic G protein–coupled receptor**. S*cience* 2007, **318**(5854):1258-1265.
68. Takemoto M, Kato HE, Koyama M, Ito J, Kamiya M, Hayashi S, Maturana AD, Deisseroth K, Ishitani R, Nureki O: **Molecular dynamics of channel rhodopsin at the early stages of channel opening**. *Plos one* 2015, **10**(6):e0131094.
69. Liu X, Xu Y, Wang X, Barrantes FJ, Jiang H: **Unbinding of nicotine from the acetylcholine binding protein: Steered molecular dynamics simulations**. *The Journal of physical chemistry B* 2008, **112**(13):4087-4093.
70. Selvam B, Wereszczynski J, Tikhonova IG: **Comparison of dynamics of extracellular accesses to the β_1 and β_2 adrenoceptors binding sites uncovers the potential of kinetic basis of antagonist selectivity**. *Chemical biology & drug design* 2012, **80**(2):215-226.

71. Clark SD, Tran HT, Zeng J, Reinscheid RK: **Importance of extracellular loop one of the neuropeptide S receptor for biogenesis and function**. *Peptides* 2010, **31**(1):130-138.

72. Peeters MC, van Westen GJ, Guo D, Wisse LE, Müller CE, Beukers MW, IJzerman AP: **GPCR structure and activation: An essential role for the first extracellular loop in activating the adenosine A2B receptor**. *The FASEB journal* 2011, **25**(2):632-643.

73. Peeters M, Wisse L, Dinaj A, Vroling B, Vriend G, Ijzerman A: **The role of the second and third extracellular loops of the adenosine A1 receptor in activation and allosteric modulation**. *Biochemical pharmacology* 2012, **84**(1):76-87.

74. Venkatakrishnan A, Deupi X, Lebon G, Tate CG, Schertler GF, Babu MM: **Molecular signatures of G protein-coupled receptors**. *Nature* 2013, **494**(7436):185-194.

75. Shi L, Javitch JA: **The second extracellular loop of the dopamine D2 receptor lines the binding-site crevice**. *Proceedings of the national academy of sciences* 2004, **101**(2):440-445.

76. Herold CL, Qi A-D, Harden TK, Nicholas RA: **Agonist versus antagonist action of ATP at the P2Y4 receptor is determined by the second extracellular loop**. *Journal of biological chemistry* 2004, **279**(12):11456-11464.

77. Hwa J, Graham RM, Perez DM: **Identification of critical determinants of α_1-adrenergic receptor subtype selective agonist binding**. *Journal of biological chemistry* 1995, **270**(39):23189-23195.

78. Massotte D, Kieffer BL: **The second extracellular loop: A damper for G protein–coupled receptors?** *Nature structural & molecular biology* 2005, **12**(4):287-288.

79. Dixon R, Sigal I, Candelore M, Register R, Scattergood W, Rands E, Strader C: **Structural features required for ligand binding to the β-adrenergic receptor**. *The EMBO journal* 1987, **6**(11):3269-3275.

80. Dohlman HG, Caron MG, DeBlasi A, Frielle T, Lefkowitz RJ: **Role of extracellular disulfide-bonded cysteines in the ligand binding function of the β_2-adrenergic receptor**. *Biochemistry* 1990, **29**(9):2335-2342.

81. Karnik SS, Sakmar TP, Chen H-B, Khorana HG: **Cysteine residues 110 and 187 are essential for the formation of correct structure in bovine rhodopsin**. *Proceedings of the national academy of sciences* 1988, **85**(22):8459-8463.

82. Noda K, Saad Y, Graham RM, Karnik SS: **The high affinity state of the β_2-adrenergic receptor requires unique interaction between conserved and non-conserved extracellular loop cysteines**. *Journal of biological chemistry* 1994, **269**(9):6743-6752.

83. Lin SW, Sakmar TP: **Specific tryptophan UV-absorbance changes are probes of the transition of rhodopsin to its active state**. *Biochemistry* 1996, **35**(34):11149-11159.

84. Wang C-D, Buck MA, Fraser CM: **Site-directed mutagenesis of α_{2A}-adrenergic receptors: Identification of amino acids involved in ligand binding and receptor activation by agonists**. *Molecular pharmacology* 1991, **40**(2):168-179.

85. Strader CD, Gaffney T, Sugg E, Candelore MR, Keys R, Patchett A, Dixon R: **Allele-specific activation of genetically engineered receptors**. *Journal of biological chemistry* 1991, **266**(1):5-8.

86. Ho BY, Karschin A, Branchek T, Davidson N, Lester HA: **The role of conserved aspartate and serine residues in ligand binding and in function of the 5-HT1A receptor: A site-directed mutation study**. *FEBS letters* 1992, **312**(2-3):259-262.

87. Strader CD, Fong TM, Tota MR, Underwood D, Dixon RA: **Structure and function of G protein-coupled receptors**. *Annual review of biochemistry* 1994, **63**(1):101-132.

88. Hwa J, Perez D: **The unique nature of the serine residues involved in α_1-adrenergic receptor binding and activation**. *Journal of biological chemistry* 1996, **271**:6322-6327.

89. Kjelsberg MA, Cotecchia S, Ostrowski J, Caron M, Lefkowitz R: **Constitutive activation of the α_{1B}-adrenergic receptor by all amino acid substitutions at a single site. Evidence for a region which constrains receptor activation**. *Journal of biological chemistry* 1992, **267**(3):1430-1433.

Chapter 3

Chapter 3: Characterisation of α_{1B}-AR upon Agonist Binding by Computational Approach

3.1 Introduction

α_1-AR function through catecholamine, particularly NE and E primarily by increasing or decreasing the intracellular production of secondary messengers such as cAMP or IP3/DAG [1]. α_1-AR are present post-junctionally to the effector organs and regulates secretion from the gland, gut contraction, glycogenolysis in liver and arrhythmias in the heart [2]. They represent important targets for drugs for the treatment of a broad spectrum of diseases including benign prostatic hyperplasia, hypertension and anxiety disorders [3, 4].

TMs of the functionally active crystal structures of the class A GPCRs known till date like opsin (active metarhodopsin II (3PQR)) [5], β_2-AR (active G protein-bound (3SN6) [6], active-like nanobody bound (3POG)) [7]; A2A-R (agonist UK432097 bound (3QAK) [8]) internally rearranges towards the cytoplasmic side that leads to cascade of bond swapping and bond forming events [9, 10] (**Figure 3-1**).

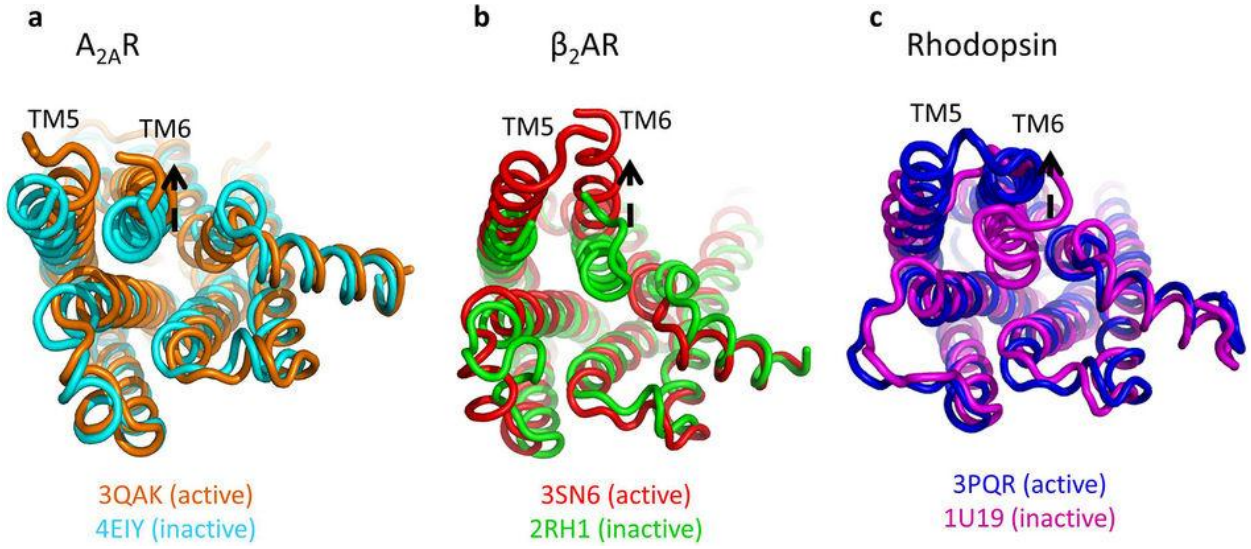

Figure 3-1: Comparison of active and inactive GPCR crystal structures [11] (Image courtesy: Libin ye et al., *Nature;* 2016;533;265-268).

Rhodopsin was the first GPCR to be crystallised initially in an inactive state with an inverse agonist 11-*cis*-retinal and provides a unique structural framework to study GPCR activation.The ligand (blue) in the inactive **(a–c)** and active **(d–f)** conformation of rhodopsin, the β_2-AR and A2A-R is embedded in a binding pocket located mainly between TM3, TM5, TM6 and TM7

(**Figure 3-2**). The binding of agonists induces related conformational changes around the interhelix interfaces that result into rotation of TM6 and rearrangement of TM5 and TM7.

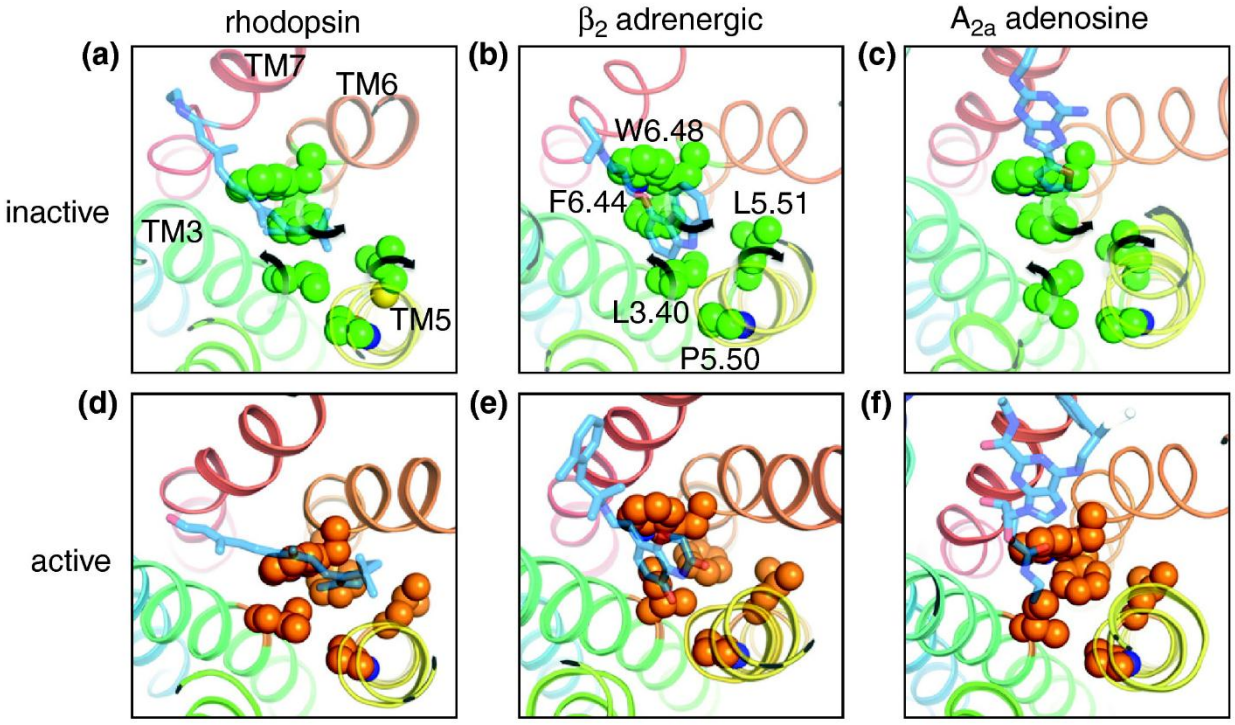

Figure 3-2: Conserved features of agonist-induced activation in three different G protein-coupled receptors through a transmission switch in the TM3–TM5–TM6 helix interfaces [12] (Image courtesy: Deupi et al., *Curr. Opin. Struct. Biol.;* 2011;21;541-551).

In rhodopsin, A2A-R and to some extent in β_2-AR, rotation of TM6 is accompanied by a translocation of $Trp^{6.48}$ [13] located close to the base of the binding pocket. In the inactive state, the retinal β-ionone ring in the case of rhodopsin (panel a) or a ribose ring that is a key feature of most A2A-R antagonists (panel c) occupies the position where $Trp^{6.48}$ will move upon activation (panels d + f). Hence, translocation of $Trp^{6.48}$ may be concluded as a common feature of GPCR activation. One helix turn towards the cytoplasmic side of TM6, sits the conserved $Phe^{6.44}$ that in all active-state structures moves towards TM5 where it leads to rearrangement of $Leu^{5.51}$ close to $Pro^{5.50}$. Also, relocation of $Ile/Leu^{3.40}$ away from $Pro^{5.50}$ further contributes to these changes in the local structure which can be transmitted through TM5 [12]. **Figure 3-3** outlines the agonist induced activation process.

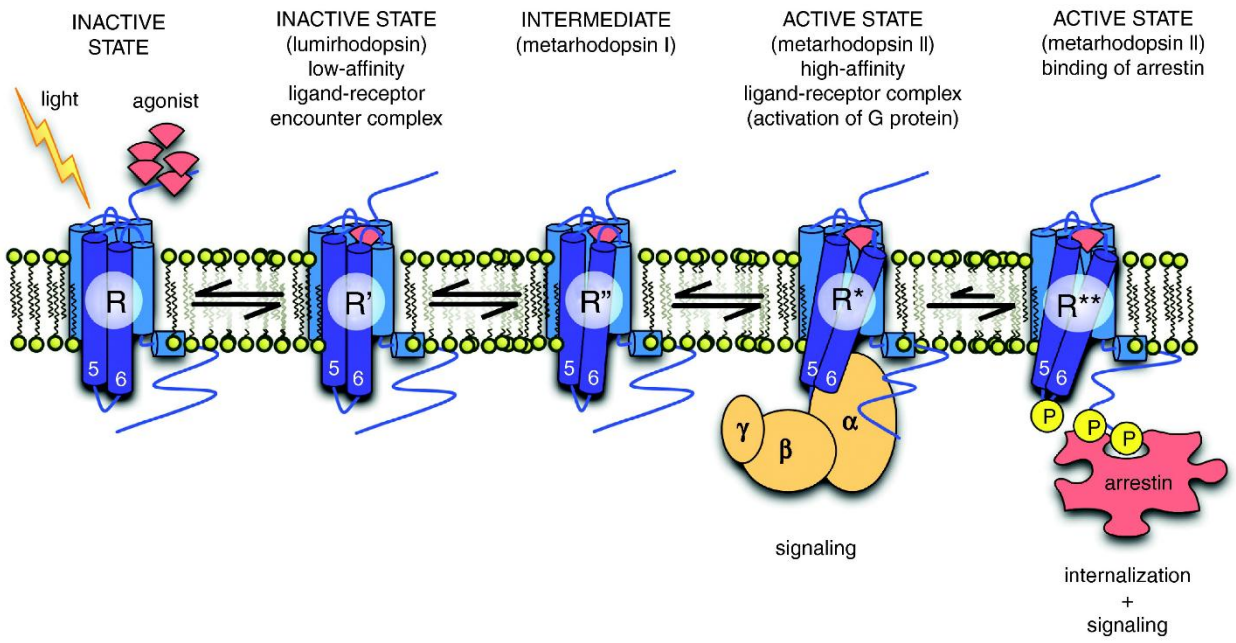

Figure 3-3: Conceptual overview of agonist-induced activation in class A GPCRs [12] (Image courtesy: Deupi et al., *Curr. Opin. Struct. Biol.;* 2011;21;541-551).

In the active state, salt bridge is broken between the $D^{3.49}$(E)RY motif in TM3 and $Glu^{6.50}$ in TM6 with an outward movement of TM6 by ~3 to 8Å (**Figure 3-4**). The cytoplasmic end of TM6 in active β_2-AR is tilted outward by 14Å and 11Å when coupled with the G protein [6] and its mimetic nanobody [7]. However, a smaller TM6 movement (~6–7Å) is observed in ligand-free opsin [5]. Ballesteros et al., predicted disruption of ionic lock between TM3 and TM6 in β_2-AR that leads to constitutive activation of the receptor. Mutation of $Glu^{6.50}$ in TM6 to glutamine or alanine (E268Q or E268A) and mutation of aspartic acid in DRY motif to asparagine (D130N) or combination of these mutants D130N/E268Q or D130N/E268A caused elevation of basal agonist-independent cAMP accumulation in transiently transfected COS-7 cells as compared with the WT receptor [14].

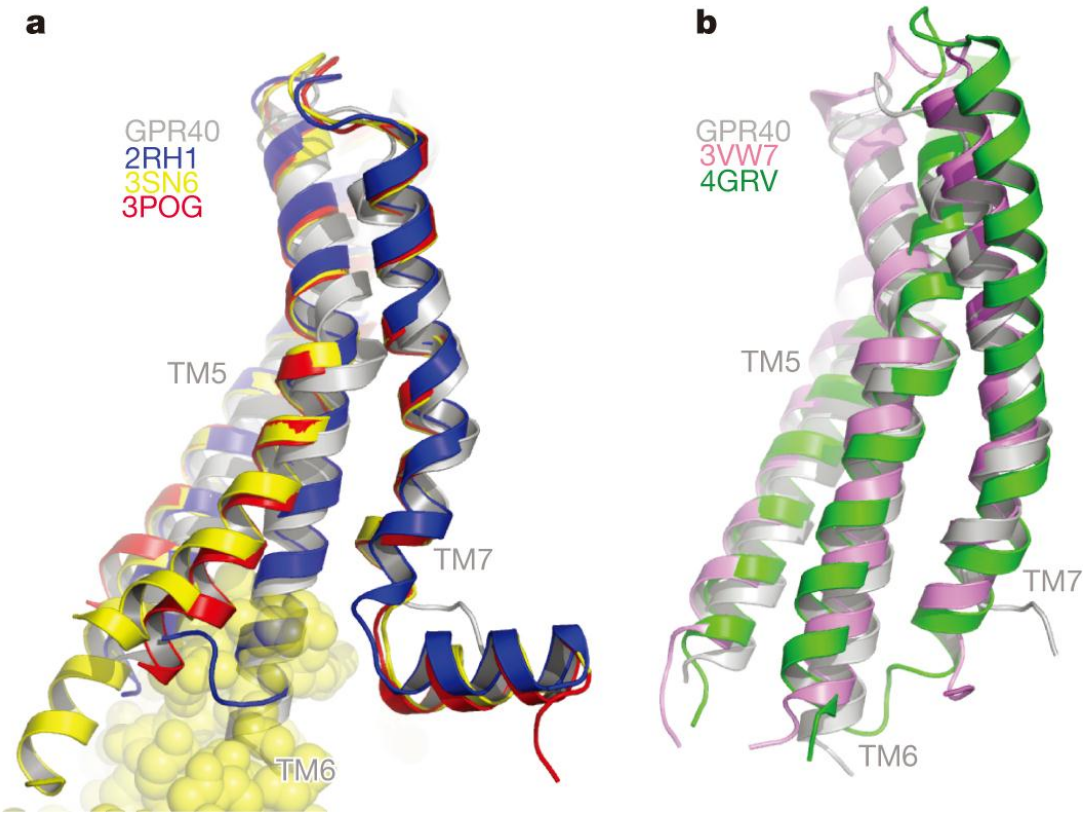

Figure 3-4: Structure alignment of active and inactive GPCR structures with an outward movement of TM by 3-8 Å [15] (Image courtesy: Srivastava A. et al., *Nature;* 2014;1-4).Structures are aligned based on equivalent residues in TM helices A) On the basis of the compendium of activation states of β_2-AR and hGPR40 (grey) TM5 and TM6 adopt an orientation most like the inactive (antagonist bound) state and B) A comparison with structurally similar peptide-binding receptors, NTSR1 (active-like 4GRV in green) and PAR1 (inactive 3VW7 in magenta), suggests receptor subclasses may have a significant impact on TM5 and TM6 orientation regardless of activation state.

Scheer et al., suggested that in α_{1B}-AR, protonation of the $Asp^{3.49}$ adjacent to $Arg^{3.50}$ shifts $Arg^{3.50}$ out of the polar pocket formed by the TMs 1, 2 and 7. This shift leads to long range conformational changes [16]. An ensemble of different conformations characterise α_1-AR to be constitutionally active and thus possess a certain degree of basal activity without binding to an agonist [17]. Cotecchia reported constitutive activity of the wild type α_{1A}- and α_{1B}-AR when the receptors were overexpressed in COS-7 cells [17]. The spontaneous activity of the α_{1B}-AR was greater than that of the α_{1A}-AR expressed at similar levels (3–4pmol/mg of protein) [18]. For the wild type α_{1D}-AR, constitutive activity and internalisation was reported for the receptor expressed in rat fibroblasts [19, 20]. Experimentally, mutation of the aspartate of the D(E)RY

motif in TM3 and Glu289$^{6.30}$ in TM6 markedly increased the constitutive activity of the α_{1B}-AR [21].

Single molecule spectroscopy experiments [22] have demonstrated that even in the absence of ligands, β_2-AR exists in equilibrium between a number of discrete conformational states [23]. Agonist binding promotes activation by shifting this equilibrium toward the active states although binding of G protein is required for their full stabilisation. Fluorescence resonance energy transfer (FRET) experiments can detect distinct conformational changes induced by E and NE and allows the calculation of activation kinetics [24]. This change in conformations leads to receptor activation and deactivation based upon binding of an agonist and inverse agonist while binding of an antagonist blocks binding of other ligands to the receptor with no signaling [25, 26].

Despite availability of the few active structures, most GPCRs lack active-state crystal structures. However, a lot has been inferred from mutagenesis, fluorescent labeling and other biophysics experiments. These experiments provided more valid information of the dynamic process than a frozen snap shot of the receptor that has been manipulated to stabilise a specific confirmation for crystallisation (chapter 1, Nygarrd et al.,). The activation mechanism is accompanied by questions which need to be resolved to understand the process of receptor activation like how ligand binding at ECS triggers signaling at intracellular G protein coupling site? how many conformational states are required before activation? how the active conformational state transits with other active states or remain stables during activation?

Many computational studies have been undertaken to study the GPCR activation mechanism [27-34] but the goal could not be attained despite of the use of supercomputers. Inactive conformations along with transitions were observed for the active structure of β_2-AR on microsecond level timeframe by cMD in a study by Dror et al., [35]. In a similar study on M2 muscarinic receptor, binding of antagonist tiotropium to the extracellular vestibule of the apo form of the receptor was observed but the structure remained inactive.

Miao et al., demonstrated the use of aMD on M2 muscarinic receptor to study receptor activation [33]. They observed direct activation of the ligand-free (apo) form of the M2 receptor through hundreds of nanosecond aMD simulations. The receptor activation was characterised by formation of a hydrogen bond between the Tyr206$^{5.58}$ – Tyr440$^{7.53}$ and outward movement of cytoplasmic end of TM6 by ~6Å (**Figure 3-5**), which is in agreement with previous GPCR

studies where TM6 has been suggested to be a switch for the conformational transitions of the M5 receptor between inactive and active states [36].

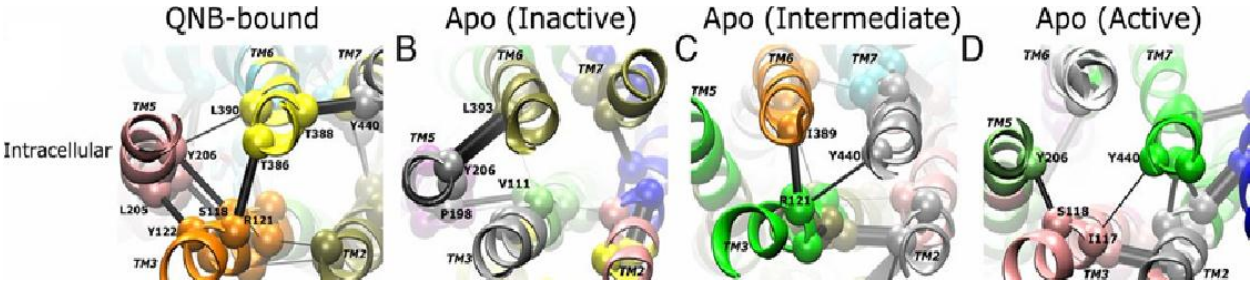

Figure 3-5: A highly dynamic transition network identified in the M2 receptor [33] (Image courtesy: Miao Y. et al., *Proc. Nat. Acad. Sci.;* 2013;110:10982-10987).

The activated M2 receptor resembles the ligand-free opsin as its G protein–coupling site can accommodate the $G_{\alpha}CT$ peptide [5]. The intermediate conformations observed for M2 receptor were different from the β_2-AR [37] as two different processes were simulated i.e., the deactivation of β_2-AR from the G protein/nanobody-coupled conformation and the activation of the M2 receptor in a ligand-free form. An allosteric pathway of M2 activation was further demonstrated by examination of conformational changes of key residues and TM domains in the aMD simulation (**Figure 3-6**).

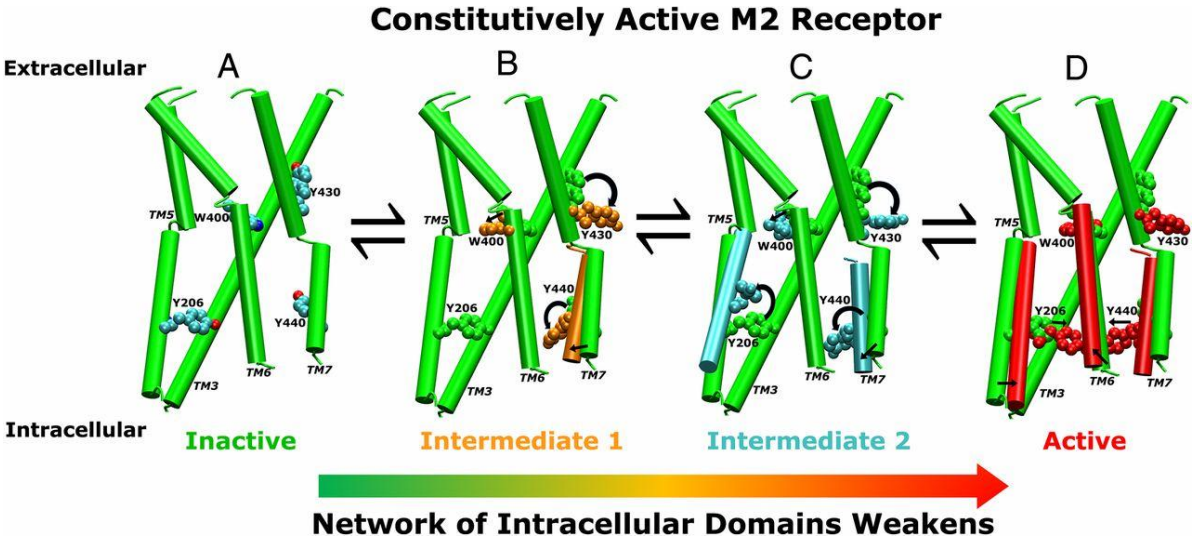

Figure 3-6: An allosteric activation pathway of the M2 receptor derived from aMD simulations [33] (Image courtesy: Miao Y. et al., *Proc. Nat. Acad. Sci.;* 2013;110:10982-10987).

The M2 receptor exists in a conformational equilibrium of the inactive, intermediate and active states. The side chain of Tyr206$^{5.58}$ reorients from the initial position between TM3 and TM6 to the lipid-exposed side of TM6 resulting in an alternative intermediate conformation. During final transition to the active sate, Tyr206$^{5.58}$ and Tyr440$^{7.53}$ relocate the side chains toward each other forming hydrogen bond and the cytoplasmic end of TM6 tilts outward by ~6 Å [33].

aMD is a sampling technique in NAMD where energy barriers are reduced to increase the transitions between the low energy states by addition of boost potential to the energy surface [38]. In the present study, we performed aMD on the homology model of the α_{1B}-AR (template: 2YCW-Turkey β_1-AR [39]) to identify the active conformation on both NE-free (apo) and NE-bound α_{1B}-AR model. Parameter selected for receptor activation was the hydrogen bond formation between the Tyr223-Tyr348.

3.2 Material and Methods

3.2.1 Classical Molecular Dynamics Simulations

The homology model of α_{1B}-AR derived from the crystal structure of Turkey β_1-AR (PDB: 2YCW resolved at 3.0Å, from chapter 2) was used for all the simulations. All MD trajectories were calculated using NAMD2.9 [40]. The protein was internally hydrated using SOLVATE program [41]. To imitate the membrane environment, the modeled hamster α_{1B}-AR was inserted into the phospholipid bilayer generated from membrane builder module of VMD1.9 [42]. The membrane consisted of 184 molecules of POPC and was equilibrated for 0.5ns. The system was neutralised by adding chloride ions and additional sodium and chloride ions were added to a final concentration of 0.15mol/L.

The parameters for NE were partly obtained from the work published on β_2-AR by Spijker. et al., [43] and remaining were derived from parameters already present in the CHARMM force field [44] for similar chemical groups. Temperature control was maintained at 310K with Langevin dynamics and a damping constant of $5ps^{-1}$ was applied to non-hydrogen atoms. Periodic boundary conditions were used with the Nosé-Hoover Langevin piston method [45] (piston period 200fs, decay rate 50fs) to maintain a constant pressure of 1.013Bar.

The Particle-mesh Ewald algorithm [46] was used to account for long-range electrostatic effects (grid resolution <1Å). The van der Waals interactions were determined using a Lennard–Jones function. The cut off radius for including atoms in the nearest-neighbor list was set to 13.5Å. 1–2 and 1–3 interactions were excluded while 1–4 interactions were scaled by multiplication with a predefined factor. All other non-bonded interactions were calculated using a switching function to smooth interactions to zero between 10 and 12Å. The integration timesteps were 2, 1, and 2fs for bonded, non-bonded and long-range electrostatic interactions respectively. The lengths of all chemical bonds were constrained by the SHAKE algorithm [47] involving hydrogen atoms at their equilibrium values while the SETTLE algorithm [48] was used to set the water geometry restrained rigid. The system was first minimised for lipids and water (1ns) while keeping the protein and ligand fixed followed by an all-atom conjugate gradient minimisation of the entire system during which protein was relaxed and allowed to move freely. After this, the system was equilibrated for 10ns at 310K and constant pressure.

The simulation was carried out both on the apo form and the ligand bound form of the α_{1B}-AR homology model along with periodic boundary conditions. Out of the two disulphide bonds in

the crystal structure of the turkey β_1-AR, one disulphide bond between Cys118 – Cys195 was maintained in all the simulations. This disulphide bond is maintained in all the class A GPCRs structures and forms an integral part of activation and signaling [6, 49-52].

3.2.2 Accelerated Molecular Dynamics

aMD implemented in NAMD is an acceleration simulation which adds boost potential and surpass low energy barriers. In our study, we performed aMD in two different ways:

(1) Dihedral aMD: in which boost potential is applied to all the dihedral angles in the system (parameters: Edihed and αdihed) and

(2) Dual-Boost aMD: in which boost potential is applied to all atoms in the system along with dihedral angles.

We performed aMD simulations starting from the final structure of 100ns cMD. Initially, dihedral aMD simulations was set up on both the apo and NE-bound form of the α_{1B}-AR model where

Edihed = Vdihed_avg + λ*Vdihed_avg and

Acceleration factor αdihed = λ*Vdihed_avg/5 in which

Vdihed_avg = average dihedral energy calculated from the 100ns cMD and

λ= adjustable acceleration parameter.

The value for acceleration factor λ = 0.3, was chosen from the previous studies by Miao et al [33] on M2 muscarinic receptor to maintain the α-helix secondary structure during the simulations. For both the apo and NE-bound form of α_{1B}-AR dihedral aMD simulations was started from the final structure of the 100ns cMD with same atomic velocity at 310K

Later, dual-boost aMD simulations was performed on the apo and NE-bound form of the α_{1B}-AR like dihedral aMD from the final structure of 100ns cMD along with input parameters (Edihed, αdihed; Etotal, αtotal) where

Edihed = Vdihed_avg + 0.3*Vdihed_avg,

αdihed = 0.3*Vdihed_avg/5,

Etotal = Vtotal_avg + 0.2*Natoms and

αtotal = 0.2*Natoms.

Etotal = total energy of the system

Vtotal_avg = average total energy calculated from the 100ns cMD

Natoms = total number of atoms in the system (including lipids ions and water)

αtotal = total acceleration of the system

We carried out only one simulation each on the apo and NE-bound form with the same atomic velocity initialisation at 310K. A 75ns production run was performed for the apo-α_{1B}-AR and 50ns for the NE-bound form of the receptor. Additionally, we performed 10ns dihedral and dual boost aMD on a set of 27 mutants in both the apo and NE-bound form of the α_{1B}-AR proposed to be involved in receptor activation. These residues were experimentally tested in our lab by Ragnarsson et al., [53, 54] and the consequences of these mutations were assessed using aMD. Each of these residues was mutated with MUTATOR pluggin implemented in NAMD2.9. The mutated form of the α_{1B}-AR was then energy minimised and equilibrated for 0.5ns each followed by a 5ns cMD production run. The final structure obtained from the 5ns production run was used as starting structure for all the 10ns dihedral and dual-boost aMD.

3.3 Results and Discussion

We performed 100ns cMD on the apo and NE-bound forms of the α_{1B}-AR homology model followed by dihedral and dual boost aMD simulations. In the cMD run for 100ns with the apo-α_{1B}-AR (**Figure 3-7A** and **3-7B**), the receptor does not deviate from the α_{1B}-AR homology model. However, substantial fluctuations were observed in full length ECL2 followed by ECL3, while ECl1 remained fairly stable during full simulation run. In contrast, the NE- bound α_{1B}-AR model showed high fluctuations in ECL2 for first 50ns with an average RMSD reaching to 3.5Å after which fluctuations became stable. No distinct fluctuations were observed for ECL1 and ECL3.

A)

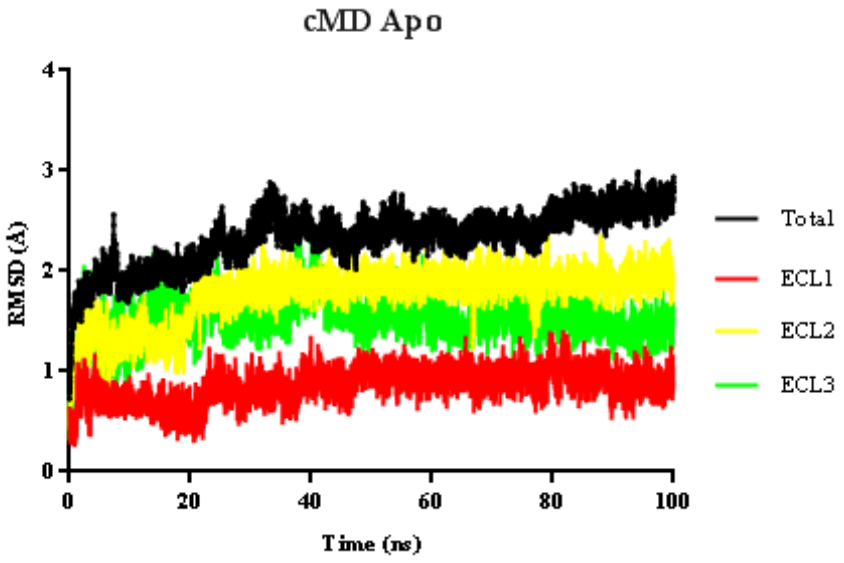

B)

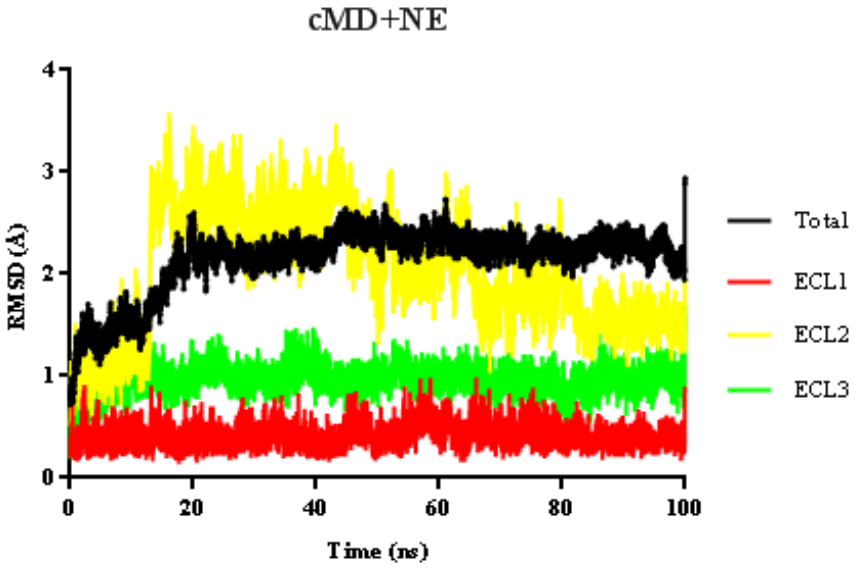

Figure 3-7: RMSD of the Cα atoms calculated from the 100ns cMD for the protein, ECL1, ECL2 and ECL3 for A) apo- α_{1B}-AR and B) NE- α_{1B}-AR.

In Dihedral aMD on apo- α_{1B}-AR for 75ns (**Figure 3-8A**), the three ECL's showed variable fluctuations during the simulation run with an overall average RMSD of 1.5Å. ECL1 remained stable throughout the simulation with an RMSD around 0.5Å while ECL3 showed initial fluctuations with an RMSD of 1.5Å and ECL2 was initially stable and fluctuated in the later part of simulation. Then, we performed dihedral aMD on the NE-bound form of the α_{1B}-AR (**Figure 3-8B**). In contrast to the apo-form, ECL2 showed markedly high fluctuations in 50ns run with RMSD averaging to ~2Å implying enhanced sampling is obtained by dihedral aMD while fewer fluctuations were observed for the ECL1 and ECL2 which remained stable

A)

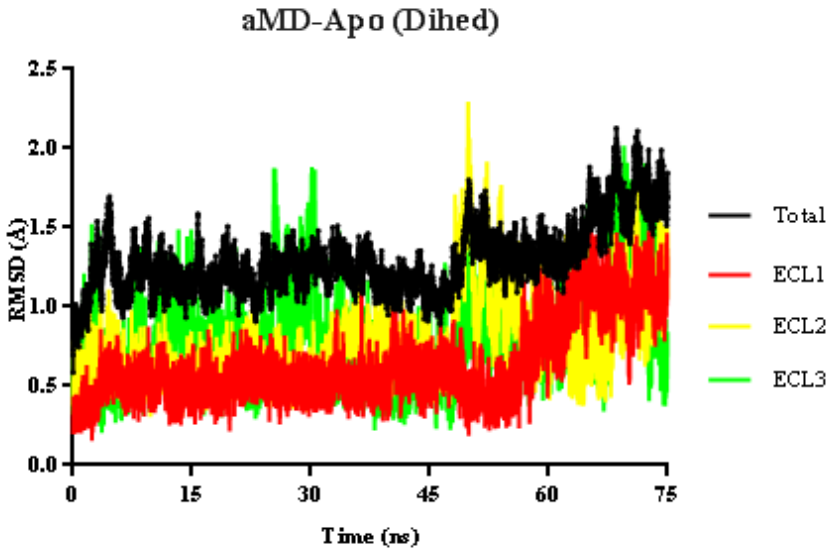

B)

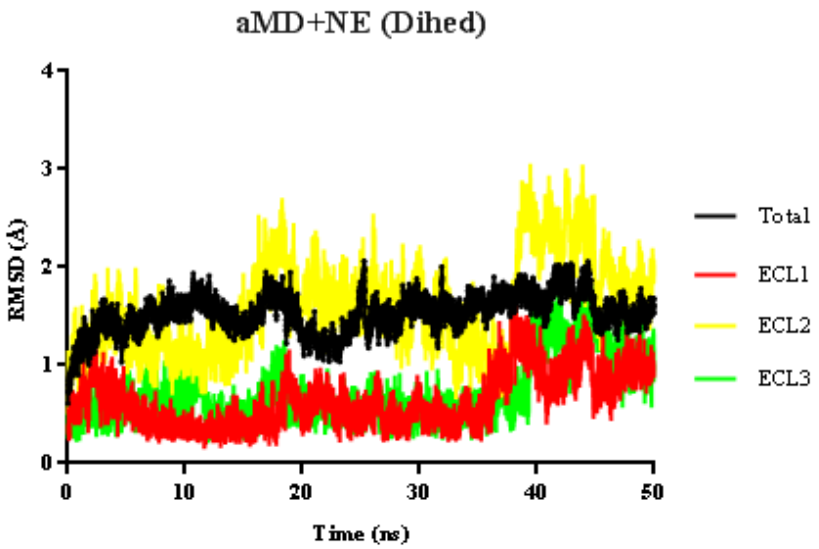

Figure 3-8: A) RMSD of the Cα atoms in apo-α_{1B}-AR calculated from the 75ns dihedral aMD for the protein, ECL1, ECL2 and ECL3. B) RMSD of the Cα atoms in NE-α_{1B}-AR calculated from the 50ns dihedral aMD for the protein, ECL1, ECL2 and ECL3.

Increased dynamics was observed in the ECS of the receptor in NE-bound form than the apo-form in dihedral aMD, but the receptor maintained a similar conformation to the apo-α_{1B}-AR (starting model after cMD) showing active conformation is not attained. In contrast in a study by Miao et al., on M2 muscarinic receptor [33], markedly higher fluctuations were observed for the

ECL3 than ECL2 in dihedral aMD in the apo and QNB-bound form of the receptor. This difference can be attributed to the different simulation process where an antagonist QNB was bound to the M2 receptor while we simulated agonist NE bound to the α_{1B}-AR homology model. The apo form showed more fluctuations in the ligand binding domain of the TM helices 3, 4, 5 and 6. Also, the receptor maintained inactive conformation similar to the X-ray structure at microsecond level Anton simulation [55] with antagonist tiotropium.

Next, we performed dual-boost aMD restarting from the final structure of the 100ns cMD which provides better sampling than dihedral aMD. Enhanced sampling provides insights in the identification of the receptor intermediates and actives which are distinct from the inactive conformation of the receptor. The apo-form of the receptor remained inactive in a 75ns simulation run despite sampling of the larger conformational space. Although, significant fluctuations (RMSD 5Å) were observed for ECL2 compared to dihedral aMD, ECL1 and ECL3 were almost stable throughout the simulation (**Figure 3-9A**) with ECL1 (RMSD 1Å) more stable than ECL3 (RMSD 2Å) because of the short length which imparts less flexibility to ECL1.

In the NE-bound form of the α_{1B}-AR, higher fluctuations were observed for ECL2 (RMSD 4Å) like that of dihedral aMD in a 50ns run (**Figure 3-9B**) while ECL1 remained stable compared to smaller fluctuations observed in dihedral aMD. ECL3 was initially stable for 20ns with an RMSD averaging to 1Å while fluctuations were observed for later part of the simulation (RMSD 2Å). Despite fluctuations observed in the ECS, the receptor maintained an inactive conformation during the simulation process suggesting that the agonist NE does not surpass the energy barriers in a 50ns run that leads to conformational transition of the receptor to pass from inactive to active-state. Significant fluctuations in the RMSD of the ECL2 suggest the role of this loop in maintaining the specific conformation necessary for receptor activation.

A)

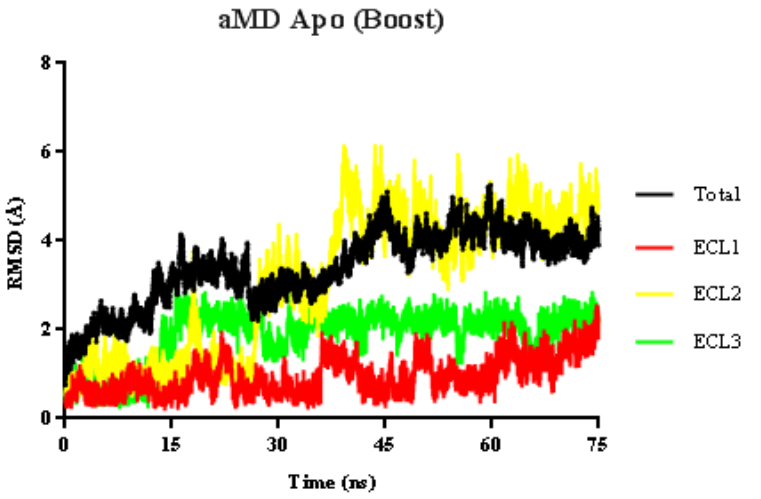

B)

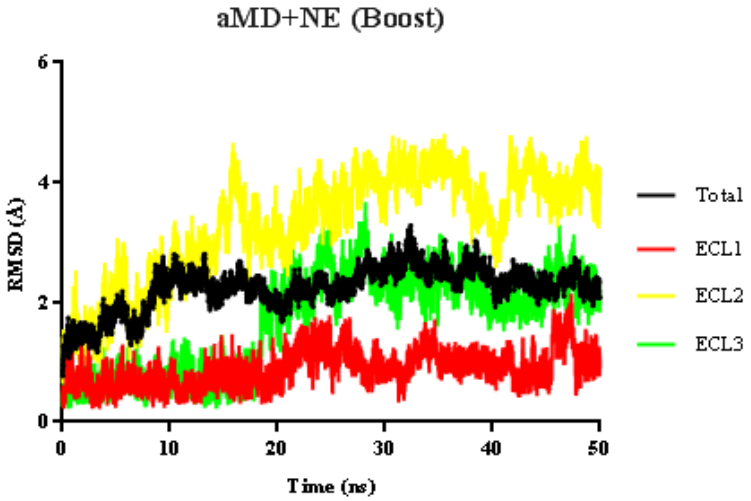

Figure 3-9: A) RMSD of the Cα atoms in apo-α_{1B}-AR calculated from the 75ns dual-boost aMD for the protein, ECL1, ECL2 and ECL3. B) RMSD of the Cα atoms in NE-α_{1B}-AR calculated from the 50ns dual-boost aMD for the protein, ECL1, ECL2 and ECL3.

3.3.1 Activation Process of α_{1B}-AR

A series of dihedral and dual-boost aMD simulations were carried out on the α_{1B}-AR in apo and NE-bound form to provide insights into the process of receptor activation. Receptor activation is characterised by formation of hydrogen bond between Tyr227 (TM5) and Tyr338 (TM7); ~6Å outward movement of the cytoplasmic end of the TM6 and breaking of the ionic lock between TM3 and TM6. We analysed the hydrogen bond formation between Tyr223 and Tyr348 as the primary criteria for receptor activation as observed in activation of M2 muscarinic receptor by Miao et al., [7] where Tyr206$^{5.58}$ and Tyr440$^{7.53}$ forms hydrogen bond in the G protein-coupling site towards the intracellular domain. The active structures reported for opsin, β_2-AR bound to Gs protein or nanobody, A2A-R are characterised by rearrangement of TM5, TM6 and TM7 while the side chains of Tyr$^{5.58}$ and Tyr$^{7.53}$ relocate towards each other in the intracellular pocket of M2 receptor compared to the inactive structures [5, 52, 56, 57].

In apo-form of the α_{1B}-AR, Tyr (-OH) – Tyr (-OH) distance shows varied degree of fluctuation from 8Å-30Å during 75ns run in dual-boost aMD while no fluctuations were observed for dihedral aMD (**Figure 3-10A**). The Tyr (-OH) – Tyr (-OH) distance remained stable around 15Å in dihedral aMD suggesting receptor remained inactive during the whole process with a similar conformation to that of the starting structure. The side chains of the two Tyr residues move to and fro between the lipid side of the membrane and center of protein during the simulation because of which TM5 and TM7 are not close enough for hydrogen bond formation and thus an increased RMSD is observed.

In NE-α_{1B}-AR, Tyr (-OH) – Tyr (-OH) distance showed varied fluctuation from 8Å-17Å during 50ns run in dual-boost aMD while the Tyr (-OH) – Tyr (-OH) distance remained stable around 15Å in dihedral aMD (**Figure 3-10B**) suggesting a similar conformation to that of the starting structure. In dual-boost aMD, the distance between Tyr223 and Tyr348 initially decreased from 15Å to 8Å over first 20ns and then increased to 15Å and became stable at 15ns. Further, the distance decreased to around 10Å and became stable till 50ns.

A)

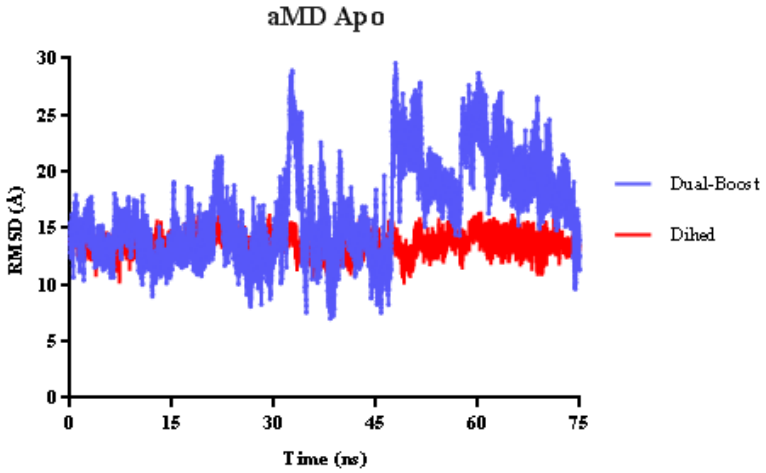

B)

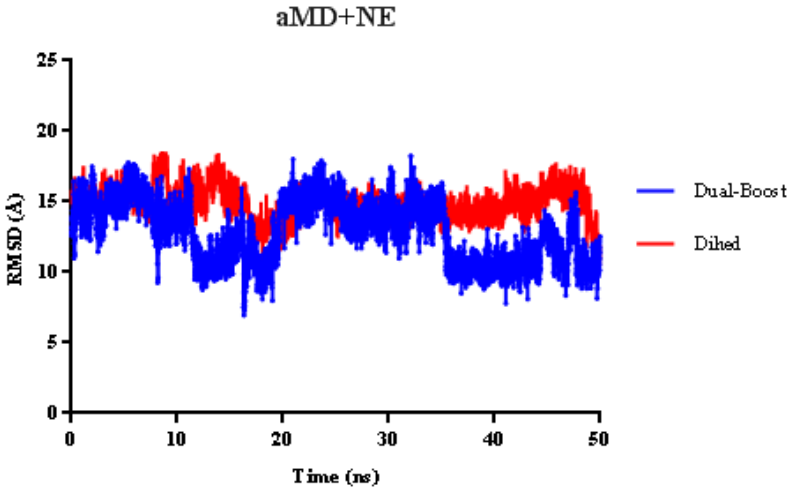

Figure 3-10: Distance between the side chain oxygen atoms of Tyr223 and Tyr348 for dihedral and dual-boost aMD for A) apo-α_{1B}-AR. B) NE-α_{1B}-AR.

Additionally, we carried out dihedral and dual-boost aMD on the apo and NE-bound form of the 27 α_{1B}-AR mutants (Y110A, W111A, L113A, G114A, R115A, C118A, V126A, P180A, L181A, G183A, W184A, K185A, N190A, C195A, G196A, T198A, E200A, Y203A, S207A, Y223F, F310A, F311A and Y348F) including 4 double mutants (C118A-C195A, Y223F-N344A, Y223F-Y348F and N344A-Y348F). These mutants were experimentally tested in our laboratory

by Ragnarsson et al., and were found to influence the NE affinity, potency and efficiency [53, 54]. Some of these residues were present at allosteric site 1 (ECL2) and 2 (ECL1) along with an overlap between the allosteric site 1 and 2 in TM5 and affected the NE egress pathway from the orthosteric binding pocket to the ECS as described in chapter 2. The double mutant C118A-C195A is a conserved disulfide bond anchoring ECL2 to TM3 while Y223F-Y348F is shown to affect signaling efficiency.

A)

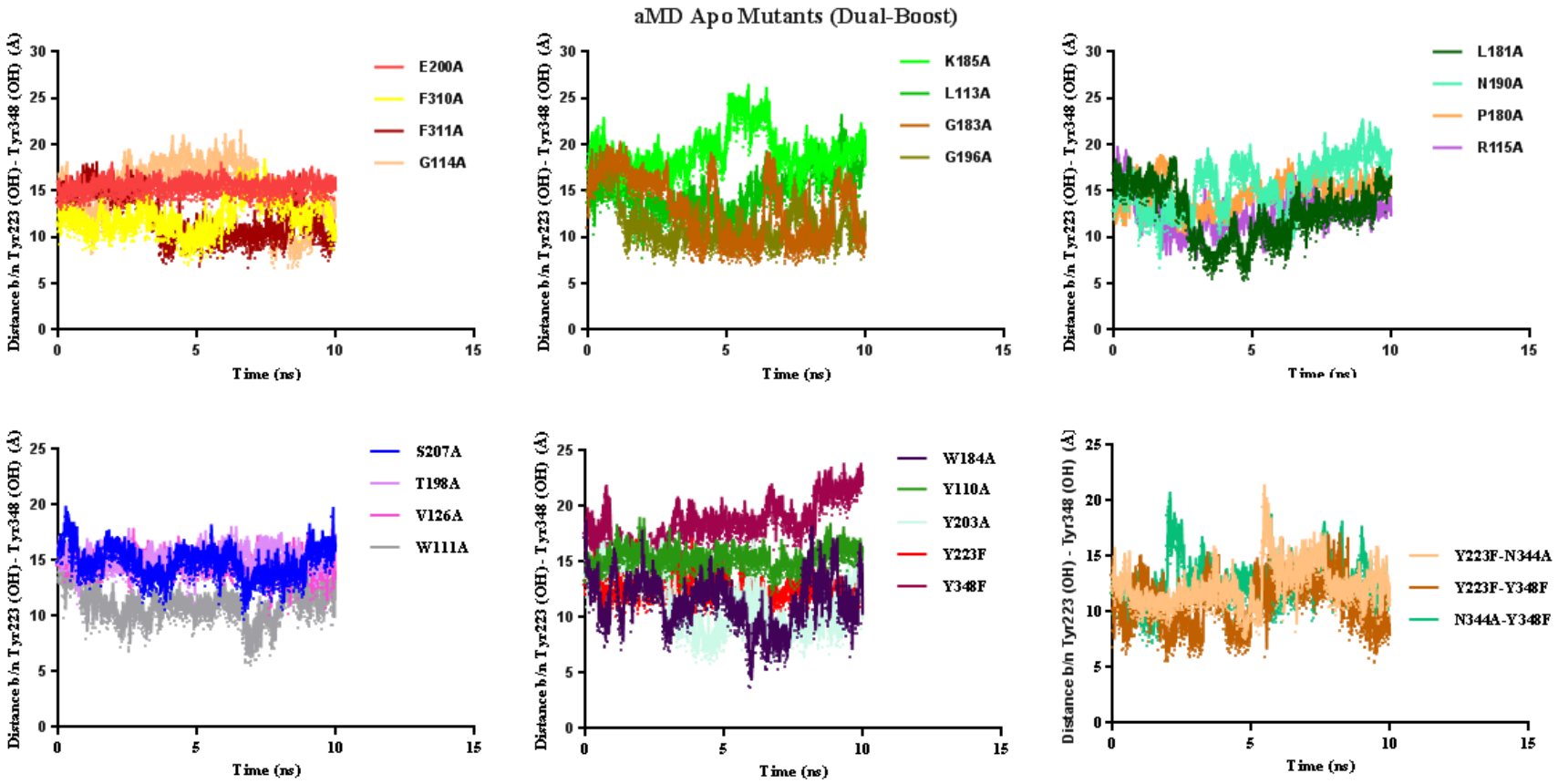
aMD Apo Mutants (Dual-Boost)
Distance b/n Tyr223 (OH) - Tyr348 (OH) (Å)
Time (ns)
E200A
F310A
F311A
G114A
K185A
L113A
G183A
G196A
L181A
N190A
P180A
R115A
S207A
T198A
V126A
W111A
W184A
Y110A
Y203A
Y223F
Y348F
Y223F-N344A
Y223F-Y348F
N344A-Y348F

B)

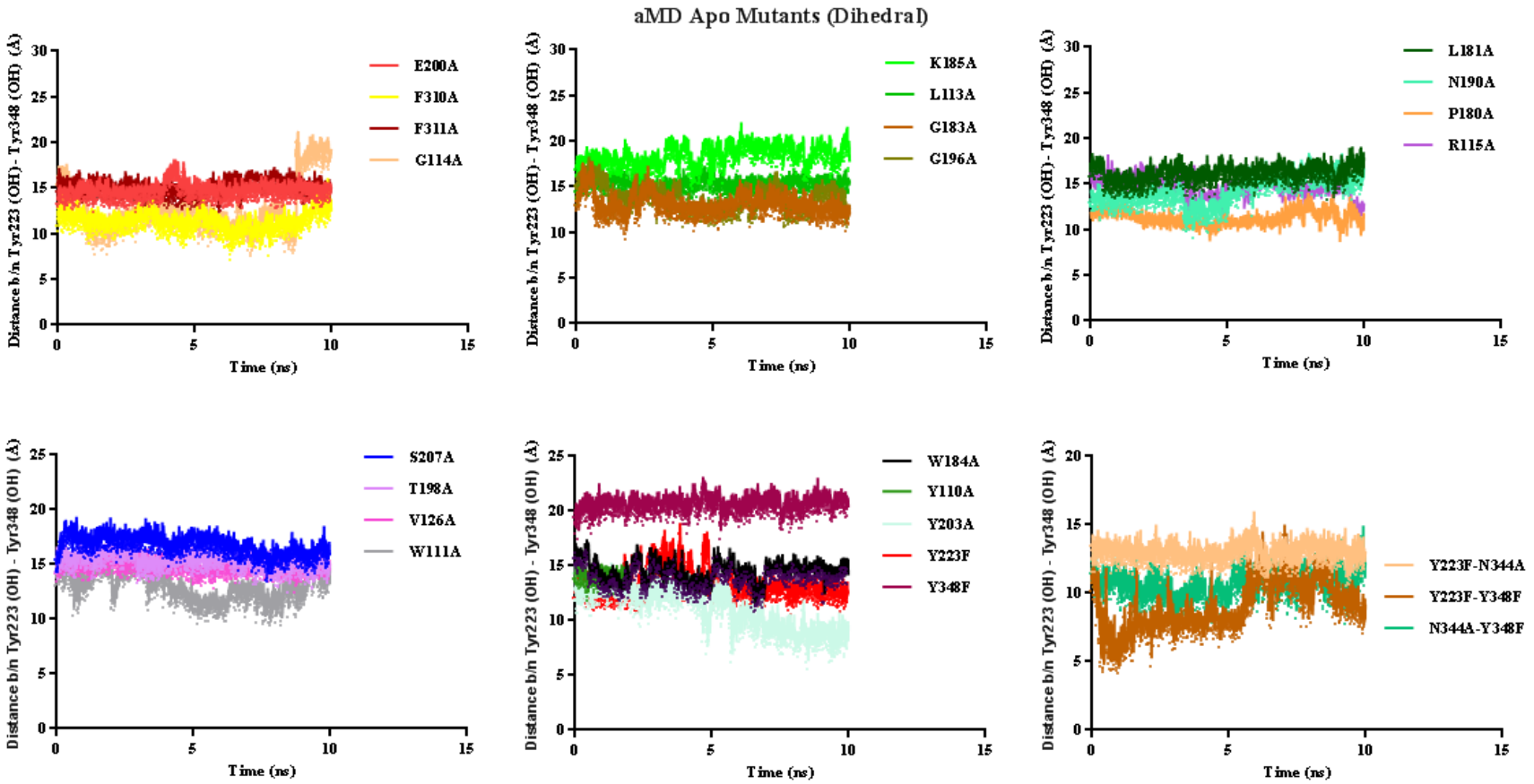

Figure 3-11: Distance between the side chain oxygen atoms of Tyr223 and Tyr348 for apo-α_{1B}-AR mutants for A) Dual-Boost and B) Dihedral aMD.

Some of the mutants identified from the experimental analysis by Ragnarsson et al., [53, 54] affect affinity and are believed to play role in receptor activation [20, 21]. Initially 5ns cMD simulations were carried out followed by 10ns aMD (Dual-Boost and Dihedral) from the final structure obtained from cMD. We observed mixed results for these mutants in dihedral and dual-boost aMD simulations (Y223F-Y348F in apo- and NE-bound α_{1B}-AR moved close to receptor activation for dual-boost and dihedral aMD while L181A and W184A in apo-α_{1B}-AR for dual-boost aMD, N190A in NE-α_{1B}-AR for dual-boost aMD and Y203A in apo-α_{1B}-AR for dihedral aMD (**Figure 3-11**)) were found moving close to activated state based on distance between Tyr223 (TM5) -Tyr348 (TM7).

The Tyr223 (-OH) – Tyr348 (-OH) distance for most of the mutants in apo-α_{1B}-AR remained stable during simulation. For mutants W111A, L181A, G183A, W184A, Y203A F310A, F311A and Y223F-Y348F, the distance between the Tyr223 and Tyr348 is reduced from ~15Å-~8Å for dual-boost aMD and for N190A, Y223F-Y348F the phe- distance reduced from ~15Å to ~5Å. This suggests internal rearrangement of the TM helices at the cytoplasmic end which rendered the side chain of two tyrosine residues close to each other suggesting movement of receptor towards active state.

The Tyr223 (-OH) – Tyr348 (-OH) distance for C118A showed decrease from ~15Å-7Å in dual-boost and dihedral aMD for apo-α_{1B}-AR and ~17Å-8Å in dual-boost aMD for NE-α_{1B}-AR in a 10ns simulation run. Mutation of C195A lead to a decrease in Tyr223 (-OH) – Tyr348 (-OH) distance in apo-α_{1B}-AR in dual-boost aMD. The distance remained stable at ~13Å in apo- and NE-α_{1B}-AR in dihedral aMD. Double mutation of C118A-C195A did not have a major impact on the Tyr223 (-OH) – Tyr348 (-OH) distance for NE-bound dual-boost and dihedral aMD where the two tyrosine residues are stabilised at 15Å while in the apo-α_{1B}-AR, the distance is reduced to ~6-7Å (**Figure 3-12**) suggesting receptor move towards active state but does not achieve activation.

The overall conformation of the receptor was found to be the same during the simulation suggesting inactive-state of the α_{1B}-AR is maintained during the simulation process. C195 in the ECL2 formed disulfide bond with C118 in the TM3. Mutation of C195 to alanine breaks the disulfide bond and thereby renders the thiol-group of C118A free. C118 in TM3 is closer to orthosteric binding site which might induce conformational changes to the α_{1B}-AR. NE had significantly reduction in potency at the C118A and C195A mutants by 285 and 1645-folds

(chapter 2). C118A mutant in TM3 leads to reduced expression and the largest reductions in NE potency arising from reductions in both NE affinity and efficacy while mutation of C195A in ECL2 reduces NE potency, affinity and efficacy. This reduction in NE affinity and efficacy by C118A and C195A mutants indicates that this disulfide bridge stabilises a conformation that facilitates both NE access to its binding site and NE signaling as shown previously for α_{1B}-AR by Ragnarsson et al., [53] and other class A GPCRs [58-68].

A)

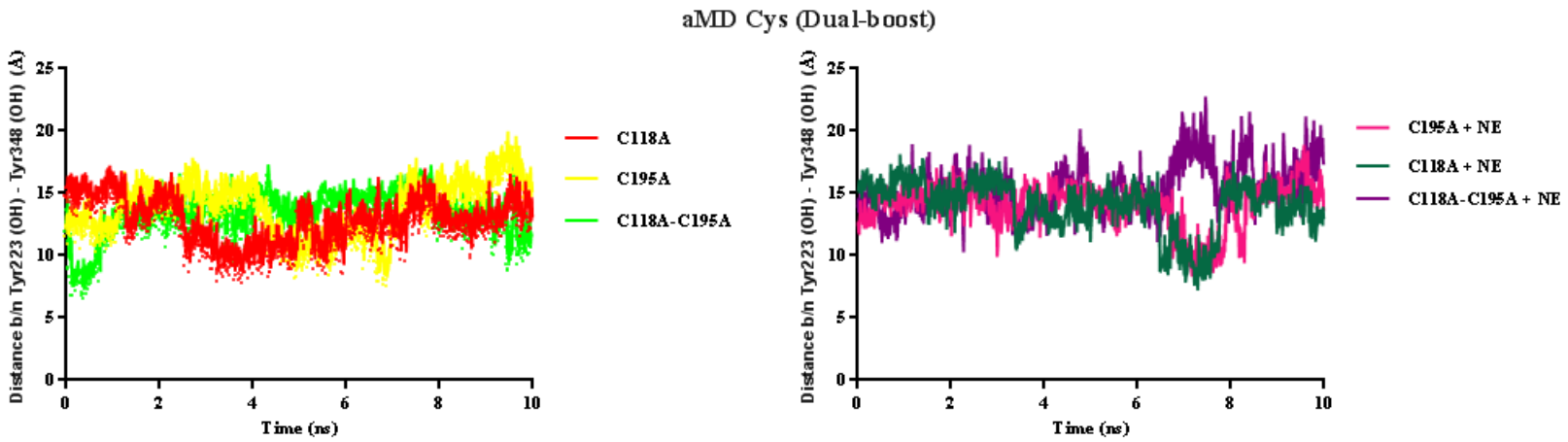

B)

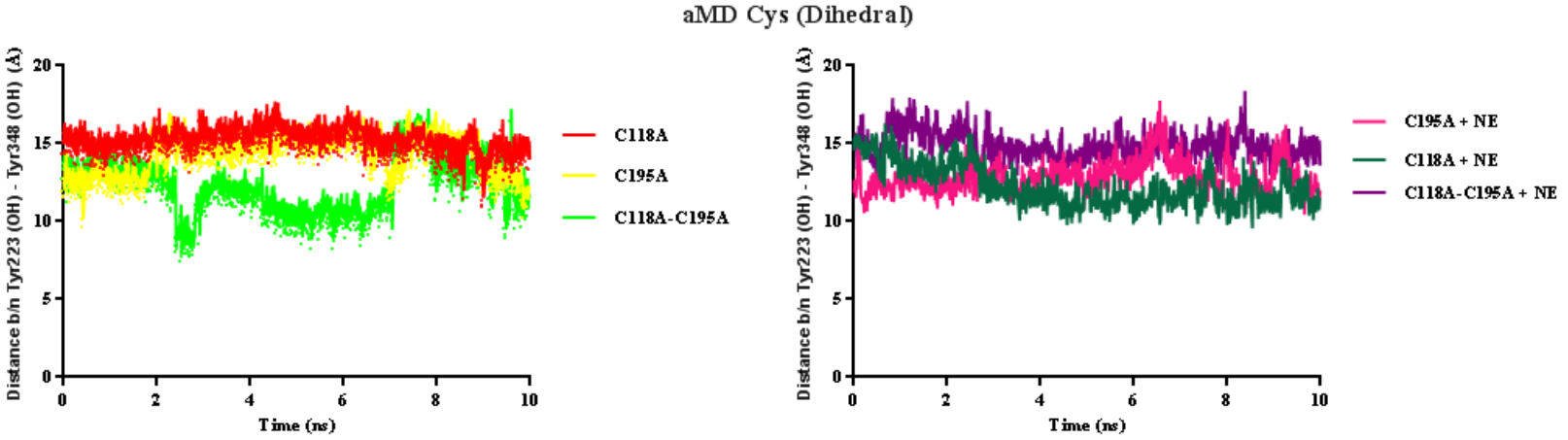

Figure 3-12: Distance between the side chain oxygen atoms of Tyr223 and Tyr348 of apo- and NE-α_{1B}-AR mutants; C118A, C195A and double mutant C118A-C195A for A) Dual-Boost and B) Dihedral aMD.

A)

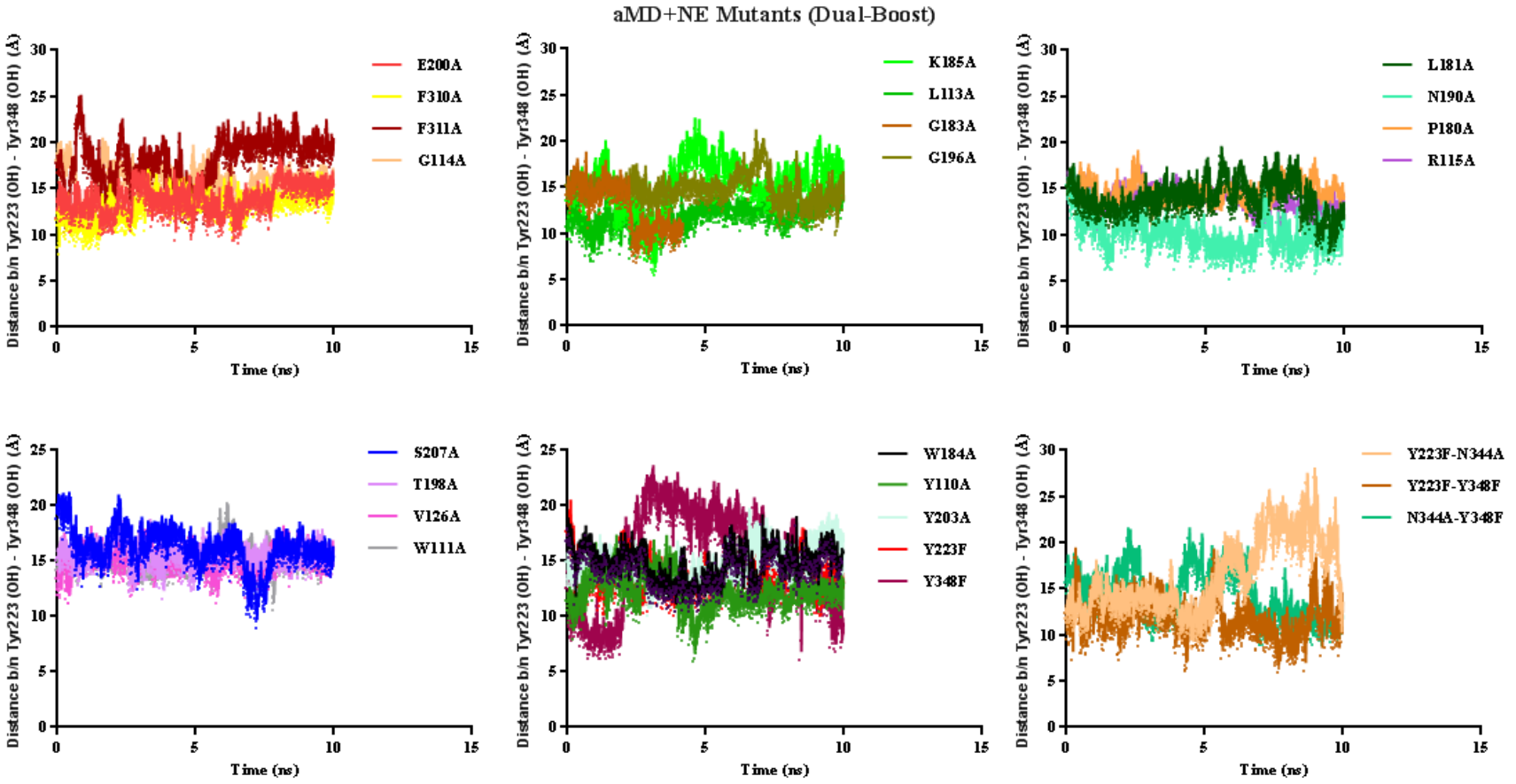
aMD+NE Mutants (Dual-Boost)
Distance b/n Tyr223 (OH) - Tyr348 (OH) (Å)
Time (ns)
E200A
F310A
F311A
G114A
K185A
L113A
G183A
G196A
L181A
N190A
P180A
R115A
S207A
T198A
V126A
W111A
W184A
Y110A
Y203A
Y223F
Y348F
Y223F-N344A
Y223F-Y348F
N344A-Y348F

B)

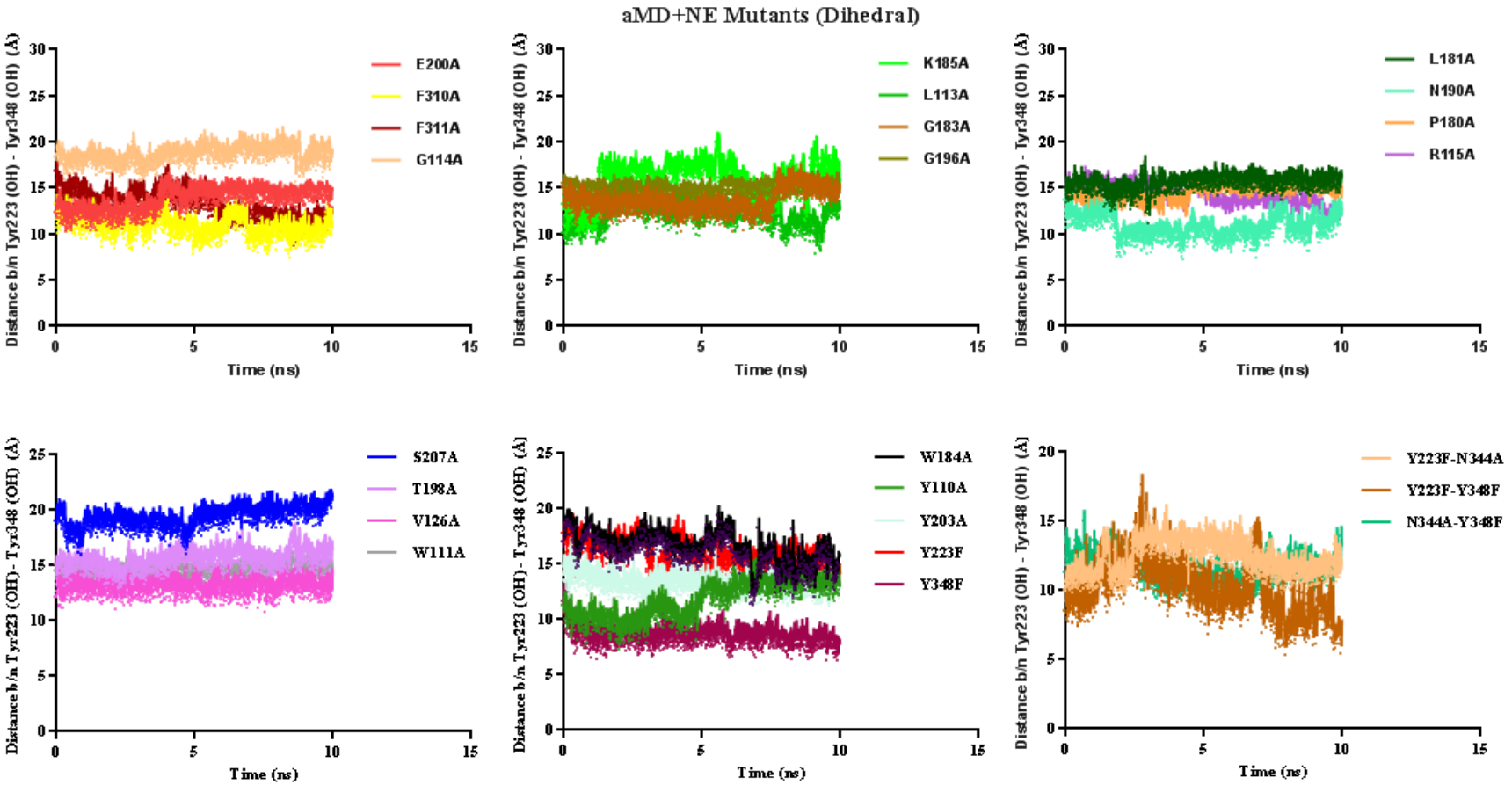

Figure 3-13: Distance between the side chain oxygen atoms of Tyr223 and Tyr348 for NE- α_{1B}-AR mutants for A) Dual-Boost and B) Dihedral aMD.

An initial reduction in the distance between tyrosine and phenylalanine residues in dual-boost aMD on Y348F of NE-α_{1B}-AR was observed from 19Å to 7Å followed by an increase from 7Å to ~23Å while it remains stable in dihedral aMD at ~8Å. Similar stability was observed in apo-α_{1B}-AR at ~20Å for dual-boost and dihedral aMD. Y110A remained stable around ~12Å with minimum distance between Tyr223 (-OH) – Tyr348 (-OH) reaching ~7Å in dual-boost aMD in NE-α_{1B}-AR with a maximum distance of ~16Å in dihedral aMD. Higher fluctuations were observed for Y110A in apo-α_{1B}-AR (**Figure 3-13**).

Dual-boost dynamics on N190A mutant of NE-α_{1B}-AR showed a significant decrease in the Tyr223 (-OH) – Tyr348 (-OH) distance from ~16Å to 6Å while no such changes were observed for N190A in other simulations. Similarly, change was observed for the W184A in apo-α_{1B}-AR where the distance between tyrosine residues reduced from 17Å to ~4Å leading to formation of weak hydrogen bond between Tyr223 (-OH) – Tyr348 (-OH) at 4.45Å (**Figure 3-14**). This contradicts with our experimental results where NE potency and affinity was reduced by 10 and 17-folds with no change in signaling efficiency compared to WT [54] (chapter 2). The reduced distance suggests intracellular rearrangement of TMs which moves the receptor towards active-state. The side chain of Tyr223 initially positioned towards lipid interface between TM5 and TM6 and the side chain of Tyr348 oriented towards TM2 flips towards each other moving the receptor towards active state along with an outward movement of TM6 by ~4Å. The distance between tyrosine residues reduced significantly for L181A in apo-α_{1B}-AR for dual-boost aMD and Y203A in apo-α_{1B}-AR for dihedral aMD from ~18Å to ~6Å and ~ 15Å to ~6Å respectively. NE potency and affinity for Y203A mutant was reduced by 1000 and 67-folds respectively while signaling efficacy is reduced by 36-folds (data not published) (**Figure 3-15**). There was no indication of any increased basal activities for any of the mutants tested that would be indicative of a constitutively active mutant.

A) B)

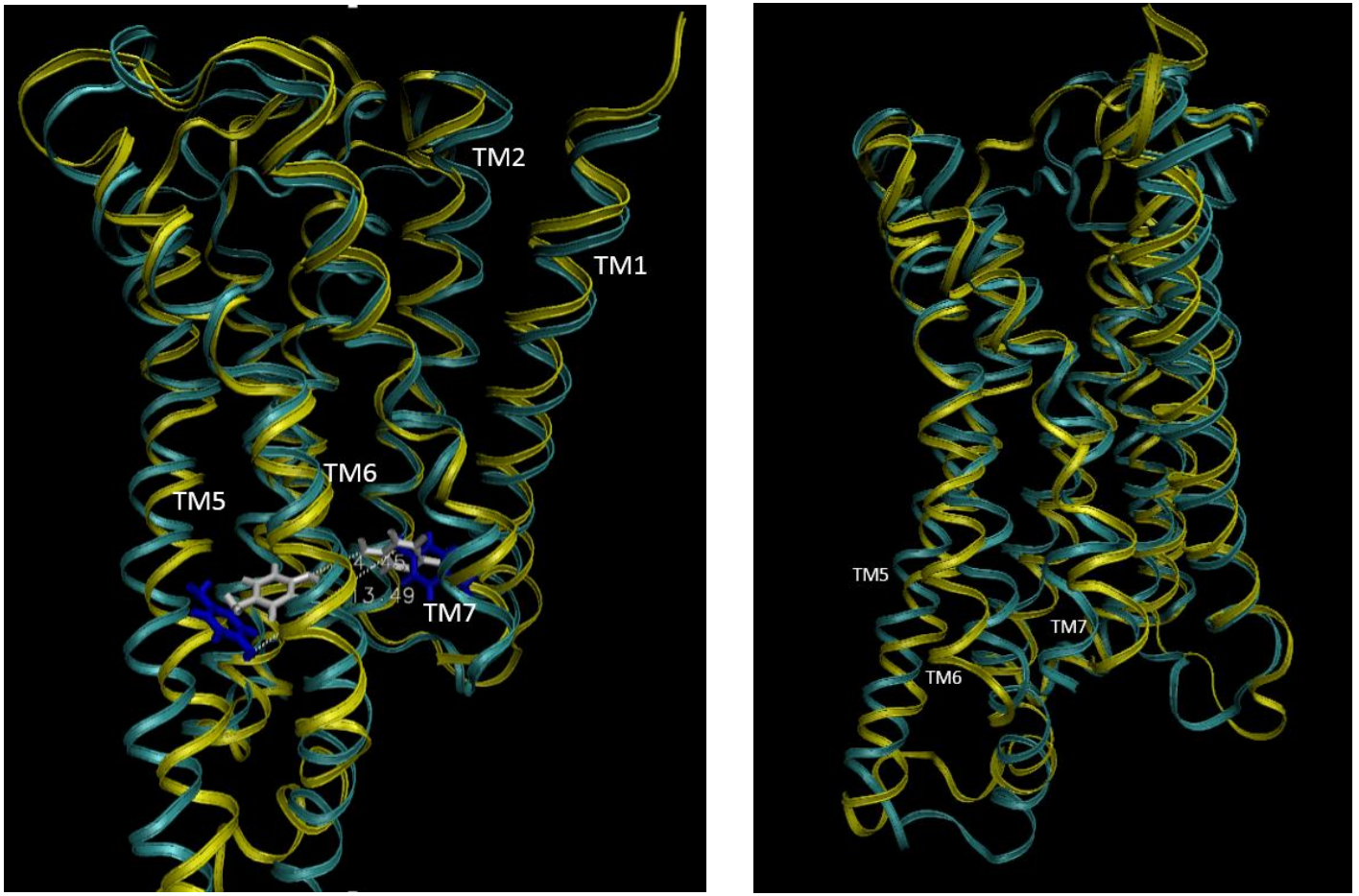

Figure 3-14: A) Reduction in Tyr223 (TM5) – Tyr348 (TM7) distance from 13.49Å to 4.45Å in dual-boost aMD between apo-α_{1B}-AR (Cyan) and W184A mutant apo-α_{1B}-AR (Yellow) in a 10ns run. Tyrosine residues for apo-α_{1B}-AR and W184A mutant apo-α_{1B}-AR are shown in Blue and Silver. B) Outward movement of TM6 of W184A mutant by ~3.75Å.

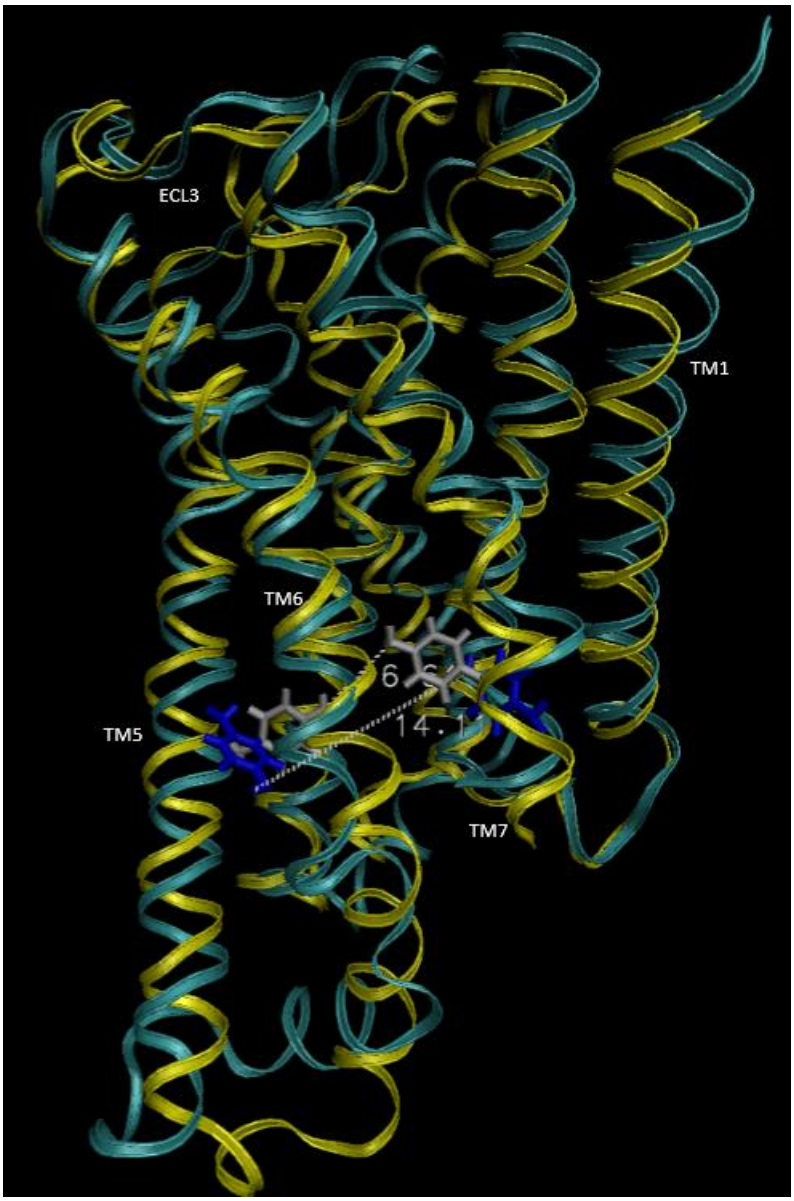

Figure 3-15: Reduction in Tyr223 (TM5) – Tyr348 (TM7) distance from 14.11Å to 6.64Å in dual-boost aMD between apo-α_{1B}-AR (Cyan) and Y203A mutant apo-α_{1B}-AR (Yellow) in a 10ns run. Tyrosine residues for apo-α_{1B}-AR and Y203A mutant apo-α_{1B}-AR are shown in Blue and Silver.

Double mutant Y223F-Y348F showed a significant decrease in Phe223– Phe348 distance in both dual-boost and dihedral dynamics in apo and NE-bound receptor where both the tyrosine residues were mutated to phenylalanine. Hence for this mutant, distance is calculated between the C-delta atoms of phenylalanine thereby forming covalent network. Thus, the Phe223 - Phe348 C-delta distance significantly decreased to 4.75Å in dihedral aMD for apo-α_{1B}-AR;

5.96Å in NE-α_{1B}-AR; 6.25Å in dual-boost aMD for apo-α_{1B}-AR; and 7.11Å in dual-boost aMD for NE-α_{1B}-AR.

Dihedral and dual-boost aMD on other α_{1B}-AR mutants did not show any significant changes and maintained inactive conformations like that of the starting structure. Almost similar window was observed for the Tyr223 (-OH) – Tyr348 (-OH) distance for few mutants in the apo-α_{1B}-AR from ~25Å to ~4Å and for the NE-α_{1B}-AR from ~28Å to ~6Å. This implies that the mutants in the apo-α_{1B}-AR induced conformational changes like the NE-α_{1B}-AR moving the receptor towards active-state by surpassing low energy barriers despite reduction in potency and affinity. This effect could be attributed to the active/inactive state which is not as clear cut and easy to explain as once thought [69, 70]. The results from our lab (data not published) shows that the classic view that active receptor has increased signaling and high affinity may not always be true. The recent papers show that there are several active receptor states and several inactive receptor states [37, 71, 72]. **Table 3-1** lists the mutants close to receptor activation based on Tyr223 (-OH) – Tyr348 (-OH) distance.

Table 3-1: List of the mutants close to receptor activation based on Tyr223 (-OH) – Tyr348 (-OH) distance.

Apo-α_{1B}-AR		**NE-α_{1B}-AR**	
Dual-Boost aMD	**Dihedral aMD**	**Dual-Boost aMD**	**Dihedral aMD**
W111A (6.61 Å)		N190A (6.11 Å)	
L181A (6.29 Å)		Y348F (7.21 Å)	Y348F (7.15 Å)
W184A (4.45 Å)			
Y203A (6.64 Å)	Y203A (6.43 Å)	Y203A (6.43 Å)	
Y223F-Y348F (6.25 Å)	Y223F-Y348F (4.75 Å)	Y223F-Y348F (7.11 Å)	Y223F-Y348F (5.96 Å)

In this study, direct activation of the apo and NE-α_{1B}-AR was not observed over the nanosecond time scale, but few mutants could be seen moving to active state over a time scale of 10ns (**Table 3-1**). This activation process at atomistic level is of pivotal importance in understanding the structure-function relationship. The receptor activation is characterised by formation of a hydrogen bond between the intracellular domains of TM5 and TM7 (Tyr223–Tyr348) which is in consonance with the results observed in previous studies for the active structures of rhodopsin [5, 52] and β_2-AR [56, 57].

The α_{1B}-AR is known to have basal activity [73, 74] which shifts the receptor from inactive to active state. When the receptor transitions from the inactive to the intermediate state and from intermediate to the active state, structural transitions within the TM helices occurs particularly with TM5, TM6 and TM7 which are known to play key role in the activation process [14, 33, 36, 52, 74]. During final transition to the active sate, Tyr223 and Tyr348 relocate the side chains toward each other forming hydrogen bond interaction and the cytoplasmic end of TM6 tilts outward by ~6Å [33].

The mutant receptor moved towards the active state in the apo-α_{1B}-AR rather than agonist bound NE-α_{1B}-AR although few mutants in NE-α_{1B}-AR were found to be close to receptor activation based on Tyr223-Tyr348 distance. This correlates with the fact that α_{1B}-AR is known to have constitutive activity [73, 74]. With agonist NE bound in the orthosteric binding site, the equilibrium between inactive and active state is shifted more towards the active state where the TM helices are connected to each other via non-covalent interactions. In contrast, the network of the apo-α_{1B}-AR in the intracellular domains is significantly weakened during the receptor activation which could further facilitate the association of the G protein and additional stabilisation of the receptor in active conformation. It could be argued that the mutants moving close to receptor activation might be constitutively active and that NE is inhibiting this activation but our functional assays on this receptor do no support this because normally we don't pick such constitutively active mutant receptors in our assay.

The ligand binding pocket in the ECS and the G protein-coupling site in intracellular domain are correlated with each other as exemplified in the activation of the M2 receptor. The intracellular domain of TM6 that shows large-scale outward movement is highly correlated with the extracellular domains of TM5, TM6 and TM7 surrounding the ligand binding site. Such changes have been justified by the conformational changes triggered by the Trp400$^{6.48}$ transmission

switch in M2 receptor. We propose similar movement of Trp307 in TM6 to be the transmission switch in our homology model of hamster α_{1B}-AR.

Relocation of Trp400 in TM6 towards Phe195 and Val199 in TM5 was found to be the key conformational change during activation of M2 receptor consistent with the previous structural studies on rhodopsin and A2A-R that suggests the conserved Trp400 to be a transmission switch which links agonist binding to the movement of the intracellular domains of TM5 and TM6 during process of GPCR activation [12]. Though, we could not observe direct activation of the α_{1B}-AR, relocation of Trp307 towards TM3 and formation of strong hydrogen bond between Asp125 in TM3 and Tyr338 in TM7 in W184A mutant be an intermediate state towards receptor activation. The second key observation for M2 receptor activation includes replacement of hydrogen bond interaction between Tyr430 in TM7 and Asp103 in TM3 with Tyr426 in TM7 that resembles breaking of a $Lys^{7.43}$ – $Glu^{3.28}$ salt bridge in rhodopsin and relocation of $Ser^{7.42}$ and $His^{7.43}$ coordinated by $Thr^{3.36}$ during agonist binding of A2A-R. These residues and interactions are known to play important roles in receptor activation.

The intracellular domain of TM7 is also correlated to its extracellular counterpart in M2 receptor in which $Tyr430^{7.43}$ flips from the ligand-binding cavity to the TM7-TM2 interface, which coincides with displacement of the NPxxY motif in the intracellular domain of TM7. Tyr338 in TM7 of W184A α_{1B}-ARmutant flips from TM7-TM2 interface towards TM3 and forms hydrogen bond with Asp125 in TM3. This rearrangement of extracellular domain in our homology model could act as a step towards receptor activation (**Figure 3-16**). Y338A mutant reduces NE potency and affinity for NE by 100 and 2-folds which results in reduction in signaling efficiency by 43-folds (chapter 2). This suggests the possible role of Tyr338 in receptor activation.

A)

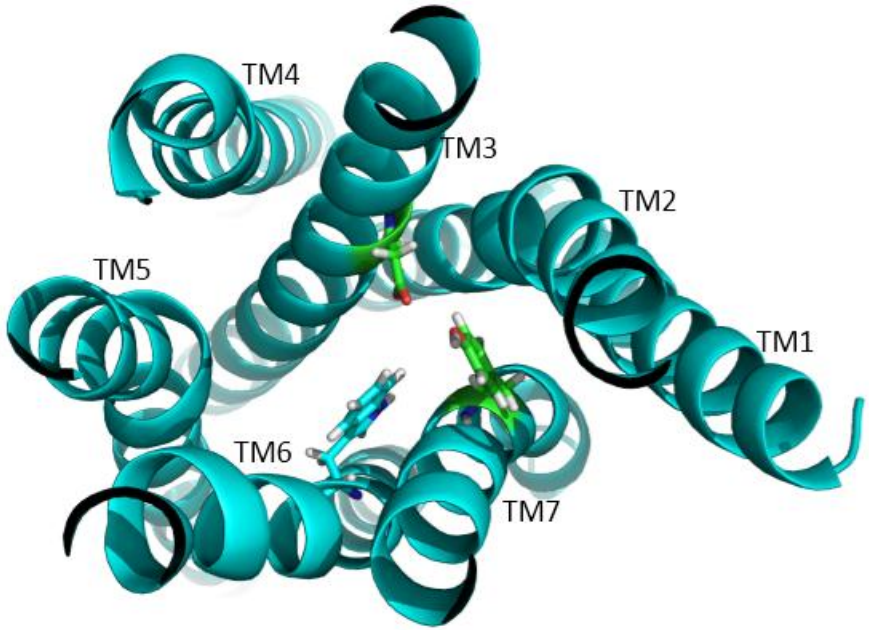

B)

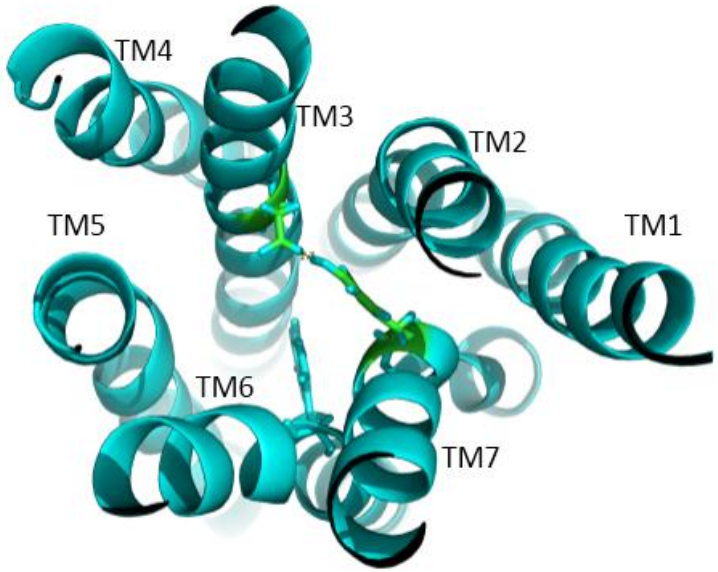

Figure 3-16: Rearrangement of A) Tyr338 in homology model of hamster α_{1B}-AR and B) W184A mutant from TM7-TM2 interface towards TM3.

A triad of Asp125 in TM3, Trp307 in TM6 and Tyr338 in TM7 in the ligand binding pocket (**Figure 3-17**) of extracellular domain of the homology model of hamster α_{1B}-AR rearranges in Y203A mutant which might play a role in receptor activation as observed by reduction in Tyr223-Tyr348 distance to 6.64Å from 13.49Å compared to WT-α_{1B}-AR. However, Y203A mutant is shown to have reduction in signaling efficiency by 36-folds and have a reduced potency and affinity of 1000 and 67-folds (chapter 2). This contradicts the fact that despite reduction in potency and affinity, Y203A mutant is shown to move the receptor towards active state but does not activate the receptor. These correlated motions between the ligand-binding pocket and intracellular domains of TM3, TM5, TM6 and TM7 might regulate GPCR activation.

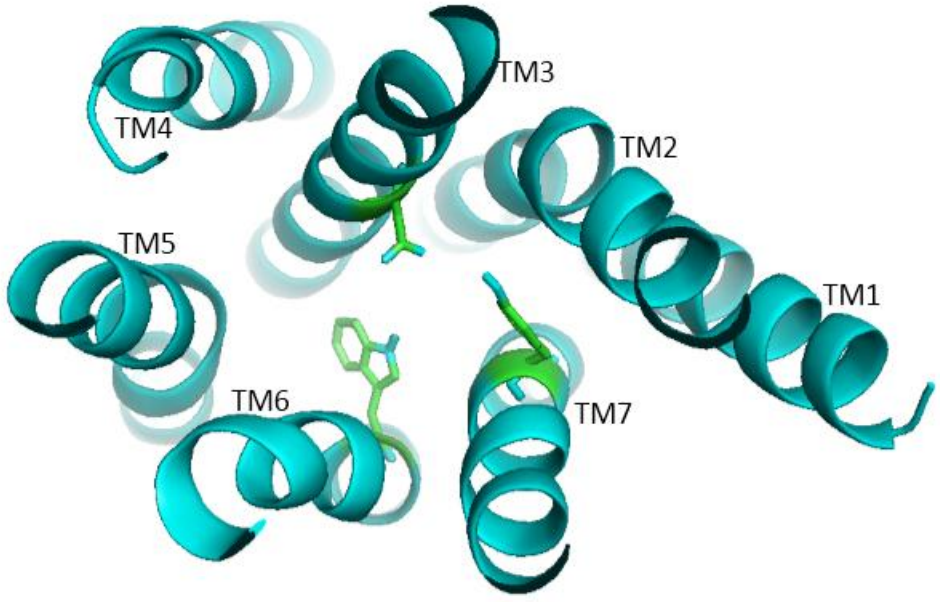

Figure 3-17: Triad of residues in TM3, TM6 and TM7 in Y203 mutant in the ligand binding pocket.

In summary, aMD on mutants induced the receptor towards active-state in significantly shorter simulation time compared to classical simulations. This study establishes the application of aMD to the study of activation process which will be highly useful for designing GPCR mutation studies and engineering small molecules for receptor-selective therapeutics [75]. Further, aMD shortens the simulation time significantly without predefined reaction coordinates as in metadynamics and ABF calculations. Thus, aMD is of extensive use to study the receptor activation process.

3.4 References

1. Fredriksson R, Lagerström MC, Lundin L-G, Schiöth HB: **The G protein-coupled receptors in the human genome form five main families. Phylogenetic analysis, paralogon groups and fingerprints**. *Molecular pharmacology* 2003, **63**(6):1256-1272.
2. Tripathi K: **Essentials of medical pharmacology**: JP Medical Ltd; 2013.
3. García-Sáinz JA, Vázquez-Prado J, Villalobos-Molina R: **α_1-adrenoceptors: Subtypes, signaling and roles in health and disease**. *Archives of medical research* 1999, **30**(6):449-458.
4. Michelotti GA, Price DT, Schwinn DA: **α_1-adrenergic receptor regulation: Basic science and clinical implications**. *Pharmacology & therapeutics* 2000, **88**(3):281-309.
5. Scheerer P, Park JH, Hildebrand PW, Kim YJ, Krauß N, Choe H-W, Hofmann KP, Ernst OP: **Crystal structure of opsin in its G protein-interacting conformation**. *Nature* 2008, **455**(7212):497-502.
6. Rasmussen SG, DeVree BT, Zou Y, Kruse AC, Chung KY, Kobilka TS, Thian FS, Chae PS, Pardon E, Calinski D: **Crystal structure of the β_2-adrenergic receptor-Gs protein complex**. *Nature* 2011, **477**(7366):549-555.
7. Rasmussen SG, Choi H-J, Fung JJ, Pardon E, Casarosa P, Chae PS, DeVree BT, Rosenbaum DM, Thian FS, Kobilka TS: **Structure of a nanobody-stabilised active state of the β_2-adrenoceptor**. *Nature* 2011, **469**(7329):175-180.
8. Lebon G, Warne T, Edwards PC, Bennett K, Langmead CJ, Leslie AG, Tate CG: **Agonist-bound adenosine A2A receptor structures reveal common features of GPCR activation**. *Nature* 2011, **474**(7352):521-525.
9. Gether U, Kobilka BK: **G protein-coupled receptors II. Mechanism of agonist activation**. *Journal of biological chemistry* 1998, **273**(29):17979-17982.
10. Dror RO, Pan AC, Arlow DH, Borhani DW, Maragakis P, Shan Y, Xu H, Shaw DE: **Pathway and mechanism of drug binding to G protein-coupled receptors**. *Proceedings of the national academy of sciences* 2011, **108**(32):13118-13123.
11. Ye L, Van Eps N, Zimmer M, Ernst OP, Prosser RS: **Activation of the A2A adenosine G protein-coupled receptor by conformational selection**. *Nature* 2016, **533**(7602):265-265.

12. Deupi X, Standfuss J: **Structural insights into agonist-induced activation of G protein-coupled receptors**. *Current opinion in structural biology* 2011, **21**(4):541-551.
13. Ballesteros JA, Weinstein H: **Integrated methods for the construction of three-dimensional models and computational probing of structure-function relations in G protein-coupled receptors**. *Methods in neurosciences* 1995, **25**:366-428.
14. Ballesteros JA, Jensen AD, Liapakis G, Rasmussen SG, Shi L, Gether U, Javitch JA: **Activation of the β_2-adrenergic receptor involves disruption of an ionic lock between the cytoplasmic ends of transmembrane segments 3 and 6**. *Journal of biological chemistry* 2001, **276**(31):29171-29177.
15. Srivastava A, Yano J, Hirozane Y, Kefala G, Gruswitz F, Snell G, Lane W, Ivetac A, Aertgeerts K, Nguyen J: **High-resolution structure of the human GPR40 receptor bound to allosteric agonist TAK-875**. *Nature* 2014, **513**(7516):124-127.
16. Scheer A, Fanelli F, Costa T, De Benedetti P, Cotecchia S: **Constitutively active mutants of the α_{1B}-adrenergic receptor: Role of highly conserved polar amino acids in receptor activation**. *The EMBO* j*ournal* 1996, **15**(14):3566-3578.
17. Cotecchia S: **Constitutive activity and inverse agonism at the α_1-adrenoceptors**. *Biochemical pharmacology* 2007, **73**(8):1076-1083.
18. Rossier O, Abuin L, Fanelli F, Leonardi A, Cotecchia S: **Inverse agonism and neutral antagonism at α_{1A}- and α_{1B}-adrenergic receptor subtypes**. *Molecular pharmacology* 1999, **56**(5):858-866.
19. García-Sáinz JA, Torres-Padilla MaE: **Modulation of basal intracellular calcium by inverse agonists and phorbol myristate acetate in rat-1 fibroblasts stably expressing α_{1D}-adrenoceptors**. *FEBS letters* 1999, **443**(3):277-281.
20. McCune DF, Edelmann SE, Olges JR, Post GR, Waldrop BA, Waugh DJ, Perez DM, Piascik MT: **Regulation of the cellular localisation and signaling properties of the α_{1B}-and α_{1D}-adrenoceptors by agonists and inverse agonists**. *Molecular pharmacology* 2000, **57**(4):659-666.
21. Greasley PJ, Fanelli F, Rossier O, Abuin L, Cotecchia S: **Mutagenesis and modeling of the α_{1B}-adrenergic receptor highlight the role of the helix 3/helix 6 interface in receptor activation**. *Molecular pharmacology* 2002, **61**(5):1025-1032.

22. Bockenhauer S, Fürstenberg A, Yao XJ, Kobilka BK, Moerner W: **Conformational dynamics of single G protein-coupled receptors in solution**. *The journal of physical chemistry* 2011, **115**(45):13328-13338.

23. Deupi X, Li X-D, Schertler GF: **Ligands stabilize specific GPCR conformations: But how?** *Structure* 2012, **20**(8):1289-1290.

24. Reiner S, Ambrosio M, Hoffmann C, Lohse MJ: **Differential signaling of the endogenous agonists at the β_2-adrenergic receptor**. *Journal of biological chemistry* 2010, **285**(46):36188-36198.

25. Bokoch MP, Zou Y, Rasmussen SG, Liu CW, Nygaard R, Rosenbaum DM, Fung JJ, Choi H-J, Thian FS, Kobilka TS: **Ligand-specific regulation of the extracellular surface of a G protein-coupled receptor**. *Nature* 2010, **463**(7277):108-112.

26. Huber T, Menon S, Sakmar TP: **Structural basis for ligand binding and specificity in adrenergic receptors: Implications for GPCR-targeted drug discovery**. *Biochemistry* 2008, **47**(42):11013-11023.

27. Borhani DW, Shaw DE: **The future of molecular dynamics simulations in drug discovery**. *Journal of computer-aided molecular design* 2012, **26**(1):15-26.

28. Bucher D, Grant BJ, Markwick PR, McCammon JA: **Accessing a hidden conformation of the maltose binding protein using accelerated molecular dynamics**. *PLoS computational biology* 2011, **7**(4):e1002034.

29. Gasper PM, Fuglestad B, Komives EA, Markwick PR, McCammon JA: **Allosteric networks in thrombin distinguish procoagulant vs. anticoagulant activities**. *Proceedings of the national academy of sciences* 2012, **109**(52):21216-21222.

30. Markwick PR, Pierce LC, Goodin DB, McCammon JA: **Adaptive accelerated molecular dynamics (Ad-AMD) revealing the molecular plasticity of P450cam**. *The journal of physical chemistry letters* 2011, **2**(3):158-164.

31. Wereszczynski J, McCammon JA: **Nucleotide-dependent mechanism of Get3 as elucidated from free energy calculations**. *Proceedings of the national academy of sciences* 2012, **109**(20):7759-7764.

32. Miao Y, Caliman AD, McCammon JA: **Allosteric effects of sodium ion binding on activation of the M3 muscarinic G protein-coupled receptor**. *Biophysical journal* 2015, **108**(7):1796-1806.

33. Miao Y, Nichols SE, Gasper PM, Metzger VT, McCammon JA: **Activation and dynamic network of the M2 muscarinic receptor**. *Proceedings of the national academy of sciences* 2013, **110**(27):10982-10987.

34. Miao Y, Nichols SE, McCammon JA: **Free energy landscape of G protein coupled receptors explored by accelerated molecular dynamics**. *Physical chemistry chemical physics* 2014, **16**(14):6398-6406.

35. Kruse AC, Hu J, Pan AC, Arlow DH, Rosenbaum DM, Rosemond E, Green HF, Liu T, Chae PS, Dror RO: **Structure and dynamics of the M3 muscarinic acetylcholine receptor**. *Nature* 2012, **482**(7386):552-556.

36. Spalding TA, Burstein ES, Henderson SC, Ducote KR, Brann MR: **Identification of a ligand-dependent switch within a muscarinic receptor**. *Journal of biological chemistry* 1998, **273**(34):21563-21568.

37. Dror RO, Arlow DH, Maragakis P, Mildorf TJ, Pan AC, Xu H, Borhani DW, Shaw DE: **Activation mechanism of the β_2-adrenergic receptor**. *Proceedings of the national academy of sciences* 2011, **108**(46):18684-18689.

38. Nelson MT, Humphrey W, Gursoy A, Dalke A, Kalé LV, Skeel RD, Schulten K: **NAMD: A parallel, object-oriented molecular dynamics program**. *International journal of high performance computing applications* 1996, **10**(4):251-268.

39. Warne T, Serrano-Vega MJ, Baker JG, Moukhametzianov R, Edwards PC, Henderson R, Leslie AG, Tate CG, Schertler GF: **Structure of a β_1-adrenergic G protein-coupled receptor**. *Nature* 2008, **454**(7203):486-491.

40. Phillips JC, Braun R, Wang W, Gumbart J, Tajkhorshid E, Villa E, Chipot C, Skeel RD, Kale L, Schulten K: **Scalable molecular dynamics with NAMD**. *Journal of computational chemistry* 2005, **26**(16):1781-1802.

41. Grubmüller H: **SOLVATE v. 1.0. Theoretical biophysics group**. *Institute for medical optics, ludwig-maximilians university, munich* 1996.

42. Humphrey W, Dalke A, Schulten K: **VMD: Visual molecular dynamics**. *Journal of molecular graphics* 1996, **14**(1):33-38.

43. Spijker P, Vaidehi N, Freddolino PL, Hilbers PA, Goddard WA: **Dynamic behavior of fully solvated β_2-adrenergic receptor embedded in the membrane with bound**

agonist or antagonist. *Proceedings of the national academy of sciences* 2006, **103**(13):4882-4887.

44. Brooks BR, Bruccoleri RE, Olafson BD, States DJ, Swaminathan S, Karplus M: **CHARMM: A program for macromolecular energy, minimisation and dynamics calculations**. *Journal of computational chemistry* 1983, **4**(2):187-217.
45. Tu K, Tobias DJ, Klein ML: **Constant pressure and temperature molecular dynamics simulation of a fully hydrated liquid crystal phase dipalmitoylphosphatidylcholine bilayer**. *Biophysical journal* 1995, **69**(6):2558-2562.
46. Darden T, York D, Pedersen L: **Particle mesh Ewald: An N· log (N) method for Ewald sums in large systems**. *The journal of chemical physics* 1993, **98**(12):10089-10092.
47. Allen MP, Wilson MR: **Computer simulation of liquid crystals**. *Journal of computer-aided molecular design* 1989, **3**(4):335-353.
48. Miyamoto S, Kollman PA: **SETTLE: An analytical version of the SHAKE and RATTLE algorithm for rigid water models**. *Journal of computational chemistry* 1992, **13**(8):952-962.
49. Peeters M, Van Westen G, Li Q, IJzerman A: **Importance of the extracellular loops in G protein-coupled receptors for ligand recognition and receptor activation**. *Trends in pharmacological sciences* 2011, **32**(1):35-42.
50. Cherezov V, Rosenbaum DM, Hanson MA, Rasmussen SG, Thian FS, Kobilka TS, Choi H-J, Kuhn P, Weis WI, Kobilka BK: **High-resolution crystal structure of an engineered human β_2-adrenergic G protein–coupled receptor**. *Science* 2007, **318**(5854):1258-1265.
51. Rosenbaum DM, Rasmussen SG, Kobilka BK: **The structure and function of G protein-coupled receptors**. *Nature* 2009, **459**(7245):356-363.
52. Park JH, Scheerer P, Hofmann KP, Choe H-W, Ernst OP: **Crystal structure of the ligand-free G protein-coupled receptor opsin**. *Nature* 2008, **454**(7201):183-187.
53. Ragnarsson L, Wang C-IA, Andersson Å, Fajarningsih D, Monks T, Brust A, Rosengren KJ, Lewis RJ: **Conopeptide ρ-TIA defines a new allosteric site on the extracellular surface of the α_{1B}-adrenoceptor**. *Journal of biological chemistry* 2013, **288**(3):1814-1827.

54. Ragnarsson L, Andersson Å, Thomas WG, Lewis RJ: **Extracellular surface residues of the α_{1B}-adrenoceptor critical for G protein–coupled receptor function**. *Molecular pharmacology* 2015, **87**(1):121-129.

55. Shaw DE, Grossman J, Bank JA, Batson B, Butts JA, Chao JC, Deneroff MM, Dror RO, Even A, Fenton CH: **Anton 2: Raising the bar for performance and programmability in a special-purpose molecular dynamics supercomputer**. *Proceedings of the international conference for high performance computing, networking, storage and analysis* 2014;41-53.

56. Rasmussen SG, Choi H-J, Fung JJ, Pardon E, Casarosa P, Chae PS, DeVree BT, Rosenbaum DM, Thian FS, Kobilka TS: **Structure of a nanobody-stabilised active state of the β_2-adrenoceptor**. *Nature* 2011, **469**(7329):175-180.

57. Rasmussen SG, DeVree BT, Zou Y, Kruse AC, Chung KY, Kobilka TS, Thian FS, Chae PS, Pardon E, Calinski D: **Crystal structure of the β_2-adrenergic receptor-Gs protein complex**. *Nature* 2011, **477**(7366):549-555.

58. Dixon R, Sigal I, Candelore M, Register R, Scattergood W, Rands E, Strader C: **Structural features required for ligand binding to the β-adrenergic receptor**. *The EMBO journal* 1987, **6**(11):3269-3275.

59. Dohlman HG, Caron MG, DeBlasi A, Frielle T, Lefkowitz RJ: **Role of extracellular disulfide-bonded cysteines in the ligand binding function of the β_2-adrenergic receptor**. *Biochemistry* 1990, **29**(9):2335-2342.

60. Fraser C: **Site-directed mutagenesis of β-adrenergic receptors. Identification of conserved cysteine residues that independently affect ligand binding and receptor activation**. *Journal of biological chemistry* 1989, **264**(16):9266-9270.

61. Karnik SS, Sakmar TP, Chen H-B, Khorana HG: **Cysteine residues 110 and 187 are essential for the formation of correct structure in bovine rhodopsin**. *Proceedings of the national academy of sciences* 1988, **85**(22):8459-8463.

62. Karnik SS, Khorana HG: **Assembly of functional rhodopsin requires a disulfide bond between cysteine residues 110 and 187**. *Journal of biological chemistry* 1990, **265**(29):17520-17524.

63. Kurtenbach E, Curtis C, Pedder E, Aitken A, Harris A, Hulme E: **Muscarinic acetylcholine receptors. Peptide sequencing identifies residues involved in**

antagonist binding and disulfide bond formation. *Journal of biological chemistry* 1990, **265**(23):13702-13708.

64. Noda K, Saad Y, Graham RM, Karnik SS: **The high affinity state of the β_2-adrenergic receptor requires unique interaction between conserved and non-conserved extracellular loop cysteines**. *Journal of biological chemistry* 1994, **269**(9):6743-6752.
65. Zhou H, Tai H-H: **Expression and functional characterisation of mutant human CXCR4 in insect cells: Role of cysteinyl and negatively charged residues in ligand binding**. *Archives of biochemistry and biophysics* 2000, **373**(1):211-217.
66. Perlman JH, Wang W, Nussenzveig DR, Gershengorn MC: **A disulfide bond between conserved extracellular cysteines in the thyrotropin-releasing hormone receptor is critical for binding**. *Journal of biological chemistry* 1995, **270**(42):24682-24685.
67. Cook JV, Eidne KA: **An intramolecular disulfide bond between conserved extracellular cysteines in the gonadotropin-releasing hormone receptor is essential for binding and activation**. *Endocrinology* 1997, **138**(7):2800-2806.
68. Lin SW, Sakmar TP: **Specific tryptophan UV-absorbance changes are probes of the transition of rhodopsin to its active state**. *Biochemistry* 1996, **35**(34):11149-11159.
69. Dror RO, Mildorf TJ, Hilger D, Manglik A, Borhani DW, Arlow DH, Philippsen A, Villanueva N, Yang Z, Lerch MT: **Structural basis for nucleotide exchange in heterotrimeric G proteins**. *Science* 2015, **348**(6241):1361-1365.
70. Manglik A, Kim TH, Masureel M, Altenbach C, Yang Z, Hilger D, Lerch MT, Kobilka TS, Thian FS, Hubbell WL: **Structural insights into the dynamic process of β_2-adrenergic receptor signaling**. *Cell* 2015, **161**(5):1101-1111.
71. Sena Jr DM, Cong X, Giorgetti A, Kless A, Carloni P: **Structural heterogeneity of the μ-opioid receptor's conformational ensemble in the apo state**. *Scientific reports* 2017,**7**: 1-7.
72. Latorraca NR, Venkatakrishnan A, Dror RO: **GPCR dynamics: Structures in motion**. *Chemical reviews* 2016, **117**(1):139-155.
73. Mhaouty-Kodja S, Barak LS, Scheer A, Abuin L, Diviani D, Caron MG, Cotecchia S: **Constitutively active α_{1B}-adrenergic receptor mutants display different phosphorylation and internalisation features**. *Molecular pharmacology* 1999, **55**(2):339-347.

74. Porter JE, Hwa J, Perez DM: **Activation of the α_{1B}-adrenergic receptor is initiated by disruption of an interhelical salt bridge constraint**. *Journal of biological chemistry* 1996, **271**(45):28318-28323.

75. Kappel K, Miao Y, McCammon JA: **Accelerated molecular dynamics simulations of ligand binding to a muscarinic G protein-coupled receptor**. *Quarterly reviews of biophysics* 2015, **48**(04):479-487.

Chapter 4

Chapter 4: Virtual Screening of the α_1-AR Modulators

4.1 Introduction

GPCRs have been predominantly classified as the leading class of target proteins [1, 2] for three reasons [3]

a) GPCRs are known to be involved widely in most cellular processes,

b) GPCRs are located on the cell surface where they are accessible to drug binding and

c)Clinical mutations in GPCRs are associated with various pathologies ranging from asthma and allergies to Parkinson's disease [4, 5].

However, fairly little is known about the mechanism by which agonist binding [6] induces the conformational changes [7] essential for G protein stimulation and intracellular signaling [8, 9]. GPCRs are increasingly associated with a high attrition rate in translating fundamental preclinical discoveries into the clinic [10]. In part, this may reflect a failure to appreciate and capture novel paradigms associated with drug action at GPCRs. Indeed, it is now well established that GPCRs possess spatially distinct and druggable allosteric sites that can be found at extracellular, TM-spanning or intracellular domains [11].

Targeting GPCR allosteric sites has the potential to lead to novel modes of GPCR subtype selectivity, signal-pathway-selective (biased) modulation [12] and importantly a "saturability" to the allosteric effect that can be exploited to "fine-tune" drug responsiveness [13]. However, many of these theoretical advantages of allosteric drugs have yet to be optimally explored in the context of disease [14-17] and this represents a significant next step for the field. Excitingly, structural biology studies have started to identify the molecular mechanisms that underlie the pharmacological effects of allosteric modulators [18] and are facilitating structure-based allosteric drug discovery at this important receptor family [19, 20].

Kobilka group has shown the role of agonists, neutral antagonists and inverse agonists in stabilising dissimilar ECS conformations of the β_2-AR initiating innovative prospects for allosteric drug targeting at GPCRs [21]. Preliminary results from experimental studies in our lab have identified an agonist induced bond swap that initiates a cascade of conformational changes that appears to explain the link between NE binding and α_{1B}-AR signaling [22-24]. Ragnarsson et al ., predicted a highly ordered ECL2 with several intramolecular interactions, a salt bridge and a conserved disulfide bond but no well-defined secondary structure in the homology model of the hamster α_{1B}-AR built from the crystal structure of the turkey-β_1-AR (PDB: 2VT4) [25].

Breaking this structurally important disulfide bond facilitated binding of the α_{1B}-AR selective allosteric antagonist, ρ-conotoxin-TIA despite reducing NE potency, affinity and efficacy [22]. Previous studies on rhodopsin activation have shown that ECL2 is displaced from the retinal binding site as a consequence of re-arrangements in the hydrogen bond network connecting ECL2 with the extracellular ends of TM4, TM5 and TM6. Together with a movement of TM5 which breaks the highly conserved ionic lock (E/DRY), these conformational shifts cause receptor activation

α_1-AR are part of a larger AR family all activated by the catecholamines; E and NE [26, 27, 28]. α_{1B}-AR mediates many effects of the sympathetic nervous system [29]. Activation of α_1-AR activates Na^+/K^+ pumps that lead to cell hyperpolarisation and decreases the propensity for abnormal heart rhythms [30, 31]. Hence, α_1-AR play role in maintaining cardiac contractility under pathological conditions such as ischaemia or pathological hypertrophy that are associated with decreased β_1-AR function [32-34] and control and regulate blood pressure [35]. However, limited agonists and antagonists are known for the α_1-AR despite their importance in patho-physiological condition and are not subtype specific [36-38]. The lack of subtype-selective agonists has limited our understanding of the characteristic structural features which requires the design and development of subtype-selective compounds [39]. Therefore, a rational drug design approach is of tremendous importance to help find the probable subtype specific new leads.

The dominant technique for the identification of new lead compounds in drug discovery is the physical screening of large libraries of chemicals against a biological target (HTS). VS is an alternative approach to computationally screen large libraries of chemicals for compounds that complement targets of known structure and experimentally test those that are predicted to bind well. It accesses many possible new ligands which can be purchased and tested. VS or *In silico* screening is a new approach attracting increasing levels of interest in the pharmaceutical industry as a productive and cost-effective technology in the search for novel lead compounds [40] (**Figure 4-1**).

VS as aninitial step in rational drug design [41] approach has emerged as a cost and time effective method for screening of millions of compound databases in recent years compared to traditional HTS [42, 43]. VS has been identified as an *in silico* method for the evaluation of the molecular properties of different scaffolds for binding affinity, interaction energy etc., and prioritises databases as actives/in-actives against a particular target [44]. Two fundamental

methods for VS are illustrated in the literature; ligand based similarity searching [21, 45] and structure based docking [46-48]. Ligand based VS is most widely used when 3D structure of the receptor/target is not known and hence all the pharmacophoric information is extracted from the known active molecule for the receptor [21]. Screening methods use one or more bioactive template for lead identification which overlooks the active hits with dissimilar structure resulting in false negative rate [49].

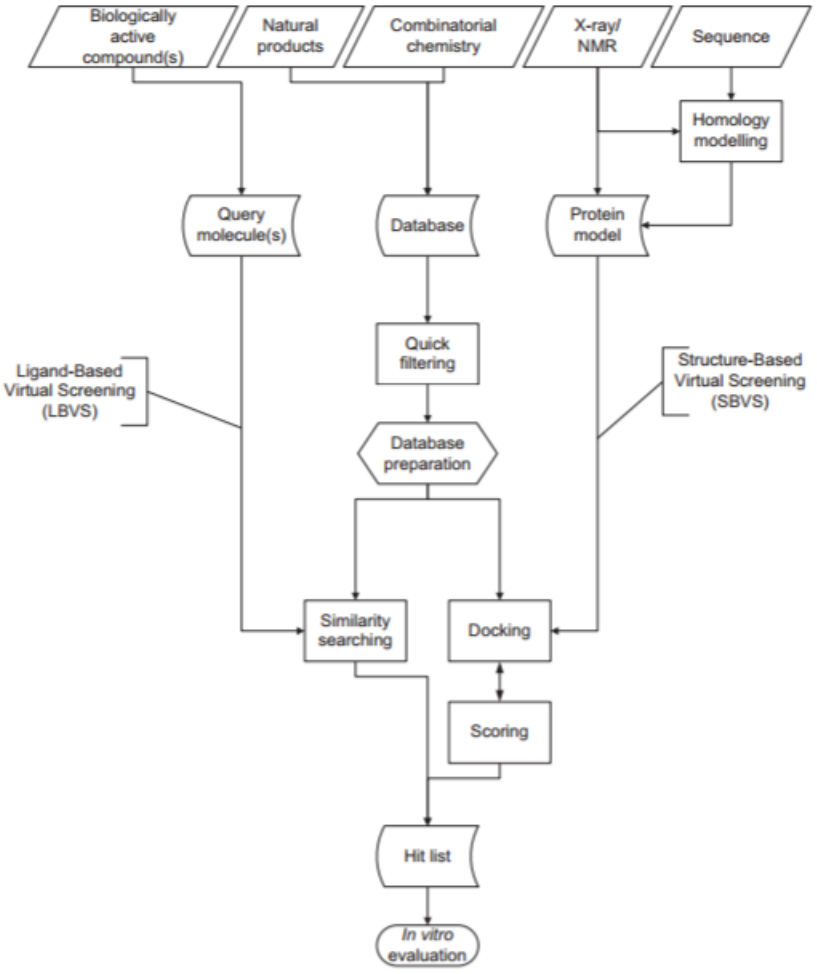

Figure 4-1: Overview of virtual screening process [50] (Image courtesy: Kalliokoski T et al., *Dissertations in health sciences;* 2010,22:1-174).

4.1.1 Concept of Virtual Screening

The basic goal of the VS is the reduction of the enormous virtual chemical space of small organic molecules to synthesise and/or screen against a specific target protein to a manageable number of the compounds that inhibit a highest chance to lead to a drug candidate [51]. Many drug candidates fail in the clinical trials because of the reasons unrelated to the potency against intended drug target. Pharmacokinetic & toxicity issues are blamed for more than half of the failure in the clinical trials [52] (**Figure 4-2**). Therefore, VS evaluates the drug likeness of the same molecules independent of their intended drug target. VS has been used to describe a process of computationally analysing large compound collections in order to prioritise compounds for synthesis or assay [53]. In our work, we have focused on receptor–ligand interactions based on molecular docking and scoring functions as a means of yielding the most detailed model in a way in which a given ligand will bind to a receptor and this will be the most informative basis to assess which ligands are useful candidates for assay.

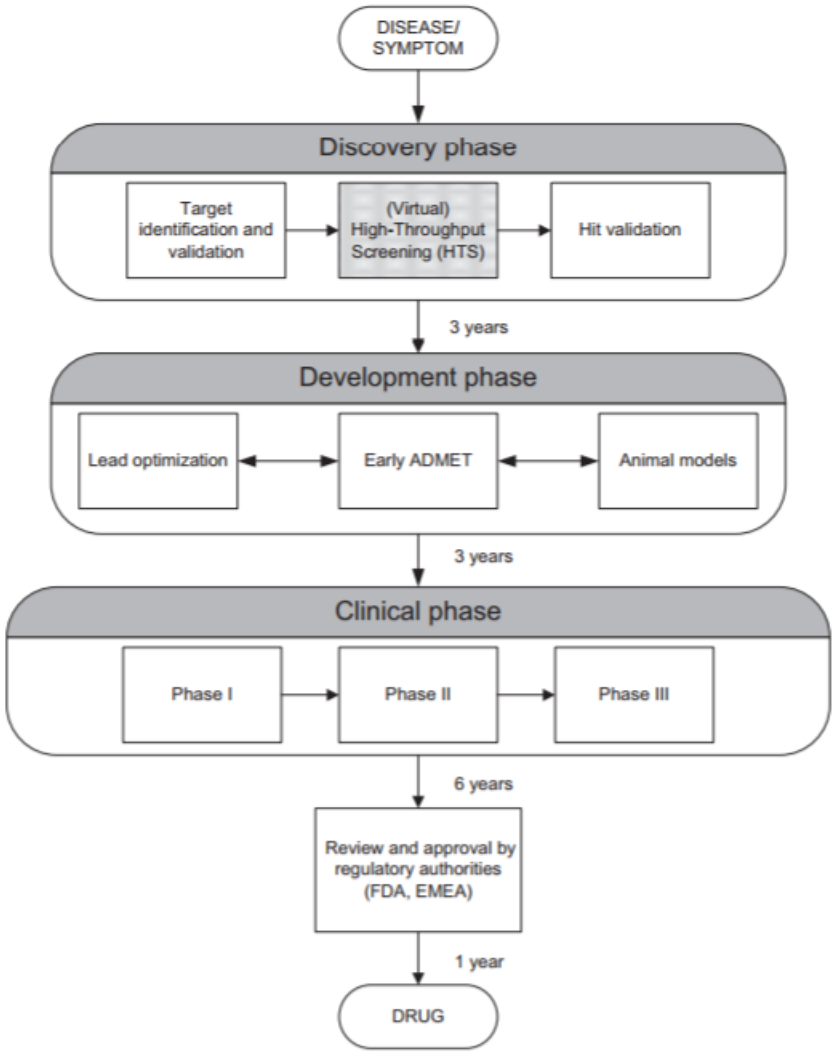

Figure 4-2: The drug development process [54] (Image courtesy: O'Driscoll C et al., P*roceedings of horizon symposium; Charting Chemical Space* 2004, 1-4).

VS of the interactions against the homology modeled receptors [55, 56] and known actives have accelerated the drug discovery process. The hits identified can then be validated for their activity by standard cell based assays. Previous VS studies on class A GPCR members such as Adenosine A2A-receptor [57], β_2-AR [58], Chemokine CXCR4 receptor [59], Dopamine D1 and D2 receptor [60] and Histamine H1 receptor [61] have successfully screened selective agonists and antagonists.

In this study, VS of the NE like compounds was performed based on the shape similarity from commercially available ZINC database [62]. However, VS of NE like compounds may result in false negative hits. The rate of false negative screened hits is nullified by validating the VS

process by a set of known compounds that are active on α_1-AR. The screened compounds were subjected to Lipinski's rule of five for drug like properties followed by docking of the resulting hits. The hits retrieved were analysed based on the scoring function [63, 64] for their binding affinity and number of hydrogen bonds formed while docking and were validated experimentally for their potency. This research is expected to open the door to the rational development of new modulators that can recognise the ECS of α_1-AR.

4.2 Material and Methods

4.2.1 Virtual Screening

Rapid Overlay of Chemical Structures (ROCS) software [65] was used for the screening of drug-like compounds library obtained from ZINC database [62]. ROCS make use of shape-based superimposition method which screens the molecule that is similar in shape to that of the query molecule. The method does not require any structural information for the screening. In ROCS, solid body optimisation method is used to maximise the volume overlap between the query and database molecules and an atom-centered Gaussian model is used to compute the geometric overlap when molecules are aligned [66].

The molecules screened are ranked according to shape coefficient, color coefficient and combined Tanimoto coefficient which integrates both shape and color scoring function. Each of these scoring function ranges from 0-1 where 0 is dissimilarity and 1 is maximum similarity and for combined Tanimoto coefficient the score ranges from 0-2. In this study, we used combined Tanimoto coefficient to rank the screened hits [67]. NE was used as a query for the screening of drug like compounds library as α_1-AR are activated by catceholamines; E and NE [28]. However, α_{1B}-AR selective pharmacophore would have been more appropriate to screen the α_{1B}-AR subtype-specific modulators but we chose to use NE as a common chemical entity to screen the database for the α_1-ARs and testing the screened hits against all the three α_1-AR (α_{1A}-AR, α_{1B}-AR and α_{1D}-AR) subtypes. NE contains conformers and therefore multi-conformer query generated by OMEGA [68, 69] software implemented in OpenEye package was used for the screening.

4.2.2 Database Selection & Preparation

Drug like compounds database was downloaded from the Zinc database which is commercial database for the millions of synthesised compounds. The compounds in drug like database are already sorted for the Lipinsky's rule of five [52]. This database contains >17 million compounds which were then expanded into a set of 3D conformers by OMEGA with 0.5rms and erange 5 kcal/mol after initial screening. OMEGA generates 3D conformations of the molecules which are most likely to be in bioactive conformation. OMEGA makes use of connection table method for generating initial set of the 3D conformers for a given molecule [68].

4.2.3 Molecular Docking

Docking studies were carried out to study the binding mode of screened potential library members against the α_{1B}-AR homology model (chapter 2) by FRED software implemented in OEDocking module of OpenEye package [70, 71]. The screened hits were tested by a blind docking strategy in the ECS that included both the orthosteric binding pocket and the auxiliary site 1 and auxiliary site 2 identified during the egress pathway of NE in chapter 2. FRED is a rigid docking tool for ultrahigh-throughput docking of >1 million compounds in single run. The receptor was prepared with receptor preparation graphical user interface of OEDocking module. The receptor grid was set to 37.32Å*34.42Å*36.62Å with other default parameters to sufficiently accommodate the ECS and orthosteric binding site to dock screened hits.

FRED systemically examines all the best possible receptor-hits pose [72] and screens them for shape complementarily and chemical features and ranks the hits based on Chemgauss4 scoring function [70]. The cut-off score was set to 7Å after visual inspection of the binding pose of hits to the receptor. The top screened hits from FRED docking were further subjected for flexible docking with AutoDock. In AutoDock, the grid maps were prepared using the AutoGrid utility with 54*52*48 points which is sufficiently large to accommodate all active site residues and grid spacing set to 0.375Å. Docking parameters were kept as per following: number of individuals in the population was set to 150, maximum number of energy evaluations was set to 2500000, maximum number of generations was set to 2700 and number of GA runs was set to 20.

4.2.4 Transient Expression of α_1-AR

COS-1 cells (ATCC, Manassas, VA) were cultured in Dulbecco's modified Eagle's medium (DMEM) supplemented with 5% fetal bovine serum (FBS) in a humidified incubator at 37ºC and 5% CO2. Cells were transiently transfected with purified plasmid DNA encoding WT α_{1A}-AR, α_{1B}-AR and α_{1D}-AR using FuGENE HD (Roche) (18µg DNA/75cm^2) following the manufacturer's protocol [22].

4.2.5 FLIPR Assay Measuring Intracellular Ca^{2+} Responses

On the day of the assay, cells were loaded with the Calcium 4 no-wash dye (Molecular Devices) by diluting the lyophilised dye in physiological salt solution and incubating for 30 min at 37°C in a 5% humidified CO2 incubator. Intracellular Ca^{2+} responses were measured in response to

increasing concentrations of agonist (NE) and test compounds (12) (10μM–100μM) in FLIPR (Molecular Devices, Sunnyvale, CA) using a cooled CCD camera with excitation at 470–495nM and emission at 515–575nM. Camera gain and intensity were adjusted for each plate to yield a minimum of 1000 arbitrary fluorescence units (AFU) baseline fluorescence. Prior to addition of NE/test compounds, 10 baseline fluorescence readings were taken followed by fluorescent readings every second for 300s. Further, intracellular Ca^{2+} responses were measured in response to second addition of agonist (NE) (100μM) to ascertain the characteristic behaviour of compounds as agonists and partial agonists. Concentration-response curves were established by plotting DeltaF/F_0 values, where F_0 is the base-line level of fluorescence and Delta F is the change in fluorescence from the baseline level against agonist concentration using Prism (GraphPad Software).

4.3 Results and Discussion

VS of the drug-like database compounds led to identification of hits which might acts as potential leads for α_1-AR. A detailed workflow of the procedure from compounds source to the screened hits and their experimental activity is outlined in **Figure 4-3**. Molecular modeling and experimental studies suggests that agonist NE and antagonist prazosin might partly have similar binding sites and residues in the receptor although prazosin's binding pocket extends above that of NE and include residues from the ECS [73]. Taking this information in account, NE was used as a 3D query to search the drug like compounds database that resulted in hits with similar chemical and pharmacophoric features. The drug like compounds database is already screened for Lipinsky's rule of five to ensure the resultant hits to be potential leads.

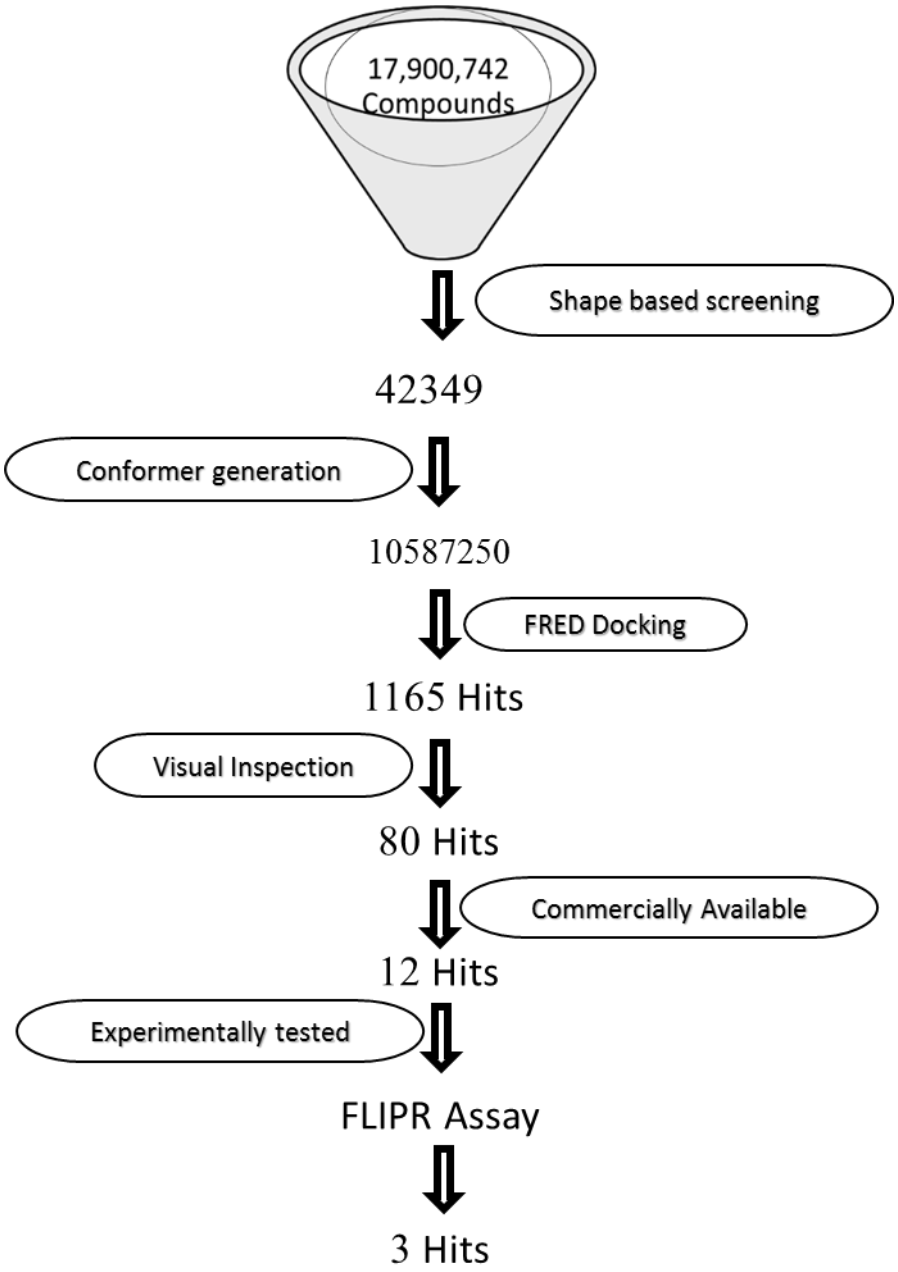

Figure 4-3: A detailed workflow of the procedure from compounds source to the screened hits and their experimental activity.

To proceed with our hypothesis of finding probable modulators based on NE structure, we made use of a similarity searching method implemented in ROCS which makes use of Gaussian based function as an algorithm for identification of molecular volume. This overlaps the query with the database compounds and screen compounds that overlay well with volume as measure of

similarity and mismatches compounds with dissimilar volume. ROCS is a shape based superimposition method that search 3D chemical space of multi-conformer ensembles based on shape screening followed by chemical features

Based on the experimental studies on α_{1B}-AR, we chose NE as our starting query for VS which binds in the similar pocket as that of antagonist prazosin [73, 74]. NE was downloaded from ZINC database and subjected to energy minimisation using MMFF94 force-field in ChemBio3D with an RMS gradient of 0.01 and iterations set to 500. The minimised structure was used for shape based screening of ~17 million drugs like compounds database. Drug like database downloaded from zinc incorporates compounds that follow Lipinsky's rule of five and might be potential subtype-specificα_1-AR leads. The compounds in the database have a molecular weight between >=150 and <= 500, number of hydrogen bond donors <=5, number of hydrogen bond acceptors <=10, number of rotatable bonds <= 7, xlogP <=5 and polar surface area <=150$Å^2$. The potential library members were ranked based on Tanimoto coefficient which is a measure of shape and color coefficients.

In ROCS, after performing shape alignment, color force field is implemented to screen chemical features like the query and to further refine hits from shape based superimpositions based on chemical similarity. The color score is a measure of the actual score of the hit divided by the color score of the query molecule. The hits ranked are measure of both shape and chemical complementary and each of them ranges from 0 to 1. The final score ranges from 0 to 2 with 0 as a measure of dissimilarity and 2 as the maximum similarity. After initial screening, a total of 42,349 hits were obtained which were then expanded into a set of conformers by OMEGA tool implemented in Openeye toolkit. The torsional sampling ranges from 5° to 60° with energy cut off set to 5Kcal/mole. OMEGA generates 3D conformers of a molecule from the SMILE format by using connection tables.

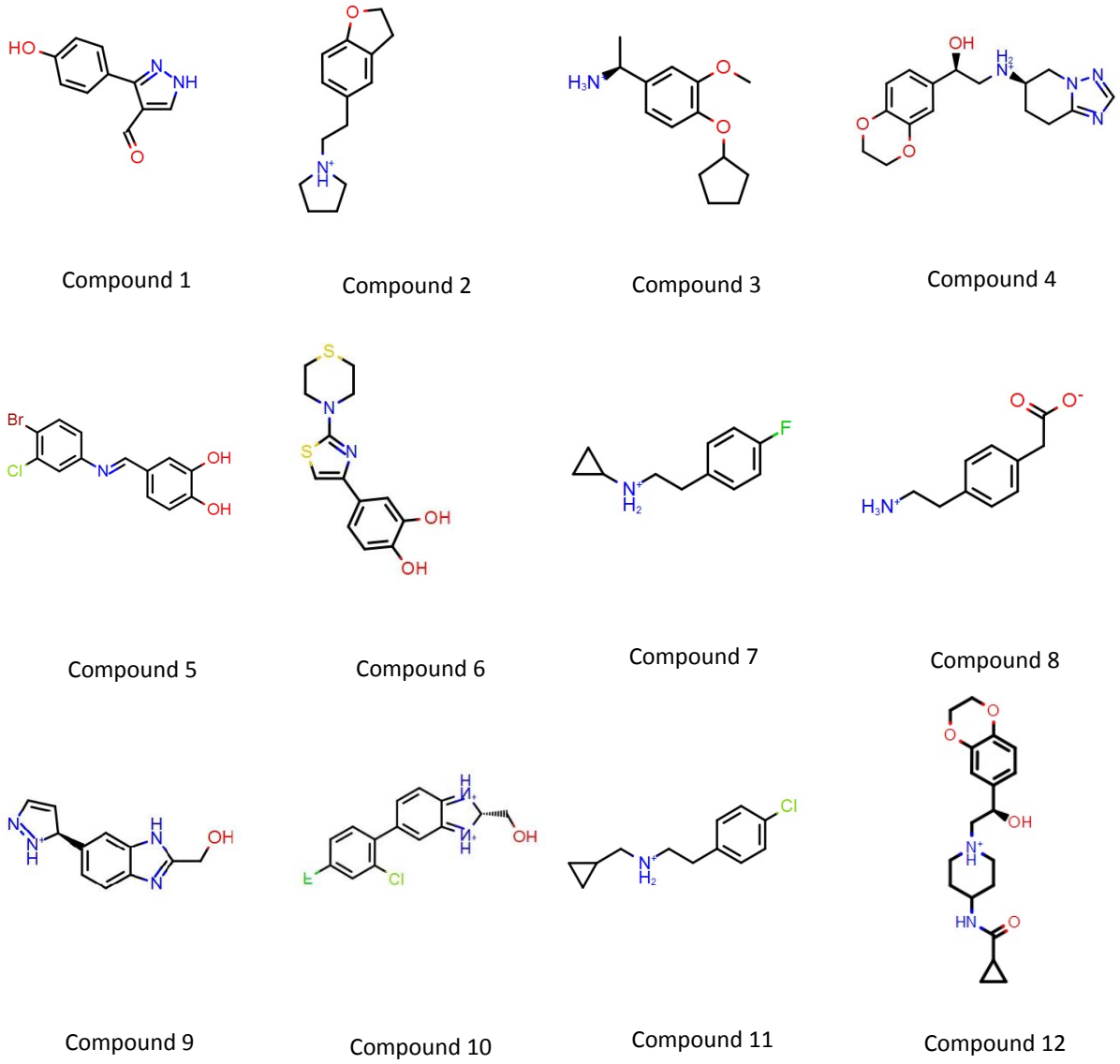

Figure 4-4: Chemical structure of 12 screened hits from virtual screening.

OMEGA generated ~1 million conformers for the initial hits which were then subjected to rigid docking in FRED tool of OEDocking. The receptor was prepared for the hydrogen atoms, energy minimised and grid generated across the orthosteric binding site and upper half of the ECS to ensure free binding of the hits in different regions of the receptor. Docking hits were ranked according to Chemgauss4 scoring function with a cut-off value of -9 which resulted in 1165 hits. These were visually inspected for their binding in the orthosteric site and ECS along with their interactions to the residues (Asp125 and Ser207) and we clustered top 20 hits into 4 groups as

hits interacting like NE (position 1, chapter 2), hits interacting with either of the residues (Asp125 and Ser207) in binding site (position 1, chapter 2), hits forming interactions with residues in ECS only (position 3, chapter 2) and hits which form interactions with residues both in orthosteric binding site and ECS (position 2, chapter 2). 12 of these were secured from the vendors and were tested for their activity on α_1-AR subtypes. **Figure 4-4** depicts the chemical structures of the 12 screened hits.

The effect of the resultant 12 hits as potential leads was measured on COS-1 cells transfected with WT-α_{1A}-AR, WT-α_{1B}-AR and WT-α_{1D}-AR. The effect was measured for increase in intracellular Ca^{2+} response with FLIPR and data was analysed by GraphPad PRISM 6.0. The hits obtained were chemically diverse to ensure the coverage of chemical space with different pharmacophoric features. The results of initial characterisation revealed that the hits that docked in the orthosteric site of the α_{1B}-AR (**Figure 4-5**) activated all the α_1-AR subtypes confirming the potential of this approach to identify new α_1-AR GPCR modulators. **Figure 4-5** shows the docked pose and binding mode of all the 12 hits in the orthosteric site A) Side view, B) Top view, C) Binding mode of top hits 1, 4, 5, 7, 10 and 12 along with cirazoline and oxymetazoline selective drugs for α_1-AR, D) Docked pose of NE, E-J) Individual docked pose of compounds 1, 4, 5, 7, 10 and 12, K) Cirazoline docking pose and L) Oxymetazoline docking pose.

A)

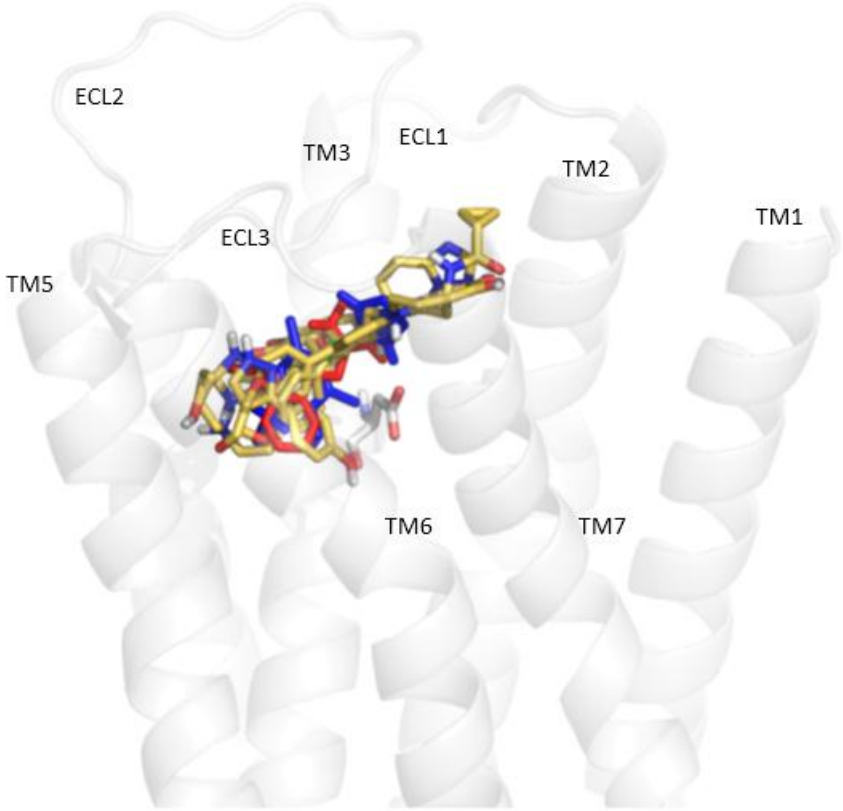
ECL2
TM3
ECL1
TM2
TM1
ECL3
TM5
TM6
TM7

B)

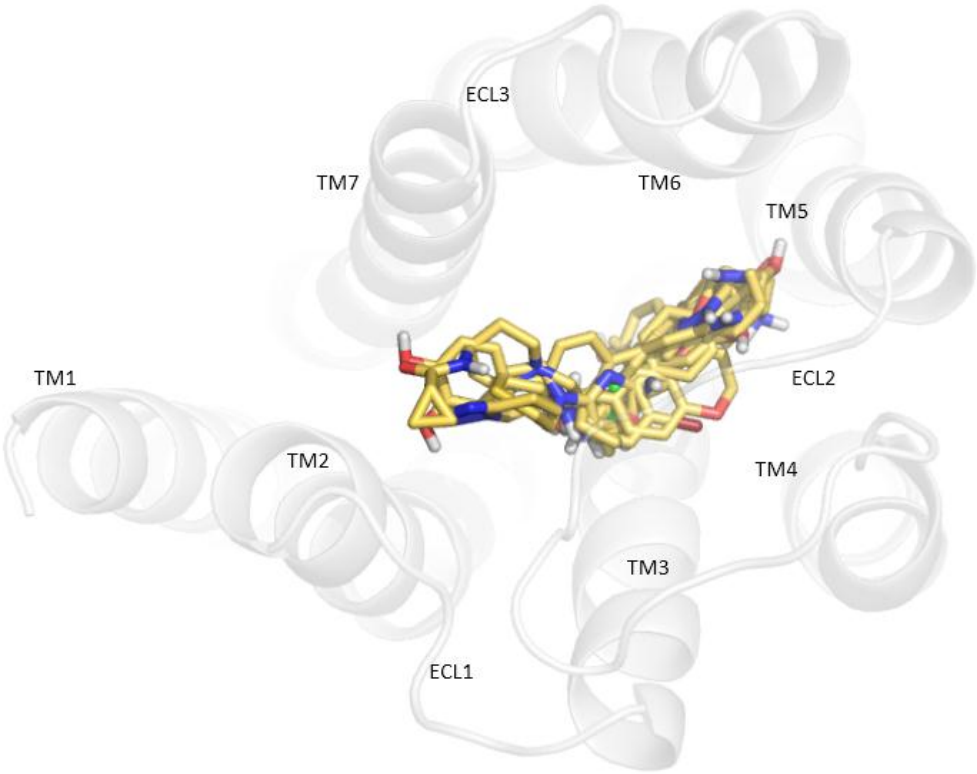
ECL3
TM7
TM6
TM5
TM1
ECL2
TM2
TM4
TM3
ECL1

C)

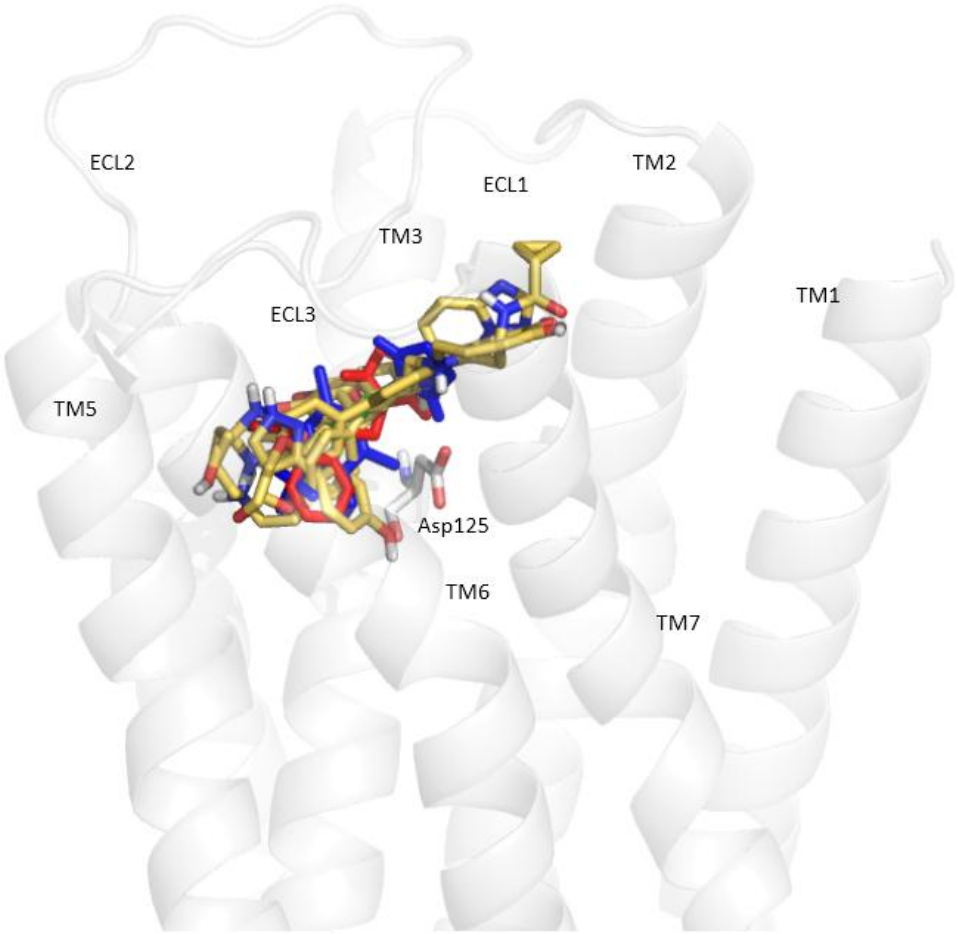

Comp 1, 4, 5, 7, 10, 12

D)

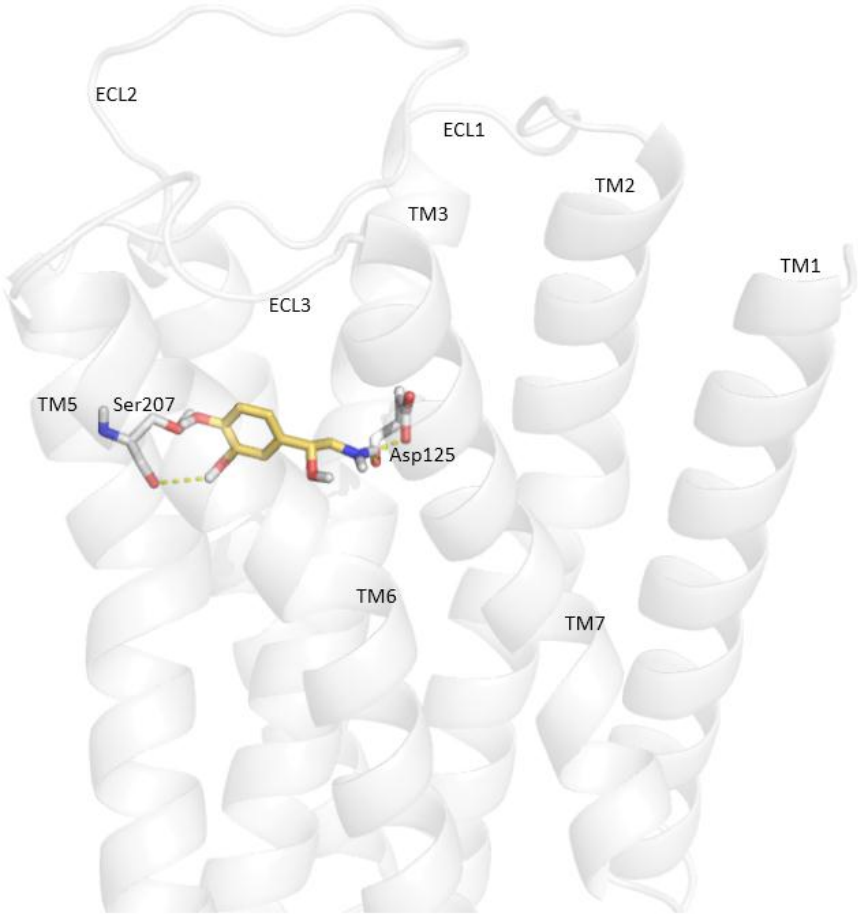

NE

E)

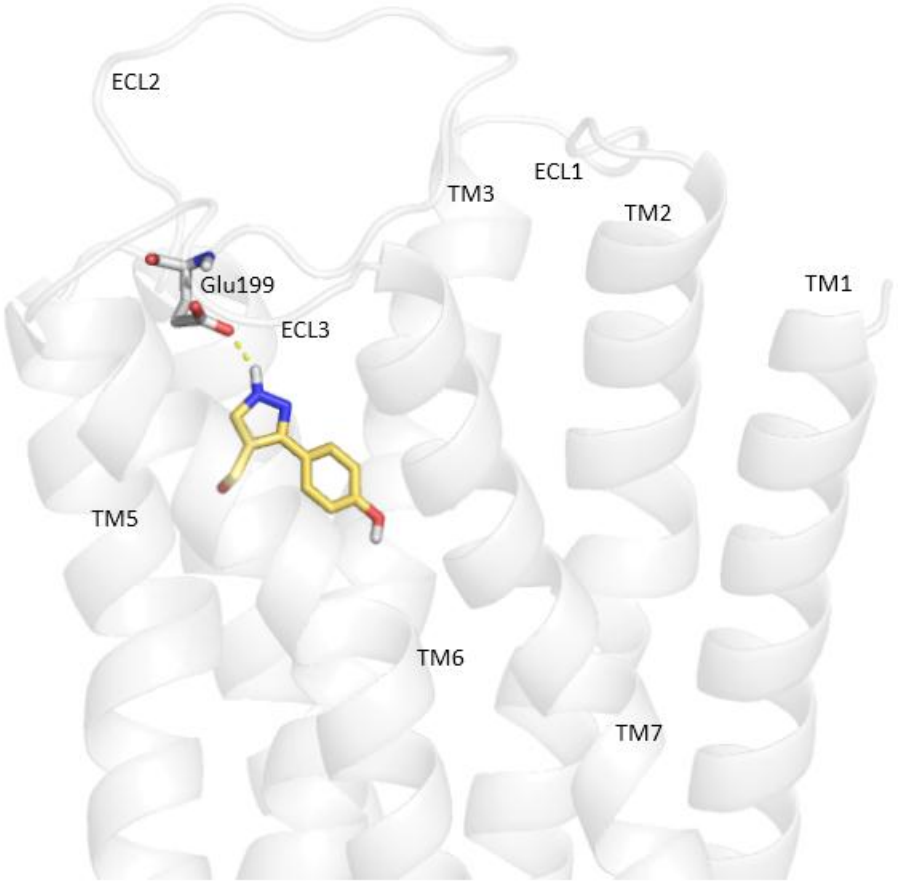

Comp 1

F)

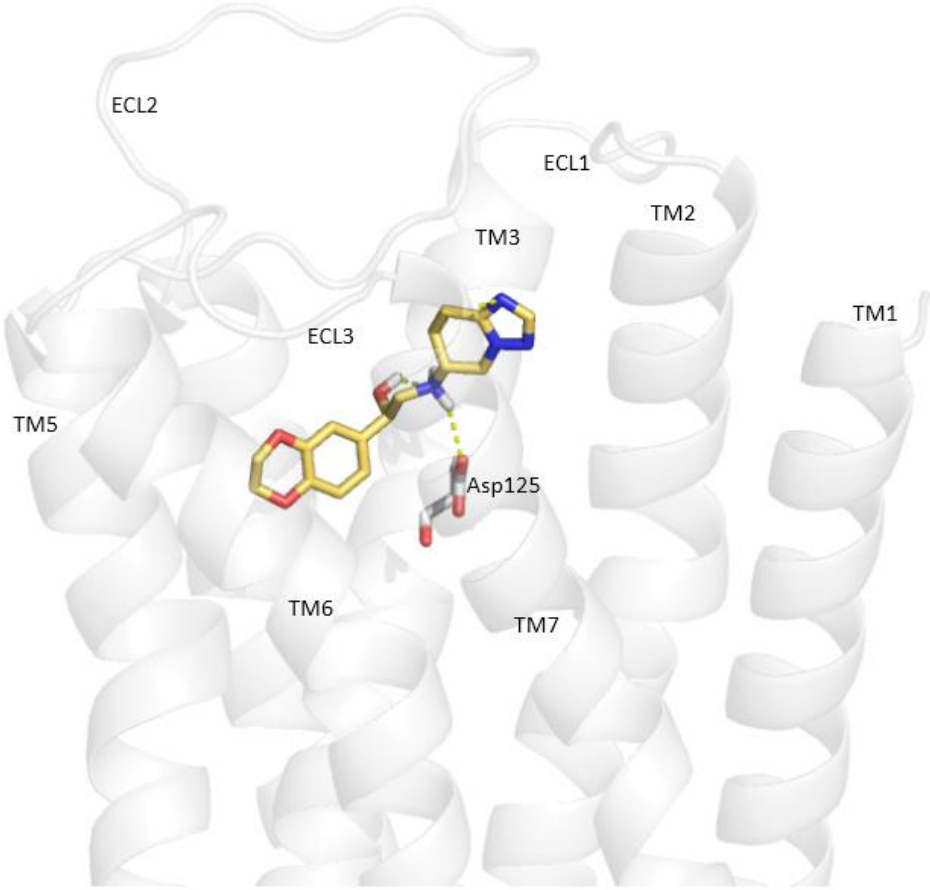

Comp 4

G)

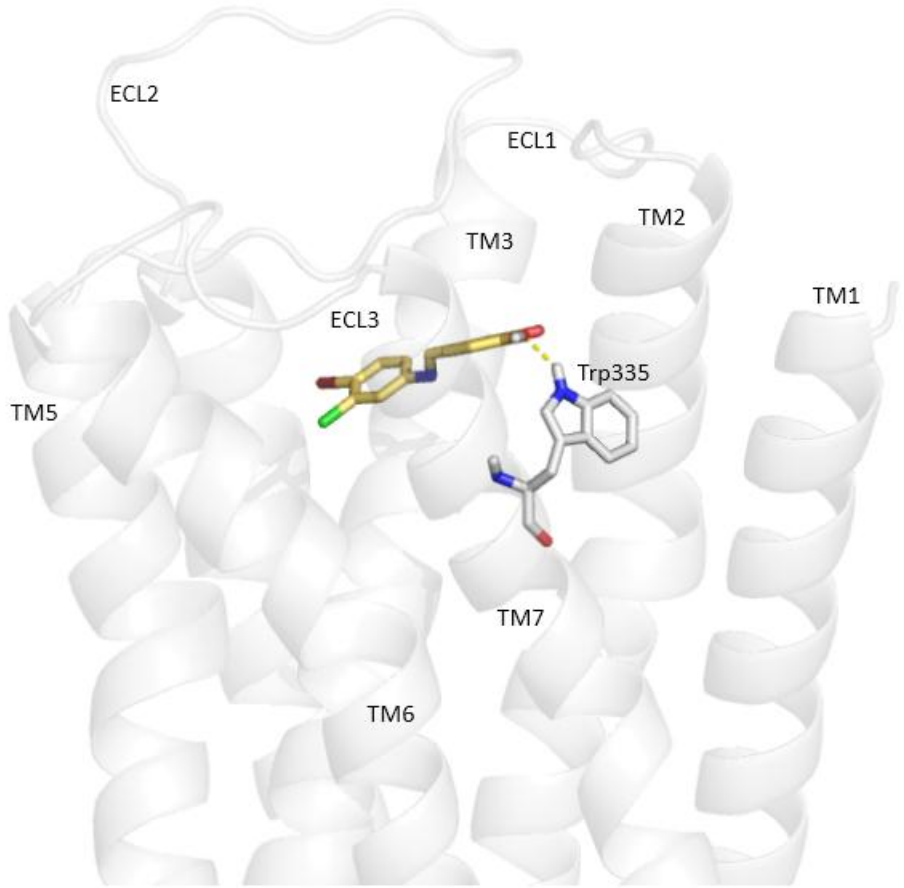

Comp 5

H)

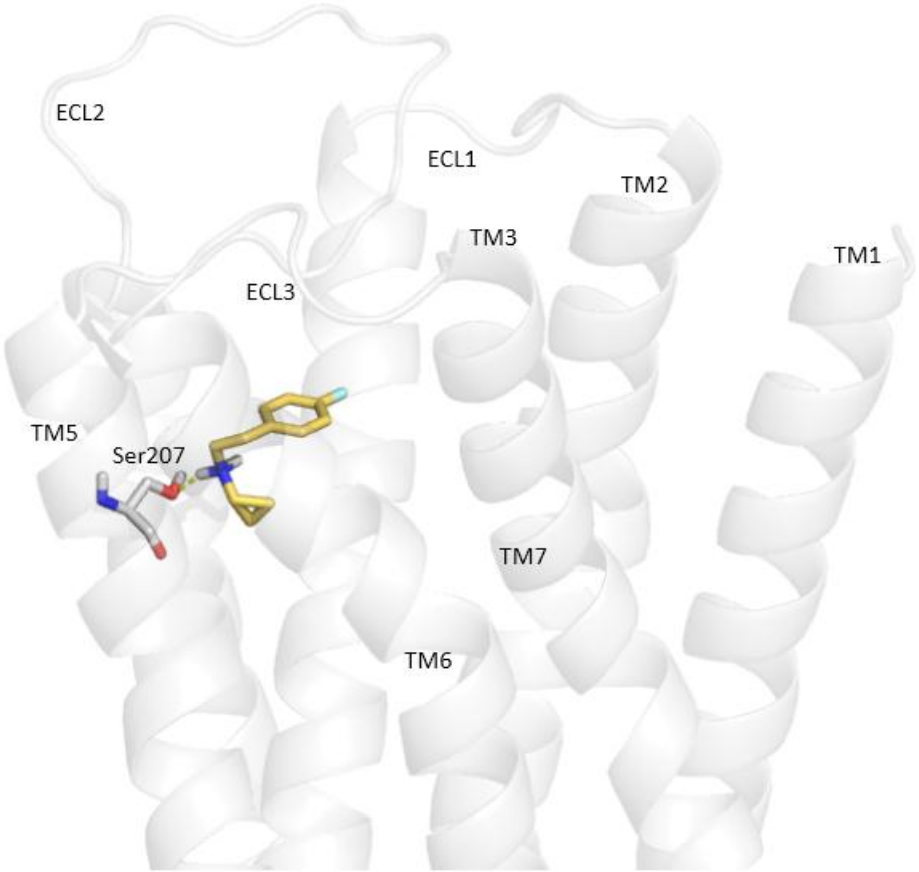

Comp 7

I)

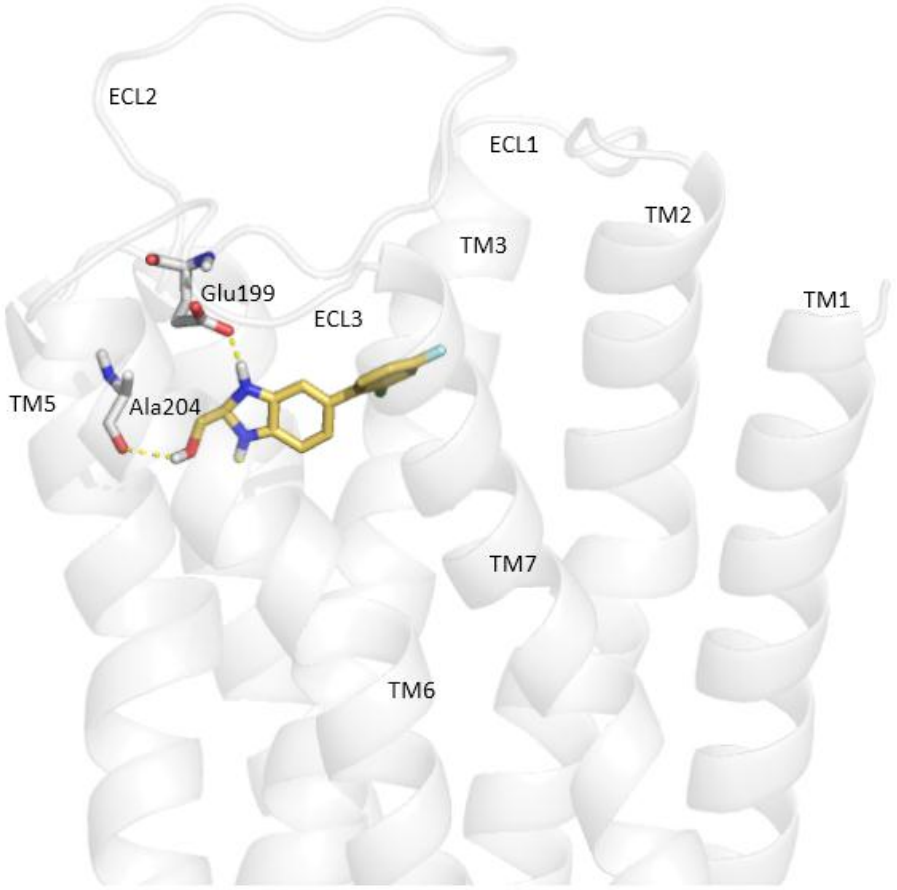

Comp 10

J)

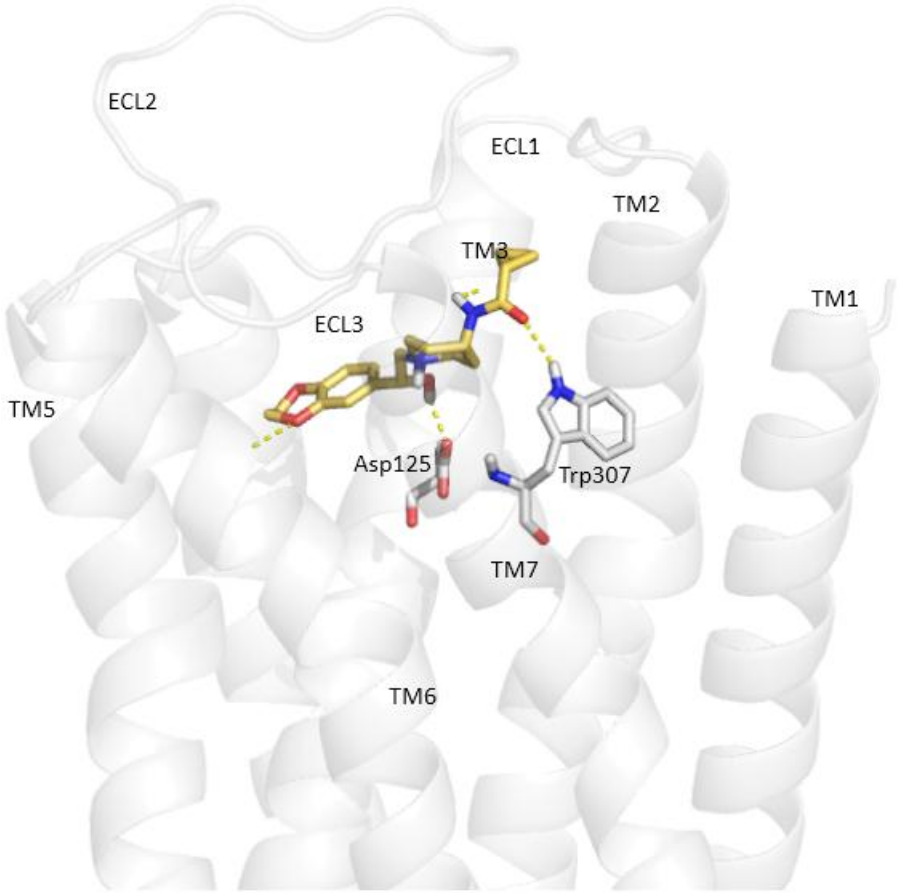

Comp 12

K)

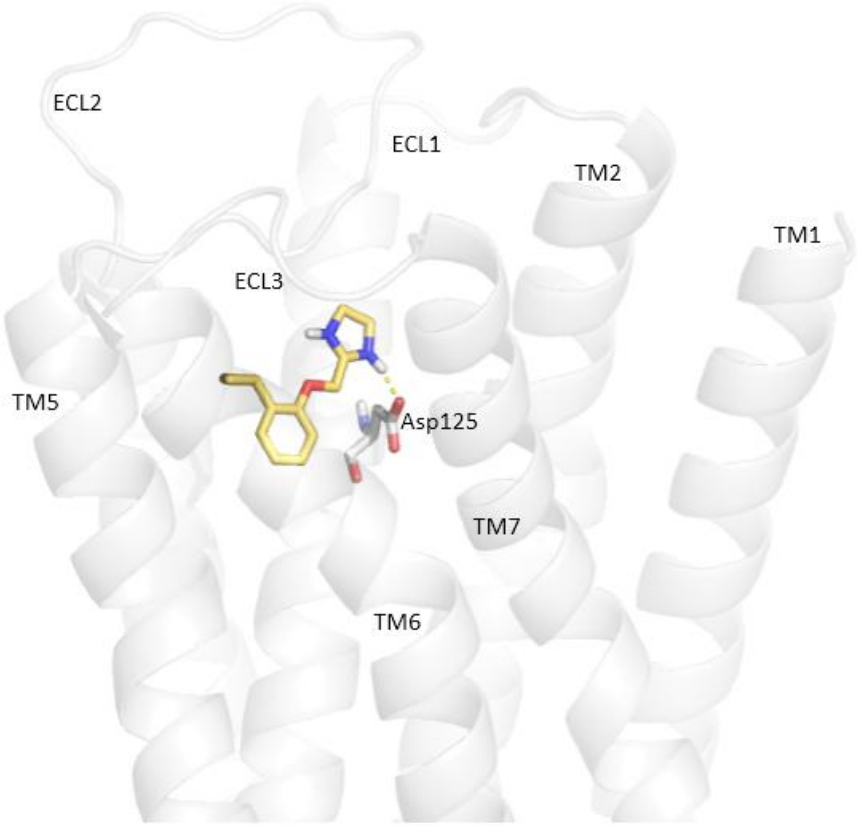

Cirazoline

L)

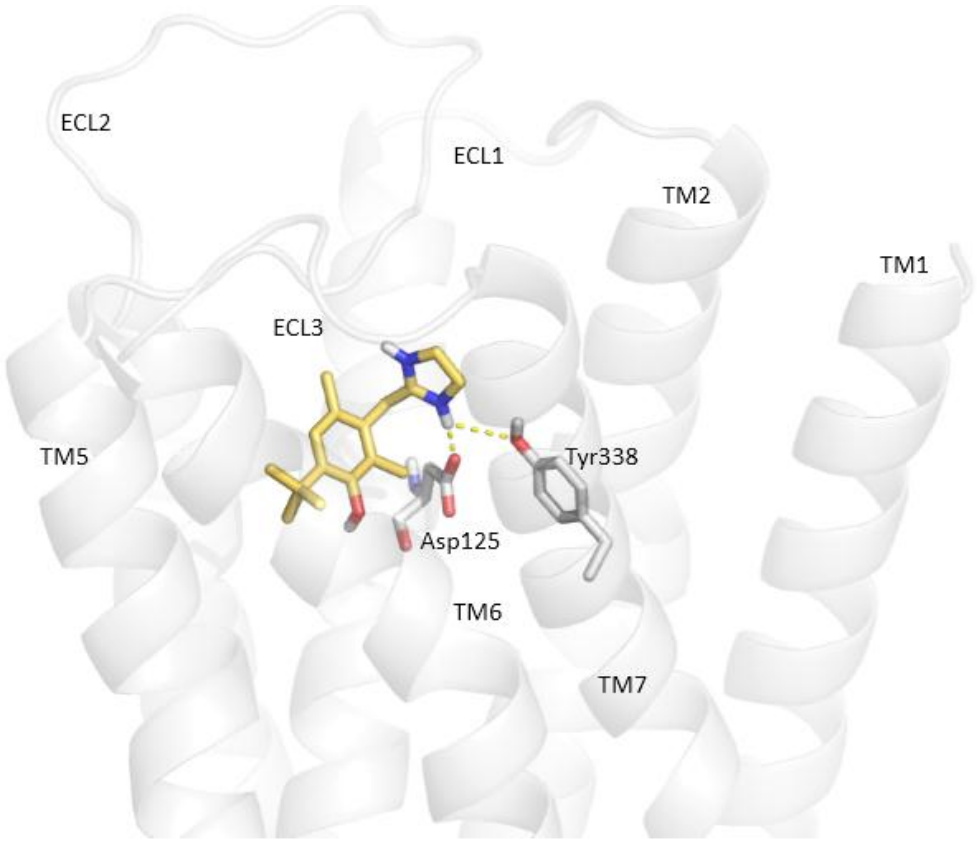

Oxymetazoline

Figure 4-5: Docking poses for 12 selected leads identified to bind within the orthosteric site of the α_1-AR A) Side view, B) Top view, C) Overlay of 1, 4, 5, 7, 10 and 12 (yellow) with the binding mode of cirazoline (red) and oxymetazoline (blue), D) NE docking pose, E–J) individual docking poses for compounds 1, 4, 5, 7, 10 and 12, K) Cirazoline docking pose and L) Oxymetazoline docking pose.

The chemical structures of the α_1-AR selective agonists NE, cirazoline and oxymetazoline are shown in **Figure 4-6**. The 12 hits docked in the orthosteric site and partially with ECS making interaction with residues at both sites. The pharmacophoric and chemical features of these hits are like existing α_1-AR agonists. A detailed SAR study of these hits could further lead to improvement in the functionality to these receptors. Further, the screened hits show the importance of the imidazole functional group to be the main chemical moiety present in the α_1-AR modulators. We did not test these hits on the β_1- or β_2-AR, dopamine or 5-HT receptors. Thus, their selectivity only to the α_1-ARs was established.

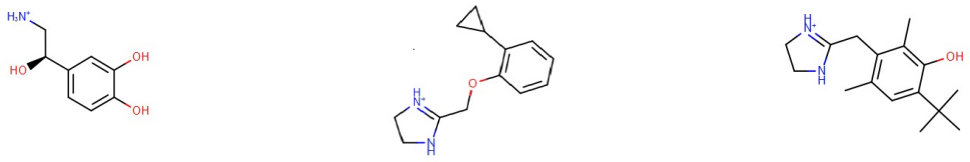

Norepinephrine Cirazoline Oxymetazoline

Figure 4-6: Chemical structures of the α_1-AR agonists NE, Cirazoline and Oxymetazoline.

The hits were tested for agonist activity and initial FLIPR screening identified 3 hits: compound 7, 10 and 12. Compound 10 is shown to have weak potency for α_{1B}-AR with effects on α_{1A} and α_{1D}-AR. For **figure 4-7** compound 10 has an EC_{50} of approx. 1µM and compound 12 has an EC_{50} of approx. 10µM. Compound 10 is a full agonist while compound 12 is a weak partial agonist. Compound 7 (5.24 ± 0.56 (nM), n=3), compound 10 (5.83 ± 0.57 (nM), n=3) and compound 12 (6.15 ± 0.23 (nM), n=3) are weak agonists for α_{1A}-AR while Compound 10 (5.49 ± 0.74 (nM), n=3) and compound 12 (7.52 ± 0.86 (nM), n=3) have similar potency on α_{1D}-AR. Compound 10 is a weak agonist for α_{1B}-AR with an EC_{50} value 4.66 ± 0.61 (nM), n=3. Compound 7 and 12 have no activity on α_{1B}-AR subtype. **Figure 4-7** shows the agonist concentration response curve at WT-α_1-AR subtypes measuring calcium accumulation using the FLIPR in response to increasing concentrations of NE and compounds 7, 10 and 12 in transiently transfected COS-1 cells.

VS and FLIPR assays lead to the identification of 3 compounds 7, 10 and 12 as agonist on α_1-ARs subtypes. However, we did not test these hits for the antagonistic activity on α_1-AR subtypes. Compound 10 is weak agonist for α_{1A}-and α_{1B}-AR subtypes while it is full agonist for α_{1D}-AR subtype. Compound 12 is weak agonist for α_{1A}- AR and α_{1D}-AR and compound 7 is weak agonist for α_{1A}-AR subtype. **Figure 4-8** shows the bar graph for potency of compounds 7, 10 and 12 compared with NE at α_1-AR WT subtypes for agonists.

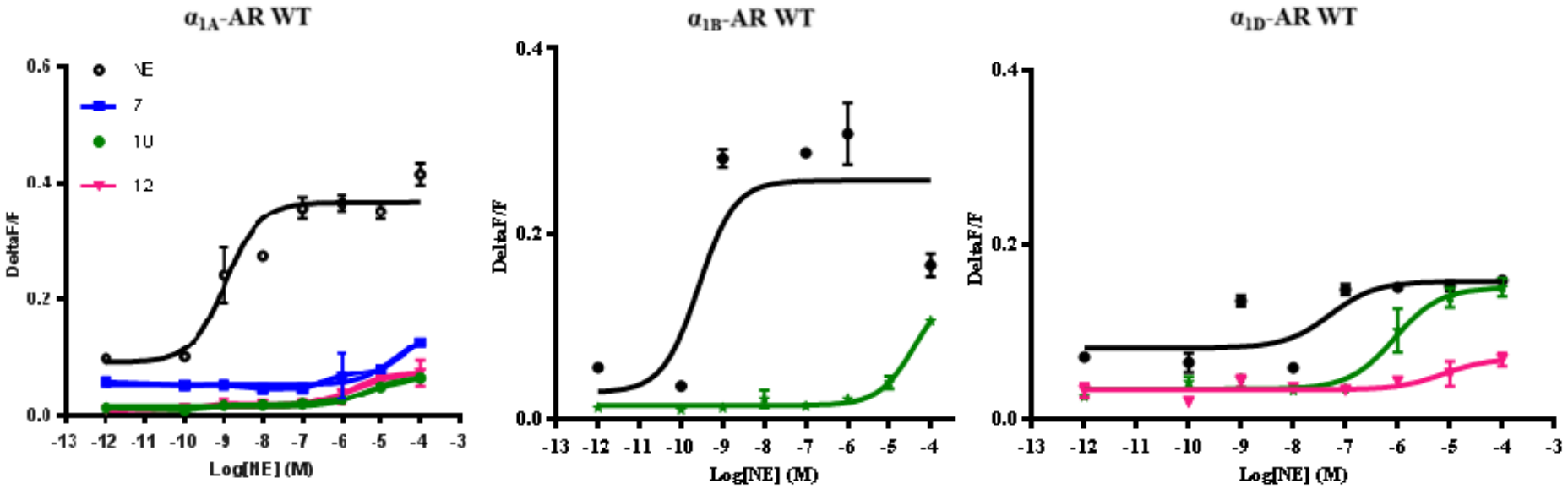

Figure 4-7: Representative agonist concentration-response curves at WT α_1-AR subtypes measuring calcium accumulation using the FLIPR in response to increase concentrations of NE and compounds 7, 10 and 12 in transiently transfected COS-1 cells. Data are means ± SEM of a representative experiment performed in triplicate showing NE, 7, 10 and 12.

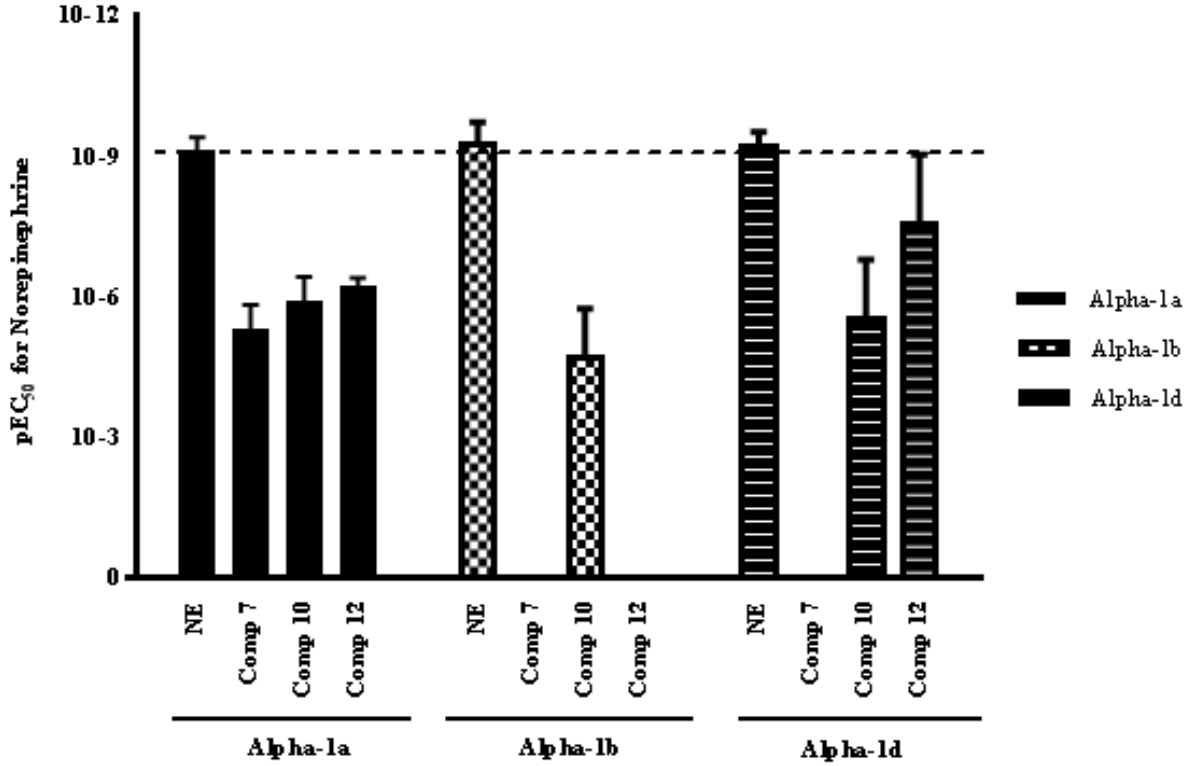

Figure 4-8: Bar graph showing potency of compounds 7, 10 and 12 compared with NE at α_1-AR WT subtypes for agonists.

In this study, we examined the implications of using a homology model of the α_{1B}-AR for the *in silico* VS of modulators as agonists. α_1-ARs are known targets for treating diseases like hypertension and benign prostatic hypertrophy which marks their importance to be relatively high in disease control. Due to lack of crystal structures, computer-aided drug design technique was employed for the ligand-based modeling and VS. Drug discovery based on crystal structures of rhodopsin, β-AR has been reported in the literature [75-78].

Most of class A GPCR ligands bind inside the TM bundle (**Figure 4-9)** but some ligands have shown binding at atypical sites commonly referred as allosteric sites or auxiliary sites. MD simulations of ligand entry into β_2-AR revealed a transient vestibule on the ECS [79] which constitute an allosteric site for the muscarinic M_2 receptor positive allosteric modulator (PAM) LY2119620 [80]. The FFA_1 receptor agonist TAK875 binds from the orthosteric site between TM3 and TM4 and extends [81] into the membrane while the $P2Y_1$ antagonist BPTU [82] and the glucagon receptor antagonist MK-0893 [83] bind at the interface between the exterior surface of the TM bundle and cell membrane. However, studies have revealed intracellular ligand binding to several chemokine receptors including CCR4, CCR5, CXCR1, CXCR2, and CX3CR1 [84]

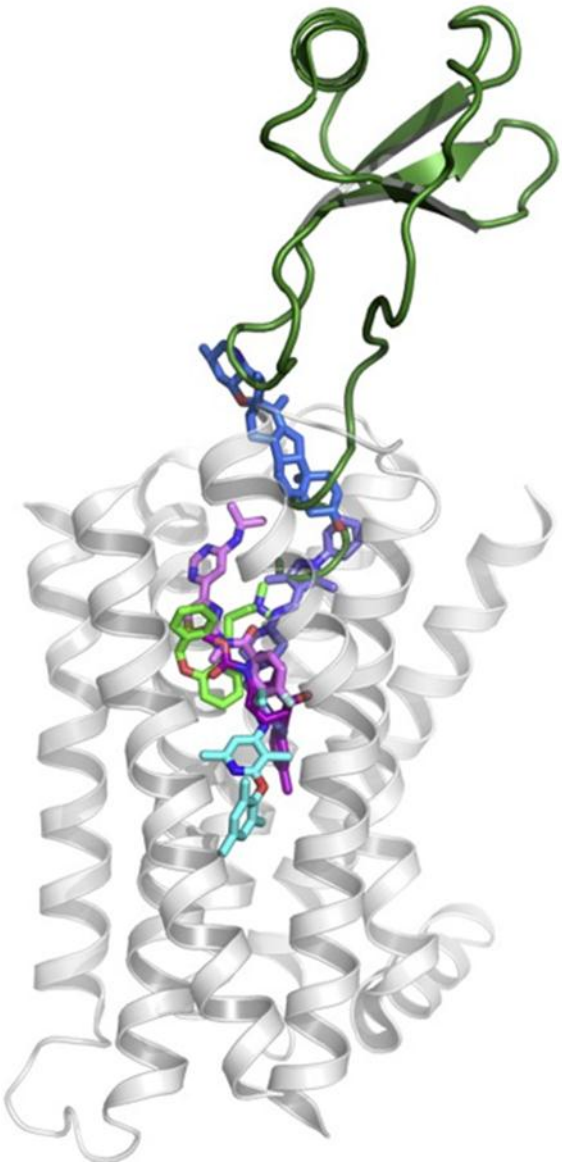

Figure 4-9: Depth of ligand binding in the TM pocket for the GPCR classes A, B, C and F. The deepest and most superficial ligand pair is displayed for each class. The histamine H_1 receptor (with light green doxepin, PDB: 3RZE) is displayed as transparent white cartoon and was used for the superposition of the other structure complexes for; class A: CXCR4-vMIP-II (dark green, PDB: 4RWS), B: CRF_1R-CP-376395 (pink, PDB: 4K5Y), C: $mGlu_1$-FITM (pink, PDB: 4OR2) and $mGlu_5$-mavoglurant (magenta, 4OO9), and F: smoothened receptor-SANT-1 (purple, PDB: 4N4W) and smoothened receptor-cyclopamine (blue, PDB: 4O9R) [85] (Image courtesy: Munk C. et al., *Curr. Opin. Pharmacol.*; 2016;30;51-58).

GPCRdb contains 13.304 mutations for 57 receptors from 10,192 publications (**Figure 4-10**). Rhee *et al.*, provided a web resource containing 390 GPCR manually annotated literature mutations for 38 receptors and comparative sequence alignments [86]. TinyGrap database in its

published release contained 10,500 GPCR mutations from 1400 articles [87]. Three functional regions for ligand binding, G protein coupling and signal transduction have been identified in a study by Madabushi et al., which agreed with over 200 function-altering *in vitro* mutants [88]. A minimal ligand binding pocket has been defined within a network of correlated mutations identified by multiple sequence and structural analysis of GPCRs through evolutionary tracing technique [89].

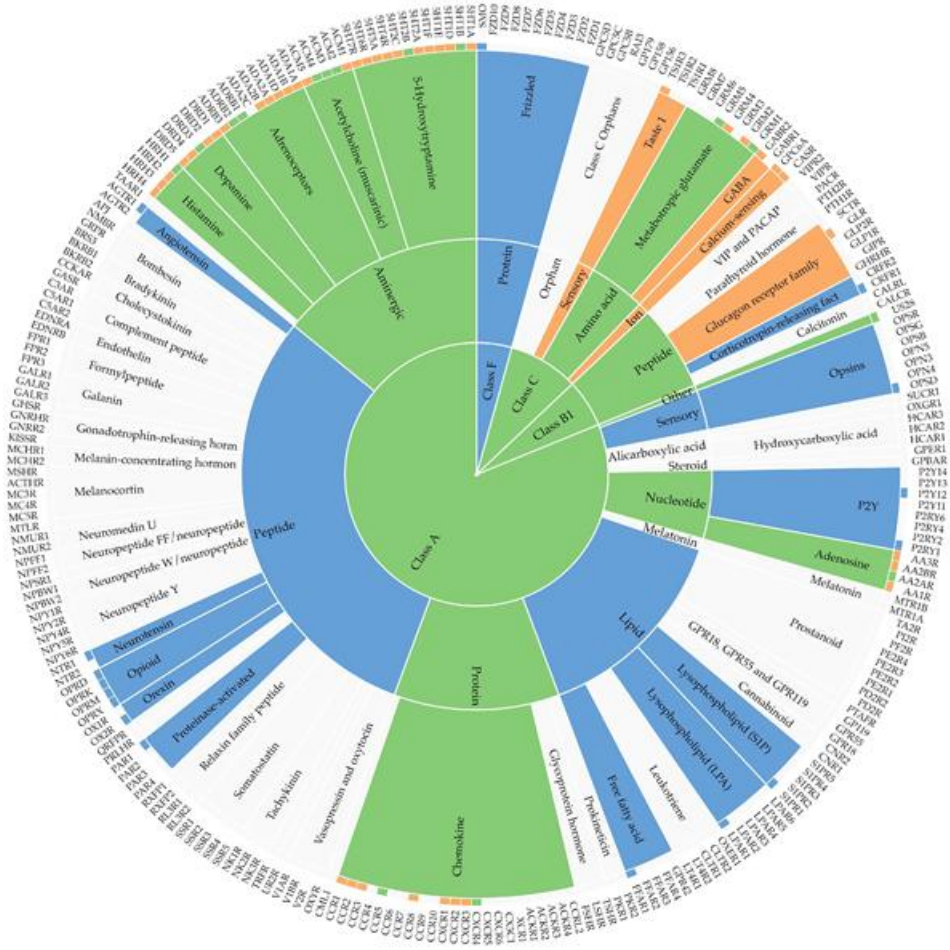

Figure 4-10: Structural and mutagenesis ligand interaction data in GPCRdb across the GPCR classes, ligand types and receptor families. Colour scheme; blue: structure complex data, orange: mutagenesis data, and green: both data types [85] (Image courtesy: Munk C. et al., *Curr. Opin. Pharmacol.;* 2016;30;51-58).

The endogenous bioamines, adrenaline, dopamine, histamine, and serotonin have a common generic pharmacophore binding site described in the literature for the natural ligands and analogues [90-92]. Mutagenesis experiments paired with several analyses have identified ligand binding (**Figure 4-11**) and efficacy-mediating residues for the serotonin, 5-HT2A, dopamine D2,

and glutamate receptors [93-95]. Four positions (6.44, 6.48, 7.45, and 7.46) were found to be conserved in most class A GPCRs indicating that they are likely to have a general function. 12 positions identified for the generic binding site comprised 12 residues on TM3 (3.32, 3.33, 3.37, and 3.40), TM5 (5.42, 5.43, 5.46, and 5.47), TM6 (6.51 and 6.52) and TM7 (7.42 and 7.43) [96]. **Figure 4-11** reveals endogenous ligand binding sites are identical in three dopaminergic receptors (DRD2−4/D_{2-4}) and six adrenoceptors (ADRB1−3/β_{1-3}, ADRA1B,D/$\alpha_{1B,D}$, and ADRA2B/α_{2B}); this is plausible given the high structural similarity of the ligands dopamine and adrenaline. However, selectivity of some compounds is achieved through differences in the binding site conferred by the next shell of amino acids through differences in passage of the ligands through the ECLs into the binding site or for drug like molecules through binding to additional residues that do vary between the receptors. In drug design, lead compounds can be inferred from nearest neighbors and tree topologies can be used to provide predictions for off-target activity for compounds. The specific ligand binding site of the aminergic ligand family shows the value of identification of the specific residues that are in contact with the ligand. This has important implications for drug design because if the binding sites can be identified for privileged structures, it provides a very useful paradigm for lead generation and optimisation as well as prediction of likely off-target activities whether they are wanted (mixed pharmacology) or unwanted (side effects).

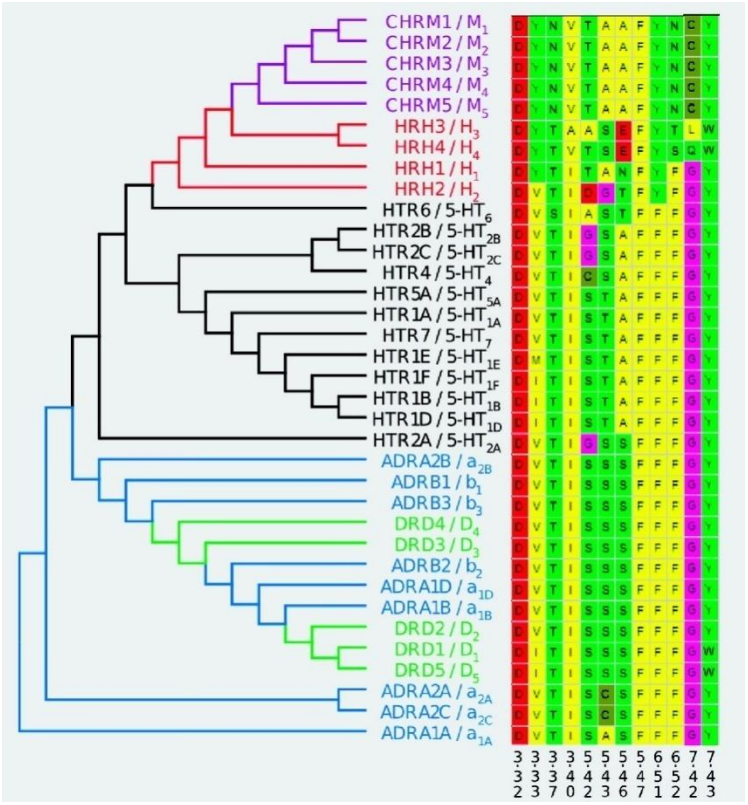

Figure 4-11: Dendogram and alignment of the human aminergic receptors based on the residue positions in the aminergic binding site as defined by evolutionary trace analysis. Receptors have been named using both the official Gene and IUPHAR conventions. The amino acids are color-coding according to physicochemical properties. The residue positions are indexed using Ballesteros−Weinstein numbering [96] (Image courtesy: David E et al., *J. Med. Chem.;* 2009;52;4429-4442).

Bremner et al., has shown high binding selectivity of ligands as antagonists for α_1-AR and were reported to have three features, (i) A basic nitrogen that is accessible and can easily be protonated at physiological pH (ii) An aromatic ring (iii) A preferably nonaromatic ring [97]. But, the difference between these subtypes was in the distances and angles between features of their pharmacophore (Hypotheses) generated by means of Catalyst software. However, Barbaro et al., excluded the above three features and proved that the typical pharmacophore (hypothesis) for the α_1-AR antagonist of antihypertensive lead drugs consists of five constraint features namely: (i) one positive ionisable portion (ii) one hydrogen bond acceptor and (iii) three hydrophobic features [98, 99].

Greene et al., stated that the α_1-agonist binding pocket is located in the TM domain near the extracellular face and that an aspartate side chain in the TM3 binds the hydrogen of the

protonated amine of both agonists and antagonists [100]. Close to this residue is also a large hydrophobic pocket containing conserved aromatic (hydrophobic) and serine/cysteine (hydrogen bond acceptor) residues suggesting that the α_1-AR agonist hypothesis consists of only three features and hence their ligands will be less firmly held to it than with the antagonist. Guimares and Daniel concluded that ideal α_1-AR agonist hypothesis contains three features namely; positive ionisable (PI), hydrogen bond acceptor (HBA) and only one hydrophobic feature (HY) [101]. Ismail et al., reported the constraint dimensions between the three features in the generated α_1-AR agonist hypothesis [102].

The role of imidazoquinazoline derivatives have been widely demonstrated in diverse biological activities including the anti-hypertensive activities through a selective α_1-antagonistic mechanism [103-105]. It was also reported that the arylpiperazinyl alkyl moiety was the key element in defining α_1-antagonist activity [106-110]. Accordingly new series of various substituted imidazo[5,1-b]quinazolines linked to arylpiperazine ring systems were designed [102]. The molecular simulation studies of these compounds revealed that some of these compounds have shown high fitting affinity with lower conformational energies with α_1-agonist hypothesis while others have high fitting affinity and low conformational energies with the α_1-antagonist hypothesis when compared to the respective lead compounds.

Evers A. and Klabunde T. performed structure-based VS for antagonists of the homology model of the α_{1A}-AR generated using bovine rhodopsin as structural template [20]. A crude topographical interaction model was derived through mutational studies and comparative affinity determinations based on ligand binding [28, 92, 111-116] and additional mutational studies performed on close relatives of the biogenic amine binding receptor family [92, 117-131]. This led to identification of essential amino acids involved in agonists and antagonist recognition.

The discovery of novel ligands derived from structure-based design is reported in work by Becker et al., [132] by using *ab initio in silico* GPCR models generated by the predict method for blind *in silico* screening when applied to a set of five different GPCR drug targets leading to a selection of <100 "virtual hit" compounds. Previous studies on β_2-AR and rhodopsin have claimed the use of inactive structures resulting in identification of antagonists or inverse agonists while the use of active-state homology models retrieves partial/full agonists. Evers et al., generated a homology model for the α_{1A}-AR and docked~23 000 ligands resulting in 24 ligands binding in the submicromolar range [20, 133]. The hit rates achieved with these models

were like those typically reached when the target protein is a crystal structure suggesting that docking into rhodopsin-based GPCR models is indeed a feasible approach for the identification of novel ligands. Varady et al.. performed VS for the D3 receptor using homology model of this receptor. Out of 20 experimentally tested compounds, eight showed K_i values better than 1μM [134].

Radestock et al., investigated the combination of two reported techniques for the improvement of homology model-based VS for antagonists of the metabotropic glutamate receptor (mGluR) subtype 5 ligands (i) ligand-supported homology modeling and (ii) ligand-receptor interaction fingerprint-based similarity (IFS) search [55]. The 3D pharmacophore models of the α_{1A}-AR, 5HT2A and D2 receptors have already been successfully used in another study to discriminate between the binders and the non-binders of these receptors [135]. The performance of the ligand-based Feature Tree, Catalyst 3D pharmacophore and Partial Least Square-Discriminant Analysis (PLS-DA) models in identifying known antagonists is remarkable. The method suggested is an improvement over the generally used ligand-based VS and could result in high enrichment rate of the true hits.

The top 1% of the ranked hits from the ligand-based VS strategies achieves excellent hit rates of active compounds. Furthermore, ligand-based VS procedures frequently outperform the VS based on docking if sufficient ligand information for the generation of relevant models is available which depends critically on the amount and quality of ligand information. The homology models are most illustrative to understand how ligands of different chemotypes potentially bind to the receptors validated by mutational and ligand SAR data. The modeled complexes provide a conclusive view on the molecular recognition process in the binding pockets. Molecular docking might reveal a novel scaffold with a "new" binding modeby addressing additional interaction sites in the protein that has not been used by known ligands.

VS is a modeling technique employed when no or limited information is available about the ligands which holds true for most of the GPCRs for which only the endogenous ligand is known. Further, due to high sequence and structural similarity between the α_1-AR subtypes, it represents a challenge for drug design for selectivity and specificity. The combined use of ROCS, VIDA and FRED played an important role in compound identification and selection.

The selection of hits is essential in VS of the compounds from large pool of database. Here, we virtually screened the drug-like compound repository from ZINC database and tested the top-

scored compounds in an experimental assay. The results of our initial characterisation revealed that several ligands that docked in the orthosteric site of the α_{1B}-AR activated the α_1-AR subtype's confirming the potential of this approach to identify new subtype GPCR modulators.The approach used can in principle be applied to any member of the GPCR family with known ligand information and site-directed mutagenesis data. This approach helped us in identifying hits which could be potential leads and be α_1-subtype specific.The current study shows that the homology model of the α_{1B}-AR is suitable for retrieving the α_1-AR partial/full agonists. Thus, there is not one optimal VS strategy for GPCRs but the chance of being successful in VS increases if different VS approaches are employed in parallel or in combination with each other.

4.4 References

1. Horn F, Bettler E, Oliveira L, Campagne F, Cohen FE, Vriend G: **GPCRDB information system for G protein-coupled receptors**. *Nucleic acids research* 2003, **31**(1):294-297.
2. Katritch V, Cherezov V, Stevens RC: **Diversity and modularity of G protein-coupled receptor structures**. *Trends in pharmacological sciences* 2012, **33**(1):17-27.
3. Goncalves JA, Ahuja S, Erfani S, Eilers M, Smith SO: **Structure and function of G protein-coupled receptors using NMR spectroscopy**. *Progress in nuclear magnetic resonance spectroscopy* 2010, **57**(2):159-180.
4. Ma P, Zemmel R: **Value of novelty?** *Nature reviews drug discovery* 2002, **1**(8):571-572.
5. Lagerström MC, Schiöth HB: **Structural diversity of G protein-coupled receptors and significance for drug discovery**. *Nature reviews drug discovery* 2008, **7**(4):339-357.
6. Gether U, Kobilka BK: **G protein-coupled receptors II. Mechanism of agonist activation**. *Journal of biological chemistry* 1998, **273**(29):17979-17982.
7. Bokoch MP, Zou Y, Rasmussen SG, Liu CW, Nygaard R, Rosenbaum DM, Fung JJ, Choi H-J, Thian FS, Kobilka TS: **Ligand-specific regulation of the extracellular surface of a G protein-coupled receptor**. *Nature* 2010, **463**(7277):108-112.
8. Tuteja N: **Signaling through G protein-coupled receptors**. *Plant signaling & behavior* 2009, **4**(10):942-947.
9. Hilger D, Masureel M, Kobilka BK: **Structure and dynamics of GPCR signaling complexes**. 2018, **25**:4-12.
10. Waring MJ, Arrowsmith J, Leach AR, Leeson PD, Mandrell S, Owen RM, Pairaudeau G, Pennie WD, Pickett SD, Wang J: **An analysis of the attrition of drug candidates from four major pharmaceutical companies**. *Nature reviews drug discovery* 2015, **14**(7):475-486.
11. Wootten D, Christopoulos A, Sexton PM: **Emerging paradigms in GPCR allostery: Implications for drug discovery**. *Nature reviews drug discovery* 2013, **12**(8):630-644.
12. Shonberg J, Lopez L, Scammells PJ, Christopoulos A, Capuano B, Lane JR: **Biased agonism at G protein-coupled receptors: The promise and the challenges-A medicinal chemistry perspective**. *Medicinal research reviews* 2014, **34**(6):1286-1330.

13. Leach K, Loiacono RE, Felder CC, McKinzie DL, Mogg A, Shaw DB, Sexton PM, Christopoulos A: **Molecular mechanisms of action and in vivo validation of an M4 muscarinic acetylcholine receptor allosteric modulator with potential antipsychotic properties**. *Neuropsychopharmacology* 2010, **35**(4):855-869.
14. Nickols HH, Conn PJ: **Development of allosteric modulators of GPCRs for treatment of CNS disorders**. *Neurobiology of disease* 2014, **61**:55-71.
15. Melancon BJ, Hopkins CR, Wood MR, Emmitte KA, Niswender CM, Christopoulos A, Conn PJ, Lindsley CW: **Allosteric modulation of seven transmembrane spanning receptors: Theory, practice and opportunities for central nervous system drug discovery**. *Journal of medicinal chemistry* 2012, **55**(4):1445-1464.
16. Williams DK, Wang J, Papke RL: **Positive allosteric modulators as an approach to nicotinic acetylcholine receptor-targeted therapeutics: Advantages and limitations**. *Biochemical pharmacology* 2011, **82**(8):915-930.
17. Nussinov R, Tsai C-J: **Allostery in disease and in drug discovery**. *Cell* 2013, **153**(2):293-305.
18. Wagner JR, Lee CT, Durrant JD, Malmstrom RD, Feher VA, Amaro RE: **Emerging computational methods for the rational discovery of allosteric drugs**. *Chemical reviews* 2016, **116**(11):6370-6390.
19. Kuntz ID: **Structure-based strategies for drug design and discovery**. *Science* 1992, **257**(5073):1078-1082.
20. Evers A, Klabunde T: **Structure-based drug discovery using GPCR homology modeling: Successful virtual screening for antagonists of the α_{1A}-adrenergic receptor**. *Journal of medicinal chemistry* 2005, **48**(4):1088-1097.
21. Taylor CM, Rockweiler NB, Liu C, Rikimaru L, Tunemalm AK, Kisselev OG, Marshall GR: **Using ligand-based virtual screening to allosterically stabilise the activated state of a GPCR**. *Chemical biology & drug design* 2010, **75**(3):325-332.
22. Ragnarsson L, Wang C-IA, Andersson Å, Fajarningsih D, Monks T, Brust A, Rosengren KJ, Lewis RJ: **Conopeptide ρ-TIA defines a new allosteric site on the extracellular surface of the α_{1B}-adrenoceptor**. *Journal of biological chemistry* 2013, **288**(3):1814-1827.

23. Greasley PJ, Fanelli F, Rossier O, Abuin L, Cotecchia S: **Mutagenesis and modeling of the α_{1B}-adrenergic receptor highlight the role of the helix 3/helix 6 interface in receptor activation**. *Molecular pharmacology* 2002, **61**(5):1025-1032.

24. Ragnarsson L, Andersson Å, Thomas WG, Lewis RJ: **Extracellular surface residues of the α_{1B}-adrenoceptor critical for G protein–coupled receptor function**. *Molecular pharmacology* 2015, **87**(1):121-129.

25. Warne T, Serrano-Vega MJ, Baker JG, Moukhametzianov R, Edwards PC, Henderson R, Leslie AG, Tate CG, Schertler GF: **Structure of a β_1-adrenergic G protein-coupled receptor**. *Nature* 2008, **454**(7203):486-491.

26. Hieble JP, Bylund DB, Clarke DE, Eikenburg DC, Langer SZ, Lefkowitz RJ, Minneman KP, Ruffolo R: **International Union of Pharmacology. X. Recommendation for nomenclature of α_1-adrenoceptors: Consensus update**. *Pharmacological reviews* 1995, **47**(2):267-270.

27. Hieble JP, Ruffolo Jr RR: **Subclassification and nomenclature of α_1-and α_2-adrenoceptors**. *Progress in drug research/Fortschritte der arzneimittel forschung/Progrès des recherches pharmaceutiques* 1996: 81-130.

28. Zhao M-M, Hwa J, Perez DM: **Identification of critical extracellular loop residues involved in α_1-adrenergic receptor subtype-selective antagonist binding**. *Molecular pharmacology* 1996, **50**(5):1118-1126.

29. Cotecchia S, Schwinn DA, Randall RR, Lefkowitz RJ, Caron MG, Kobilka BK: **Molecular cloning and expression of the cDNA for the hamster α_1-adrenergic receptor**. *Proceedings of the national academy of sciences* 1988, **85**(19):7159-7163.

30. Wang Y, Gao J, Mathias R, Cohen I, Sun X, Baldo G: **α-adrenergic effects on Na^+/K^+ pump current in guinea-pig ventricular myocytes**. *The journal of physiology* 1998, **509**(1):117-128.

31. Nishimaru K, Kobayashi M, Matsuda T, Tanaka Y, Tanaka H, Shigenobu K: **α-adrenoceptor stimulation-mediated negative inotropism and enhanced Na^+/Ca^{2+} exchange in mouse ventricle**. *American journal of physiology-Heart and circulatory physiology* 2001, **280**(1):H132-H141.

32. Simpson P: **Norepinephrine-stimulated hypertrophy of cultured rat myocardial cells is an α_1-adrenergic response**. *Journal of clinical investigation* 1983, **72**(2):732-738.

33. Rokosh DG, Simpson PC: **Knockout of the $\alpha_{1A/C}$-adrenergic receptor subtype: The $\alpha_{1A/C}$ is expressed in resistance arteries and is required to maintain arterial blood pressure**. *Proceedings of the national academy of sciences* 2002, **99**(14):9474-9479.

34. Heusch G: **Alpha adrenergic mechanisms in myocardial ischemia**. *Circulation* 1990, **81**: 1-13.

35. Tanoue A, Koshimizu T-a, Shibata K, Nasa Y, Takeo S, Tsujimoto G: **Insights into α_1-adrenoceptor function in health and disease from transgenic animal studies**. *Trends in endocrinology & metabolism* 2003, **14**(3):107-113.

36. King H, Goetz A, Ward S, Saussy Jr D: **AH11110A is selective for the α_{1B} subtype of α_1-adrenoceptors**. *Society for neuroscience abstract 1994*. 526.

37. Goetz AS, King HK, Ward SD, True TA, Rimele TJ, Saussy DL: **BMY7378 is a selective antagonist of the D subtype of α_1-adrenoceptors**. *European journal of pharmacology* 1995, **272**(2):R5-R6.

38. Giardinà D, Crucianelli M, Melchiorre C, Taddei C, Testa R: **Receptor binding profile of cyclazosin, a new α_{1B}-adrenoceptor antagonist**. *European journal of pharmacology* 1995, **287**(1):13-16.

39. Schlyer S, Horuk R: **I want a new drug: G protein-coupled receptors in drug development**. *Drug discovery today* 2006, **11**(11):481-493.

40. Beuming T, Lenselink B, Pala D, McRobb F, Repasky M, Sherman W: Docking and virtual screening strategies for GPCR drug discovery..*Methods in molecular biology*2015,1335:251-276.

41. Reddy AS, Pati SP, Kumar PP, Pradeep H, Sastry GN: **Virtual screening in drug discovery-A computational perspective**. *Current protein and peptide science* 2007, **8**(4):329-351.

42. Stahura FL, Bajorath J: **Virtual screening methods that complement HTS**. *Combinatorial chemistry & high throughput screening* 2004, **7**(4):259-269.

43. Bleicher KH, Böhm H-J, Müller K, Alanine AI: **Hit and lead generation: Beyond high-throughput screening**. *Nature reviews drug discovery* 2003, **2**(5):369-378.

44. Jacob L, Hoffmann B, Stoven V, Vert J-P: **Virtual screening of GPCRs: An *in silico* chemogenomics approach**. *BMC bioinformatics* 2008, **9**(1):363-379.

45. Kinnings SL, Jackson RM: **LigMatch: A multiple structure-based ligand matching method for 3D virtual screening**. *Journal of chemical information and modeling* 2009, **49**(9):2056-2066.

46. Ghosh S, Nie A, An J, Huang Z: **Structure-based virtual screening of chemical libraries for drug discovery**. *Current opinion in chemical biology* 2006, **10**(3):194-202.

47. Kolb P, Ferreira RS, Irwin JJ, Shoichet BK: **Docking and chemoinformatic screens for new ligands and targets**. *Current opinion in biotechnology* 2009, **20**(4):429-436.

48. Lundstrom K: **An overview on GPCRs and drug discovery: Structure-based drug design and structural biology on GPCRs**. *Methods in molecular biology* 2009, **552**: 51-66.

49. Triballeau N, Acher F, Brabet I, Pin J-P, Bertrand H-O: **Virtual screening workflow development guided by the "receiver operating characteristic" curve approach. Application to high-throughput docking on metabotropic glutamate receptor subtype 4**. *Journal of medicinal chemistry* 2005, **48**(7):2534-2547.

50. Kalliokoski T: **Accelereating three-dimensional virtual screening: New software and approaches for computer-aided drug discovery**. *Dissertations in health sciences* 2010,**22**:1-174.

51. Tondi D, Slomczynska U, Costi MP, Watterson DM, Ghelli S, Shoichet BK: **Structure-based discovery and in-parallel optimisation of novel competitive inhibitors of thymidylate synthase**. *Chemistry & biology* 1999, **6**(5):319-331.

52. Lipinski CA: **Lead-and drug-like compounds: The rule-of-five revolution**. *Drug discovery today: Technologies* 2004, **1**(4):337-341.

53. Shoichet BK: **Virtual screening of chemical libraries**. *Nature* 2004, **432**(7019):862-865.

54. O'Driscoll C: **A virtual space odyssey**.*Proceedings of horizon symposium: Charting chemical space* 2004, 1-4.

55. Weil T, Renner S: **Homology model-based virtual screening for GPCR ligands using docking and target-biased scoring**. *Journal of chemical information and modeling* 2008, **48**(5):1104-1117.

56. Katritch V, Rueda M, Lam PCH, Yeager M, Abagyan R: **GPCR 3D homology models for ligand screening: Lessons learned from blind predictions of adenosine A2A**

receptor complex. *Proteins: Structure, function, and bioinformatics* 2010, **78**(1):197-211.

57. Langmead CJ, Andrews SP, Congreve M, Errey JC, Hurrell E, Marshall FH, Mason JS, Richardson CM, Robertson N, Zhukov A: **Identification of novel adenosine A2A receptor antagonists by virtual screening**. *Journal of medicinal chemistry* 2012, **55**(5):1904-1909.
58. De Graaf C, Rognan D: **Selective structure-based virtual screening for full and partial agonists of the β_2-adrenergic receptor**. *Journal of medicinal chemistry* 2008, **51**(16):4978-4985.
59. Neves MA, Simões S, e Melo MLS: **Ligand-guided optimisation of CXCR4 homology models for virtual screening using a multiple chemotype approach**. *Journal of computer-aided molecular design* 2010, **24**(12):1023-1033.
60. Kołaczkowski M, Bucki A, Feder M, Pawłowski M: **Ligand-optimised homology models of D1 and D2 dopamine receptors: Application for virtual screening**. *Journal of chemical information and modeling* 2013, **53**(3):638-648.
61. de Graaf C, Kooistra AJ, Vischer HF, Katritch V, Kuijer M, Shiroishi M, Iwata S, Shimamura T, Stevens RC, de Esch IJ: **Crystal structure-based virtual screening for fragment-like ligands of the human histamine H1 receptor**. *Journal of medicinal chemistry* 2011, **54**(23):8195-8206.
62. Irwin JJ, Shoichet BK: **ZINC-A free database of commercially available compounds for virtual screening**. *Journal of chemical information and modeling* 2005, **45**(1):177-182.
63. Hamza A, Wei N-N, Hao C, Xiu Z, Zhan C-G: **A novel and efficient ligand-based virtual screening approach using the HWZ scoring function and an enhanced shape-density model**. *Journal of biomolecular structure and dynamics* 2013, **31**(11):1236-1250.
64. Baber JC, Shirley WA, Gao Y, Feher M: **The use of consensus scoring in ligand-based virtual screening**. *Journal of chemical information and modeling* 2006, **46**(1):277-288.
65. ROCS; OpenEye Scientific Software: http://www.eyesopen.com/rocs Santa Fe N.
66. Hawkins PC, Skillman AG, Nicholls A: **Comparison of shape-matching and docking as virtual screening tools**. *Journal of medicinal chemistry* 2007, **50**(1):74-82.

67. Pérez-Nueno VI, Ritchie DW, Rabal O, Pascual R, Borrell JI, Teixidó J: **Comparison of ligand-based and receptor-based virtual screening of HIV entry inhibitors for the CXCR4 and CCR5 receptors using 3D ligand shape matching and ligand-receptor docking**. *Journal of chemical information and modeling* 2008, **48**(3):509-533.
68. Hawkins PC, Skillman AG, Warren GL, Ellingson BA, Stahl MT: **Conformer generation with OMEGA: Algorithm and validation using high quality structures from the protein databank and cambridge structural database**. *Journal of chemical information and modeling* 2010, **50**(4):572-584.
69. OMEGA; OpenEye Scientific Software: http://www.eyesopen.com/omega Santa Fe N.
70. McGann M: **FRED and HYBRID docking performance on standardised datasets**. *Journal of computer-aided molecular design* 2012, **26**(8):897-906.
71. FRED; OpenEye Scientific Software: http://www.eyesopen.com/oedocking Santa Fe N.
72. McGann M: **FRED pose prediction and virtual screening accuracy**. *Journal of chemical information and modeling* 2011, **51**(3):578-596.
73. Morrow AL, Creese I: **Characterisation of α_1-adrenergic receptor subtypes in rat brain: A reevaluation of $^{[3H]}$WB4104 and $^{[3H]}$prazosin binding**. *Molecular pharmacology* 1986, **29**(4):321-330.
74. Ishiguro M, Futabayashi Y, Ohnuki T, Ahmed M, Muramatsu I, Nagatomo T: **Identification of binding sites of prazosin, tamsulosin and KMD-3213 with α_1-adrenergic receptor subtypes by molecular modeling**. *Life sciences* 2002, **71**(21):2531-2541.
75. Costanzi S: **On the applicability of GPCR homology models to computer-aided drug discovery: A comparison between *in silico* and crystal structures of the β_2-adrenergic receptor**. *Journal of medicinal chemistry* 2008, **51**(10):2907-2914.
76. Jin F, Lu C, Sun X, Li W, Liu G, Tang Y: **Insights into the binding modes of human β_3-adrenergic receptor agonists with ligand-based and receptor-based methods**. *Molecular diversity* 2011, **15**(4):817-831.
77. Christopher JA, Brown J, Doré AS, Errey JC, Koglin M, Marshall FH, Myszka DG, Rich RL, Tate CG, Tehan B: **Biophysical fragment screening of the β_1-adrenergic receptor: Identification of high affinity arylpiperazine leads using structure-based drug design**. *Journal of medicinal chemistry* 2013, **56**(9):3446-3455.

78. Huber T, Menon S, Sakmar TP: **Structural basis for ligand binding and specificity in adrenergic receptors: Implications for GPCR-targeted drug discovery**. *Biochemistry* 2008, **47**(42):11013-11023.

79. Dror RO, Pan AC, Arlow DH, Borhani DW, Maragakis P, Shan Y, Xu H, Shaw DE: **Pathway and mechanism of drug binding to G protein-coupled receptors**. *Proceedings of the national academy of sciences* 2011, **108**(32):13118-13123.

80. Kruse AC, Ring AM, Manglik A, Hu J, Hu K, Eitel K, Hübner H, Pardon E, Valant C, Sexton PM: **Activation and allosteric modulation of a muscarinic acetylcholine receptor**. *Nature* 2013, **504**(7478):101-106.

81. White JF, Noinaj N, Shibata Y, Love J, Kloss B, Xu F, Gvozdenovic-Jeremic J, Shah P, Shiloach J, Tate CG: **Structure of the agonist-bound neurotensin receptor**. *Nature* 2012, **490**(7421):508-513.

82. Zhang D, Gao Z-G, Zhang K, Kiselev E, Crane S, Wang J, Paoletta S, Yi C, Ma L, Zhang W: **Two disparate ligand binding sites in the human P2Y1 receptor**. *Nature* 2015, **520**(7547):317-321.

83. Jazayeri A, Dor AS, Lamb D, Krishnamurthy H, Southall SM, Baig AH, Bortolato A, Koglin M, Robertson NJ, Errey JC: **Extra-helical binding site of a glucagon receptor antagonist**. *Nature* 2016, **533**(7602):274-274.

84. Scholten D, Canals M, Maussang D, Roumen L, Smit M, Wijtmans M, De Graaf C, Vischer H, Leurs R: **Pharmacological modulation of chemokine receptor function**. *British journal of pharmacology* 2012, **165**(6):1617-1643.

85. Munk C, Harpsøe K, Hauser AS, Isberg V, Gloriam DE: **Integrating structural and mutagenesis data to elucidate GPCR ligand binding**. *Current opinion in pharmacology* 2016, **30**:51-58.

86. van Rhee AM, Jacobson KA: **Molecular architecture of G protein-coupled receptors**. *Drug development research* 1996, **37**(1):1-38.

87. Edvardsen Ø, Reiersen AL, Beukers MW, Kristiansen K: **tGRAP, the G protein coupled receptors mutant database**. *Nucleic acids research* 2002, **30**(1):361-363.

88. Madabushi S, Gross AK, Philippi A, Meng EC, Wensel TG, Lichtarge O: **Evolutionary trace of G protein-coupled receptors reveals clusters of residues that determine**

global and class-specific functions. *Journal of biological chemistry* 2004, **279**(9):8126-8132.

89. Moitra S, Tirupula KC, Klein-Seetharaman J, Langmead CJ: **A minimal ligand binding pocket within a network of correlated mutations identified by multiple sequence and structural analysis of G protein-coupled receptors**. *BMC biophysics* 2012, **5**(1):13-29.
90. Jacoby E: **A novel chemogenomics knowledge-based ligand design strategy: Application to G protein-coupled receptors**. *Molecular informatics* 2001, **20**(2):115-123.
91. Kristiansen K: **Molecular mechanisms of ligand binding, signaling and regulation within the superfamily of G protein-coupled receptors: Molecular modeling and mutagenesis approaches to receptor structure and function**. *Pharmacology & therapeutics* 2004, **103**(1):21-80.
92. Shi L, Javitch JA: **The binding site of aminergic G protein–coupled receptors: The transmembrane segments and second extracellular loop**. *Annual review of pharmacology and toxicology* 2002, **42**(1):437-467.
93. Sung Y-M, Wilkins AD, Rodriguez GJ, Wensel TG, Lichtarge O: **Intramolecular allosteric communication in dopamine D2 receptor revealed by evolutionary amino acid covariation**. *Proceedings of the national academy of sciences* 2016, **113**(13):3539-3544.
94. Rodriguez GJ, Yao R, Lichtarge O, Wensel TG: **Evolution-guided discovery and recoding of allosteric pathway specificity determinants in psychoactive bioamine receptors**. *Proceedings of the national academy of sciences* 2010, **107**(17):7787-7792.
95. Kang HJ, Wilkins AD, Lichtarge O, Wensel TG: **Determinants of endogenous ligand specificity divergence among metabotropic glutamate receptors**. *Journal of biological chemistry* 2015, **290**(5):2870-2878.
96. Gloriam DE, Foord SM, Blaney FE, Garland SL: **Definition of the G protein-coupled receptor transmembrane bundle binding pocket and calculation of receptor similarities for drug design**. *Journal of medicinal chemistry* 2009, **52**(14):4429-4442.
97. Bremner JB, Coban B, Griffith R, Groenewoud KM, Yates BF: **Ligand design for α_1-adrenoceptor subtype selective antagonists**. *Bioorganic & medicinal chemistry* 2000, **8**(1):201-214.

98. Betti L, Botta M, Corelli F, Floridi M, Giannaccini G, Maccari L, Manetti F, Strappaghetti G, Tafi A, Corsano S: **α_1-adrenoceptor antagonists. 4. 1 pharmacophore-based design, synthesis, and biological evaluation of new imidazo-, benzimidazo- and indoloarylpiperazine derivatives**. *Journal of medicinal chemistry* 2002, **45**(17):3603-3611.

99. Barbaro R, Betti L, Botta M, Corelli F, Giannaccini G, Maccari L, Manetti F, Strappaghetti G, Corsano S: **Synthesis and biological activity of new 1, 4-benzodioxan-arylpiperazine derivatives. Further validation of a pharmacophore model for α_1-adrenoceptor antagonists**. *Bioorganic & medicinal chemistry* 2002, **10**(2):361-369.

100. Greene J, Kahn S, Savoj H, Sprague P, Teig S: **Chemical function queries for 3D database search**. *Journal of chemical information and computer sciences* 1994, **34**(6):1297-1308.

101. Guimarães S, Moura D: **Vascular adrenoceptors: An update**. *Pharmacological reviews* 2001, **53**(2):319-356.

102. Ismail MA, Aboul-Enein MN, Abouzid KA, Serya RA: **Ligand design and synthesis of new imidazo [5, 1-b] quinazoline derivatives as α_1-adrenoceptor agonists and antagonists**. *Bioorganic & medicinal chemistry* 2006, **14**(4):898-910.

103. Chern J-W, Shiau C-Y, Lu G-Y: **Studies on quinazolinones. 3: 1 novel and efficient route to the synthesis of conformationally restricted analogues of ketanserin and SGB-1534 as antihypertensive agents**. *Bioorganic & medicinal chemistry letters* 1991, **1**(11):571-574.

104. Chern JW, Tao PL, Yen MH, Lu GY, Shiau CY, Lai YJ, Chien SL, Chan CH: **Studies on quinazolines. 5. 2, 3-Dihydroimidazo [1, 2-c] quinazoline derivatives: A novel class of potent and selective α_1-adrenoceptor antagonists and antihypertensive agents**. *Journal of medicinal chemistry* 1993, **36**(15):2196-2207.

105. Jen T, Dienel B, Bowman H, Petta J, Helt A, Loev B: **Amidines. 2. New class of antihypertensive agents. 1,2,3,5-tetrahydroimidazo [2, 1-b] quinazolines**. *Journal of medicinal chemistry* 1972, **15**(7):727-731.

106. Romeo G, Ambrosini G, Guccione S, De Blasi A, Russo F: **Pyrimido [5, 4-b] benzofuran and pyrimido [5, 4-b] benzothiophene derivatives ligands for α_1-and 5HT1A-receptors**. *European journal of medicinal chemistry* 1993, **28**(6):499-504.

107. Seki N, Nishiye E, Itoh T, Suzuki H, Kuriyama H: **Electrical and mechanical properties of the capsular smooth muscles of the rabbit prostate in relation to the actions of the α_1-adrenoceptor blocker, YM-12617**. *British journal of pharmacology* 1988, **93**(3):702-714.

108. Hess HJ, Cronin TH, Scriabine A: **Antihypertensive 2-amino-4(3H)-quinazolinones**. *Journal of medicinal chemistry* 1968, **11**(1):130-136.

109. Campbell SF, Davey MJ, Hardstone JD, Lewis BN, Palmer MJ: **2, 4-Diamino-6, 7-dimethoxyquinazolines. 1.2-[4-(1,4-benzodioxan-2-ylcarbonyl) piperazin-1-yl] derivatives as α_1-adrenoceptor antagonists and antihypertensive agents**. *Journal of medicinal chemistry* 1987, **30**(1):49-57.

110. Melchiorre C, Angeli P, Bolognesi M, Chiarini A, Giardina D, Gulini U, Leonardi A, Marucci G, Minarini A, Pigini M: **α_1-adrenoreceptor antagonists bearing a quinazoline or a benzodioxane moiety**. *Pharmacochemistry library* 2000, **31**:181-190.

111. Hwa J, Perez D: **The unique nature of serine interactions for α_1-adrenergic receptor agonist binding and activation**. *Journal of biological chemistry* 1996, **271**(11):6322-6327.

112. Hwa J, Graham RM, Perez DM: **Identification of critical determinants of α_1-adrenergic receptor subtype selective agonist binding**. *Journal of biological chemistry* 1995, **270**(39):23189-23195.

113. Hamaguchi N, True TA, Saussy DL, Jeffs PW: **Phenylalanine in the second membrane-spanning domain of α_{1A}-adrenergic receptor determines subtype selectivity of dihydropyridine antagonists**. *Biochemistry* 1996, **35**(45):14312-14317.

114. Hamaguchi N, True TA, Goetz AS, Stouffer MJ, Lybrand TP, Jeffs PW: **α_1-adrenergic receptor subtype determinants for 4-piperidyl oxazole antagonists**. *Biochemistry* 1998, **37**(16):5730-5737.

115. Waugh DJ, Gaivin RJ, Zuscik MJ, Gonzalez-Cabrera P, Ross SA, Yun J, Perez DM: **Phe-308 and Phe-312 in transmembrane domain 7 are major sites of α_1-adrenergic receptor antagonist binding. Imidazoline agonists bind like antagonists**. *Journal of biological chemistry* 2001, **276**(27):25366-25371.

116. Waugh DJ, Zhao M-M, Zuscik MJ, Perez DM: **Novel aromatic residues in transmembrane domains IV and V involved in agonist binding at α_{1A}-adrenergic receptors**. *Journal of biological chemistry* 2000, **275**(16):11698-11705.

117. Almaula N, Ebersole BJ, Zhang D, Weinstein H, Sealfon SC: **Mapping the binding site pocket of the serotonin 5-hydroxytryptamine2A receptor ser3.36(159) provides a second interaction site for the protonated amine of serotonin but not of lysergic acid diethylamide or bufotenin**. *Journal of biological chemistry* 1996, **271**(25):14672-14675.

118. Boess FG, Monsma FJ, Sleight AJ: **Identification of residues in transmembrane regions III and VI that contribute to the ligand binding site of the serotonin 5-HT6 receptor**. *Journal of neurochemistry* 1998, **71**(5):2169-2177.

119. Chen S, Xu M, Lin F, Lee D, Riek P, Graham RM: **Phe310 in transmembrane VI of the α_{1B}-adrenergic receptor is a key switch residue involved in activation and catecholamine ring aromatic bonding**. *Journal of biological chemistry* 1999, **274**(23):16320-16330.

120. Fraser CM, Wang C-D, Robinson DA, Gocayne JD, Venter JC: **Site-directed mutagenesis of M1 muscarinic acetylcholine receptors: Conserved aspartic acids play important roles in receptor function**. *Molecular pharmacology* 1989, **36**(6):840-847.

121. Fu D, Ballesteros JA, Weinstein H, Chen J, Javitch JA: **Residues in the seventh membrane-spanning segment of the dopamine D2 receptor accessible in the binding-site crevice**. *Biochemistry* 1996, **35**(35):11278-11285.

122. Javitch JA, Li X, Kaback J, Karlin A: **A cysteine residue in the third membrane-spanning segment of the human D2 dopamine receptor is exposed in the binding-site crevice**. *Proceedings of the national academy of sciences* 1994, **91**(22):10355-10359.

123. Javitch JA, Fu D, Chen J: **Residues in the fifth membrane-spanning segment of the dopamine D2 receptor exposed in the binding-site crevice**. *Biochemistry* 1995, **34**(50):16433-16439.

124. Javitch JA, Ballesteros JA, Weinstein H, Chen J: **A cluster of aromatic residues in the sixth membrane-spanning segment of the dopamine D2 receptor is accessible in the binding-site crevice**. *Biochemistry* 1998, **37**(4):998-1006.

125. Javitch JA, Ballesteros JA, Chen J, Chiappa V, Simpson MM: **Electrostatic and aromatic microdomains within the binding-site crevice of the D2 receptor: Contributions of the second membrane-spanning segment**. *Biochemistry* 1999, **38**(25):7961-7968.

126. Javitch JA, Shi L, Simpson MM, Chen J, Chiappa V, Visiers I, Weinstein H, Ballesteros JA: **The fourth transmembrane segment of the dopamine D2 receptor: Accessibility in the binding-site crevice and position in the transmembrane bundle**. *Biochemistry* 2000, **39**(40):12190-12199.

127. Kao H-T, Adham N, Olsen MA, Weinshank RL, Branchek TA, Hartig PR: **Site-directed mutagenesis of a single residue changes the binding properties of the serotonin 5HT2 receptor from a human to a rat pharmacology**. *FEBS letters* 1992, **307**(3):324-328.

128. Roth B, Shoham M, Choudhary M, Khan N: **Identification of conserved aromatic residues essential for agonist binding and second messenger production at 5-hydroxytryptamine2A receptors**. *Molecular pharmacology* 1997, **52**(2):259-266.

129. Roth BL, Willins DL, Kristiansen K, Kroeze WK: **5-Hydroxytryptamine$_2$-family receptors (5-hydroxytryptamine (2A), 5-hydroxytryptamine (2B), 5-hydroxytryptamine (2C)): Where structure meets function**. *Pharmacology & therapeutics* 1998, **79**(3):231-257.

130. Shi L, Javitch JA: **The second extracellular loop of the dopamine D2 receptor lines the binding-site crevice**. *Proceedings of the national academy of sciences* 2004, **101**(2):440-445.

131. Simpson MM, Ballesteros JA, Chiappa V, Chen J, Suehiro M, Hartman DS, Godel T, Snyder LA, Sakmar TP, Javitch JA: **Dopamine D4/D2 receptor selectivity is determined by a divergent aromatic microdomain contained within the second, third, and seventh membrane-spanning segments**. *Molecular pharmacology* 1999, **56**(6):1116-1126.

132. Becker OM, Marantz Y, Shacham S, Inbal B, Heifetz A, Kalid O, Bar-Haim S, Warshaviak D, Fichman M, Noiman S: **G protein-coupled receptors: *In silico* drug discovery in 3D**. *Proceedings of the national academy of sciences* 2004, **101**(31):11304-11309.

133. Evers A, Hessler G, Matter H, Klabunde T: **Virtual screening of biogenic amine-binding G protein coupled receptors: Comparative evaluation of protein-and ligand-based virtual screening protocols**. *Journal of medicinal chemistry* 2005, **48**(17):5448-5465.

134. Varady J, Wu X, Fang X, Min J, Hu Z, Levant B, Wang S: **Molecular modeling of the three-dimensional structure of dopamine 3 (D3) subtype receptor: Discovery of novel and potent D3 ligands through a hybrid pharmacophore-and structure-based database searching approach**. *Journal of medicinal chemistry* 2003, **46**(21):4377-4392.

135. Klabunde T, Evers A: **GPCR antitarget modeling: Pharmacophore models for biogenic amine binding GPCRs to avoid GPCR-mediated side effects**. *Chembiochem* 2005, **6**(5):876-889.

Chapter 5

Chapter 5: Conclusion & Future Perspectives

5.1 Conclusions

GPCRs comprise of the largest class of membrane proteins in humans with more than 800 members [1] which act as gatekeepers to signal transduction in eukaryotes [2]. They are encoded by about 26% of the human genome [3] and represent a majority of present as well as potential future drug targets [4]. They demonstrate common appearance in architecture with 7TM helices (**Figure 1**); classified into 5 classes and subclasses and are the largest target class of approximately ~30-40% of FDA-approved marketed drugs[5]. GPCRs are flexible chemical sensors that harmonise cellular reaction with extracellular stimuli [6]. In view of their importance in physiology and disease conditions an understanding of structure and function is of key significance in drug discovery for researchers in the basic and applied sciences[7].

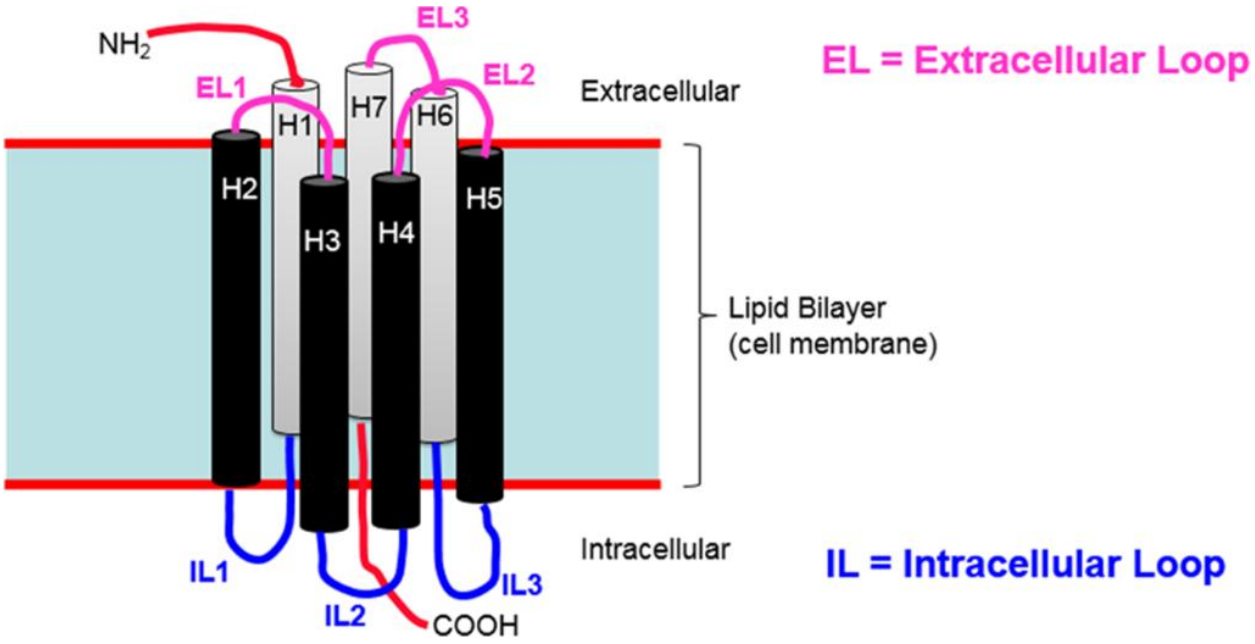

Figure 5-1: A schematic diagram of the general structure of GPCRs[8] (Image courtesy: Clark T. Beilstein *J. Org. Chem.;* 2017;13;1071-1078).

GPCRs are the most heavily investigated drug targets in the pharmaceutical industry [9]. Incredible and remarkable efforts has been put forward by both industry and academia to understand the GPCR structure and function [10]. The process of GPCR activation has evolved from the classical inactive-active two-state model to a complex view of GPCR conformational ensembles associated with ligands, allosteric modulators, ions and downstream signaling proteins [11, 12]. Conformational flexibility of GPCRs has paused challenges in crystallisation and

limited our understanding to delineate their function and elucidate the structure-function relationship [13].

Breakthroughs with recent advancement in technology such as X-ray crystallography have surmounted the hitch of GPCR crystallisation and resulted in high-resolution structures of over 30 GPCRs providing structural basis for drug design and functional studies (**Figure-2**) [6, 14]. This evolvement has ushered new era to gain and comprehend insights into receptor-ligand binding and enabled wide applications of computational approaches in GPCR research which led to several groundbreaking studies in the last few years [15, 16]. While a large fraction of human GPCRs has yet to be crystallised, molecular modeling plays a pivotal role in the simulation of these GPCRs [8, 17]. This pipeline progress is inquisitive to exploit information in biophysics, pharmacology, molecular biology and computational queries [18]. Advance evidence on receptors and their connections and communications within and between receptors has been characterised by X-ray crystallography, NMR spectroscopy, Biochemistry, Biophysics and Bioinformatics. Here, we have provided brief overview on class A GPCR structure and functions in reference to α_1-AR with a focus on the applications and perspectives of molecular modeling in GPCR ligand design.

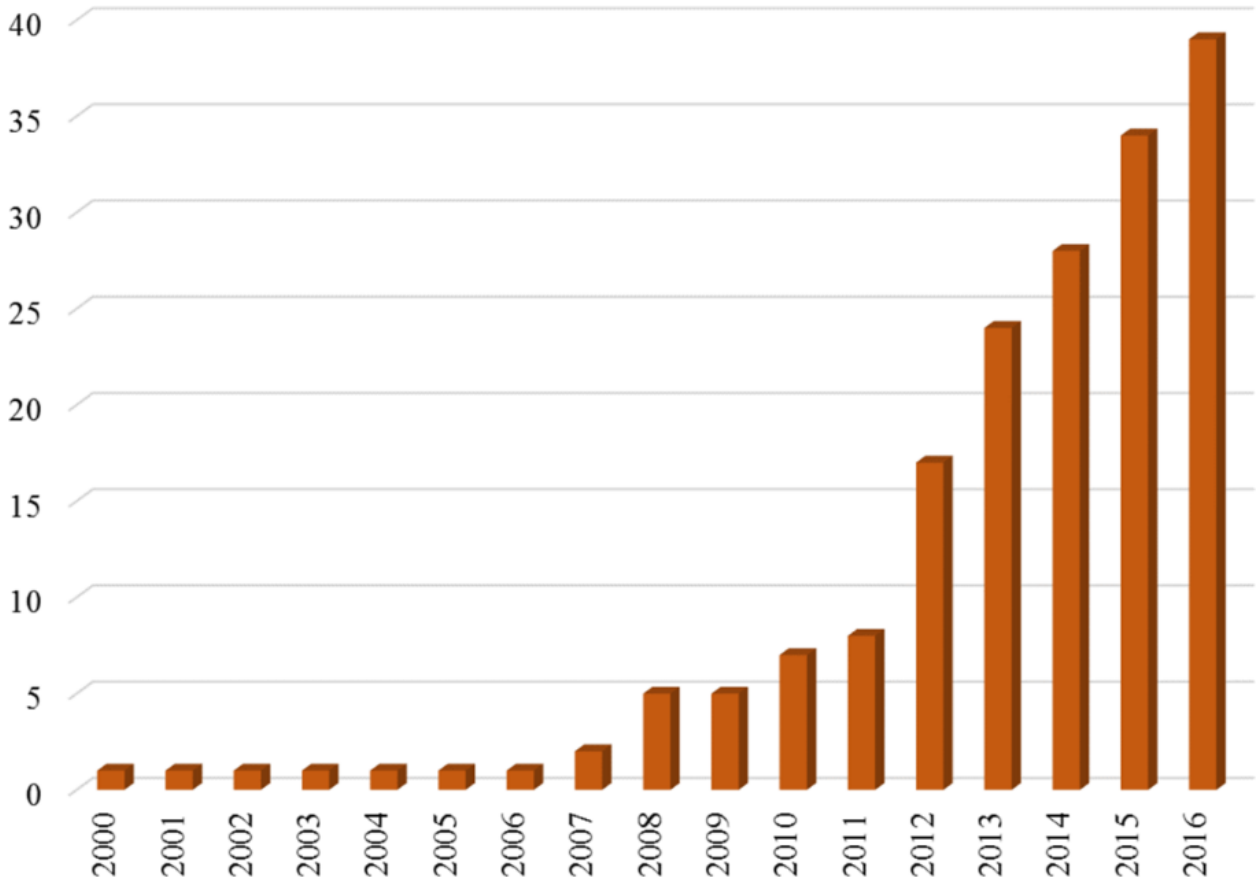

Figure 5-2: The cumulative number of different GPCRs for which X-ray structures were available in a given year. The data represent a total of 174 structures on 91 ligand–receptor complexes for 39 different receptors. The data are taken from http://gpcrdb.org/structure/statistics (2nd February 2017) [8] (Image courtesy: Clark T. Beilstein, *J. Org. Chem.;* 2017;13;1071-1078).

In addition to GPCRs exploitation in specific labs, GPCR network was established in 2010 as part of a much larger network to study significant biological and biomedical complications. As a consequence, leveraging through modeling has become more reliable and will further improve as additional experimental structures are determined [19]. The first successful structural elucidation of β_2-AR and the adenosine A2A-R by GPCR network led to progress of set-up with feedback loops that could be used as a prototype for the structural resolution of other GPCR structures through wet-lab and computational techniques [20-23]. The structures elucidated could be leveraged to understand the structures of related GPCRs through comparative analysis and homology-based modeling of structures and their related complexes [24].

X-ray structures of different class A, class B, class C and frizzled GPCRs spanning large sections of the phylogenetic tree have been published [19]. This gives opportunity to pharmaceutical

researchers to use these structures for drug design purposes. The recent structures of non-class A GPCRs may serve as invaluable templates for ligand design for the difficult target classes. Although both classes (B and C) are attractive drug target families, very few small molecule drugs targeting class B or C GPCRs are in the market. This reflects the impact of their apparently highly demanding binding sites in terms of druggability. During the past few years, crystallography of GPCRs has experienced exponential growth resulting in the determination of the structures of distinct receptors (9 of them in 2012 alone) [25].

The structures obtained from structural biology techniques were in inactive conformation in conjunction with inverse agonists that reduce basal activity or neutral antagonists that maintain basal activity. The adrenergic, rhodopsin and adenosine receptor systems are also described by agonist-bound active-state structures including a structure of the receptor-G protein complex for the β_2-AR. Crystallisation of the agonist-bound active-state structures of β_2-AR revealed subtle changes in the binding pocket associated with an 11Å outward movement of the cytoplasmic end of TM6 and rearrangements of TM5 and TM7 that are remarkably similar to those observed for opsin, an active form of rhodopsin. These structure provides insights into the process of agonist binding and activation [22].

For class A receptors, some structures with approved marketed drugs are available. These include the complexes of: maraviroc in CCR5, tiotropium in M3 receptor, adenosine in A2A-R, carvedilol in β_1-AR, doxepin in H_1 receptor (H_1-R), ergotamine in 5HT1B as well as 5HT2B receptors and voraxapar in the protease-activated receptor PAR-1. In addition to the new X-ray structures from classes B and C, a first structure of an agonist bound M2 receptor structure with allosteric modulator as well as two very high-resolution structures of A2A-R and δ-opioid receptors (δ-OR) were reported providing first insight into the allosteric regulation, biased signaling and solvent networks in GPCRs.

Structural difference ensues between the receptors based on the sequence composition for eg., ECL2 forms a β-hairpin lid at the ligand binding pocket in rhodopsin unlike other class A structures [26]. GPCRs are known to bind ligands of diverse shape and size in a pocket at the extracellular side of the TM helices [27] (**Figure 4-7**; Chapter 4). Different ligands are known to bind topologically equivalent residues up to an extent in TM3, TM6 and TM7 at positions 3.32, 3.33, 3.36, 6.48, 6.51 and 7.39 [28]. Additional details revealed by high-resolution structures illustrated the receptors as allosteric machines that are controlled not only by ligands but also by

ions, lipids, cholesterol and water. H_2O molecules facilitates indirect contact between the ligand and receptor [29] such as A2A-R, β_1-AR, CXCR4, δ-OR, κ-OR, PAR-1 and sphingosine-1-phosphate receptor 1 (S1P1). X-ray structures show water mediated contacts between the ligands and receptor [30].

A crystal structure of the A2A-R bound to an antagonist contained three distinct water clusters which were visible at 1.8Å [31] on the extracellular face in the TM core and at the intracellular face near the E/DRY motif. Water molecules in the central TM region are coordinated to a Na^+ ion that may play a role in receptor activation. In the agonist bound A2A-R, the ligand induced change in TM3 prevents binding of water molecules [23, 32]. Thus, the presence of water and activation-induced changes in conformation which alters receptor hydration may be common feature in GPCRs [33-36]. The high degree of involvement of water molecules in GPCR ligand binding makes rational ligand design very difficult without corresponding to X-ray structure. This is because the SAR is greatly changed when a bridging water entity is replaced. The knowledge that water location is crucial in GPCRs has led to studies which explicitly investigate the thermodynamic properties of water molecules in GPCR X-ray structures to answer the question; Can specific water molecules be replaced by ligand atoms? [37].

Biochemical and biophysical techniques such as NMR and hydrogen-deuterium exchange coupled with mass spectrometry provided complementary insights into ligand-dependent dynamic equilibrium between different functional states. This wealth of data helped redefine our knowledge of how GPCRs recognise such a diverse array of ligands and how they transmit signals across the cell membrane. It also shed light on structural basis of GPCR allosteric modulation and biased signaling. A new class of ligands termed bitopic or dualsteric ligands have been reported to target at both orthosteric and allosteric sites simultaneously [38, 39]. The development of bitopic ligands is based on the combination of high affinity (*via* orthosteric sites) and high selectivity (*via* allosteric sites). Moreover, some recent reports [40, 41] showed that bitopic ligands possess either orthosteric or allosteric properties under different conditions. Both allosteric modulators and bitopic ligands of GPCRs possess advantages over orthosteric ones, so the discovery of allosteric modulators or bitopic ligands of GPCRs has become a new strategy in drug design.

The biogenic amine binding class of GPCRs has provided excellent targets for the treatment of several CNS diseases such as schizophrenia (mixed D2/D1/5HT2), psychosis (mixed D2/$5HT_{2A}$),

depression (5HT1) or migraine (5HT1). This GPCR subfamily has also proven to provide druggable targets for other disease areas such as allergies (H1), asthma (β_2), ulcers (H2), or hypertension (α_1 antagonist, β_1 antagonist) [42]. The α_1-ARs subdivided into the α_{1A}, α_{1B} and α_{1D}subtypes [43] are involved in blood pressure maintenance by modulating the vascular muscle tone. α_1-AR antagonists such as indoramin and prazosin are employed as antihypertensitive agents. In addition, α_{1A} antagonists such as alfuzosin and prazosin are effective in the management of benign prostatic hypertrophy.

Crystal structures provide robust structural framework for computational modeling of receptor dynamics, ligand docking and structure and ligand based virtual screening processes. Computational approach like homology modeling, molecular dynamics, molecular docking, pharmacophore mapping, structure and ligand based virtual screening are used to study ligand-receptor interactions in the drug discovery and development process [44] (**Figure 5-3**). MD simulations have become an essential technique among all tools available to design new drugs. Initially developed to investigate molecular models with a limited number of atoms, computers now enable investigations of large macromolecular systems with a simulation time reaching the microsecond range [45].

MD techniques are being increasingly applied to GPCRs to study protein dynamics, explore druggability and optimise lead compounds [46]. MD simulations allow the exploration of allosteric and cryptic binding pockets [47], understanding the mechanisms of allosteric modulation [48], discovery of allosteric modulators for the μ opioid receptor [49], fragment-based drug discovery by SILCS (Site Identification by Ligand Competitive Saturation) [50]. MD simulations which are frequently an integral part of these modeling protocols allows refinement and exploration of GPCR structures to a degree that is not possible with static models alone. Despite the best efforts of the pharmaceutical industry to design novel GPCR targeting drugs, attrition rates along R&D pipelines remain high with many candidates eventually failing to demonstrate sufficient efficacy in clinical trials [51].

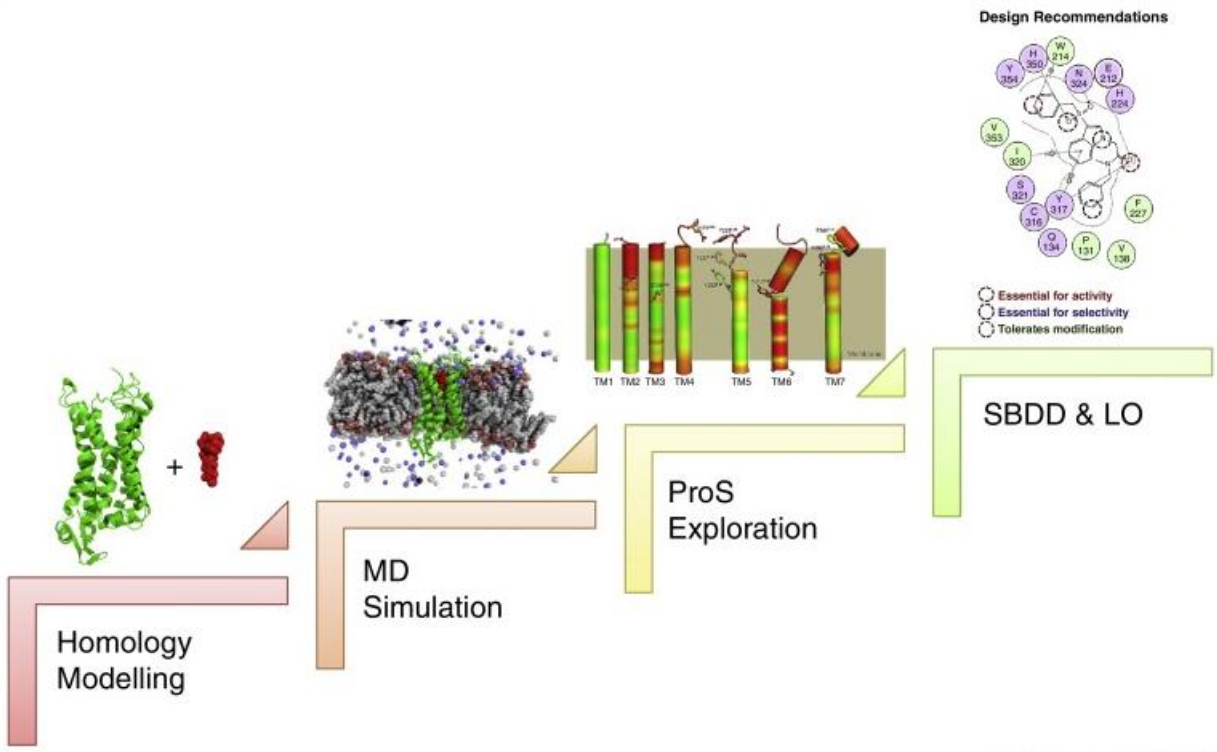

Figure 5-3: Schematic summarisation of interaction maps derived from structural models and MD data that can be used to provide synthesis recommendations [52] (Image courtesy: Heifetz A., *Biochemistry*; 2013;52;8246-8260).

The biogenic amine binding receptors represents a challenge for ligand design with respect to the problem of selectivity considering the high sequence (and probably structural) similarity of the ligand binding site. Due to lack of crystal structures, computer-aided drug design for GPCRs was achieved by applying ligand-based modeling techniques [53, 54]. Literature survey revealed generation of many GPCR models which were mainly used to explain the binding of known GPCR agonists/antagonists [55-59]. A large amount of GPCR ligand binding site data is available from mutagenesis and structures which can be used to direct new mutagenesis experiments to the positions that are most likely to have an effect on ligand binding. The orthosteric pocket present in TMs is very well suited for drug design with a blend of polar and lipophilic areas (**Figure 5-4**) [60]. Mutants designed to discriminate between these molecules can provide more unambiguous elucidation of affinity and selectivity for receptor residue hotspots [28].

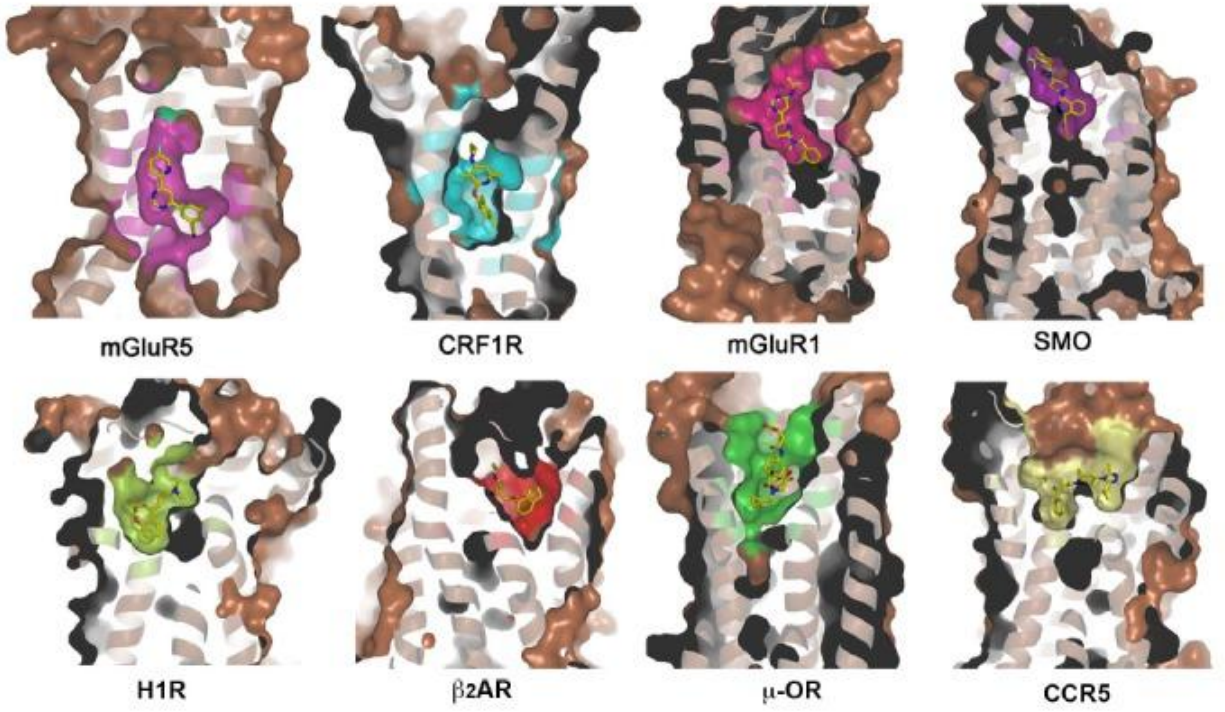

Figure 5-4: Ligand-binding pockets of mGluR5, CRF1R, mGluR1, SMO, H1R, β_2AR, μ-OR and CCR5. Receptors are shown in cartoon and surface representations. Ligands are shown as yellow sticks [61] (Image courtesy: Zhang D. *Mol Cells*.; 2015;38;836–842.).

The ligand interactions may unlock a rational design of ligands with the exact desired pharmacological activity that is agonism versus antagonism as well as potentially biased agonism by the ligand interaction fingerprints approach which has been shown to discriminate agonists from antagonists based on their receptor interactions as well as increase the hits rate from VS [62]. Similar ligands are likely to have similar binding sites. Thus, it would be interesting to implement a mutation design for ligands of interest. Another intriguing outlook is to extend the concept of data-driven mutation design to other functional sites, that is the binding sites of G proteins [63, 64], β-arrestin [65] and dimerisation interfaces [66].

The use of VS processes has substantiated high hit rates in the identification of new ligand chemotype as lead compounds as well as in lead optimisation through virtual screen libraries (*e.g.* the ZINC database is a free database of ~80 million commercially available compounds) by docking compounds into receptor models and then scoring the best fit using computational programs such as AutoDock, GOLD, GLIDE (Schrödinger, LLC) [67, 68]. Virtual screen hit

rates of 3–10% have been reported for a range of GPCR targets including the adenosine A2A-R [69], histamine H_1 [70] and the chemokine receptor, CXCR7 [71].

Many crystal structures have been deciphered from the discovery of bovine rhodopsin and first human GPCR structure with a diffusible ligand. Hence, modeling has become a reliable tool to anticipate additional 3D structures to be discovered based on available experimental structures. Additionally valuable inputs could be obtained by characterisation of GPCRs crystallised with widening range of ligands and intracellular proteins required for receptors transition from inactive to active phase. Previous studies have significantly shown the specific role of distinct agonists and antagonists in studying the ECS conformations [72], thereby opening up new possibilities for allosteric drug targeting at GPCRs [73]. Primary results from the Lewis laboratory have identified an agonist-induced bond swap that initiates a cascade of conformational changes that appears to explain the link between NE binding and α_1-AR signaling [74, 75].

The goal of this project was to extend these studies to define how the ECS conformation of the α_1-AR changes during agonist activation through understanding of NE egress pathway. The contacts NE make with surrounding residues in TMs and ECLs during egress may help in receptor subtype selectivity of ligand binding and design of specific drugs with higher efficacy and longer duration of action. Two parallel approaches were initiated to define the role of residues lining the primary and secondary binding sites. Residues predicted from binding site server lining the orthosteric site were mutated experimentally for their role in signaling while the role of residues at secondary sites were predicted from MD simulations. Moreover, only a few specific agonists and antagonists are known till date for the α_1-AR. Therefore, a ligand based or structure based approach will help in finding possible new leads. The outcomes of this research will provide a new understanding of GPCR activation mechanisms by simulating the new hits and understanding their binding pattern in comparison to known ligands. This research is expected to open the door to the rational development of new modulators that can recognise the ECS of GPCRs in distinct conformational states.

In the present PhD thesis, I made use of computational techniques in conjunction with experimental assays to delineate the residues involved in egress pathway. The process of receptor activation in the apo and NE-bound form of the built homology model was investigated by the aMD simulations. The residues known from previous experimental studies were mutated

individually along with some double mutants to further characterise their rolein the process of receptor activation [74, 75]. Moreover, we were also interested in studying the putative ligand binding residues in the active site and the importance of the ECS in agonist binding. This was followed by ligand based VS to identify hits as new ligand chemotype for the α_1-AR and its subtypes. The α_1-AR has been an important target for drug design but slight is known about the receptor function in dearth of crystal structure. Despite recent progress in GPCRs structure, function and mechanism; the rational development of the next generation of GPCR-targeted drugs including allosteric inhibitors and biased agonists has met with limited success [76].

The aim of this project was to study the changes in ECS conformation of the α_{1B}-AR upon agonist binding and receptor activation computationally with rational design of modulators.
The specific outcomes achieved include:

1. Development of new molecular model that describes the conformational changes of α_1-AR by NE.
2. Characterisation of the egress pathway of NE from the orthosteric binding site that lead to identification of additional contributions to NE affinity.
3. Determination of the effects of selected ECS residues on agonist binding and NE signaling.
4. Understand the α_{1B}-AR activation process in both apoand NE-bound form.
5. Identification of new modulators acting at different α_1-AR subtypes.

Chapter 1 is an introductory chapter on the GPCRs which gives a brief overview of the structure, function, pharmacology and regulation of GPCRs. A broad picture of GPCR network is presented and classified into subclasses of which the biggest is class A and accounts for ~85% of the genes [77]. The mechanism of GPCRs activation is proposed on the rhodopsin structures [78, 79] although crystal structures of ARs have shed light on the GPCR activation process where the receptor is shown to exist in an equilibration between the inactive and active conformations. Biophysical studies has provided direct structural analyses of conformational changes in the receptor molecule as an important first step towards a more profound understanding of GPCR function at a molecular level [80]. A brief outline of adrenergic modulators that binds at the orthosteric and allosteric sites is presented with their limitations such as selectivity, clinical efficacy and undesirable effects on receptor regulation [81, 82].

The main focus is on the findings of the studies done on Class A GPCRs with special reference to α_1-ARs. This chapter outlines a basic understanding of the GPCR along with the implementation of computational techniques to corroborate the structures of closely related GPCRs from existing structures based on sequence analysis. Further use of computational tools (homology modeling, molecular docking, MD and VS) has been shown to study the α_1-AR for drug discovery and development.The present work is an effort to address the issues pertaining to the activation process of the α_{1B}-AR and how the binding of the known ligand (agonist, NE) affect the ECS of the receptor and stabilise specific conformations. The ligand-based *in silico* drug discovery approach is implemented to address rational development of leads which could prove to bepotential α_1-AR modulators.

Chapter 2 is a research chapter on characterising the egress pathway of NE, a α_1-AR agonist. Homology model of the α_{1B}-AR built using the turkey-β_1-AR template was used for docking of NE at the orthosteric binding site. Validation of the docking model was carried out by site directed mutagenesis studies and testing the above mutants using radiolabelled, functional and binding studies that helped us to gain insights into the role played by the residues lining the egress pathway. Egress pathway identified critical involvement of residues from TM3, TM5, TM7, ECL1 and ECL2; in particular W121 (TM3), C195 (ECL2), Y203 (TM5) and S207 (TM5) which affect the signaling efficiency [75, 83]. Egress pathway identified 3 distinct positions *viz.* 1, 2 and 3. Position 1 is the orthosteric binding site that included residues from TM3, TM5, TM7, ECL1 and ECL2. Position 2 is the auxiliary site 1 that included residues from ECL2 and TM5.

Position 3 is the auxiliary site 2 that included residues from ECL1 and TM3. An overlap between orthosteric site and auxiliary site 1 is observed including residues from TM5. The negatively charged ECS provides retention site for positively charged Iigands as allosteric modulators which affect the signaling process. Hence, ECS represents an important secondary site for drug design and might be subtype specific [72, 84].

RAMD study on the β_2-AR suggested that the ligands access the primary binding site via the ECS revealing that specific residues in the ECS were important for ligand entry and exit [83, 85]. In contrast, ligand exits through the TM helices as observed in rhodopsin [86-88] where ECL2 covers the entrance to the binding pocket [89]. Ligand exit involved the breakage of the Asp192-Lys305 salt bridge that linked the ECL2 to the extracellular top of the TM7. Guo D et al., investigated the molecular basis of ligand dissociation process (antagonist ZM241385) in the adenosine A2A-R [90] where ZM241385 follows a multi-step dissociation pathway from the A2A-R by first breaking the hydrogen bond network formed by the triad of Glu169 in ECL2, Thr256 in TM6 and His264 in TM7 and moving further away from the binding pocket into the extracellular domain and bulk solvent. Thus, it is plausible to suggest an importance of the ECS as a secondary site for ligand binding.

The ECS of GPCRs is remarkably diverse and therefore represents an ideal target for the discovery of subtype-selective drugs. However, the functional role of the ECS in receptor activation or conformational coupling of this surface to the native ligand binding pocket is not fully understood. Small molecule drugs that bind within the TM core exhibit different efficacies towards G protein activation (agonist, neutral antagonist and inverse agonist) and also stabilise distinct conformations of the ECS. The use of NMR spectroscopy around a central structural feature in the ECS of the β_2-AR i.e., a salt bridge linking ECL 2 and ECL3 could be beneficial to investigate the ligand-specific conformational changes. Thus, conformational coupling between the ECS and the orthosteric binding site might demonstrate that drugs targeting this diverse surface could function as allosteric modulators with high subtype selectivity. Moreover, these studies could provide new insights into the dynamic behavior of GPCRs not addressable by static and inactive-state crystal structures.

Chapter 3 is a research chapter to understand the activation process of the apo and NE-bound form of the α_{1B}-AR by aMD. TMs of the functionally active crystal structures of the class A GPCRs like opsin [91] (active metarhodopsin II (3PQR)); β_2-AR (active G protein bound

(3SN6) [63], active-like nanobody bound (3POG)) [22]; A2A-R (agonist UK432097 bound (3QAK) [23]) internally rearranges towards the cytoplasmic side that leads to cascade of bond swapping and bond forming events [92, 93]. The rotation of TM6 is accompanied by a translocation of $Trp^{6.48}$ located close to the base of the binding pocket in rhodopsin, A2A-R and to some extent in β_2-AR.

Ballesteros et al., predicted disruption of ionic lock between TM3 and TM6 in the β_2-AR that leads to constitutive activation of the receptor [94]. Inactive conformations along with transitions were observed for the active structure of β_2-AR on microsecond level timeframe using cMD in a study by Dror et al., [95]. Miao et al., demonstrated the use of aMD on M2 muscarinic receptor [96] where the receptor activation was characterised by formation of a hydrogen bond between the $Tyr206^{5.58}$ – $Tyr440^{7.53}$ and outward movement of cytoplasmic end of TM6 by ~6Å which is in agreement with previous GPCR studies where TM6 has been suggested to be a switch for the conformational transitions between inactive and active states [97].

We performed dihedral aMD by applying boost potential to all the dihedral angles in the system (parameters: E_{dihed} and α_{dihed}) and dual-boost aMD by applying boost potential to all atoms in the system along with dihedral angles. The residues known from the experimental studies in our lab were mutated individually along with some double mutants to further characterise their role in receptor activation [74, 75]. aMD identified movement of tyrosine residues in close proximity to form weak hydrogen bond for W184A and double mutant Y223F-Y348F in a 10ns simulation. The direct activation of the apo and NE-α_{1B}-AR was not observed over the nanosecond time scale but few mutants could be seen moving close to active state over a time scale of 10ns (**Table 3-1, Chapter 3**). The residues identified showed reduced distance between Tyr223 (-OH) – Tyr348 (-OH) suggesting movement of receptor towards active state. This activation process at atomistic level is of pivotal importance in understanding the structure-function relationship. The receptor activation is characterised by formation of a hydrogen bond between the intracellular domains of TM5 and TM7 (Tyr223–Tyr348) which is in consonance with the results observed in previous studies for the active structures of rhodopsin [91, 98] and β_2-AR [99, 100]. aMD applied to α_{1B}-AR in apo and NE-bound state have shown almost similar results in apo-state and NE-bound receptor thereby suggesting theirsimilar inclination towards activation with both dihedral and dual-boost dynamics.

Chapter 4 reflects the VS of the α_{1B}-AR modulators. VS provide a cost and time effective method to interrogate *in silico* databases containing millions of compounds to identify potential binders to a receptor of interest. Chris de Graaf and Didier Rognan used selective structure-based VS for full and partial agonists of the β_2-AR [101]. Previous VS studies on class A GPCR member like A2A-R [69], β_2-AR [101], Chemokine CXCR4 receptor [102], Dopamine D1 and D2 receptor [103] and Histamine H1 receptor [62] have successfully screened selective agonists and antagonists.

Evers A. and Klabunde T. performed structure-based VS for antagonists of the homology model of the α_{1A}-AR generated using BRh as structural template [42]. Previous studies on β_2-AR and rhodopsin have claimed the use of inactive structures resulting in identification of antagonists or inverse agonists while the use of active-state homology models retrieves partial/full agonists. Evers et al., generated a homology model for the α_{1A}-AR [42] and docked ~23 000 ligands resulting in 24 ligands binding in the submicromolar range [104]. The role of imidazoquinazoline derivatives have been widely demonstrated in diverse biological activities including the anti-hypertensive activities through a selective α_1-antagonistic mechanism [105-107].

We screened approximately 17.9 million drug-like compounds from the ZINC database using ROCS software. The initial results identified 80"hits" which were confirmed by flexible docking to likely bind either in the orthosteric site or in line to allosteric sites along the ligand unbinding pathway (chapter 2). To corroborate the potential of screened hits to target the α_1-AR, we selected 12 hits for pharmacological evaluation acrossthe three α_1-AR subtypes. VS and molecular docking of the screened hits from the drug like compounds database identified 3 hits from 12 compounds which were similar to the query molecule NE. *In vitro* studies of hits supported our study and identified compound 7 to be weak agonist for α_{1A}-AR, compound 12 to be weak agonist forα_{1A}-AR and α_{1D}-AR subtypes while compound 10 to be weak agonist for α_{1A}-AR and α_{1B}-AR and subtypes and full agonist for α_{1D}-AR subtype.

The combined use of ROCS, VIDA and FRED played a vital role in compound identification and selection. This selection of hits is essential in VS of the compounds from large pool of database. The current study showed that the homology model of the α_{1B}-AR is suitable for retrieving the α_1-AR partial/full agonists.The results of our initial characterisation revealed that several ligands that docked in the orthosteric site of the α_{1B}-AR activated all the three α_1-AR subtypes confirming the potential of this approach to identify new modulators. The approach used can in

principle be applied to any member of the GPCR family with known ligand information and site-directed mutagenesis data.

In summary, this project has increased our understanding of GPCR structure¸ function and shed light on the aspect of receptor activation process, role of the ECS in identification of residues as allosteric/auxiliary sites by modeling, dynamics and VS followed by their experimental validation. We addressed the exit pathway of NE from the homology model of hamster α_{1B}-AR by SMD simulations and succeeded in getting close to active state of the receptor for few single and double mutants which have been proven experimentally to contribute in the signaling efficacy. Although the direct receptor activation could not be observed for the apo and NE-bound form of the α_{1B}-AR, the use of aMD has shown the movement of the receptor towards active state for the mutants in significantly shorter simulation time compared to classical simulations.

This study established the application of aMD to the study of activation process which will be highly useful for designing GPCR mutation studies and engineering small molecules for receptor-selective therapeutics. The novel modulators for the α_1-ARs were identified by using known endogenous ligand, NE as a query to search leads among the database with millions of compounds confirming the potential of this approach to identify new α_1-AR subtype GPCR modulators. The atomic-level descriptions of the process as observed in this study will deepen our understanding of ligand-GPCR interactions and will lay the structural foundation for future rational design of drugs with optimised binding kinetics.

The different studies conducted with this project have increased our understanding of the α_1-AR. This project work provided useful insights into the role of residues lining the orthosteric sites, ECS and TM helices adding their specific role in activation and providing subtype specificity. This project has open doors to new possibilities in drug design targeting allosteric sites along with structure based drug design. The combined use of computational and experimental technique is beneficial in setting an environment for understanding of basics and surpassing the high cost associated with either technique.

5.2 Future Perspectives

This PhD project has unbolted and raised additional questions to be countered that comprehend the basis behind the working mechanism of this class and subset of receptor. Though experimental data is available to validate the computational results obtained from molecular modeling, molecular docking, homology modeling, MD and VS, but further insight is needed to join the hanging patches. Future work that could provide more insight into above studies includes:

1. Building new molecular model from the latest active GPCRs and their comparison with the inactive GPCRs and their subsequent models.
2. Free Energy perturbation simulations on the apo and NE-bound receptor to determine contribution of each residue in ligand binding.
3. Long range accelerated simulations to study the receptor activation/inactivation using different parameters (different atomic velocity initialisation).
4. Steered dynamic simulations on the new hits to determine the egress pathway and additional contributions of residues.
5. Ligand based virtual screening for the antagonist prazosin.
6. Structure based virtual screening using imidazole as the basic pharmacophore.
7. Structure and fragment based drug design on the existing modulators.

5.3 Publications

1. Brust, Andreas; Croker, Daniel; Colless, Barbara; Ragnarsson, Lotten; Andersson, Asa; Jain, Kapil; Caraballo, Sonia; Castro, Joel; Brierley, Stuart; Alewood, Paul; Lewis, Richard: **Conopeptide-derived κ-opioid agonists (conorphins): potent, selective and metabolic stable dynorphinA mimetics with anti-nociceptive properties**. *Journal of medicinal chemistry* 2016, **59**(6):2381-2395.

5.4 References

1. Fredriksson R, Lagerström MC, Lundin L-G, Schiöth HB: **The G protein-coupled receptors in the human genome form five main families. Phylogenetic analysis, paralogon groups, and fingerprints**. *Molecular pharmacology* 2003, **63**(6):1256-1272.
2. Pierce KL, Premont RT, Lefkowitz RJ: **Seven-transmembrane receptors**. *Nature reviews molecular cell biology* 2002, **3**(9):639-650.
3. Fagerberg L, Jonasson K, von Heijne G, Uhlén M, Berglund L: **Prediction of the human membrane proteome**. *Proteomics* 2010, **10**(6):1141-1149.
4. Lagerström MC, Schiöth HB: **Structural diversity of G protein-coupled receptors and significance for drug discovery**. *Nature reviews drug discovery* 2008, **7**(4):339-357.
5. Hopkins AL, Groom CR: **The druggable genome**. *Nature reviews drug discovery* 2002, **1**(9):727-730.
6. Granier S, Kobilka B: **A new era of GPCR structural and chemical biology**. *Nature chemical biology* 2012, **8**(8):670-673.
7. Marinissen MJ, Gutkind JS: **G protein-coupled receptors and signaling networks: Emerging paradigms**. *Trends in pharmacological sciences* 2001, **22**(7):368-376.
8. Clark T: **G protein-coupled receptors: Answers from simulations**. *Beilstein journal of organic chemistry* 2017, **13**(1):1071-1078.
9. Filmore D: **It's a GPCR world**. *Modern drug discovery* 2004, **7**:24-28.
10. Heifetz A, Schertler GF, Seifert R, Tate CG, Sexton PM, Gurevich VV, Fourmy D, Cherezov V, Marshall FH, Storer RI: **GPCR structure, function, drug discovery and crystallography: Report from academia-industry international conference (UK royal society) chicheley hall, 1–2 september 2014**. *Naunyn-schmiedeberg's archives of pharmacology* 2015, **388**(8):883-903.
11. Park PS-H, Lodowski DT, Palczewski K: **Activation of G protein–coupled receptors: Beyond two-state models and tertiary conformational changes**. *Annual review of pharmacology and toxicology* 2008, **48**:107-141.
12. Cong X, Topin J, Golebiowski J: **Class A GPCRs: Structure, function, modeling and structure-based Ligand Design**. *Current pharmaceutical design* 2017, **23**(29):4390-4409.

13. Salom D, Padayatti PS, Palczewski K: **Crystallisation of G protein-coupled receptors**. *Methods in cell biology* 2013, **117**:451-468.
14. Ghosh E, Kumari P, Jaiman D, Shukla AK: **Methodological advances: The unsung heroes of the GPCR structural revolution**. *Nature reviews molecular cell biology* 2015, **16**(2):69-81.
15. Millar RP, Newton CL: **The year in G protein-coupled receptor research**. *Molecular endocrinology* 2010, **24**(1):261-274.
16. Mason JS, Bortolato A, Congreve M, Marshall FH: **New insights from structural biology into the druggability of G protein-coupled receptors**. *Trends in pharmacological sciences* 2012, **33**(5):249-260.
17. Hinsen K: **The molecular modeling toolkit: A new approach to molecular simulations**. *Journal of computational chemistry* 2000, **21**(2):79-85.
18. Ciancetta A, Sabaddin D, Federico S, Spalluto G, Moro S: **Advances in computational techniques to study GPCR–ligand recognition**. *Trends in pharmalogical sciences* 2014, **36**(12):878-890.
19. Stevens RC, Cherezov V, Katritch V, Abagyan R, Kuhn P, Rosen H, Wüthrich K: **GPCR Network: A large-scale collaboration on GPCR structure and function**. *Nature reviews drug discovery* 2013, **12**(1):25-34.
20. Soriano-Ursúa MA, Trujillo-Ferrara JG, Correa-Basurto J, Vilar S: **Recent structural advances of β_1 and β_2-adrenoceptors yield keys for ligand recognition and drug design**. *Journal of medicinal chemistry* 2013, **56**(21):8207-8223.
21. Li J, Jonsson AL, Beuming T, Shelley JC, Voth GA: **Ligand-dependent activation and deactivation of the human adenosine A2A receptor**. *Journal of the american chemical society* 2013, **135**(23):8749-8759.
22. Rasmussen SG, Choi H-J, Fung JJ, Pardon E, Casarosa P, Chae PS, DeVree BT, Rosenbaum DM, Thian FS, Kobilka TS: **Structure of a nanobody-stabilised active state of the β_2-adrenoceptor**. *Nature* 2011, **469**(7329):175-180.
23. Lebon G, Warne T, Edwards PC, Bennett K, Langmead CJ, Leslie AG, Tate CG: **Agonist-bound adenosine A2A receptor structures reveal common features of GPCR activation**. *Nature* 2011, **474**(7352):521-525.

24. Costanzi S: **On the applicability of GPCR homology models to computer-aided drug discovery: A comparison between *in silico* and crystal structures of the β_2-adrenergic receptor**. *Journal of medicinal chemistry* 2008, **51**(10):2907-2914.

25. Katritch V, Cherezov V, Stevens RC: **Structure-function of the G protein–coupled receptor superfamily**. *Annual review of pharmacology and toxicology* 2013, **53**:531-556.

26. Wheatley M, Wootten D, Conner MT, Simms J, Kendrick R, Logan R, Poyner DR, Barwell J: **Lifting the lid on GPCRs: The role of extracellular loops**. *British journal of pharmacology* 2012, **165**(6):1688-1703.

27. Venkatakrishnan A, Deupi X, Lebon G, Tate CG, Schertler GF, Babu MM: **Molecular signatures of G protein-coupled receptors**. *Nature* 2013, **494**(7436):185-194.

28. Munk C, Harpsøe K, Hauser AS, Isberg V, Gloriam DE: **Integrating structural and mutagenesis data to elucidate GPCR ligand binding**. *Current opinion in pharmacology* 2016, **30**:51-58.

29. Lie MA, Thomsen R, Pedersen CN, Schiøtt B, Christensen MH: **Molecular docking with ligand attached water molecules**. *Journal of chemical information and modeling* 2011, **51**(4):909-917.

30. Congreve M, Dias JM, Marshall FH: **Structure-based drug design for G protein-coupled receptors**. *Progress in medicinal chemistry* 2014, **53**:1-63.

31. Liu W, Chun E, Thompson AA, Chubukov P, Xu F, Katritch V, Han GW, Roth CB, Heitman LH, IJzerman AP: **Structural basis for allosteric regulation of GPCRs by sodium ions**. *Science* 2012, **337**(6091):232-236.

32. Xu F, Wu H, Katritch V, Han GW, Jacobson KA, Gao Z-G, Cherezov V, Stevens RC: **Structure of an agonist-bound human A2A adenosine receptor**. *Science* 2011, **332**(6027):322-327.

33. Lau P-W, Grossfield A, Feller SE, Pitman MC, Brown MF: **Dynamic structure of retinylidene ligand of rhodopsin probed by molecular simulations**. *Journal of molecular biology* 2007, **372**(4):906-917.

34. Hurst DP, Grossfield A, Lynch DL, Feller S, Romo TD, Gawrisch K, Pitman MC, Reggio PH: **A lipid pathway for ligand binding is necessary for a cannabinoid G protein-coupled receptor**. *Journal of biological chemistry* 2010, **285**(23):17954-17964.

35. Grossfield A, Pitman MC, Feller SE, Soubias O, Gawrisch K: **Internal hydration increases during activation of the G protein-coupled receptor rhodopsin**. *Journal of molecular biology* 2008, **381**(2):478-486.

36. Orban T, Jastrzebska B, Gupta S, Wang B, Miyagi M, Chance MR, Palczewski K: **Conformational dynamics of activation for the pentameric complex of dimeric G protein-coupled receptor and heterotrimeric G protein**. *Structure* 2012, **20**(5):826-840.

37. Bortolato A, Tehan BG, Bodnarchuk MS, Essex JW, Mason JS: **Water network perturbation in ligand binding: Adenosine A2A antagonists as a case study**. *Journal of chemical information and modeling* 2013, **53**(7):1700-1713.

38. Kamal M, Jockers R: **Bitopic ligands: All-in-one orthosteric and allosteric**. *F1000 biology reports* 2009, **1**:77-79.

39. Lane JR, Sexton PM, Christopoulos A: **Bridging the gap: Bitopic ligands of G protein-coupled receptors**. *Trends in pharmacological sciences* 2013, **34**(1):59-66.

40. Lane JR, Donthamsetti P, Shonberg J, Draper-Joyce CJ, Dentry S, Michino M, Shi L, López L, Scammells PJ, Capuano B: **A new mechanism of allostery in a G protein–coupled receptor dimer**. *Nature chemical biology* 2014, **10**(9):745-752.

41. Maggio R, Scarselli M, Capannolo M, Millan MJ: **Novel dimensions of D3 receptor function: Focus on heterodimerisation, transactivation and allosteric modulation**. *European neuropsychopharmacology* 2015, **25**(9):1470-1479.

42. Evers A, Klabunde T: **Structure-based drug discovery using GPCR homology modeling: Successful virtual screening for antagonists of the α_{1A} adrenergic receptor**. *Journal of medicinal chemistry* 2005, **48**(4):1088-1097.

43. Zhong H, Minneman KP: **α_1-adrenoceptor subtypes**. *European journal of pharmacology* 1999, **375**(1):261-276.

44. Heifetz A, James T, Morao I, Bodkin MJ, Biggin PC: **Guiding lead optimisation with GPCR structure modeling and molecular dynamics**. *Current opinion in pharmacology* 2016, **30**:14-21.

45. Mortier J, Rakers C, Bermudez M, Murgueitio MS, Riniker S, Wolber G: **The impact of molecular dynamics on drug design: Applications for the characterisation of ligand–macromolecule complexes**. *Drug discovery today* 2015, **20**(6):686-702.

46. McRobb FM, Negri A, Beuming T, Sherman W: **Molecular dynamics techniques for modeling G protein-coupled receptors**. *Current opinion in pharmacology* 2016, **30**:69-75.

47. Frembgen-Kesner T, Elcock AH: **Computational sampling of a cryptic drug binding site in a protein receptor: Explicit solvent molecular dynamics and inhibitor docking to p38 MAP kinase**. *Journal of molecular biology* 2006, **359**(1):202-214.

48. Kaczor AA, Rutkowska E, Bartuzi D, Targowska-Duda KM, Matosiuk D, Selent J: **Computational methods for studying G protein-coupled receptors (GPCRs)**. *Methods in cell biology* 2016, **132**:359-399.

49. Bartuzi D, Kaczor AA, Matosiuk D: **Interplay between two allosteric sites and their influence on agonist binding in human μ opioid receptor**. *Journal of chemical information and modeling* 2016, **56**(3):563-570.

50. Faller CE, Raman EP, MacKerell AD, Guvench O: **Site identification by ligand competitive saturation (SILCS) simulations for fragment-based drug design**. *Methods in molecular biology* 2015, **1289**:75-87.

51. Guo D, Hillger JM, IJzerman AP, Heitman LH: **Drug-target residence time: A case for G protein-coupled receptors**. *Medicinal research reviews* 2014, **34**(4):856-892.

52. Heifetz A, Barker O, Morris GB, Law RJ, Slack M, Biggin PC: **Toward an understanding of agonist binding to human Orexin-1 and Orexin-2 receptors with G protein-coupled receptor modeling and site-directed mutagenesis**. *Biochemistry* 2013, **52**(46):8246-8260.

53. Flohr S, Kurz M, Kostenis E, Brkovich A, Fournier A, Klabunde T: **Identification of nonpeptidic urotensin II receptor antagonists by virtual screening based on a pharmacophore model derived from structure-activity relationships and nuclear magnetic resonance studies on urotensin II**. *Journal of medicinal chemistry* 2002, **45**(9):1799-1805.

54. Marriott DP, Dougall IG, Meghani P, Liu Y-J, Flower DR: **Lead generation using pharmacophore mapping and three-dimensional database searching: Application to muscarinic M3 receptor antagonists**. *Journal of medicinal chemistry* 1999, **42**(17):3210-3216.

55. Bröer BM, Gurrath M, Höltje H-D: **Molecular modeling studies on the ORL1-receptor and ORL1-agonists**. *Journal of computer-aided molecular design* 2003, **17**(11):739-754.
56. Chambers JJ, Nichols DE: **A homology-based model of the human 5-HT2A receptor derived from an *in silico* activated G protein-coupled receptor**. *Journal of computer-aided molecular design* 2002, **16**(7):511-520.
57. Freddolino PL, Kalani MYS, Vaidehi N, Floriano WB, Hall SE, Trabanino RJ, Kam VWT, Goddard WA: **Predicted 3D structure for the human β_2-adrenergic receptor and its binding site for agonists and antagonists**. *Proceedings of the national academy of sciences* 2004, **101**(9):2736-2741.
58. Furse KE, Lybrand TP: **Three-dimensional models for β-adrenergic receptor complexes with agonists and antagonists**. *Journal of medicinal chemistry* 2003, **46**(21):4450-4462.
59. Jöhren K, Höltje H-D: **A model of the human M2 muscarinic acetylcholine receptor**. *Journal of computer-aided molecular design* 2002, **16**(11):795-801.
60. Lu M, Wu B: **Structural studies of G protein-coupled receptors**. *IUBMB life* 2016, **68**(11):894-903.
61. Zhang D, Zhao Q, Wu B: **Structural studies of G protein-coupled receptors**. *Molecules and cells* 2015, **38**(10):836-842.
62. de Graaf C, Kooistra AJ, Vischer HF, Katritch V, Kuijer M, Shiroishi M, Iwata S, Shimamura T, Stevens RC, de Esch IJ: **Crystal structure-based virtual screening for fragment-like ligands of the human histamine H1 receptor**. *Journal of medicinal chemistry* 2011, **54**(23):8195-8206.
63. Rasmussen SG, DeVree BT, Zou Y, Kruse AC, Chung KY, Kobilka TS, Thian FS, Chae PS, Pardon E, Calinski D: **Crystal structure of the β_2-adrenergic receptor-Gs protein complex**. *Nature* 2011, **477**(7366):549-555.
64. Standfuss J, Edwards PC, D'antona A, Fransen M, Xie G, Oprian DD, Schertler G: **The structural basis of agonist-induced activation in constitutively active rhodopsin**. *Nature* 2011, **471**(7340):656-660.
65. Kang Y, Zhou XE, Gao X, He Y, Liu W, Ishchenko A, Barty A, White TA, Yefanov O, Han GW: **Crystal structure of rhodopsin bound to arrestin by femtosecond X-ray laser**. *Nature* 2015, **523**(7562):561-567.

66. Huang J, Chen S, Zhang JJ, Huang X-Y: **Crystal structure of oligomeric β_1-adrenergic G protein–coupled receptors in ligand-free basal state**. *Nature structural & molecular biology* 2013, **20**(4):419-425.

67. Sirci F, Istyastono EP, Vischer HF, Kooistra AJ, Nijmeijer S, Kuijer M, Wijtmans M, Mannhold R, Leurs R, de Esch IJ: **Virtual fragment screening: Discovery of histamine H3 receptor ligands using ligand-based and protein-based molecular fingerprints**. *Journal of chemical information and modeling* 2012, **52**(12):3308-3324.

68. Kontoyianni M, Liu Z: **Structure-based design in the GPCR target space**. *Current medicinal chemistry* 2012, **19**(4):544-556.

69. Langmead CJ, Andrews SP, Congreve M, Errey JC, Hurrell E, Marshall FH, Mason JS, Richardson CM, Robertson N, Zhukov A: **Identification of novel adenosine A2A receptor antagonists by virtual screening**. *Journal of medicinal chemistry* 2012, **55**(5):1904-1909.

70. Graaf Cd, Kooistra A, Vischer H, Katritch V, Kuijer M, Shiroishi M, Shimamura T, Iwata S, Stevens R, de Esch I: **Crystal structure-based virtual screening for novel fragment-like ligands of the human histamine H1 receptor**. *Journal of medicinal chemistry* 2011, **54**(23):8195-8206.

71. Yoshikawa Y, Oishi S, Kubo T, Tanahara N, Fujii N, Furuya T: **Optimised method of G protein-coupled receptor homology modeling: Its application to the discovery of novel CXCR7 ligands**. *Journal of medicinal chemistry* 2013, **56**(11):4236-4251.

72. Bokoch MP, Zou Y, Rasmussen SG, Liu CW, Nygaard R, Rosenbaum DM, Fung JJ, Choi H-J, Thian FS, Kobilka TS: **Ligand-specific regulation of the extracellular surface of a G protein-coupled receptor**. *Nature* 2010, **463**(7277):108-112.

73. Wang C-IA, Lewis RJ: **Emerging opportunities for allosteric modulation of G protein-coupled receptors**. *Biochemical pharmacology* 2013, **85**(2):153-162.

74. Ragnarsson L, Wang C-IA, Andersson Å, Fajarningsih D, Monks T, Brust A, Rosengren KJ, Lewis RJ: **Conopeptide ρ-TIA defines a new allosteric site on the extracellular surface of the α_{1B}-adrenoceptor**. *Journal of biological chemistry* 2013, **288**(3):1814-1827.

75. Ragnarsson L, Andersson Å, Thomas WG, Lewis RJ: **Extracellular surface residues of the α_{1B}-adrenoceptor critical for G protein–coupled receptor function**. *Molecular pharmacology* 2015, **87**(1):121-129.

76. Cavero I, Kaplan HR: **Drug discovery paradigms: Past, present, future-A centennial symposium of the american society for pharmacology and experimental therapeutics: 6 april 2008, san diego, USA**. *Expert opinion on drug discovery* 2008, **3**(9):1145-1154.

77. Chou K-C: **Prediction of G protein-coupled receptor classes**. *Journal of proteome research* 2005, **4**(4):1413-1418.

78. Schertler GF, Villa C, Henderson R: **Projection structure of rhodopsin**. *Nature* 1993, **362**(6422):770-772.

79. Okada T, Ernst OP, Palczewski K, Hofmann KP: **Activation of rhodopsin: New insights from structural and biochemical studies**. *Trends in biochemical sciences* 2001, **26**(5):318-324.

80. Gether U: **Uncovering molecular mechanisms involved in activation of G protein-coupled receptors**. *Endocrine reviews* 2000, **21**(1):90-113.

81. Smith NJ, Bennett KA, Milligan G: **When simple agonism is not enough: Emerging modalities of GPCR ligands**. *Molecular and cellular endocrinology* 2011, **331**(2):241-247.

82. Violin JD, Crombie AL, Soergel DG, Lark MW: **Biased ligands at G protein-coupled receptors: Promise and progress**. *Trends in pharmacological sciences* 2014, **35**(7):308-316.

83. Wang T, Duan Y: **Ligand entry and exit pathways in the β_2-adrenergic receptor**. *Journal of molecular biology* 2009, **392**(4):1102-1115.

84. Deupi X, Li X-D, Schertler GF: **Ligands stabilise specific GPCR conformations: But how?** *Structure* 2012, **20**(8):1289-1290.

85. Johnston JM, Filizola M: **Showcasing modern molecular dynamics simulations of membrane proteins through G protein-coupled receptors**. *Current opinion in structural biology* 2011, **21**(4):552-558.

86. Palczewski K, Kumasaka T, Hori T, Behnke CA, Motoshima H, Fox BA, Le Trong I, Teller DC, Okada T, Stenkamp RE: **Crystal structure of rhodopsin: A G protein-coupled receptor**. *Science* 2000, **289**(5480):739-745.

87. Nygaard R, Frimurer TM, Holst B, Rosenkilde MM, Schwartz TW: **Ligand binding and micro-switches in 7TM receptor structures**. *Trends in pharmacological sciences* 2009, **30**(5):249-259.

88. Standfuss J, Edwards PC, D'Antona A, Fransen M, Xie G, Oprian DD, Schertler GF: **Crystal structure of constitutively active rhodopsin: How an agonist can activate its GPCR**. *Nature* 2011, **471**(7340):656-660.

89. Bokoch MP, Zou Y, Rasmussen SG, Liu CW, Nygaard R, Rosenbaum DM, Fung JJ, Choi H-J, Thian FS, Kobilka TS: **Ligand-specific regulation of the extracellular surface of a G protein-coupled receptor**. *Nature* 2010, **463**(7277):108-112.

90. Guo D, Pan AC, Dror RO, Mocking T, Liu R, Heitman LH, Shaw DE, IJzerman AP: **Molecular basis of ligand dissociation from the adenosine A2A receptor**. *Molecular pharmacology* 2016, **89**(5):485-491.

91. Scheerer P, Park JH, Hildebrand PW, Kim YJ, Krauß N, Choe H-W, Hofmann KP, Ernst OP: **Crystal structure of opsin in its G protein-interacting conformation**. *Nature* 2008, **455**(7212):497-502.

92. Gether U, Kobilka BK: **G protein-coupled receptors II. Mechanism of agonist activation**. *Journal of biological chemistry* 1998, **273**(29):17979-17982.

93. Dror RO, Pan AC, Arlow DH, Borhani DW, Maragakis P, Shan Y, Xu H, Shaw DE: **Pathway and mechanism of drug binding to G protein-coupled receptors**. *Proceedings of the national academy of sciences* 2011, **108**(32):13118-13123.

94. Ballesteros JA, Jensen AD, Liapakis G, Rasmussen SG, Shi L, Gether U, Javitch JA: **Activation of the β_2-adrenergic receptor involves disruption of an ionic lock between the cytoplasmic ends of transmembrane segments 3 and 6**. *Journal of biological chemistry* 2001, **276**(31):29171-29177.

95. Kruse AC, Hu J, Pan AC, Arlow DH, Rosenbaum DM, Rosemond E, Green HF, Liu T, Chae PS, Dror RO: **Structure and dynamics of the M3 muscarinic acetylcholine receptor**. *Nature* 2012, **482**(7386):552-556.

96. Miao Y, Nichols SE, Gasper PM, Metzger VT, McCammon JA: **Activation and dynamic network of the M2 muscarinic receptor**. *Proceedings of the national academy of sciences* 2013, **110**(27):10982-10987.

97. Spalding TA, Burstein ES, Henderson SC, Ducote KR, Brann MR: **Identification of a ligand-dependent switch within a muscarinic receptor**. *Journal of biological chemistry* 1998, **273**(34):21563-21568.

98. Park JH, Scheerer P, Hofmann KP, Choe H-W, Ernst OP: **Crystal structure of the ligand-free G protein-coupled receptor opsin**. *Nature* 2008, **454**(7201):183-187.

99. Rasmussen SG, DeVree BT, Zou Y, Kruse AC, Chung KY, Kobilka TS, Thian FS, Chae PS, Pardon E, Calinski D: **Crystal structure of the β_2-adrenergic receptor-Gs protein complex**. *Nature* 2011, **477**(7366):549-555.

100. Rasmussen SG, Choi H-J, Fung JJ, Pardon E, Casarosa P, Chae PS, DeVree BT, Rosenbaum DM, Thian FS, Kobilka TS: **Structure of a nanobody-stabilised active state of the β_2-adrenoceptor**. *Nature* 2011, **469**(7329):175-180.

101. De Graaf C, Rognan D: **Selective structure-based virtual screening for full and partial agonists of the β_2-adrenergic receptor**. *Journal of medicinal chemistry* 2008, **51**(16):4978-4985.

102. Neves MA, Simões S, e Melo MLS: **Ligand-guided optimisation of CXCR4 homology models for virtual screening using a multiple chemotype approach**. *Journal of computer-aided molecular design* 2010, **24**(12):1023-1033.

103. Kołaczkowski M, Bucki A, Feder M, Pawłowski M: **Ligand-optimised homology models of D1 and D2 dopamine receptors: Application for virtual screening**. *Journal of chemical information and modeling* 2013, **53**(3):638-648.

104. Evers A, Hessler G, Matter H, Klabunde T: **Virtual screening of biogenic amine-binding G protein coupled receptors: Comparative evaluation of protein and ligand-based virtual screening protocols**. *Journal of medicinal chemistry* 2005, **48**(17):5448-5465.

105. Chern J-W, Shiau C-Y, Lu G-Y: **Studies on quinazolinones. 3: Novel and efficient route to the synthesis of conformationally restricted analogues of ketanserin and SGB-1534 as antihypertensive agents**. *Bioorganic & medicinal chemistry letters* 1991, **1**(11):571-574.

106. Chern JW, Tao PL, Yen MH, Lu GY, Shiau CY, Lai YJ, Chien SL, Chan CH: **Studies on quinazolines. 5. 2, 3-Dihydroimidazo [1, 2-c] quinazoline derivatives: A novel class of potent and selective α_1-adrenoceptor antagonists and antihypertensive agents**. *Journal of medicinal chemistry* 1993, **36**(15):2196-2207.

107. Jen T, Dienel B, Bowman H, Petta J, Helt A, Loev B: **Amidines. 2. A new class of antihypertensive agents. 1, 2, 3, 5-tetrahydroimidazo [2, 1-b] quinazolines**. *Journal of medicinal chemistry* 1972, **15**(7):727-731.